THE UNIVERSITY
of EDINBURGH

The functional regulation of kisspeptin receptor by calmodulin and Ca^{2+}/calmodulin-dependent protein kinase II

Abdirahman M Jama BSc (Hons), MSc

Medical Research Council, Centre for Reproductive Health

47 Little France Crescent

Edinburgh

EH16 4TH

This thesis is submitted to the University of Edinburgh for the degree of

Doctor of Philosophy

2014

Table of Contents

Declaration

I hereby declare that the work presented within this thesis was carried out by me during the course of my PhD and that it has not been submitted for any other degree or qualification. Where I have used the work of others, the sources of information have been detailed clearly in the presentation.

Abdirahman M. Jama

Publications

Per-reviewed

JAMA, A. M., GABRIEL, J., AL-NAGAR, A. J., MARTIN, S., BAIG, S. Z., SOLEYMANI, H., CHOWDHURY, Z., BEESLEY, P. & TOROK, K. 2011. Lobe-specific functions of Ca2+.calmodulin in alphaCa2+.calmodulin-dependent protein kinase II activation. *The Journal of biological chemistry, 286, 12308-16.*

GORDIENKO, D., POVSTYAN, O., SUKHANOVA, K., RAPHAEL, M., HARHUN, M., DYSKINA, Y., LEHEN'KYI, V., **JAMA, A**., LU, Z. L., SKRYMA, R. & PREVARSKAYA, N. 2015. Impaired P2X signalling pathways in renal microvascular myocytes in genetic hypertension. *Cardiovascular research, 105, 131-42.*

Manuscripts in preparation

The functional regulation of kisspeptin receptor by Ca^{2+}/calmodulin (in preparation)

Inhibitory effect of KISS1R phosphorylation by αCaMKII (in preparation)

Acknowledgements

Thank you to Dr Zhiliang Lu for giving me the opportunity to do a PhD. The closure of the HRSU at the beginning of my second year brought unique challenges and made me who I am today, an independent scientist. During those turbulent times Professor Dr Philippa Saunders and Professor Dr Richard Sharpe showed me kindness in allowing me to continue in the centre for reproductive health. Thank you to Mr Robin Sellar and Dr Kevin Morgan for helping me to iodinate the kisspeptin ligand. This research was funded by the Medical Research Council and the Wellcome Trust. The research was carried out in the Queen's Medical Research Institute, University of Edinburgh and St George's University of London. Thank you to my collaborator – Professor Dr Kevin O'Byrne of Kings College London. Thank you to Dr Katalin Török of St George's University of London, for the guidance she has shown me throughout my PhD.

The inspiration, motivation, and hunger to succeed come from my family. Thank so much for supporting me when times were hard. With your love and material support I kept on going until I realised my final goal, therefore, I dedicate this thesis to you.

Abstract

The kisspeptin receptor (KISS1R), functioning as a metastasis suppressor and gate-keeper of GnRH neurons, is a potent activator of intracellular Ca^{2+}. The surge in cytoplasmic Ca^{2+} mediates the exocytosis of GnRH from GnRH neurons. However, the regulatory processes which enable KISS1R to sense increasing intracellular Ca^{2+} and avoid Ca^{2+} excitotoxicity via a signalling off-switch mechanism remain unclear. This thesis provides evidence for the interaction between KISS1R and the Ca^{2+} regulated proteins of calmodulin (CaM), and αCa^{2+}/CaM-dependent-protein kinase II (α-CaMKII). Binding of CaM to KISS1R was shown with three independent approaches. Firstly, cell-free spectrofluorimeter assays showed that CaM selectively binds to intracellular loop (IL) 2 and IL3 of the KISS1R. Secondly, KISS1R co-immunoprecipitation experiments identified ligand/Ca^{2+}-dependent binding of KISS1R to HEK-293 endogenous CaM. Thirdly, confocal experiments showed CFP-CaM co-localises with YFP-KISS1R. The functional relevance of CaM binding was examined with alanine substitution of critical residues of the CaM binding motifs in IL2 and IL3 of KISS1R. This approach revealed that the receptor activity (relative maximum responsiveness) was increased in the mutated residues of the juxtamembrane regions of IL3 and the N-terminus of IL2 relative to wild-type KISS1R. The Ca^{2+}/CaM regulated αCaMKII was also found to interact with KISS1R by selectively phosphorylating T77 of IL1. Phosphomimetic mutations of T77 into E or D created a receptor that was unable to elicit inositol phosphate production upon ligand stimulation. Finally, *in vivo* studies using ovariectomised rats that were intracerebroventricularly administered with a cell-permeable αCaMKII inhibitor augmented the effects of kisspeptin ligand stimulation of plasma luteinizing hormone levels. Taken together, this thesis demonstrates that the KISS1R-G protein coupling is regulated by Ca^{2+}-dependent CaM binding and αCaMKII-mediated KISS1R phosphorylation.

List of Figures

List of Tables

Abbreviation

ACTH	Adrenocorticotrophic hormone
AC	Adenylate cyclase
Arc	Arcuate
AVP	Arginine vasopressin
AVPV	Anteroventral periventricular
Badan-CaM	6-bromoacetyl-2-dimethylaminonaphthalene labelled calmodulin
BSA	Bovine serum albumin
Ca^{2+}	Ionised calcium
CaM	Calmodulin
αCaMKII	Ca^{2+}/calmodulin dependent protein kinase II
DA-CaM	Calmodulin labelled with donor 5-((((2-iodoacetyl)amino)ethyl)amino)naphthalene-1-sulfonic acid (1,5-IAEDANS) and acceptor dimethylamino-3,5-dinitrophenyl (DDP).
DAG	Diacyl glycerol
DMEM	Dulbecco's Modified Eagle's Medium
ECL	Extracellular loop
ERK	Extracellular signal–regulated kinase
FCS	Foetal Calf Serum
FRET	Fluorescence Resonance Energy Transfer
FSH	Follicle-stimulating hormone
GnRH	Gonadotropin releasing hormone
GPCRs	G-protein coupled receptors
GPR54	Kisspeptin receptor
GRK2	G-protein coupled receptor kinase 2
HPLC	High-performance liquid chromatography
HPG	Hypothalamic–pituitary–gonadal axis

ICL	Intracellular loop
IHH	Isolated hypogonadotropic hypogonadism
IP_3	Inositol trisphosphates
Co-IP	Coimmunoprecipitation
LH	Luteinizing hormone
MAPK	Mitogen-activated protein kinase
ME	Median eminence
MMP	Matrix-metalloproteases
NPAF	Neuropeptide AF
NPFF	Neuropeptide FF
NPSF	Neuropeptide SF
NPVF	Neuropeptide VF
NPY	Neuropeptide Y
OVX	Ovariectomized
PBS	Phosphate buffered saline
PIP2	Phosphatidylinositol bisphosphate
POA	Preoptic area
RFRPs	RFamide related peptides
SAR	Structure activity relationships
SEM	Standard error of mean
TA-CaM	2-chloro-(epsilon-amino-Lys75)-[6-[4-(N,N-diethylamino)phenyl]- 1,3,5-triazin-4-yl]CaM
TM	Transmembrane

1. Introduction

1.1. Overview

The introduction is divided into four parts; in the first part I give an overview of GPCR structure and function that is most conserved. The second part is an introduction to the biochemistry and physiology of kisspeptin receptor and its cognate ligands. In the final two parts I introduce calmodulin and αCaMKII structure and function.

1.2. G protein coupled receptors

G protein coupled receptors (GPCRs) are 7-transmembrane cell-surface proteins that are partly exposed to the extracellular milieu and recognise a multitude of signals such as photons, ions, nucleotides, lipids and biogenic amines, to peptides and larger proteins (Schlyer and Horuk, 2006). This makes GPCRs indispensable cell surface proteins that transduce a vast array of intracellular signals, and have provided pharmacologists a reservoir of drug targets. In fact, 30 % of pharmacological drugs on the market target GPCRs (Jacoby et al., 2006, Schlyer and Horuk, 2006, Overington et al., 2006). This section will provide an overview of GPCR trafficking, their structural & functional properties, and interacting proteins.

1.2.1. Trafficking to the cell surface

The process of GPCR maturation requires nascent receptors to fold correctly, ready for export from the endoplasmic reticulum (ER) to their place of residence on the cell surface (Figure 1.1) (Duvernay et al., 2005, Radford and Dobson, 1999, Sanders and Nagy, 2000, Trombetta and Parodi, 2003). The ER quality control system (QCS) determines the fate of nascent GPCRs by controlling their trafficking and routing within the cell (Ellgaard and Helenius, 2001, Cahill et al., 2002). Therefore, ER QCS must utilise a variety of complex systems such as folding proteins, retention factors, enzymes, escort proteins, and chaperones in order to sort receptors depending on their maturation status. Molecular chaperones are accessory components of the ER QCs, and serve to target misfolded proteins (Hartl and Hayer-Hartl, 2002, Sitia and Braakman, 2003). The important regions in chaperone-protein

interactions include unpaired cysteines, immature glycans, or exposed motifs in the hydrophobic domains of misfolded proteins (Ellgaard and Helenius, 2001, Tan et al., 2004, Dong et al., 2007). To this end molecular chaperones aim to stabilise structurally unstable nascent polypeptides in order to rescue correct folding and prevent aggregation (Hartl and Hayer-Hartl, 2002). In the event that the nascent polypeptides fail to fold correctly then they are targeted to the proteasomes for destruction (Werner et al., 1996; Schubert et al., 2000).

Several GPCR-interacting chaperones have been identified; e.g. the mammalian RanBP2 is thought to bind to the red/green opsins and promote their proper folding and trafficking to the cell surface (Ferreira et al., 1996). The ODR4 assists olfactory receptors in their proper folding and ER exit (Dwyer et al., 1998). Calreticulin and calnexin bind several GPCRs including gonadotropin-releasing hormone receptor (GnRHR), luteinizing hormone receptor (LHR), follicle-stimulating hormone receptor (FSHR), vasopressin receptor (V2R), and thyrotropin receptor (TSHR) (Schrag et al., 2003, Helenius et al., 1997, Vassilakos et al., 1998, Rozell et al., 1998, Brothers et al., 2006, Morello et al., 2001). Calreticulin and calnexin bind oligosaccharides containing terminal glucose residues of proteins, which aid in degradation. During protein processing, glucose residues are removed from the core oligosaccharide, which is added during N-linked glycosylation. In the event of misfolded proteins, "overseer" enzymes will re-add glucose residues in the rough ER for the purpose of calreticulin/calnexin to bind and prevent proteins to proceed to the Golgi (Helenius et al., 1997, Schrag et al., 2003). One example of this is V2R R337X mutant, which results in the increased interaction between the mutant receptor calnexin and increase ER retention and inhibition of cell surface expression (Morello et al., 2001).

The receptor activity modifying proteins (RAMPs) are another class of molecular chaperones that aid GPCR trafficking. RAMPs are known to interact with receptors like the vasoactive intestinal polypeptide (VIP), the pituitary adenylate cyclase-activating peptide receptor (PACAP), the calcitonin receptor-like receptor (CALCRL), the glucagon receptor, the parathyroid hormone receptor (PTH1R and PTH2R) (Christopoulos et al., 2003).

The unfolded protein response (UPR) pathway is a cellular stress response that is activated when misfolded proteins accumulate in the lumen of the ER. Several proteins are involved in the UPR pathway such as the transmembrane kinase endoribonuclease IRE1, activating transcription factor 6, BiP/Grp78, and the pancreatic ER kinase (Yang et al., 1998). Misfolded proteins induce a cascade of interactions starting with BiP dissociating from its three proximal sensors and binds to the misfolded proteins in an attempt to refold them, BiP dissociation releases the sensors from a negative inhibition which then transduces the UPR-inducible genes and decreases protein expression (Forman et al., 2003). Normal functioning of the UPR pathway will reduce new protein translocation and increase protein refolding or degradation (Harding et al., 2002; Kaufman, 2002). However, overwhelming the UPR pathway may lead to apoptosis (Forman et al., 2003).

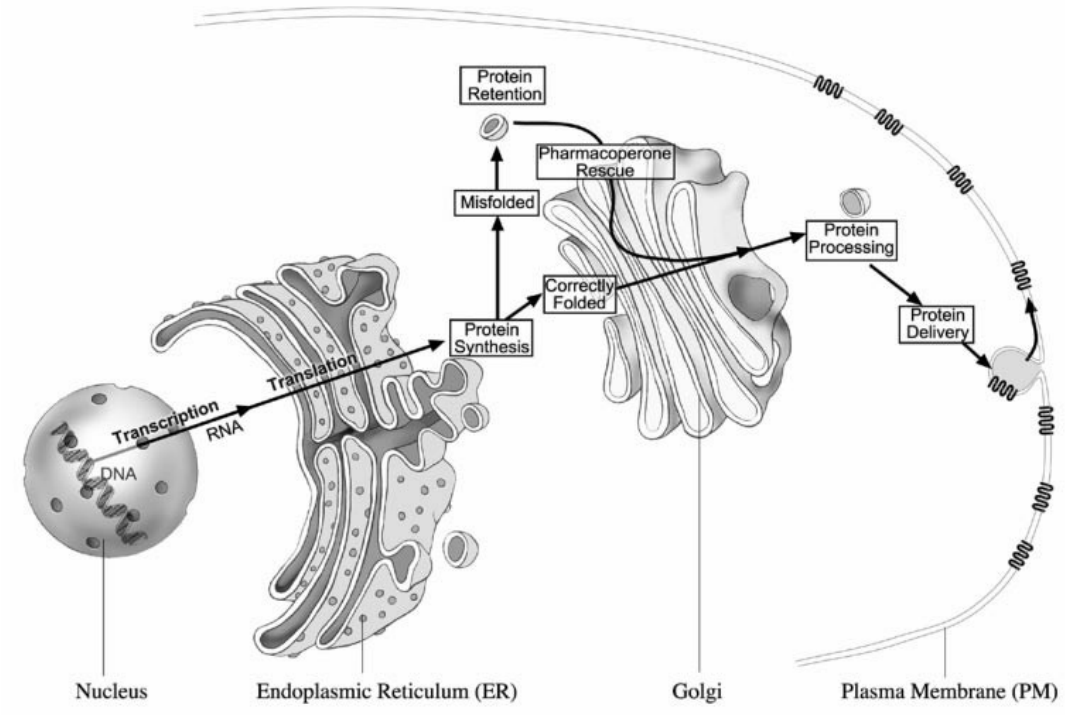

Figure 1.1 GPCR trafficking. GPCRs are transcribed in the nucleus, then translated and simultaneously incorporated into the lumen of the ER where they are correctly folded. In the event of misfolding GPCRs will be assisted or degraded in the ER. Subject to correct folding GPCRs are trafficked to the Golgi and then further transported to the plasma membrane [as reviewed in (Conn et al., 2007)]

1.2.2. Overview of GPCR structure and function

Signal transduction is the fundamental process that orchestrates cellular physiology. Membrane proteins are upstream signalling units, and one of the most diverse membrane protein families is GPCRs. These 7-transmembrane proteins respond to a variety signals from the extracellular milieu, ranging from hormones, neurotransmitters, lipids, and to photons and converting them into cellular responses via heterotrimeric G-proteins and other GPCR interacting proteins [as reviewed in (Katritch et al., 2012)]. Pharmacological drugs that alter GPCR activity are already used in the treatment of asthma, migraines, and cardiac malfunction. Therefore, determining the structure of GPCRs is critical for advancing our understanding of fundamental biology, but also for disease modulation. In the last 15 years the structure of 18 different Class A (rhodopsin-like) GPCRs have been solved (Figure 1.2). GPCRs are grouped into five major classes and numerous subclasses (Figurer 1.3). These structures validate the common 7-transmembrane (7-TM) architecture, as well as show a structural diversity among GPCR, which are fundamental to their specialised functions. The solved structures are composed of closely related GPCR subtypes (β_1AR and β_2AR) with sequence identity of 65 %, different subfamilies (D3R, β_2AR, and H_1R) with sequence similarity of ~35 %, and from different sub-branches of the same α-branch (β_2AR and A_{2A}AR) with ~30 % identity. Furthermore, there are solved structures from different branches i.e. α- and γ- branches of class A GPCRs (β_2AR and CXCR4) with 25% identity (Figure 1.3) [as reviewed in (Katritch et al., 2012).

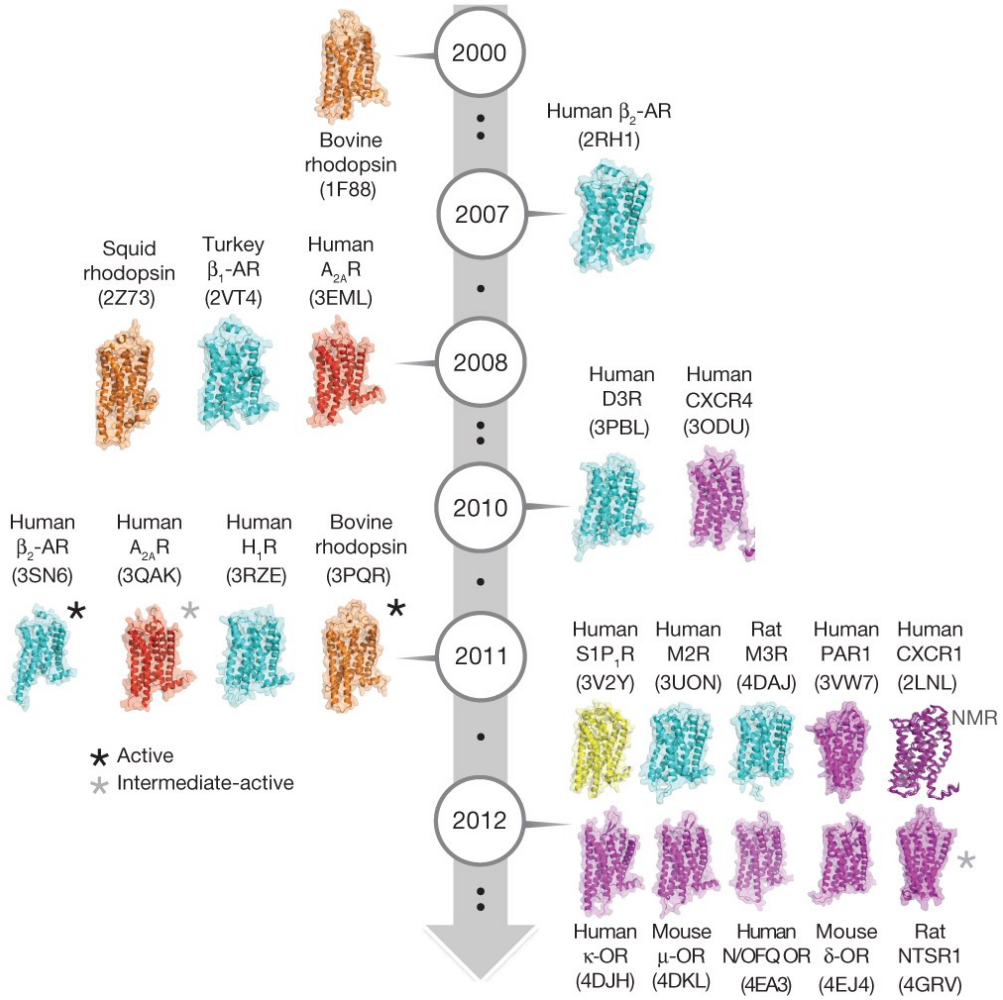

Figure 1.2 Time-line of solved GPCR structures. Time-line of GPCR structures by year of publication. A representative set of GPCRs are shown. The active GPCR structures are marked with black asterisks and the intermediate-active conformation is represented in grey asterisks. The Protein Data Bank accession numbers are presented below the structures. Obtained with permission from Nature Publishing Group (license number 3341491031788) [as reviewed in (Venkatakrishnan et al., 2013)]

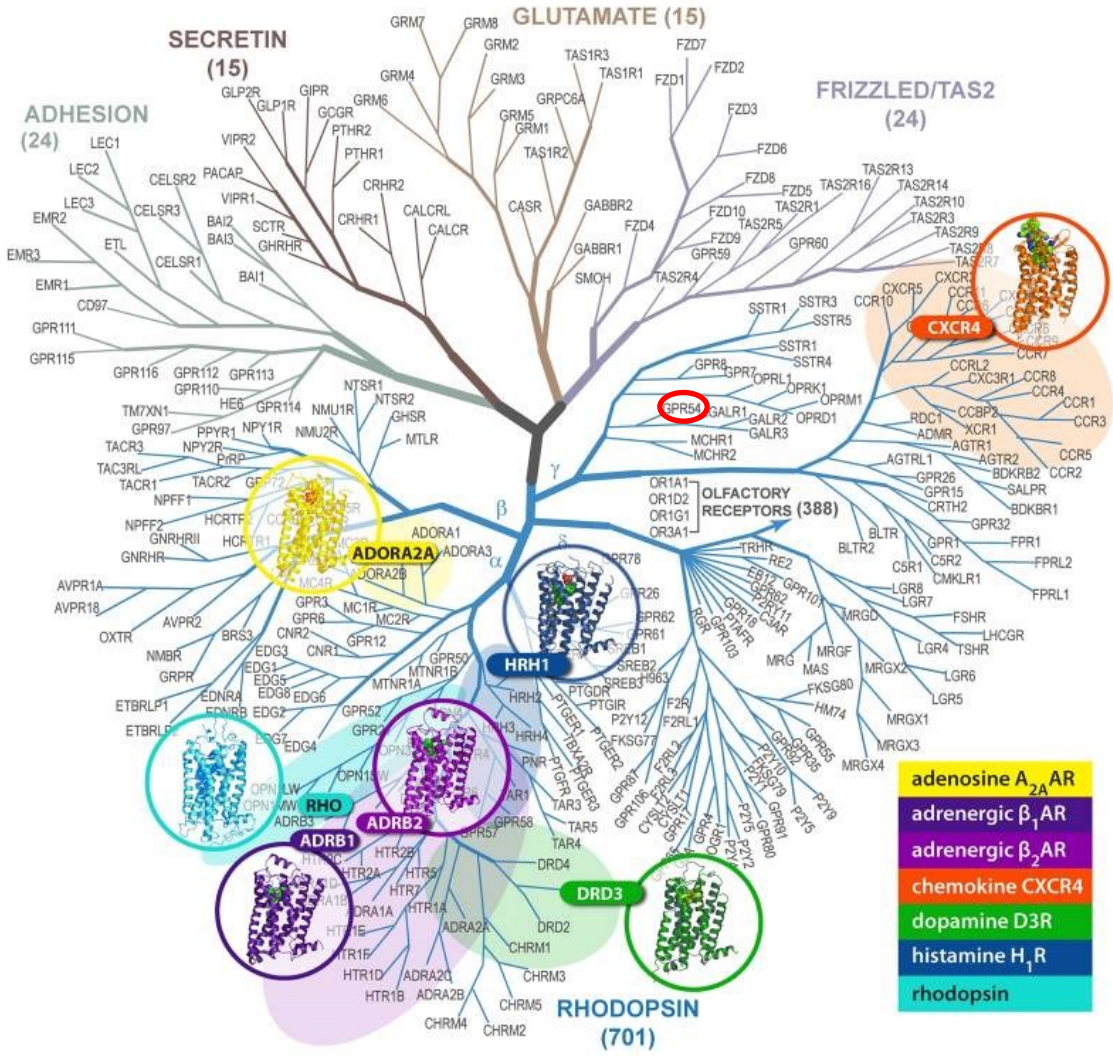

Figure 1.3 Sequence homology tree of human GPCRs. The solved GPCR structures are superimposed onto their respective locations on the tree dependent on the sequence similarly between the TM domains (>35 % homology). The highlighted areas represent close homology with the solved structures. GPR54, also known as the kisspeptin receptor (KISS1R), is emphasised (red circle) because of its importance in this thesis (see later sections). Obtained with permission from Elseveir B.V. (license number 3341500821570) [as reviewed in (Katritch et al., 2012)].

GPCRs are composed of seven transmembrane α-helical domains which are connected by three extracellular loops (ECL1–3) and three intracellular loops (ICL1–3) (Figure 1.4). The EC region in conjunction with the N-terminus is responsible for ligand recognition (Lagerstrom and Schioth, 2008). The IC region interacts with intracellular proteins such as G proteins, arrestins and other GPCR interacting proteins. Furthermore, the IC region of GPCRs is usually composed of helix VIII and a C-terminus palmitoylation site that functions to anchor the receptor to the plasma membrane (Maeda et al., 2010a, Tobin et al., 2008). The most conserved GPCR region is the 7TM helical bundle, which contain signature motifs such as the 'ionic lock' (composed of D[E]RY) in helix III, the NPxxY motif in helix VII, and the WxP motif in helix VI (Nygaard et al., 2009).

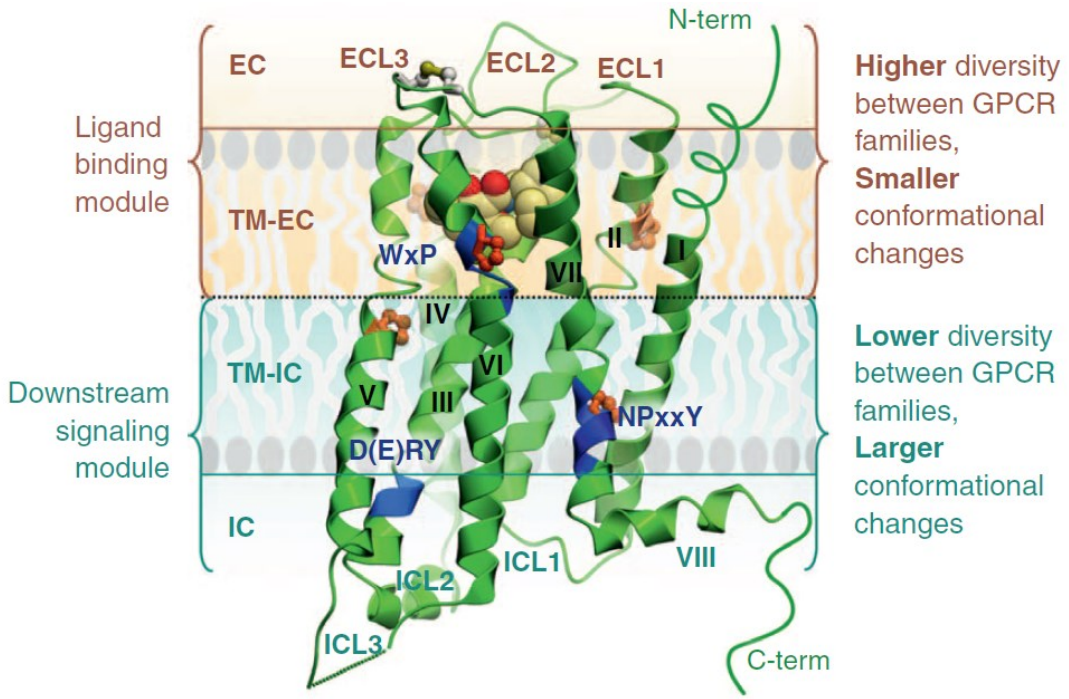

Figure 1.4 The modularity of GPCRs. The major regions and features of GPCRs are shown using as example the solved structure of Dopamine receptor (D3R) (PDB 3PBL). The extracellular region (EC) is formed of 3 extracellular loops (ECL) and an N-terminus. The 7-transmembrane helical bundle contain strategically positioned flexible proline residues that make 'kinks' and divide the receptor into two modules; the EC (extracellular) and IC (intracellular) modules. The EC module is also composed of TM-EC and is highly diverse in its structure and ligand binding properties. The IC module (also composed of TM-IC region) is more conserved, but undergoes greater structural change upon GPCR activation. The IC module is responsible for interfacing with downstream effectors such as G proteins and arrestins. The blue ribbon denotes highly conserved motifs that are also functionally important in class A GPCRs. Helix VIII in many GPCRs is responsible for anchoring the receptor to the membrane via a palmitoylation site. Obtained with permission from Elseveir B.V. (license number 3341500821570) [as reviewed in (Katritch et al., 2012)].

The 7-TM helical bundle serves to transduce ligand binding signals into G-protein regulation. GPCRs are sufficiently similar in their sequence to constitute a family and different enough to have divergent functions. A structure based-sequence alignment study of the different GPCR structures, which includes both active and inactive conformations, revealed a shared network of 24 inter-TM contacts that are mediated by 36 topologically equivalent residues as represented by the Ballesteros–Weinstein numbering scheme (Figure 1.5) [as reviewed in (Venkatakrishnan et al., 2013)]. Some of the topologically equivalent amino acids have been reported to be functionally important and include highly conserved residues (Madabushi et al., 2004): For instance, Asn 1.50, Asp 2.50, Trp 4.50 and Pro 7.50. Furthermore, they can tolerate amino acid substitutions. For instance, the non-covalent contact between 2.42 and 3.46 is observed in all structures, but the amino acids are different in different structures. For example, the bovine rhodopsin corresponding residues are Ile 75 contacting Leu 131 and for the human k-OR it is Tyr 97 contacting Met 152. Therefore, the consensus network may provide a rigid structural scaffold that maintains the GPCR fold irrespective of conformational change or evolution driven sequence change. The spatial location of the consensus network within the receptor is largely in the middle and cytoplasmic side of the TM bundle and predominately located between TM1-TM2, TM3-TM4, TM4-TM5, and TM3-TM6-TM7. An important region is TM3, which is thought to be a ‘structural hub’, because of its extensive interfacing with other TM regions (Figure 1.5) [as reviewed in (Venkatakrishnan et al., 2013)].

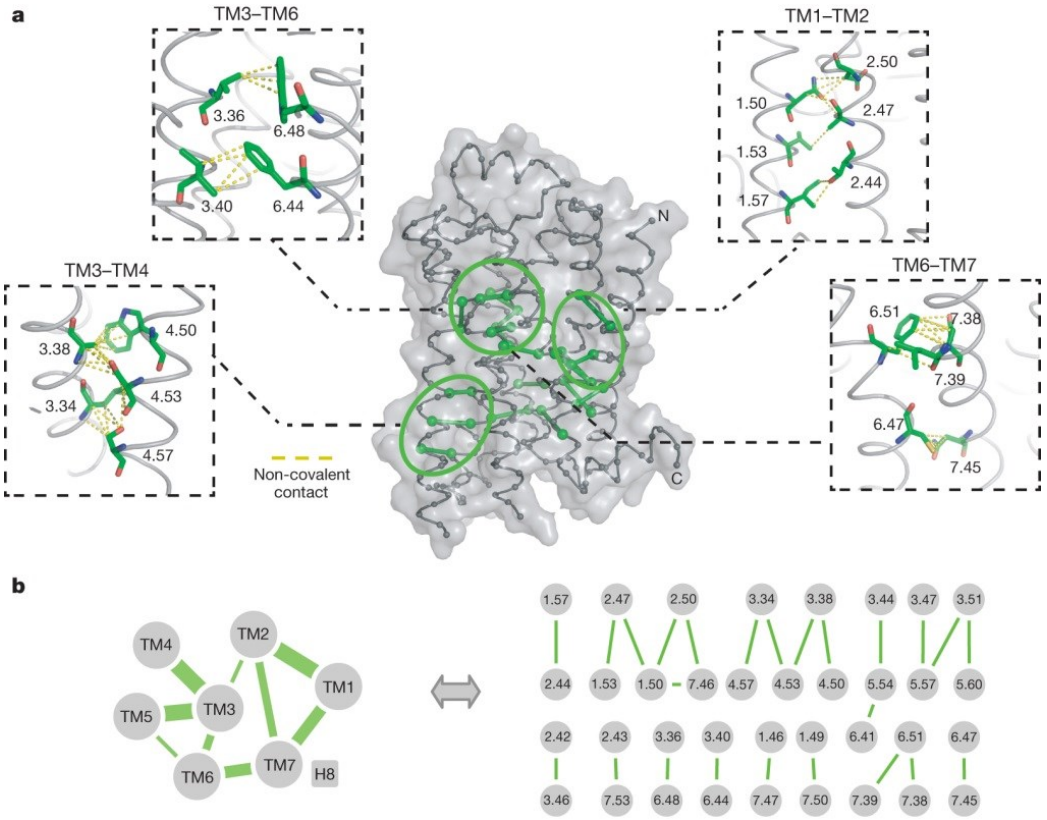

Figure 1.5 Conserved GPCR inter-helical non-covalent contacts. The structure based sequence alignments of 17 solved structures were used to determine the consensus network that is common among all GPCR structures irrespective of their conformational state. A network of 24 inter-TM contacts between 36 topological equivalent residues (represented as Ballesteros-Weinstein numbering scheme) is presented (**a**) with a representative structure of inactive β_1-AR. (**b**), Left, schematic representation of the conserved inter-helical contacts, the TM domains are presented as grey circles and the green line denotes the contacts with the thickness of the line being proportional to the number of contacts. (**b**), Right, Ballesteros-Weinstein numbering of the 36 topological equivalents with their respective contacts (the line here is uniform). Obtained with permission from Nature Publishing Group (license number 3341491031788) [as reviewed in (Venkatakrishnan et al., 2013)]

Upon receptor activation, G proteins interact with the cytoplasmic end of TM3 and intracellular loop 2 (Arg 3.50 of the DRY motif) (Rasmussen et al., 2011b). A case in point is rhodopsin; a salt bridge between Arg 3.50 and Glu 6.30 is broken upon receptor activation. This observation is commonly referred to as an 'ionic lock' and is thought to exist in the inactive state of some receptors (Lebon et al., 2012). A study of the active-state structures of rhodopsin (metarphodopsin II) bound a peptide mimicking the C-terminal tail of G_t and of β2-AR bound to the G protein (G_s) gives insights into the consensus structure that forms the interface between TM and G-proteins. The interface is formed of ~8 residues in TM3, TM5, and TM6 (Figure 1.6) [as reviewed in (Venkatakrishnan et al., 2013)]. Upon receptor activation, the TM-G protein interface is created with a considerable movement of TM5 and TM6 (Figure 1.6). An interesting and emerging observation is that G-protein coupling to receptor brings bidirectional regulation between the ligand-binding site and the G-protein binding site (Hino et al., 2012). Furthermore, G-protein coupling has been shown to induce a receptor conformation that is more sensitive to agonist (100- fold higher affinity) (Whorton et al., 2007).

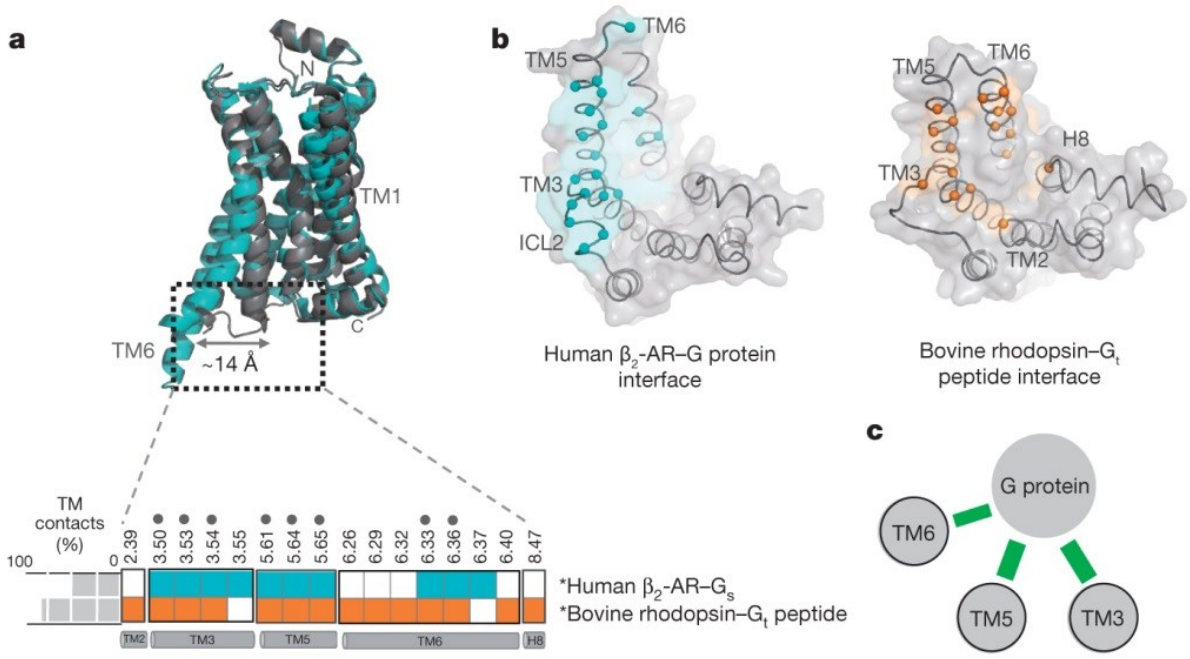

Figure 1.6 The receptor–G protein interface. (**a**), Comparison of β_2-AR TM movements between the active (cyan) and inactive (grey) conformations. The TMs that interface G_s protein and G_t peptides are presented in parentheses. The Ballesteros-Weinstein numbering is used to depict equivalent residues and the black dots represent residues that interact with the G_s and G_t peptides in both β2-AR (cyan) and rhodopsin (orange). (**b**), Intracellular view of β2-AR and rhodopsin with the highlighted residues that compose the interface between G-proteins. (**c**) A representation of the GPCR TM domains and G-protein (grey circles) interactions (green lines). The thickness of the green lines is proportional to the number of consensus contacts. Obtained with permission from Nature Publishing Group (license number 3341491031788) [as reviewed in (Venkatakrishnan et al., 2013)]

1.2.2.1. The ternary complex model

A molecule that binds to a GPCR and initiates a positive physiological response is referred to as an agonist. The power of an agonist to produce a response is referred to as efficacy. The concentration of agonist required to produce an effect of given intensity is termed as potency. Conversely, a molecule that binds to a receptor and induces a depression in basal physiological function is referred to as inverse-agonist. Furthermore, a molecule that binds a receptor but does not induce a physiological response is termed as an antagonist. One way to express this is the ternary complex (Figure 1.7). There exists equilibrium between agonist, GPCR and G-proteins, and the changing concentrations can make the equilibria shift. For example, an increase in agonist will shift the equilibria left of Figure1.7 creating an agonist-active receptor complex. An increase of receptors will increase the potency and efficacy of available agonists if not otherwise saturating (Kenakin, 2002b).

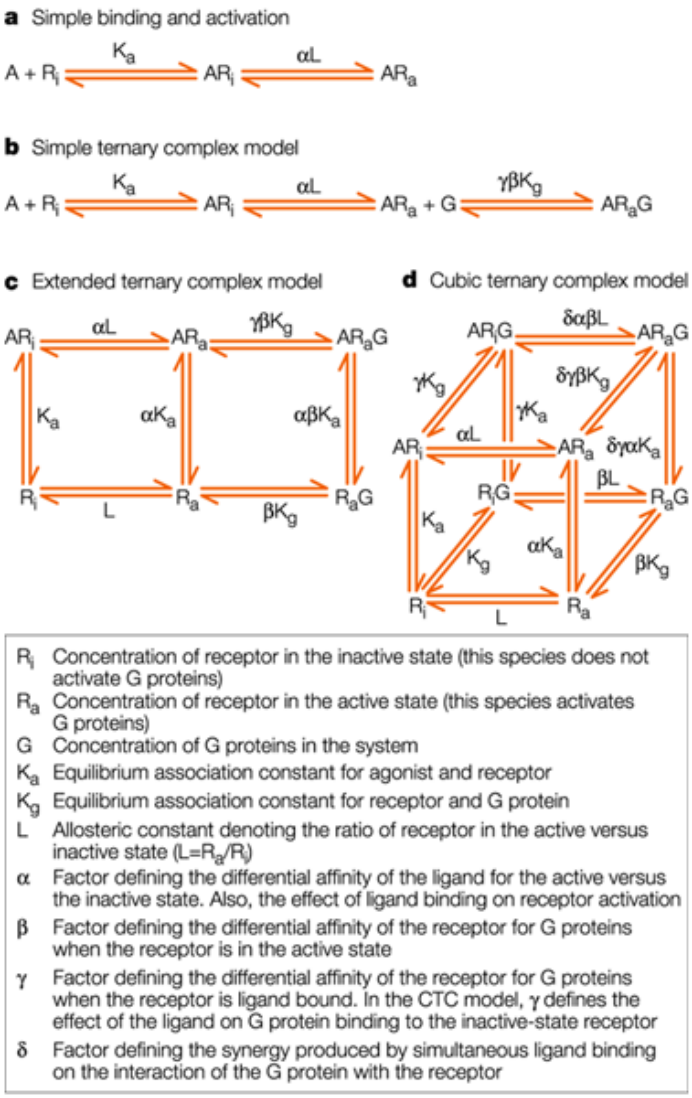

Figure 1.7 Commonly used models for GPCR equilibria. (a) In the classical receptor activation model, agonist (A) binding to an inactive receptor (R_i) forms a complex (AR_i) which in turns creates an active agonist-receptor complex (AR_a). In the case of antagonists, the ligand binds the receptor but does not create an active complex, and an inverse agonist reverses the equilibria from the active complex to an inactive complex. (**b**) A deeper understanding GPCR pharmacology incorporates G-proteins in a ternary AR_aG complex model. (**c**) The expanded ternary complex model captures the spontaneous formation of the active-state receptor (R_a) independent of agonist binding. The activation of the receptor from R_i to R_a modifies the affinity of the receptor for G-proteins (α, β and γ) and determines the efficacy. (**d**) The cubic ternary complex model allows for the formation of Ri complexed with G protein and the affinity is modified by the factors δ, β and γ. Obtained with permission from Nature Publishing Group (license number 3460351409397) [as reviewed in (Kenakin, 2002b)

1.2.3. Desensitization and endocytosis

Cell signalling is fine-tuned to convey cellular physiology and therefore the receptors that initiate signalling must be turned off by a mechanism known as desensitization. Receptor desensitization is the process whereby overstimulation leads to reduced receptor response to the extracellular milieu. The level of desensitization is dependent on the amount and duration of the overstimulation, as well as the intracellular interacting proteins [as reviewed in (Ferguson, 2001, Kelly et al., 2008). The classical model of GPCR desensitization starts with inhibitory phosphorylation of the receptor intracellular loops and/or tail, which leads to G protein uncoupling (Figure1.7). The inhibitory phosphorylation is carried out by protein kinases such as cAMP-dependent protein kinase (PKA), G protein-coupled receptor kinases (GRKs), and protein kinase C (PKC) (Benovic et al., 1986, Benovic et al., 1985). Receptor desensitization by internalisation is initiated when β-arrestins associate with the phosphorylated receptors, recruiting β2-adaptin and clathrin, and therefore promoting endocytosis by clathrin-coated pits (Figure 1.8)(Ferguson et al., 1996, Lohse et al., 1992, Zhang et al., 1996). The internalised receptors can be dephosphorylated by phosphatases and recycled back to the plasma membrane. However, sustained receptor down-regulation involves proteolytic degradation by proteasomes and reduced protein expression (Ferguson, 2001, Ritter and Hall, 2009, Kelly et al., 2008).

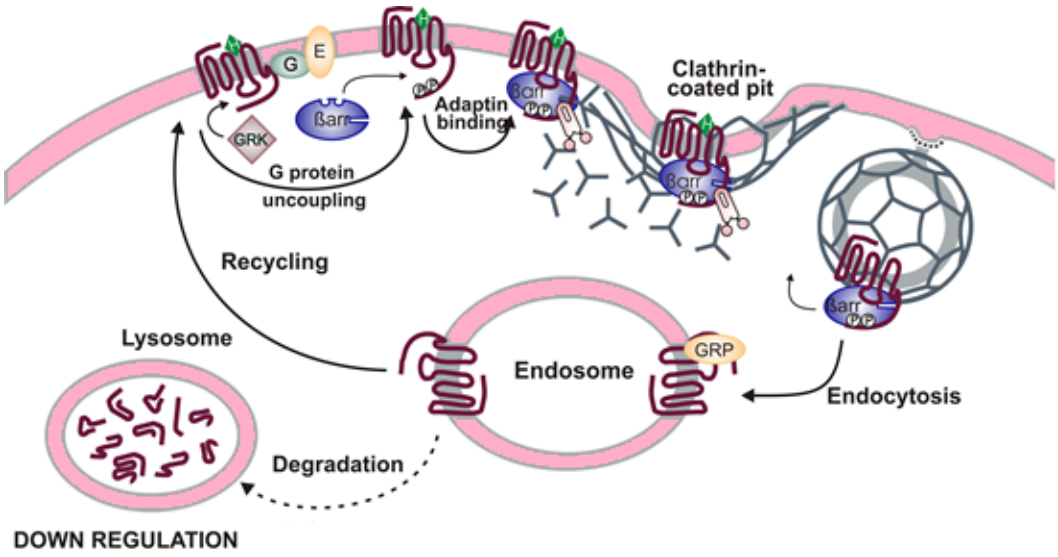

Figure 1.8 Cartoon illustration of GPCR desensitization by endocytosis. The process of GPCR desensitization begins with the inhibitory phosphorylation (**P**) of hormone (**H**) stimulate GPCRs by protein kinases such as G-protein-coupled receptor kinase (**GRK**). Thereafter, β-arrestins (**βarr**) bind and inhibit G-protein (**G**) coupling. βarr also recruit β2-adaptin and clathrin, promoting endocytosis by clathrin coated pits. Recycling of GPCRs are then dephosphorylated by G protein-coupled receptor phosphatase (**GRP**) and reintegrated back into the plasma membrane.[adapted from (Dhami and Ferguson, 2006)].

1.2.4. The Receptosome: GPCR interacting proteins (GIPs)

The classical understanding of G protein-coupled receptor (GPCR) signaling is that an agonist binds to the extracellular region of the receptor which promotes a conformational change that favours the interaction of heterotrimeric G proteins. GPCRs are commonly referred to as 'guanine nucleotide exchange factors', because GPCRs catalyses the exchange of GDP for GTP on the Gα subunit. This nucleotide exchange induces the dissociation of Gα and Gβγ subunits (Figure 1.9). There are four main subtypes of Gα, including Gαs, Gαi, Gα12/13 and Gαq. Upon activation the Gα•GTP complex regulates the activity of effectors such as adenylyl cyclase, RhoGEF and phospholipase Cβ (PLCβ). These molecules generate second messengers such as cyclic AMP, DAG and IP_3 that further modulate downstream effectors, such as protein kinase A (PKA) and protein kinase C (PKC). The βγ subunits also have their unique cellular function of regulating ion channel conductivity (Ritter and Hall, 2009).

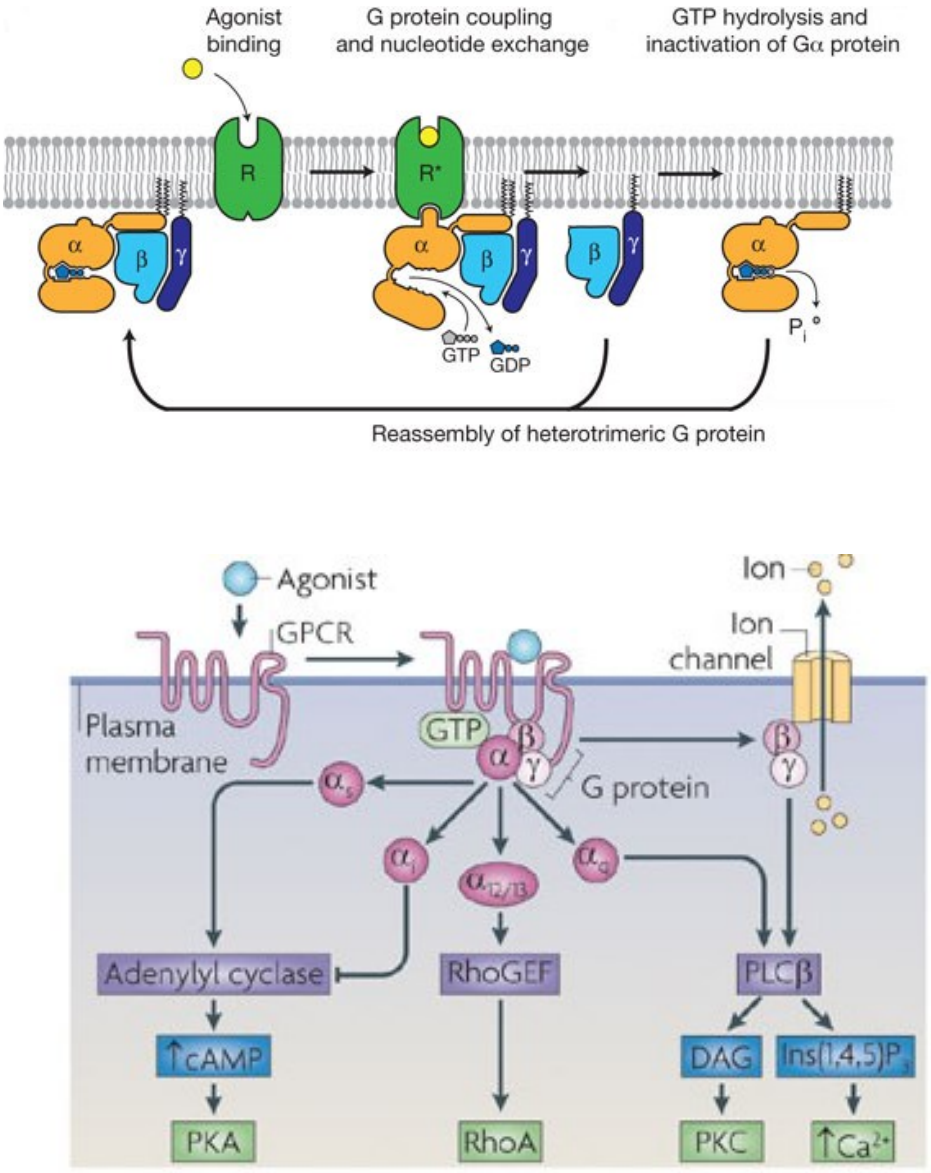

Figure 1.9 The classical GPCR signalling pathway. Agonist binding to the receptor EC region induces conformational changes to the IC region and promotes heterotrimeric G-proteins (α, β, and γ) to bind to the receptor. Upon formation of the receptor G-protein complex, the α subunit exchanges guanosine diphosphate (GDP) for guanosine triphosphate (GTP), resulting in the dissociation of the α and βγ subunits from the receptor. The activated subunits regulate their respective downstream effector proteins. The heterotrimeric G-proteins reassemble after the hydrolysis of GTP to GDP. Adapted and obtained with permission from Nature Publishing Group. Top panel obtained from [as reviewed in (Rasmussen et al., 2011b)(license number 3342240463377)]. Bottom panel adapted from [as reviewed in (Ritter and Hall, 2009)(license 3343410290024)].

The process of evolutionary adaptation of proteins to new environmental cues has generated more than 1000 GPCRs that are dedicated to cell-cell communication and the recognition of light, taste, and smell (Mansuy et al., 2011, Zhao and Kriegsfeld, 2009, Quaynor et al., 2007). Before the turn of the century, the up-stream GPCR signal transduction pathways were believed to be simple. It was thought of in the following terms. Specific ligands activate GPCRs, which in turn cause the rearrangement of the transmembrane regions and intracellular domains. This conformational change enables a limited number of heterotrimeric G proteins to undergo structural changes. An exchange between GDP-GTP takes place within the G protein, leading to the separation of Gα-GTP and Gβγ subunits. Subsequently, both subunits bind and regulate various molecular effectors (Jacobi et al., 2007). However, GPCRs are now understood to interact with an increasing repertoire of GPCR interacting proteins (GIPs).

GIPs took centre stage with the discovery of 'receptosomes' composed of inactivation-no-afterpotential D (INAD) (Tobet and Schwarting, 2006, Barrow and Trowsdale, 2006), Ste5 (Kirby et al., 2010, Aydin et al., 2010), and arrestins (Makri et al., 2008). Subsequently, an increasing number of GIPs have been discovered [as reviewed in (Duvernay et al., 2005, Salvi et al., 2006)]. GIPs interact with different intracellular regions of GPCRs and are responsible for targeting GPCRs to particular regions of the cell. In addition, GIPs are responsible for 'fine tuning' GPCR activity. Although complex there are lessons to be learnt in order to appreciate common interacting proteins.

The concept of 'receptosomes', which describes the GPCR signaling complexes, was first described with the study of the phototransduction cascade in *Drosophila*. The GPCR that was implicated in this cascade was rhodopsin, eliciting the classical pathway that results in the regulation of ion channels and thus enabling a photon of light to excite a photoreceptor cell. The rhodopsin signaling complex, composed of direct and indirect protein associations is responsible for the efficacy of the cascade. The signaling complex is composed of the scaffolding protein INAD and Gαq, PLCβ, store-operated Ca^{2+} entry channels [TRP], nonspecific cationic conductance channels [TRPL], εPKC and Ca^{2+}/calmodulin. INAD acts as a

scaffolding protein because it contains 5 PDZ domains (Clarkson et al., 2008). PDZ domains are the most common protein interaction, responsible for signaling units (Clarkson et al., 2008).

Another example is the GPCR - α-factor pheromone receptor in the budding yeast *Saccharomyces cerevisiae*. In this example, the receptor upon activation enables the release of the Gβγ subunit, which then interacts with the scaffolding protein Ste5, causing it to translocate to the membrane. Afterwards, Ste5 via Ste20 recruits MAPKKK (Ste11), the MAPKK (Ste7), and the MAPK (Fus3) (Kirby et al., 2010). The two examples given above are interactions that are, on the whole, not physically associated with GPCRs.

The visual arrestin was one of the first proteins shown to physically bind to GRK phosphorylated rhodopsin (Ang et al., 2000). Arrestin proteins and G-protein coupled receptor kinases (GRKs) have historically been the most common GIPs and are now understood to be critical in the GPCR desensitisation, internalization, trafficking, and signalling. The GRK family is composed of seven member genes. The expression of GRK1 and 7 is found in the retinal rods and cones, respectively. GRK4 expression is limited to the cerebellum, kidney and testis. The expression of GRK3, 5 and 6 are expressed widely in mammalian tissues. Arrestins consist of four-members in the family. The expression of arrestin 1 and 4 are found in retinal rods and cones, respectively Arrestin 2 and 3 (they are also known as β-arrestin 1 and β-arrestin 2) are ubiquitously expressed [as reviewed in (Reiter and Lefkowitz, 2006)].

Increasing evidence is now emerging that the function of GRKs and arrestins are not only restricted to desensitisation and internalization, but extend to inducing downstream signaling via interacting proteins (Figure 10). GRKs and arrestin have the ability to scaffold signaling proteins and translocate them to receptors. Initial experiments that determined β-arrestin dependent signaling revealed the recruitment of the proto-oncogene Src (c-Src) to the receptor and thereafter resulting in the activation of the extra-cellular signal-regulated kinase (ERK1 or 2). The c-Src family proteins of Hck, Yes and Fgr, which are non-receptor tyrosine kinases are also recruited to the receptor via β-arrestins. β-Arrestins are able to scaffold JNK, ERK1 and 2, MAPK, MAPKKK and MAPKK with the receptor. Furthermore, GRK 5 and

6 is required for β-arrestin dependent ERK activation by V2R, β_2AR and $AT_{1A}R$ receptors, GRK2 and 3 appear to attenuate the β-arrestin dependent ERK activation. This would suggest that the GRKs are competing are competing with each other in order to provide a balance between signaling and desensitization and to coordinate the different pathways dependent on extracellular stimuli. Because GRK2 and 3 require G-protein activation and GRK5 and 6 actually reside at the plasma membrane their unique locations will further facilitate divergent signaling by receptors [as reviewed in (Reiter and Lefkowitz, 2006)].

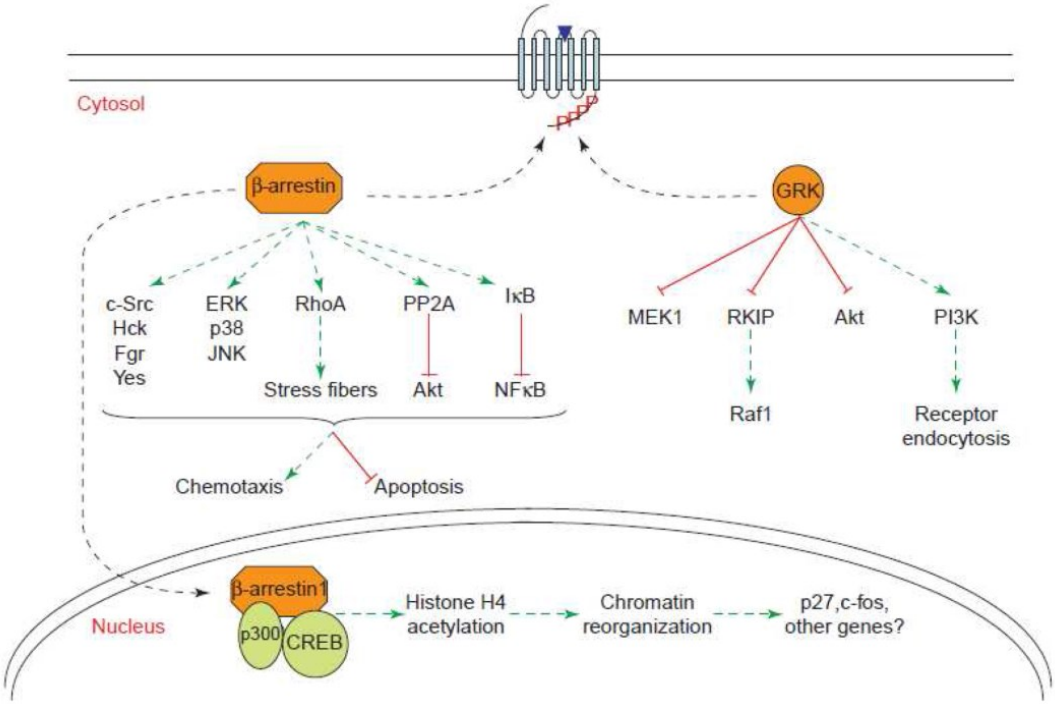

Figure 1.10 The downstream signaling cascade of GRK and arrestin signaling. Ligand binding to the GPCR promotes the recruitment and activation of GRKs and arrestins. They either activate (green line) or inhibit (red line) downstream pathways. β-arrestin 1 can translocate into the nucleus and regulate gene expression. Obtained with permission (license number - 3463340582990) from Elservier (Reiter and Lefkowitz, 2006),

Upon direct GPCR binding, arrestins 2 and 3 stoichiometerically bind clathrin of the clathrin-based endocytic vesicles [as reviewed in (Duvernay et al., 2005, Salvi et al., 2006)]. GPCR endocytosis and trafficking is initiated by arrestins recuiting intracellular trafficking proteins, such as the *N*-ethylmaleimide-sensitive factor (NSF), the endocytic protein AP2, phosphoinositides, and the ADP-ribosylation factor ARF6, along with its exchange factor ARNO. ARF6 recuits COP1 coatomers to regulate vesicle budding. Some GPCRs undergo internalisation through a non-arrestin dependent manner (Tung and Lee, 2012, Cavallaro and Christofori, 2004).

Furthermore, Arrestin 3 is ubiquitinylated upon binding to E3 ubiquitin ligase Mdm2 (Evans et al., 2008). This is necessary for β_2-adrenergic receptor (β_2-AR) internalization, as well as for β_2-AR ubiquitinylation and degradation (Evans et al., 2008, Cavallaro and Christofori, 2004, Tung and Lee, 2012). Arrestin 3 is also important for agonist-dependent internalization and degradation of the yeast pheromone receptor Ste2p and Ste3p and the vasopressin V2 receptor (Dalkyz et al., 2000, Yaphe et al., 2000).

GPCRs can interact with multiple proteins that enhance the efficiency and diversity of G-protein-mediated signaling. One prominent example includes the Homer proteins, which can interact with mGluR1, mGluR5 and the $InsP_3$ receptors, thereby linking these receptors to increase the efficiency of mGluR-stimulated Ca^{2+} signaling (Brakeman et al., 1997, Xiao et al., 1998, Tu et al., 1998). Other enhancers of GPCR signaling are members of the A-Kinase anchoring protein (AKAP) family, which interact with β-adrenergic receptors (β_2AR) to tether protein kinase A (PKA) in the vicinity of the receptor and increase the efficiency of PKA-mediated phosphorylation of various substrates, including the receptor itself. The increased interaction with β_2AR enhances receptor resensitization resulting in a more robust β_2AR-mediated ERK signaling (Shih et al., 1999, Fraser et al., 2000, Tao et al., 2003, Gardner et al., 2006).

The most extensively studied example of GIPs that can regulate receptor pharmacology are the receptor activity modifying proteins; RAMP 1, RAMP2 and RAMP3. The discovery of RAMP proteins is a classic example of research through serendipity. They were identified in experiments that attempted to search for the

receptor that was activated by calcitonin gene-related peptide (CGRP). In order to express functional CGRP receptor it required the co-expression of calcitonin receptor-like receptor (CAlCRl; also known as CRlR), with RAMP1. Furthermore, when RAMP2 and CAlCRl were co-expressed it resulted in formation of receptors activated not by CGRP, but a related peptide termed as adrenomedullin. Additionally, CAlCRl and RAMP3 can interact to form adrenomedullin receptor subtypes. Surprisingly, the co-expression of RAMP and a distinct receptor known as the calcitonin receptor (CAlCR) creates the formation of receptors with unique pharmacological properties. Moreover, the preferential activation of some RAMP–CAlCR combinations are brought about by a distinct peptide known as amylin. It is now evident that the pharmacological properties of CAlCR and CAlCRl are dependent by cell type, depending on RAMP expression. Furthermore, RAMPs can affect CAlCR and CAlCR surface expression levels [as reviewed in (Ritter and Hall, 2009)]

Table 1.1 GIPs that regulate G-protein mediated signalling. Adapted from Nature Publishing Group with permission [as reviewed in (Ritter and Hall, 2009), (license 3343410290024)].

Interactor	Associated GPCR	Site of interaction	Impact on GPCR
AKAP79 (AKAP5) and AKAP250 (AKAP12, gravin)	β_2AR and β_1AR	CT	Thethers PKA near to the receptor
Calmodulin	5-HT_{1A}	IL3	Competes with PKC for GPCR phosphorylation
	5-HT_{2A}	IL2 and CT	Impairs G protein coupling
	5-HT_{2c}	CT	Promotes arrestin-dependent ERK activation
	D2R	IL3	Modulates G protein signalling
	mGluR7	CT	Regulates GPCR phosphorylation
	PTH1R	CT	Inhibits GPCR activity
	V2R	CT	Enhances GPCR-induced Ca^{2+} signalling
	μOPR	IL3	Inhibits G protein coupling
Homer	mGluR1 and mGluR5	CT	Regulates GPCR signalling and localisation
INAD	Rhodopsin	CT	Enhances speed and efficiency of GPCR signalling
JAK2	AGTR1 and PTAFR	CT	Promotes Jak-STAT signalling
LARG (ARHGEF12)	LPAR2	CT	Facilitates GPCR-mediated activation of Rho
MAGI3	Frizzled 4 and LPAR2	CT	Enhances GPCR-mediated activation of the MAPK ERK
MUPP1 (MPDZ)	$GABA_B$ and MT_1	CT	Enhances GPCR-mediated Gαi signalling
Neurochondrin	MCHR1	CT	Disrupts G protein-mediated signalling
NHERF1 (EBP50, SLC9A3R1)	PTH1R	CT	Enhances Gαq-mediated receptor signalling
	β_2AR and $_\kappa$OPR	CT	Mediates activation of Na^+-H^+ exchange
NHERF2 (SLC9A3R2)	LPAR2	CT	Enhances Gαq-mediated receptor signalling
	mGluR5 and P2RY1	CT	Prolongs GPCR-mediated Ca^{2+} signalling
	PTH1R	CT	Enhances Gαq-mediated receptor

			signalling
P85	SSTR2	IL2 AND CT	Mediates Survival signalling by receptor
PDZ-RhoGEF (ARHGEF11)	LPAR2	CT	Facilitates GPCR-mediated activation of Rho
Periplakin	MCHR1 and μOPR	CT	Impairs G protein-mediated signalling
Spinophilin	D2R	IL3	Reduces G protein and arrestin-mediated signalling
	α_2AR and mAChR	IL3	Reduces GPCR-mediated Ca^{2+} signalling

1.3. The kisspeptin system

1.3.1. RFamides and their cognate receptors

RFamides are neuropeptides that share at their C-terminus an arginine-phenylalanine-amide (RF-NH2) motif. Mammalian genomes contain five RFamide genes that are expressed to create precursor polyproteins that are later proteolytically cleaved to make physiologically active ligands (Figure 1.11). Although the grouping of these ligands is based on their C-terminus homology, the N-terminus is where the greatest diversity exists and confers onto the peptides their unique binding and signalling characteristics. One sure way of differentiating between these ligands is through a method of structure-activity relationship (SAR), in where the 3D structure and amino acid sequence of the peptides is related to its biological activity. SAR enables researchers to group RFamides in order to determine the chemical groups that evoke a target biological response in an organism of interest. This becomes of particular interest when concerned with the rational design of antagonist (Bass et al., 2013).

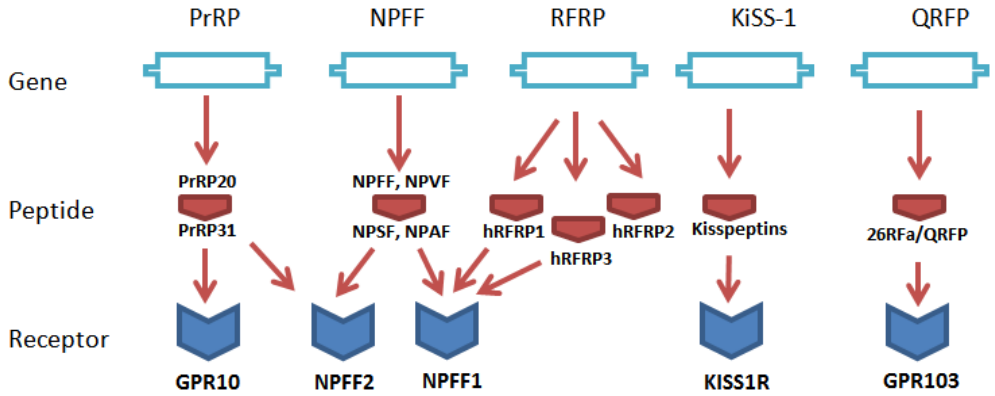

Ligand	hNPFF2
	K_i (nM)
NPFF	5.2 ± 2.4
(1DMe)Y8Fa	5.3 ± 1.0
NPFF-OH	4200 ± 800
rNPSF	37 ± 12
hNPY	4000 ± 1200
hNPY18-36	1200 ± 200
hPrRP20	23 ± 5
hPrRP31	19 ± 4
hRFRP-1	15 ± 2
hRFRP-3	55 ± 4
hPrRP24–31	32 ± 5

Figure 1.11 The RFamide family of peptides and their cognate receptors. *Top*, The genes that encode PrRP (prolactin releasing peptide), NPFF (Neuropeptide FF), RFRP (RFamide related peptide), KiSS-1 (kisspeptin), and QRFP (pyroglutamylated RFamide peptide) bind their respective G-protein coupled receptors (GPCRs). Cross-talk between PrRP, NPFF, and RFRP peptides and their targets is indicated by arrows [adapted from (Jhamandas and Goncharuk, 2013)]. *Below*, a table of relative binding affinities of RFamids to human NPFF2, adapted from (Engström et al., 2003)

The physiological roles RFamides is the subject of intense research, but currently we know that RFamides are master regulators of endocrine function, and are associated with the regulation of important pituitary hormones. These hormones include luteinising hormone (LH), follicle stimulating hormone (FSH), prolactin, growth hormone, adrenocorticotrophic hormone (ACTH), arginine vasopressin (AVP), and oxytocin. The downstream endocrine effects of RFamides are the regulation of mammalian growth, reproduction, maternal physiology, stress responses, blood pressure, and diuresis (Bechtold and Luckman, 2007, Osugi et al., 2006).

Some RFamides show an affinity for more than one GPCR, for example NPFF is known to bind NPFF1 and NPFF2 (Engström et al., 2003) (Figure 1.11). Additionally, both these receptors are also known to exhibit affinity for neuropeptide Y (an RYamide), as well as orexin and cholecystokinin peptides. This promiscuity may function to complement RFamide function in a yet unknown cross-talk mechanism (Engström et al., 2003, Bonini et al., 2000).

Table 1.2 Amino acid sequence comparison between human RFamide peptides. [adapted from (Findeisen et al., 2011)].

Peptide	Amino Acid Sequence	Reference
KP54	GTSLSPPPESSGSRQQPGLSAPHSRQI-PAPQGAVLVQREKDLPNYNWNSFGL RF-NH2	(Kotani et al., 2001, Ohtaki et al., 2001)
KP14	DLPNYNWNSFGLRF-NH2	
KP13	LPNYNWNSFGLRF-NH2	
KP10	YNWNSFGLRF-NH2	
NPFF	SQAFLFQPQRF-NH2	(Tsutsui et al., 2000)
NPAF	AGEGLNSQFWSLAAPQRF-NH2	
RFRP1 (NPSF)	MPHSFANLPLRF-NH2	(Ubuka et al., 2009, Hinuma et al., 2000)
RFRP3 (NPVF)	VPNLPQRF-NH2	
26RFa	TSGPLGNLAEELNGYSRKKGGFSFRF-NH2	(Bruzzone et al., 2006, Chartrel et al., 2003)
PrRP31	SRTHR-HSMEIRTPDINPAWYASRGIRPVGRF-NH2	(Hinuma et al., 2000, Langmead et al., 2000)
PrRP20	TPDINPAWYASRGIRPVGRF-NH2	

The first RFamide to be discovered was neuropeptide FF (NPFF-FLFQPQRFa). The amino acid sequence of NPFF is conserved amongst mammalian species. NPFF expression is highest in the hypothalamus and to a lesser extent in the peripheral tissue (Hinuma et al., 2000). The precursor mRNA also encodes for NPSF (SLAAPQRFa), and NPVF (VPNLPQRFa) peptides (Bonini et al., 2000, Liu et al., 2001). NPFF is known to control the neuronal processing of noxious stimuli by opioids (Chen et al., 2006, Mouledous et al., 2010). As well as playing a significant role in the autonomic nervous system's control of cardiovascular response, neuroendocrine regulation, and feeding (Panula, 2009, Jhamandas and Goncharuk, 2013). RFRPs have been shown to act on the pituitary and hypothalamus to facilitate prolactin release, inhibit GnRH release, and increase food intake (Johnson et al., 2007, Clarke et al., 2008, Hinuma et al., 2000). RFRP1 acts in the hypothalamus to inhibit dopaminergic neuronal activity (Samson et al., 2003). RFRP3 has emerged as important regulator of reproductive function (Murakami et al., 2008).

1.3.2. Kisspeptins and KISS1R

The kisspeptin ligands (KPs) are products of the *KiSS1* gene. The initial discovery of the *KiSS1* gene occurred in Hershey, Pennsylvania, USA, where it gained its name after the famous Hershey's chocolates kisses (Lee et al., 1996a). The *KiSS1* gene encodes for a 145 amino acid (aa) propeptide that is cleaved to form C-terminally amidated 54 aa peptide (KP54). Further cleavage creates peptide fragments called KP14, KP13, and KP10 (denoting the number of amino acids) (Figure 1.12). KPs are cognate ligands for the once orphaned GPCR called GPR54 (also known as, KISS1R, AXOR12; HH8; HOT7T175; and KISS-1R). However, for this purpose of this thesis it will be referred to as KISS1R. All of the KP ligands have similar binding and signalling properties on KISS1R. Although the biochemical properties of the KP ligands are similar, the *in vivo* bioactivity of KP10 is greater than the other ligands. The termination of biological activity of KP ligands is brought about by the matrix-metalloproteases 2 and 9 (MMP-2/9)[as reviewed in (Oakley et al., 2009)].

The *KiSS1* mRNA expression profile by in situ hybridisation determined that levels are high in the pancreas, placenta, testis, small intestine, liver, and the

hypothalamus (Lee et al., 1996a, Ohtaki et al., 2001, Muir et al., 2001). Furthermore, *KiSS1* mRNA expressing neurons have been identified in the hypothalamus (Kelly et al., 2013). Additionally, the expression profile of the KISS1R protein is high in the placenta, hypothalamus, and pituitary. The role of KISS1R expression became self-evident in 2003 when clinical mutations of the KISS1R encoding gene showed individuals with hypogonadotropic hypogonadism (HH) (Seminara et al., 2003, de Roux et al., 2003). KP ligands and KISS1R function is now known to be critically important in the regulation of the reproductive axis [as reviewed in (Pineda et al., 2010)].

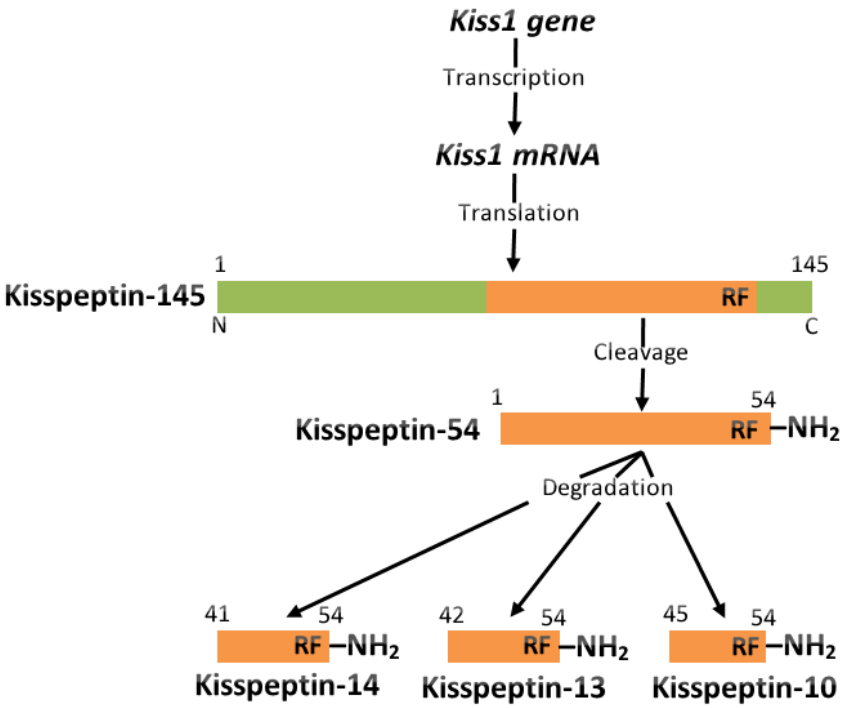

Figure 1.12 The cleavage products of Kisspeptin-145. The *KiSS1* gene upon transcription and translation produces kispeptin 145 prepropeptide that is cleaved to make the kisspeptin 54 and then further cleaved to create the kisspeptin 14, 13, and 10 peptides. Note the RF (denoting Arginine and Phenylalanine) at the C-terminus [adapted from (Oakley et al., 2009)].

The KISS1R shares 45 % sequence homology with the galanin receptor (GAL1), this is a high sequence homology between two GPCRs. This would suggest that KISS1R and GAL1 share a common ancestor, however, the KP ligands do not bind nor activate GAL1 and vice versa (Lee et al., 1999). The KISS1R amino acid sequence is conserved amongst mammals, for example the sequence similarity between rat KISS1R and human KISS1R is 85%, and the transmembrane domains comprise 98% identity. Furthermore, the sequence similarity between mouse and human KISS1R is 82%. Thus, the KISS1R has structurally and functionally diversified from its closely related GPCR, but remains conserved among primate and rodent species (Kotani et al., 2001, Ohtaki et al., 2001, Muir et al., 2001).

The principle signal transduction mechanism of KISS1R is through heterotrimeric G proteins (Figure 1.13). The G-protein q/11 enables phospholipase C_β (PLC_β) to hydrolyse phosphatidylinositol 4, 5-bisphosphate (PIP2) to form diacyl glycerol (DAG) and inositol 1, 4, 5-trisphosphate (IP_3). DAG activates protein kinase C (PKC) and IP_3 binds its cognate receptors on the endoplasmic reticulum (ER), causing calcium puffs (Constantin et al., 2009, Liu et al., 2008, Muir et al., 2001, Stafford et al., 2002, Kotani et al., 2001). The surge in cytoplasmic Ca^{2+} results in the stimulation of extracellular signal–regulated kinase (ERK) 1 and ERK2 kinase (Kotani et al., 2001). DAG function is important in the depolarization of gonadotropin releasing hormone neurons (GnRH neurons), by means of activating nonselective cation channel (TRPC), and at the same time inhibiting inwardly rectifying potassium channels (Kir) (Liu et al., 2008, Pielecka-Fortuna et al., 2008).
With the use of a GnRH promoter driven green fluorescent protein (GFP) reporter, researchers have been able to identify GnRH neurons in mouse brain slices, and carry out electrophysiological tests. Using this method, KP ligands were found to be potent activators of GnRH neurons by increasing their rate of action potentials (Han et al., 2005, Quaynor et al., 2007). One of the signalling mechanisms of action is through the inhibition of γ-amino-butyric acid (GABA). GABA is inhibitory neurotransmitter that is known inhibit GnRH secretion from GnRH neurons through neuronal hyperpolarisation (Clarkson and Herbison, 2006). KP ligands have been shown to suppress the effects of $GABA_B$ receptor in GnRH neurons (Zhang et al., 2009). Like other GPCRs, the KISS1R is desensitised through the process of

internationalisation and interactions with β-arrestin and G-protein coupled receptor kinase 2 (GRK2) (Pampillo et al., 2009).

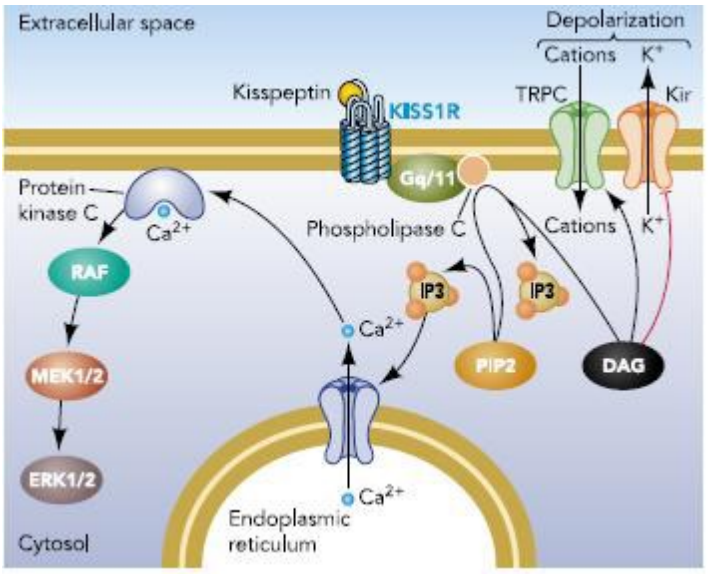

Figure 1.13 The signal transduction mechanism of KPs and KISS1R. KP ligand binding to KISS1R induces G protein q/11 to activate phospholipase C (PLC) and enable the cleavage of phosphoinositide 4, 5-bisphosphate (PIP2) to form diacyl glycerol (DAG) and inositol 1,4,5-trisphosphate (IP_3). IP_3 activates its cognate receptors on the endoplasmic reticulum and promotes the increase of intracellular Ca^{2+}. This process activates protein kinase C (PKC) and a kinase phosphorylation cascade (RAF, MEK1/2, ERK1/2) is initiated. In the case of gonadotropin releasing hormone neurons (GnRH neurons), depolarization is known to be controlled by DAG activating nonselective cation channel (TRPC), and at the same time inhibiting inwardly rectifying potassium channel (Kir) (d'Anglemont de Tassigny and Colledge, 2010).

Prior to the discovery of kisspeptins' cognate GPCRs (being known), KPs were exclusively thought to be metastasis inhibitors, hence their early name, metastin. Although the KP/KISS1R pathway is appreciated for its role in the regulation of the reproductive axis, this pathway also has a role in modulating disease states. The KP/KISS1R system functions as anti-metastatic in some types of cancers such as pancreatic cancer, melanoma, and gastric carcinoma (Masui et al., 2004, Shoji et al., 2009). The molecular mechanisms that underlie this anti-metastatic function are poorly understood and require further investigation. However, KISS1R is known to inhibit the action of MMP-9, increase the expression of the tissue inhibitor of matrix metalloprotease-1 (TIMP-1), and increase the activity of focal adhesion kinase (FAK). This leads to the inhibition of cell migration, development of focal adhesions and stress fibres (Kotani et al., 2001, Makri et al., 2008). The impact of the KP/KISS1R system has been shown to inhibit cell proliferation, motility, invasion, and chemotaxis (Kotani et al., 2001, Ohtaki et al., 2001).

1.3.3. KISS1R Agonists

All the natural cognate ligands for KISS1R (KP54, 14, 13, and 10) have similar binding and signalling characteristics to each other (Kotani et al., 2001). The similarity is caused by the conserved C-terminal region of the KP ligands (Figure 1.12 and Table 1.2). As a result, researchers used the N-terminally truncated KP10 as a template for structure-activity studies (Gutiérrez-Pascual et al., 2009, Ohtaki et al., 2001). They found that the five C-terminal residues are critical for KISS1R activation (Niida et al., 2006). Ala scanning mutagenesis studies revealed that KP10's critical residues were Phe6, Arg9, and Phe10, Ala substitution here would result in loss of agonistic activity (Niida et al., 2006, Gutiérrez-Pascual et al., 2009, Orsini et al., 2007). A nuclear magnetic resonance study using KP13 corroborated the importance of these three residues as they lie on the surface of a helix and are thought to constitute the pharmacophore site (Orsini et al., 2007).

Several compounds that have KP10-like agonist activity have been developed. For example the down-sized FM052a and FM053a are equipotent to KP10 (Niida et al., 2006). Further optimization of these analogues created another agonist; H-Amb-Nal(2)-Gly-Leu-Arg-Trp-NH2 (compound 34), which is reported to

be 4 times more potent than KP10 (Tomita et al., 2006). Another analogue termed FTM145 was created to inhibit proteinase degradation and increase bioactivity by inserting (E)-alkene dipeptide isostere at the Gly-Leu site (Tomita et al., 2008). Similarly, the [*D*-Y]1KP10 analog, although having a lower binding affinity for KISS1R is reported to have a higher *in vivo* bioactivity because of a resistance to proteolytic degradation compared to KP10 (Curtis et al., 2010).

1.3.4. The role of kisspeptin in reproduction and puberty

During the developmental stages of mammals, gonadotropin releasing hormone (GnRH) expressing neurons originate in the olfactory placode, where they migrate and colonise a region of the basal forebrain known as the preoptic area (POA) and the mediobasal hypothalamus (Wray et al., 1989b, Schwanzel-Fukuda and Pfaff, 1989, Wray, 2002). GnRH neurons are surrounded by terminals of KP expressing neurons (Irwig et al., 2004). The anatomical architecture of the hypothalamus, median eminence (ME), and the pituitary gland create precise control of the gonadotropin cells of the pituitary. GnRH neurons extend their projections onto the external secretory zone of the ME, where GnRH neuronal terminals interact with the primary capillary bed of the hypophyseal portal system (Page and Dovey-Hartman, 1984).

The mammalian brain expresses KP neurons in the arcuate (Arc) nucleus and the anteroventral periventricular nucleus (AVPV) (Navarro et al., 2009, Mayer et al., 2010). The KP neurons of the AVPV are thought to be responsible for the onset of puberty (Mayer et al., 2010). In the female brain, KP neurons of the AVPV control preovulatory surge of LH. The male neonatal masculisation process creates an AVPV that expresses low numbers of KP neurons relative to females. The pulsatile section of GnRH is thought to be regulated by the KP neurons of the Arc (d'Anglemont de Tassigny and Colledge, 2010, Colledge, 2004).

In order to insure the survival of all species, reproductive function is fine-tuned by central and peripheral signals that coordinate the hypothalamic pituitary gonadal (HPG) axis (Fink, 2000). The hypothalamus is where sparsely distributed neurons secrete GnRH, which acts on gonadotropin cells of the anterior pituitary to

secrete follicle stimulating hormone (FSH) and luteinizing hormone (LH). The gonads generate gametes that secure for future generations a continued genome, as well as synthesising peptide hormones and sex steroids (Fink, 2000, Schwartz, 2000a).

The HPG axis is governed by feed-forward loops (Figure 1.14). In order to establish homeostatic regulation, other forms of feedback regulatory loops are present. GnRH neurons are critical units in the hypothalamic component of the HPG axis, because the subsequent secretion of GnRH regulates downstream processes. Therefore, regulating GnRH pulsatile secretion is critical for synchronising the axis (Santoro et al., 1986, Belchetz et al., 1978). GnRH neurons are regulated by hypothalamic afferent neurons (Maeda et al., 2010b). The HPG axis of males and females is differentiated to give unique capabilities at puberty. This sexual dimorphism arises from the stages of foetal and postnatal development to bring about differences in the timing of puberty, the reproductive brain circuits, and the sexual dimorphic role of the HPG axis in adulthood (Fink, 2000, Herbison, 2006, Schwartz, 2000a). These differences give rise to female-specific roles in the ovarian cycle, lactation, and pregnancy (Roa et al., 2006, Schwartz, 2000b, Smith and Grove, 2002).

The reproductive system is important for general health, energy homeostasis, and immune/inflammatory state (Fernandez-Fernandez et al., 2006, Tena-Sempere, 2007, Tomaszewska-Zaremba and Herman, 2009). Furthermore, the reproductive system is responsive to environmental cues, such as stress conditions and photoperiods (Kinsey-Jones et al., 2009, Li et al., 2010, Simonneaux et al., 2009). The GnRH pulse generator interacts with circulating hormones, neurotransmitters, and neuropeptides (Fink, 2000, Herbison, 2006, Schwartz, 2000b). Additionally, GnRH neurons are regulated by many interacting glial and trans-synaptic inputs (Herbison, 2006, Ojeda et al., 2006, Ojeda et al., 2009). Glial cells are emerging as important regulators of puberty onset and adult reproductive function due to their facilitatory role, for example glial cells are known to stimulate GnRH neurons via glutamate and growth factors (Ojeda et al., 2006, Ojeda et al., 2009). Afferent neurons that regulate the pulsatile secretion of GnRH have been partially elucidated

(Herbison, 2006, Ojeda et al., 2008). Neurotransmitters such as glutamate and norepinephrine are known to be major excitatory factors, whereas endogenous opioids and GABA are inhibitory signals (Ojeda et al., 2009). However, in particular cases GABA can excite GnRH neurons (Herbison and Moenter, 2011). Briefly, some other participating factors that regulate reproductive function are as follows; members of the RF-amide superfamily and GnIH (Clarke et al., 2009, Navarro et al., 2006, Smith and Clarke, 2010). Tachykinins including NKB (Lehman et al., 2010), as well as metabolic neuropeptides like NPY and nesfatin-1(García-Galiano et al., 2010, Pralong, 2010).

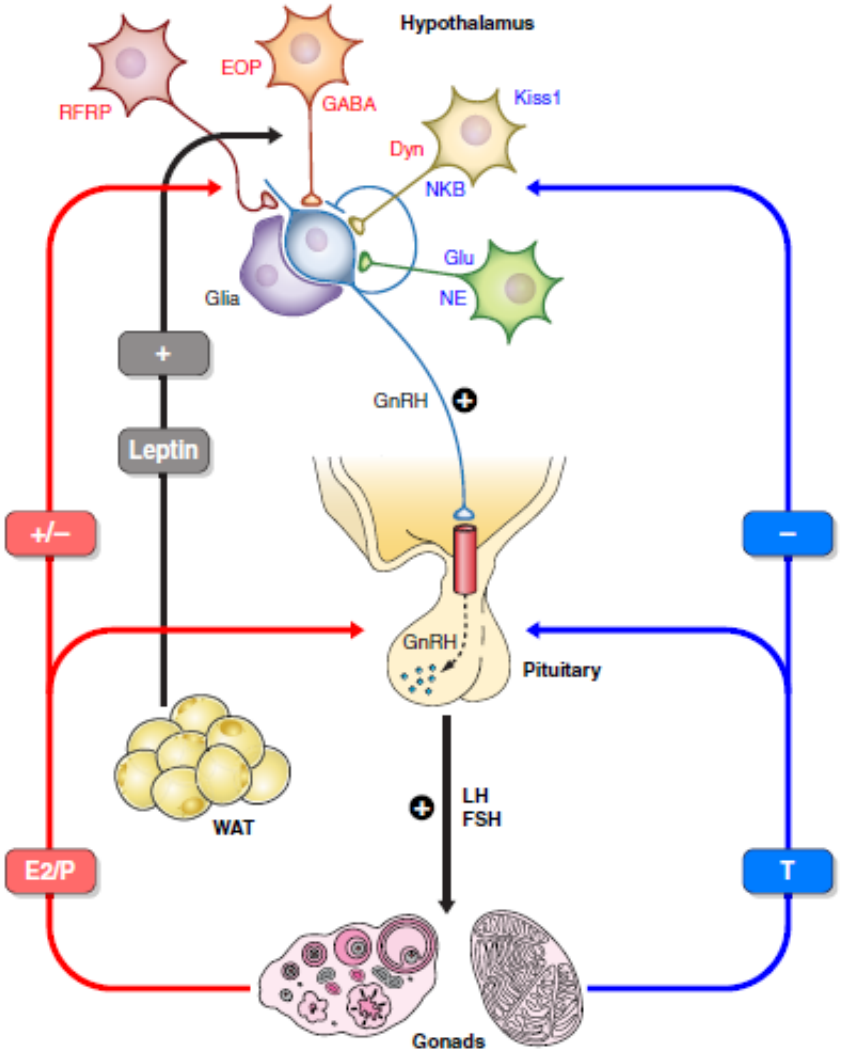

Figure 1.14 The hypothalamic-pituitary-gonadal (HPG) axis. Hypothalamic GnRH neurons are regulated by afferent neurons. GnRH is released into the blood system via the hypophysial portal. GnRH levels drive the pulsatile secretion of FSH and LH in the pituitary, which in turn regulate gonadal function (both the testes and ovaries are present). The axis is regulated by feedback regulatory loops, such as gonadal steroids like testicular testosterone (**T**), which is inhibitory to GnRH/LH/FSH (negative feedback). However, ovarian steroids mainly progesterone (**P**) and estradiol (**E2**) have dual roles, they can function as positive or negative feedback subject to the stages of the ovarian cycle. Metabolic hormones also regulate the HPG axis. These include the leptin, which is produced in white adipose tissue (**WAT**). Other abbreviations include – RFR, RF-related peptides; Glu, glutamate; NE, norepinephrine; NKB, neurokinin-B; EOP, endogenous opioid peptides; Dyn, dynorphin; GABA, γ-aminobutyric acid. Obtained with permission from the American Physiological Society (license number 3337131130885) (Pinilla et al., 2012).

1.3.5. The role of kisspeptin and KISS1R in pathology

The first reported cases of disease causing mutations of the *KISS1R* gene was shown by de Roux and colleagues of 2003 and quickly followed by Seminara and colleagues in 2003, in the same year. Both groups independently reported the presence of deletions leading to inactivating mutations of the *KISS1R* gene in patients with sporadic or familial forms hypogonadotropic hypogonadism (IHH), a rare condition leading to impaired gonadotropin secretion and infertility (de Roux et al., 2003, Seminara et al., 2003). These observations were further corroborated with mice engineered to lack KISS1R function, these studies were a phenocopy of the affected patients (Funes et al., 2003, Seminara et al., 2003). These findings were needed to realise the critical role of KISS1R and KP ligands in the reproduction system. Later studies confirmed these observations with *KiSS1* null mice (d'Anglemont de Tassigny et al., 2007, Lapatto et al., 2007). However, the *KiSS1* KO mice showed a less severe reproductive phenotype than KISS1R-deficient mice (Colledge, 2009). This may be due to the compensatory role of other RF-amides.

Patients suffering from clinical inactivating mutations of KISS1R responded to exogenous GnRH administration, partially rescuing their reproductive phenotype (Seminara et al., 2003). Furthermore, precocious puberty (time of vaginal opening) was observed with the chronic central administration of KP ligand into pre-pubertal female rats (Navarro et al., 2004). Conversely, a KP antagonist (p234) delayed puberty in female rats [as reviewed in (Pineda et al., 2010)]. Another supporting piece evidence for the role of KP in puberty is the observed increased expression of *KiSS1* mRNA in the hypothalamus of pubertal monkeys of both sexes (Shahab et al., 2005).

Several reports have suggested that the timing of the onset of puberty in girls has become earlier over the last 30 years. A major contributor to this is the increasing levels obesity in children (Kaplowitz, 2008). However, little is known about the mechanistic processes that govern this. KP neurons have been found to express leptin receptors, suggesting that the increase in leptin from white adipose tissue may regulate the HPG axis via KP neurons (Smith et al., 2006). Furthermore, leptin

deficient mice (ob/ob mice) exhibited reduced *KiSS1* mRNA levels in the arcuate nucleus of the hypothalamus (Smith et al., 2006).

The first described function of KPs was an anti-metastasis factor in human melanoma cell-lines (Becker et al., 2005, Takino et al., 2003). KPs inhibit RhoA-mediated tumor necrosis factor-alpha (TNFα) induced nuclear factor-kappa (NF-kB) pathway and thus suppresses cancer development and metastasis in breast cancer proliferation, migration, and invasion (Lee et al., 1996a). Furthermore, upon KP ligand binding, the KISS1R has been shown to inhibit cell proliferation, motility, chemotaxis and metastasis (Hori et al., 2001, Kotani et al., 2001, Lee and Welch, 1997, Ohtaki et al., 2001, Yan et al., 2001). The expression level of KP is inversely related to the metastatic potential of many types of tumours, such as in malignant melanoma, bladder, ovarian, gastric, breast, esophageal, uveal melanoma, osteosarcoma, renal and pancreatic cancers (Sanchez-Carbayo et al., 2003a, Dhar et al., 2004, Hata et al., 2007, Hesling et al., 2004, Ikeguchi et al., 2004, Lee et al., 1996b, Lee and Welch, 1997, Martins et al., 2008, Masui et al., 2004, Mitchell et al., 2006, Nagai et al., 2009, Shirasaki et al., 2001, Yi et al., 2008, Yoshioka et al., 2008, Sanchez-Carbayo et al., 2003b)

The clinical mutations of KPs and KISS1R are extremely rare (Cerrato et al., 2006). Nevertheless, they have provided insights into the role of KPs and KISS1R in reproduction. For example, inactivating clinical mutations of human KISS1R have been reported with a 155-nt deletion between intron 4 and exon 5, the R331X and X399X mutations, and the homozygous L148S mutation, all of which lead to IHH (Seminara et al., 2003, de Roux et al., 2003). Furthermore, C223R, R297L, L102P, and F272S substitutions have been reported to cause IHH in patients (Semple et al., 2005, Tenenbaum-Rakover et al., 2007, Nimri et al., 2011, Todman et al., 2005) . Additionally, an insertion at 1001_1002C has been reported which shifts the open-reading frame leading to IHH (Lanfranco et al., 2005). An illustration of the clinical mutations of KISS1R is presented in Figure 1.15.

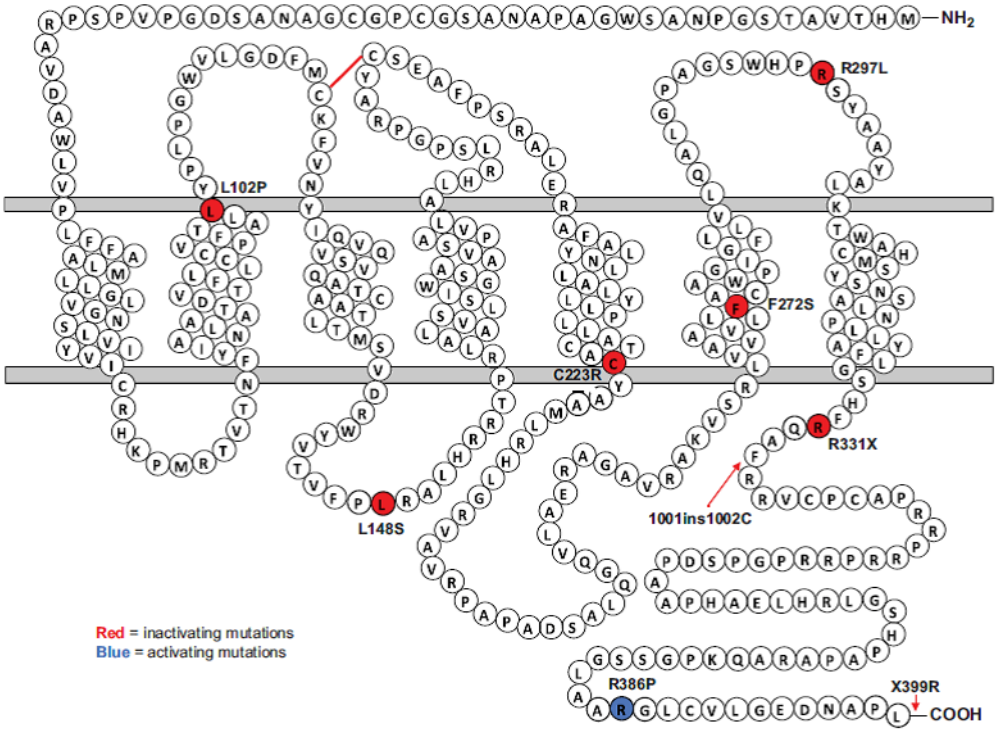

Figure 1.15 Schematic representation of human KISS1R with clinical mutations. The inactivating mutations are indicated in red and the activating mutation is indicated in blue. The insertion site is indicated in red arrow. [as reviewed in (Pinilla et al., 2012)].

Two clinical missense mutations in the *KiSS1* gene (KPs) have been reported (P74S and H90D) and are reported to cause central precocious puberty. The mechanism of action here is the increased stability of KP54 and thus increased bioactivity (Silveira et al., 2010). Another clinical mutation that leads to precocious puberty is reported in the KISS1R R386P. This autosomal dominant mutation has been demonstrated in vitro to prolong KISS1R activity as a measure of IP_3 production upon KP stimulation (Teles et al., 2008).

1.3.6. Cell-line models of GnRH neurons.

Researchers have developed physiologically relevant *in vitro* assays to study KP and KISS1R function. The challenge was that the intracellular molecular pathways that modulate GnRH neuronal function have been hindered by the low number and sparse distribution of these neurons in the hypothalamus (King et al., 1982, Wray et al., 1989a). Although, primary cell cultures circumvent this, the challenge is how to separate GnRH neurons from other cells. Thus researchers turned to the use of cell-lines derived from GnRH neurons. These immortalised cell-lines commonly referred to as 'GnRH neurons' bear some limitations, mainly from the immortalisation procedure and the unknown developmental stage at which the GnRH neurons were transformed.

The GT1-7 cell-line was created by incorporating a hybrid gene encoding for the SV40 T-antigen driven by the GnRH promoter into the mouse genome. This approach targets tumorigenesis to specific hypothalamic neurons that express GnRH. This GT1-7 cell-line was found to express endogenous GnRH mRNA, secrete GnRH in response to depolarization, and display neuronal, but not glial markers. It also appeared to show extended neurites (Mellon et al., 1990). However, constitutive expression of the immortalization agent – SV40 T-antigen may interfere with the normal functioning of cellular processes. Indeed, epidemiological and molecular evidence exists that links the expression of T-antigen to various molecular regulation pathways (Slack et al., 1999, Seinsoth et al., 2003, May et al., 2004, Cotsiki et al., 2004). Thus, the expression of the T-antigen may hinder the usefulness of the GT1-7 cell-line.

Alternative to GT1-7 cells, researchers created the GnV3 cell-line. This cell-line is derived from adult GnRH neurons of the rat hypothalamus. This was done by generating two lentiviral constructs: in the first construct, the GnRH promoter was cloned 5' to the tetracycline transactivator sequence; in the second construct, the TRE was cloned 5' to v-myc (the immortalization agent) and followed by the minigene encoding resistance to puromycine at the 3' (Salvi et al., 2006). These constructs enabled the researchers to conditionally, with the use of doxycycline, induce significant increase in cell proliferation, and with puromycine select for cells derived from GnRH neurons. Whereas in the absence of doxycycline GnV3 cells stop proliferating and develop many features common to GnRH neurons, such as electrophysiological, morphological similarities to neurons and they have been reported to express and secrete GnRH (Salvi et al., 2006, Mansuy et al., 2011).

1.4. Ca^{2+}/calmodulin

The chemical element calcium was created in the furnaces of stars when oxygen and neon bound successive α particles. Now calcium is the fifth most abundant element on earth and its ionised version [Ca^{2+}] is a principle regulator of cell signalling. Binding of Ca^{2+} to cognate proteins alters their shape, charge, and interactions. Moreover, cells must maintain a 20,000-fold gradient between their intracellular and extracellular Ca^{2+} concentrations. In contrast, Mg^{2+} levels barely differs across the plasma membrane. Why is Ca^{2+} vigorously removed from the cytosol? One explanation is that Ca^{2+} precipitates phosphate. Therefore, cells have adapted mechanisms to sequester and utilise cytosolic Ca^{2+} for signal transduction purposes. Moreover, Ca^{2+} cannot be chemically altered, thus cells have to chelate, compartmentalise, or extrude it. To this end, hundreds of proteins have evolved affinities for Ca^{2+} over a million-fold range (nM to mM), that function to buffer Ca^{2+} levels or to induce cellular processes (Clapham, 2007). The cell's "professional" protein chelator of Ca^{2+} is the EF hand domain, which was first described after the E and F regions of parvalbumin (Nakayama and Kretsinger, 1994). The EF hand motifs contain negatively charged oxygen atoms that cradle Ca^{2+}. The best studied EF hand protein is calmodulin. Below I describe calmodulin's structural features and its interactions with GPCRs.

1.4.1 Structural features of calmodulin

The name calmodulin is in fact an abbreviation for calcium modulator protein and is also represented in short form as CaM. CaM is relativity small with 148 amino acids and a molecular weight of 16.7 kDa (Figure 1.16) (Babu et al., 1985, da Silva and Reinach, 1991, Gnegy, 1993), The structure of CaM can be thought of as a dumbbell, in that the two globular domains are separated by a linker region (Persechini and Kretsinger, 1988, Kuboniwa et al., 1995). The linker region is 26 amino acids long and connects the last alpha helix of the N-terminal domain and the first alpha helix of the C-terminal domain. The linker region also functions to distance the two globular domains (Meador et al., 1993). The two globular domains of CaM each have two helix-loop-helix EF-hand regions that bind Ca^{2+}. The CaM N-terminal domain has a 10-fold lower affinity for Ca^{2+} than the C-terminal globular (Linse et al., 1991)

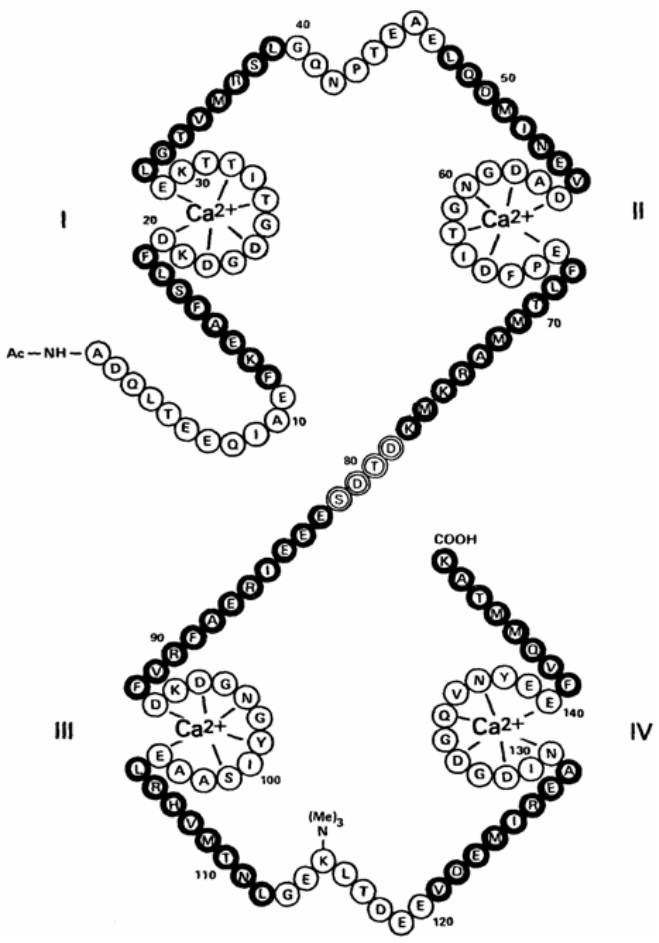

Figure 1.16 Calmodulin sequence schematic. The calmodulin protein contains two Ca^{2+} binding EF-hand regions in the N-terminal (represented as – I and II), and the C-terminus (shown as - III and IV). The alpha-helical regions are highlighted with bold circles. With permission from Elsevier (license number - 3298511476737) (Cohen and Klee, 1988)

1.4.2. Calmodulin conformational states

There are three CaM conformational states; the first is the Ca^{2+} free CaM, otherwise known as apocalmodulin, the second is Ca^{2+} bound CaM, which is represented as Ca^{2+}/CaM, and third is the Ca^{2+}/CaM-bound to target protein. The main characterising feature of the apocalmodulin conformation is the retention of hydrophobic residues imbedded inside the structure of the globular domains (Jurado et al., 1999). The retention of the hydrophobic core is maintained by strongly twisted and tightly packed bundle of four antiparallel α-helices which makes inter-helix angles of 128^{o} - 137^{o} (Jurado et al., 1999)

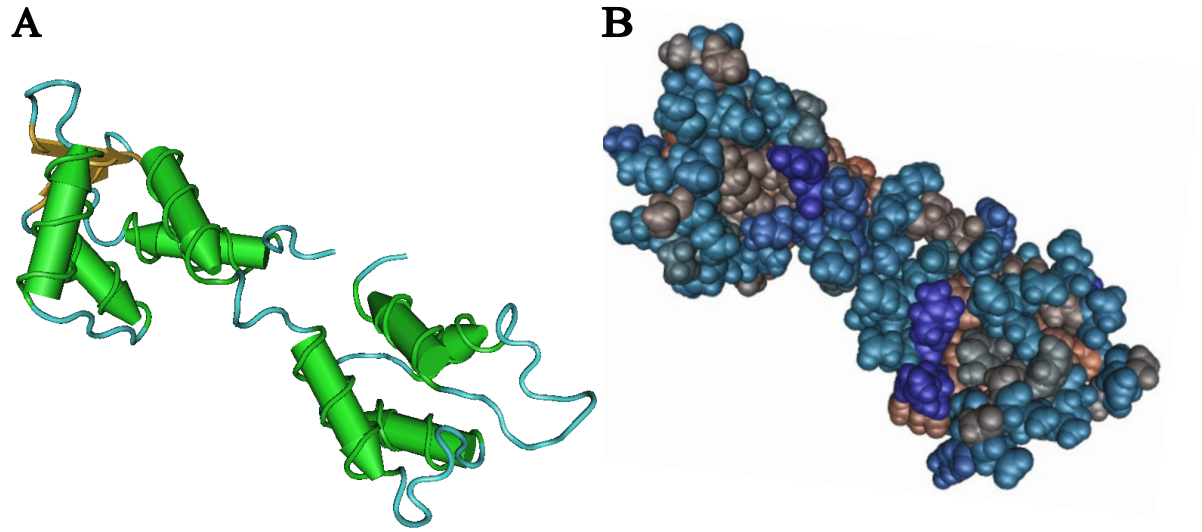

Figure 1.17 The apocalmodulin structure. The Ca^{2+}-free CaM is compact with hydrophobic residues retained inside the structure and hydrophilic amino acids covering the outside of the protein. Panel A- the worm rendering shows that the globular domains consist of anti-parallel α-helices that form inter-helix angles of 128^{o} - 137^{o}. Panel B- the space filled rendering shows blue and brown colours, which denote hydrophilic and hydrophobic residues, respectively. This structure was created using Cn3D program with PDB ID; 1CFD. The structure was previously obtained using nuclear magnetic resonance (NMR) spectroscopy (Kuboniwa et al., 1995).

The Ca^{2+}/CaM structure, however, has decreased angles of 86^{o} – 101^{o} due to the opening of the EF-hand regions. The conformation of the Ca^{2+}/CaM induces the hydrophobic residues to swing outwards forming a hydrophobic cup at both globular domains (Figure 1.18). The hydrophobic cups of Ca^{2+}/CaM bind to hydrophobic regions of target proteins (Kuboniwa et al., 1995). The stretching of the central α-helix observed in the crystal structure is indeed a crystallographic artefact and in solution it functions as a 'flexible tether' (Persechini and Kretsinger, 1988).

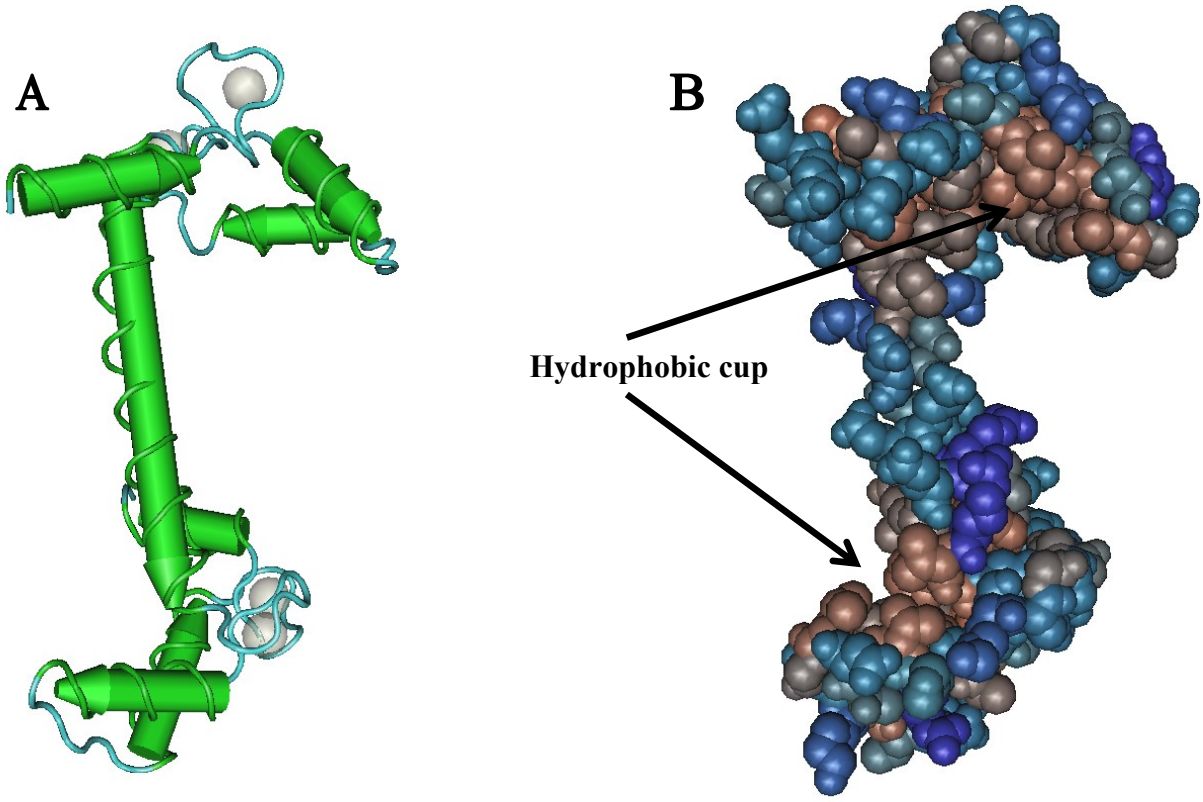

Figure 1.18 The Ca^{2+}/CaM structure. The crystal structure of Ca^{2+}/CaM shows that the EF-hand regions swing out and expose the once hidden hydrophobic core. Panel A is a worm rendering and panel B is a space filled representation and shows hydrophilic to hydrophobic residues depicted as blue to brown colours. The rendering was created using Cn3D program with PDB ID; 3CLN, obtained from (Babu et al., 1988).

Ca^{2+}/CaM is thought to interact with approximately ~100 proteins (Fallon and Quiocho, 2003). The solved structure of Ca^{2+}-CaM bound αCaMKII peptide (290-314aa) has revealed that the two globular domains compact and the hydrophobic cups interact with bulky hydrophobic residues of the target peptide (Meador et al., 1993). It is therefore not surprising, that αCaMKII $T_{305/306}$ autophosphorylation inhibits Ca^{2+}/CaM binding (Hanson and Schulman, 1992b).

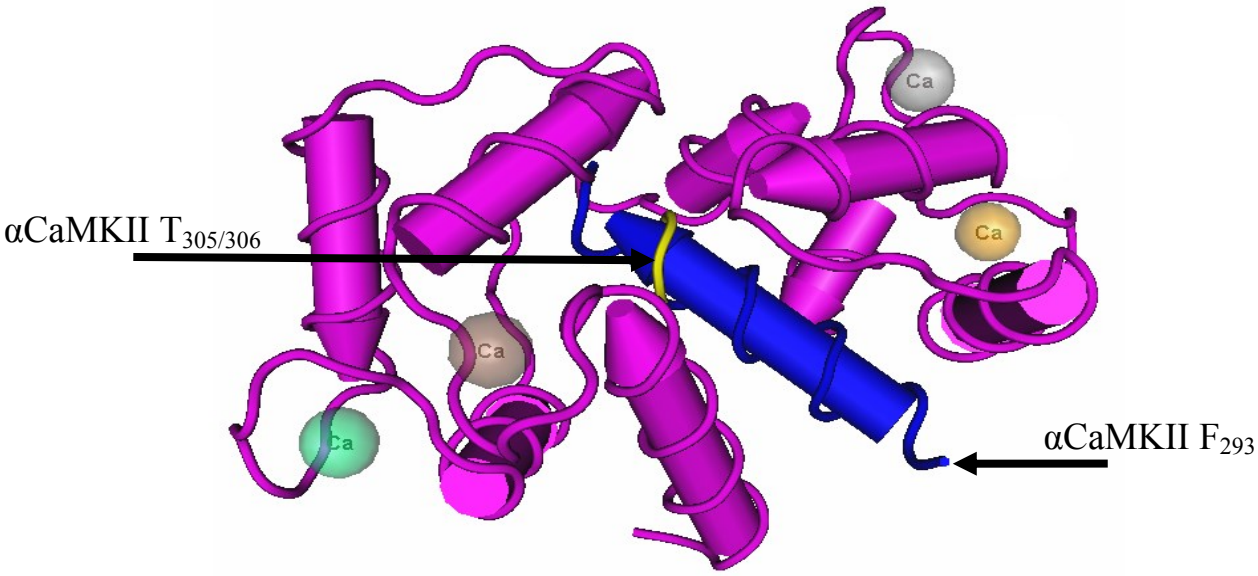

Figure 1.19 The structure of Ca^{2+}/CaM bound αCaMKII 290-314 aa peptide. The Ca^{2+}/CaM bound to αCaMKII peptide is compacted due to the unwinding central helix in order to enable the hydrophobic cups to interact with the hydrophobic residues of the peptide. The worm rendering was created using Cn3D program with PDB ID; 1CM1, obtained from (Wall et al., 1997).

1.4.3. Calmodulin binding to GPCRs

CaM has been shown to interact with several GPCRs and modulate their function [as reviewed in (Ritter and Hall, 2009)] (Table 1.3). For example CaM has been shown to bind to the third intracellular loop of the μ-opioid receptor and attenuate G-protein coupling (Wang et al., 2000, Wang et al., 1999) Furthermore, single-nucleotide polymorphisms in the G-protein coupling domain of the μ-opioid receptor were found to increase the receptor basal activity by altering CaM binding (Wang et al., 2001). Additionally, previous reports have shown that CaM interacts with the 5-hydroxytryptamine receptors 1A, 2A, and 2C (5-HT). The 5-HT_{1A} receptor contains two CaM binding sites in the third intracellular loop, which incidentally is a protein kinase C (PKC) binding site. The binding of CaM and PKC to the 5-HT_{1A} receptor is antagonistic and therefore important in modulating receptor activity (Turner et al., 2004). The 5-HT_{2A} contains two CaM binding sites, one in the second intracellular loop and the other within the C-terminal region. Binding of CaM to the C-terminal region of 5-HT_{2A} antagonises PKC binding, however, CaM binding the second intracellular loop attenuates G-protein coupling (Denis et al., 2012). The 5-HT_{2C} receptor also binds CaM at the C-terminal region (Becamel et al., 2002, Labasque et al., 2008). Moreover, CaM binding stabilises the 5-HT_{2C}/β-arrestin complex resulting in G-protein-independent ERK1/2 signalling (Teles et al., 2008).

CaM also binds metabotropic glutamate receptor 5 (mGluR5) at the C-terminal tail, which also overlaps a PKC phosphorylation site. CaM and PKC interactions with mGluR5 appear to be antagonistic with one another (Minakami et al., 1997). CaM binding stabilises mGluR5 surface distribution, while PKC phosphorylation abolishes CaM binding and promotes receptor internalisation Lee *et al*. (2008). CaM binding is also reported occur at the C-terminal tail of several Class B receptors, which results in the modulation of the agonist-stimulated activity of vasoactive intestinal peptide, calcitonin, glucagon-like peptide, parathyroid hormone, and pituitary adenylate cyclase activating corticotrophin releasing hormone receptors (Mahon and Shimada, 2005). Taken together, these observations suggest that CaM binding to GPCRs affect receptor trafficking, as well as G-protein-dependent and independent signalling.

Table 1.3 Calmodulin binding to GPCRs.

Associated GPCR	Site of Interaction	Impact on GPRCR	Reference
5-HT1A	IL3	Impairs PKC biding for receptor phosphorylation	(Turner et al., 2004)
5-HT2A	IL2 and CT	Inhibits G protein coupling	(Turner and Raymond, 2005)
5-HT2C	CT	Induces arrestin-dependent ERK activation	(Labasque et al., 2008)
D2R	IL3	Regulates G protein signalling	(Bofill-Cardona et al., 2000, Liu et al., 2007)
mGluR5	CT	Promotes receptor expression	(Minakami et al., 1997, Lee et al., 2008)
mGluR7	CT	Modulates receptor phosphorylation	(Nakajima et al., 1999, Sorensen et al., 2002)
PTH1R	CT	Inhibits GPCR activity	(Mahon and Shimada, 2005)
V2R	CT	Enhances GPCR-induced Ca^{2+} signalling	(Nickols et al., 2004)
μOPR	IL3	Regulates GPCR signalling and localization	(Wang et al., 1999)

1.5. αCaMKII

1.5.1. Structure and regulation

α-Ca^{2+}/calmodulin dependent protein kinase II (αCaMKII) is Ser/Thr protein kinase that is regulating by Ca^{2+}/CaM binding. This oligomeric protein kinase holoenzyme is composed of four domains; an N-terminal catalytic domain, regulatory domain, variable linker domain, and the C-terminal association domain. The monomeric molecular weight is ~54 kDa (Figure 1.20). The structure of αCaMKII is hexagonal with the association domain at the centre governing the oligomerisation. Extending outwards is the variable linker domain, which is responsible for sub-cellular localisation of the enzyme. Adjacent to the variable linker domain is the regulatory domain that contains the Ca^{2+}/CaM binding site and the inhibitory autophosphorylation site of T305/306. Also present is the T286 autophosphorylation site, which plays a role in enzyme activation and stabilises the active conformation [as reviewed in (Coultrap and Bayer, 2012)]

The structure of αCaMKII is analogous to 'petals on a flower'. The first structural study of αCaMKII was with electron microscopy. The derived images/models revealed a hexagonal structure consisting of a smaller inner and a larger outer ring. The smaller inner ring was calculated to be ~6 nm in radius, containing 6 subunits in the top and bottom monomer. The inner ring is organised around a hollow centre. The larger outer ring extends to ~15 nm from the core and is made of 12 catalytic domains (Morris and Torok, 2001).

In that early study of Morris and Török, 2001, they found that the single partial EM images gave a less defined outer ring in αCaMKII obtained from the rat brain compared when purified from recombinant baculovirus expressed cell-lines The authors suggest that the rat brain purified αCaMKII exhibits a higher degree of disorder because of basal autophosphorylation, as well as the contribution of βCaMKII, which is another isoform endogenous to the rat brain (Morris and Torok, 2001).

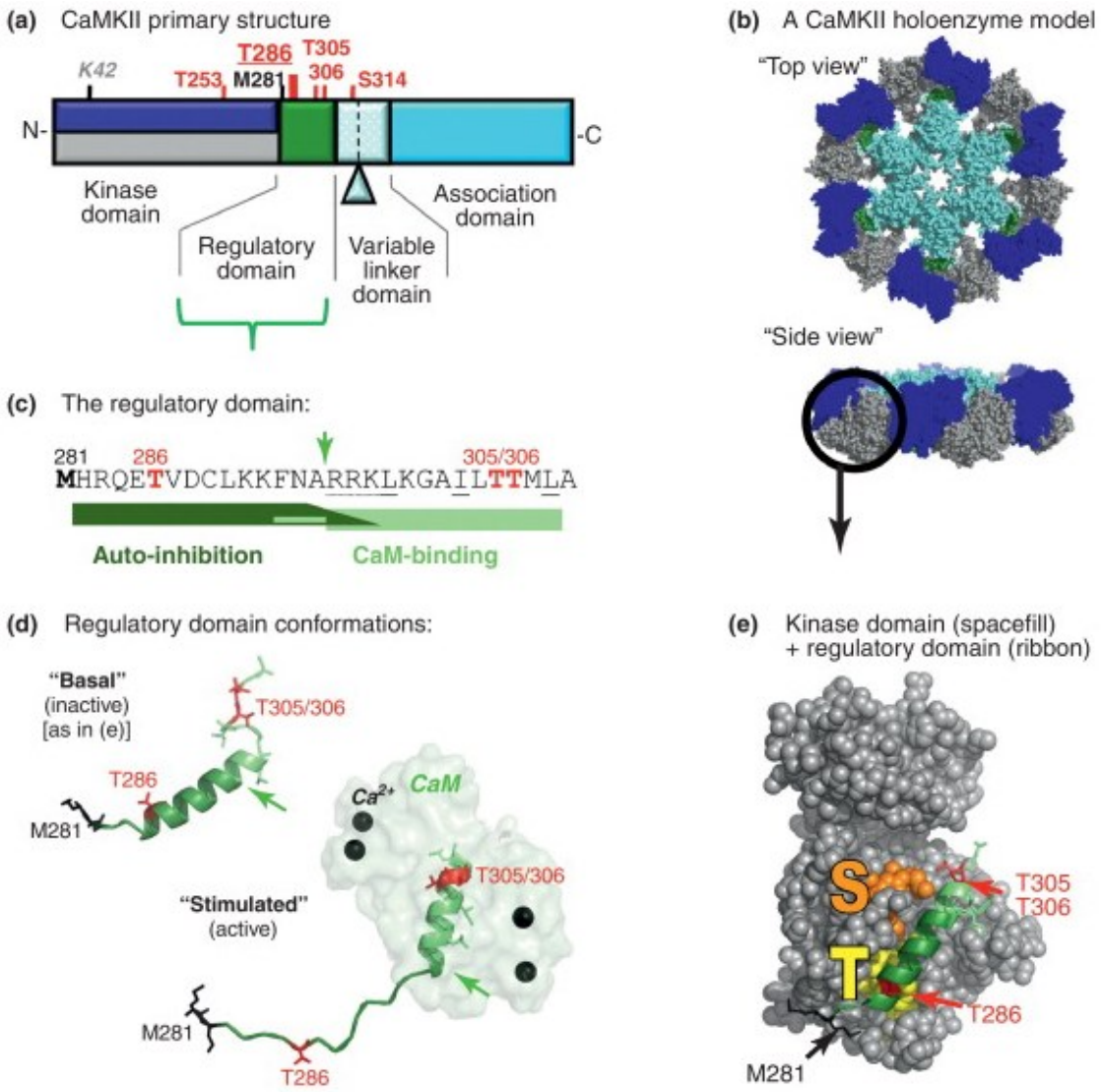

Figure 1.20 Illustration of αCaMKII structure and regulation. (a) An illustration depicting the primary structure of αCaMKII, with the variable linker domain being subject to alternative splicing as indicated with a triangle. Functionally important residues are indicated, with phosphorylation sites in red. (b) A structural model of αCaMKII is shown in two different views angles. The 12meric holoenzyme model is derived from several partial crystal structures (Rosenberg et al., 2006, Hoelz et al., 2003, Rosenberg et al., 2005). (c) The amino acid sequence of the regulatory domain, with autoinhibitory and CaM-binding regions are shown in dark and light green, respectively. The oxidation site – M281 is represented in black. The green arrow indicates the N terminus of the core CaM-binding region (R296) and is carried forward in panel (d); which shows the structural transition of the regulatory domain upon Ca^{2+}/CaM binding (Rellos et al., 2010). (e) Crystal structure of the basal state of the human γ-CaMKII regulatory domain (identical to αCaMKII), which is held in place partly by T-site (yellow) interaction, resulting in blocking access to the S-site, substrate binding regions (orange). The phosphorylation (red) and oxidation sites that generate autonomous activity (T286) are shown (Hudmon and Schulman, 2002a, Coultrap et al., 2010, Erickson et al., 2008). Also, the inhibition of CaM-binding (T305/306) sites are marked (Hudmon and Schulman, 2002a, Colbran and Soderling, 1990, Hanson and Schulman, 1992a, Colbran, 1993). Representations in panels d and e are based on Protein Data Bank (PDB) files 2VN9 and 2WEL (Rellos et al., 2010). Obtained with permission from Elsevier B.V. (license number - 3298510548633) [as reviewed in (Coultrap and Bayer, 2012).

1.5.2. T286 autophosphorylation

The binding of Ca^{2+}/CaM to αCaMKII induces T286 autophosphorylation in a inter subunit fashion and stabilises flanking hydrophobic residues that enables the regulatory domain to separate from the S-site (Yang and Schulman, 1999, Lisman et al., 2002, Colbran, 2004). The autophosphorylation of T286 confers onto αCaMKII a ~1,300-fold increase in affinity for Ca^{2+}/CaM and gives the interaction a positive cooperativity, which essentially means grouped activation of the catalytic domains by Ca^{2+}/CaM (Waxham et al., 1998). Furthermore, T286 autophosphorylation is thought to endow αCaMKII with autonomous activity i.e. Ca^{2+}/CaM independent activity (Colbran, 2004).

However, Tzortzopoulos and colleagues (2004) found that the activity of T286 autophosphorylated αCaMKII in low Ca^{2+} represented ~5% of maximal activity (Tzortzopoulos et al., 2004). The perplexing question therefore is; how is it possible for αCaMKII to be active in the absence of Ca^{2+} (autonomous activity) and be almost inactive in the presence of low Ca^{2+}? One possible way to consolidate these two observations may come from the CaM trapping hypothesis. CaM dissociation from αCaMKII is ~0.4 seconds, however, CaM dissociation from T286 autophosphorylated αCaMKII is several minutes (Meyer et al., 1992, Torok et al., 2001). Therefore, T286 autophosphorylated αCaMKII protomers may interact with other proteins, like CaM to convey autonomous activity.

1.5.3. T305/306 autophosphorylation

The inhibitory T305/306 autophosphorylation site is firmly within the Ca^{2+}/CaM binding domain of αCaMKII (Hashimoto et al., 1987, Miller and Kennedy, 1986). Furthermore, the autophosphorylation is thought occur in an intra-subunit fashion (Mukherji and Soderling, 1994). The rate of T305/306 autophosphorylation is similar to the rate of enzyme inactivation, which was previously determined to be ~1 minute at 37ºC (Jama et al., 2009, Lee and Yasuda, 2009). Other reports have demonstrated that Ca^{2+}/CaM binding inhibits T305/306 autophosphorylation (Patton et al., 1990, Meador et al., 1993, Hanson and Schulman, 1992a). This is corroborated with observations that EGTA induces a ‘burst’ of T305/306 autophosphorylation (Lou and Schulman, 1989, Jama et al., 2009). Taken

together, these studies suggest that αCaMKII catalytic activity is regulated by T305/306 autophosphorylation and Ca^{2+}/CaM binding.

1.5.4. Other posttranslational modifications

The well-studied mechanisms of αCaMKII regulation are Ca^{2+}/CaM binding and the above mentioned autophosphorylation events. However, several other less studied mechanisms may contribute to αCaMKII regulation. For example the T253 phosphorylation is thought to target αCaMKII to the post synaptic density without altering its enzyme activity (Migues et al., 2006). *In vitro* S314 phosphorylation has been demonstrated, but no function has been shown to date (Colbran and Soderling, 1990, Hanson and Schulman, 1992a). Recent studies have shown M281 oxidation, which like T286 is thought to impart Ca^{2+}/CaM independent activity (autonomous activity) (Erickson et al., 2008). M281 oxidation has pathological roles in smooth muscle and cardiomyocytes (Luo et al., 2013, Scott et al., 2012, He et al., 2011, Swaminathan et al., 2011).

1.5.5. αCaMKII binding GPCRs

There are more than 100 proteins in the genomic database that contain the αCaMKII consensus sequence of Arg-X-X-Ser/Thr (Pearson et al., 1985, White et al., 1998)(Pearson *et al*., 1985; White *et al*., 1998). The role of these possible substrates is of particular interest in understanding the Ca^{2+} transduction pathway. Among these putative interactions is thought to contain GPCRs. One example of GPCR regulation by αCaMKII is the Ca^{2+} dependent phosphorylation of the M4 muscarinic acetylcholine receptor (M4R) (Guo et al., 2010). The Gαi/o-coupled M4Rs inhibits adenylyl cyclase and therefore lowering the cAMP production (Wess, 1996, Nathanson, 2000). The increase in cytoplasmic Ca^{2+} activates αCaMKII, thereafter phosphorylating T145 M4R (intracellular loop 2). The phosphorylation potentiates M4R efficacy in suppressing cAMP production (Guo et al., 2010). Another example is αCaMKII phosphorylation of the limbic dopamine receptor (D3R) at S229 (intracellular loop 3). D3R is similar to M4R in that they are both Gαi/o-coupled GPCRs. However, unlike the reported M4R potentiation, the αCaMKII dependent phosphorylation of D3R reduces D3R efficacy in suppressing cAMP production (Liu et al., 2009).

1.6. Aims and Objectives

Previous reports have shown that some GPCRs are regulated by CaM and αCaMKII. Herein I address the mechanisms by which CaM and αCaMKII confer onto the KISS1R temporal sensing of cytoplamic Ca^{2+} concentrations before the stages of receptor desensitisation. I have discovered CaM-binding and αCaMKII consensus motifs in the primary amino acid sequence of the human KISS1R. I attempt to answer fundamental questions. For example, does CaM bind to the KISS1R and if so where? What is the functional relevance of the potential interaction? Also, the hypothesis was investigated whether αCaMKII can phosphorylate the KISS1R. This thesis provides, in my opinion, convincing evidence for the existence of a negative feedback loop regulating KISS1R activity. The vision of this thesis is to propose novel concepts in the development of co-agonists that may one day usher in hormone therapies for KISS1R associated diseases.

2. Materials and Methods

2.1. Introduction

This chapter includes the materials and the laboratory techniques used in the research project presented within this thesis. All used materials that were obtained from external sources and any work that was not performed by me have been acknowledged.

2.2. Peptides and Proteins

The derived peptides from the kisspeptin receptor (KISS1R), gonadotropin releasing hormone receptor (GnRHR), the C-terminal regions of G-protein α subunits, and the kisspeptin-10 ligand were synthesised by EZbioLab, USA with >95 % purity. Alpha-Ca^{2+}/calmodulin dependent protein kinase II (αCaMKII) was expressed using the baculovirus expression system and was kindly provided by Dr K. Török, St Georges University of London. Pyruvate kinase (PK), Syntide-2 and lactate dehydrogenase (LDH) proteins were purchased from Sigma-Aldrich Inc. Wild-type calmodulin (CaM) and fluorescently tagged CaM probes were first expressed, FLPC purified, labelled and then HPLC purified. The CaM probes that were used were DA-CaM and TA-CaM which were kindly provided by Dr K. Török. The CaM ^{C34}-badan was created in Dr K. Török's lab. The point mutants CaM1, CaM2, CaM3, CaM4, CaM12, CaM34, and CaM1234 were obtained from Dr. Nael Nadif Kasri, Catholic University of Leuven, Belgium. CaM mutants were generated by mutation of the first coordinating Asp of the Ca^{2+} binding EF-hand motifs to Ala.

2.3. Transforming of competent cells

DNA constructs were transformed into ultra-competent *E.coli* cells XL-10 (obtained from Stratagene, Cheadle, UK). Briefly, the cells were first thawed on ice and incubated with 1.5 μL β-mercaptoethanol for 10 minutes, followed by 30 minute incubation on ice with 10 ng of the DNA vector. The cells were then heat shocked at 42°C for 35 seconds and allowed to cool on ice. After cooling (~3 minutes), 450 μL of S.O.C medium (Invitrogen, Paisley) was added into the tubes containing bacteria and incubated at 37°C in the shaker for 1 hour. Finally, the bacteria were streaked out

on to LB-agar (Luria Broth) plates containing 100μg/mL of ampicillin or 40 μg/mL of kanamycin and incubated at 37°C overnight.

2.4. Preparation of DNA plasmids

The LB-agar plates were removed from the 37°C incubator and a single bacterial colony was picked with a sterile toothpick and placed into a 5 mL LB medium starting culture containing 100 μg/mL of ampicillin or 40 μg/mL of kanamycin. The bacterial cultures were grown at 37°C in the shaker for ~8 hours. Then 1mL of the starting culture was inoculated into 250 mL of LB medium containing the necessary concentrations of antibiotics (100μg/mL of ampicillin and 50μg/mL of kanamycin) and incubated for ~16 hours at 37°C in the shaker. The bacterial cells were harvested by centrifugation at 6000 x g for 15 minutes at 4°C, followed by purifying the DNA vectors using Qiagen maxi-preparation columns (Qiagen, Crawley, UK) according to the provided protocol and eluted in distilled and deionised H_2O. A Nanodrop spectrophotometer (Nanodrop Technologies, Delaware, USA) was used to determine DNA vector concentration and purity. The DNA concentration was measured at 260nm wavelength (extinction coefficient $0.020 \mu g/mL^{-1}$ cm^{-1}) and the purity was determined using the ratio absorption of 260/280 nm wavelength.

2.5. Preparation of glycerol stocks

The transformed bacteria were preserved using Glycerol stocks. To do this 300 μL of 80% (w/v) glycerol was mixed into 700 μL of bacterial culture, frozen on dry ice and stored at -80°C. In order to recover the transformed bacteria, the frozen glycerol stock vials was placed into dry-ice and a small piece was scraped off the surface of the frozen culture and streaked onto LB-agar plates containing the necessary concentrations of antibiotics and incubated overnight at 37 °C.

2.6. Agarose gel electrophoresis

Agarose gels were prepared with 1 % (w/v) agarose in TAE buffer (320 mM acetic acid, 40 mM Tris, 1 mM EDTA, pH7.2). DNA samples were separated at 120 V for 40 minutes and stained with ethidium bromide and visualised under ultraviolet light using a GeneFlash transilluminator (Syngene Bio Imaging, Cambridge, UK). The DNA material was excised from the agarose gels and processed using a QIAquick gel extraction kit (Qiagen, Crawley, UK) according to supplied protocol.

2.7. KISS1R cDNA victors and Site-directed mutagenesis

The FLAG-KISS1R cDNA that was used in this project was kindly provided by Dr Andy V Babwah, The University of Western Ontario, Canada. Briefly, the human KISS1R cDNA was obtained from OriGene Technologies (Rockville, MD – NM_032551.3) and a FLAG-epitope was introduced at the amino terminus of KISS1R. The FLAG-KISS1R was cloned into *NheI* and *NotI* sites of a pEGFP-C vector backbone obtained from Invitrogen (Pampillo et al., 2009).

The Wt-CaM cDNA contained in the pAED 4 vector and cloned into *NdeI* and *PstI* restriction sites was kindly provided by Dr Katalin Török, St George's University of London. All the FLAG-KISS1R and CaM mutations were introduced using the Site-Directed Mutagenesis Kit from Agilent Technologies (Cheshire, UK) and validated by di-deoxy sequencing (Lu et al., 1997).

2.8. Co-immunoprecipitation

FLAG-KISS1R expressing cells were stimulated with KP-10 using 150 mm dishes. After stimulation the cells were washed with Ca^{2+} free PBS and placed on ice for 30 minutes. This was followed by lysing the cells with NP40 lysis buffer (0.7 mL) containing NaCl 250 mM, K^{+}-HEPES (pH7) 5 mM, Glycerol 10 % (w/v), NP-40 0.5 % (w/v), EDTA 2 mM, Phenylmethylsulfonyl fluoride (PMSF) 1 mM and Leupeptin 1mg/mL. The lysed cells were sonicated at 6 amplitude microns for 30 seconds. Heavier cellular organelles were separated from whole cell lysates by centrifugation at 14,000 rpm for 10 minutes. 40 µL ANTI-FLAG M2 affinity Gel (Sigma-Aldrich) was incubated with the lysates on a rotating wheel overnight in the

cold room. The samples were then spun down at 5,000 rpm for 30 seconds. The supernatant was removed with a narrow Hamilton syringe. At this stage the samples were washed with 0.5 ml of TBS. The process of spinning and washing was repeated three times. The elution was carried out using 3 X FLAG peptide (Sigma-Aldrich) at 150 ng/μL and incubated with gentle agitation for 30 minutes 2-8ºC. Afterwards the samples were spun at 8200 x g for 30 seconds and the supernatant was removed liked before. The samples were then stored in -20ºC . The pellets were dissolved in SDS sample buffer and were resolved by SDS-polyacrylamide gel electrophoresis (SDS-PAGE) and transferred to PVDF membrane (NEN Life Sciences) for protein immunoblotting. PVDF membranes were blocked in 4% bovine serum albumin, 50 mM Tris-HCl, pH 7.0, 0.05% Tween-20 and 0.05 % NP40 blocking solution.

The primary antibodies of rabbit FLAG were purchased from Sigma-Aldrich. Mouse calmodulin antibodies were purchased from Millipore. Both antibodies were used at 1:1000. These were visualised by complementary anti-rabbit and anti-mouse secondary antibodies at a dilution of 1:5000 (Upstate). The imaging was carried out using a LiCor machine.

2.9. Expression and purification of calmodulin

A starter culture of 10 mL of 2xTY medium (16 g/L bacto-tyrptone, 10 g/L yeast extract, and 5 g/L of NaCl) containing 100 μg/mL ampicillin was inoculated with one bacterial colony of BL21 – Gold transformed with $pAED_4$-CaM vector. The starter culture was incubated in a shaking incubator, shaking at 125 revolutions per minute (RPM) for 8 hours at 37°C until bacterial growth reached an absorbance of 0.6- 0.8 (A_{600}) per mL. Thereafter, 200 μL of the starter culture was aliquoted into 2 L culture flasks containing 500 mL 2XTY medium with 100 μg/mL ampicillin and incubated at 37°C at 80 RPM overnight**.** In order to induce CaM expression 300 μM of isopropyl β-D-1-thiogalactopyranoside (IPTG) was added into the 2 L culture flasks and allowed to incubate for a further 150 minutes at 37ºC, 125 RPM. Afterwards, the bacterial cultures were pelleted by centrifugation at 16000 g for 30 minutes at 4ºC. The pellet was suspended in 20 mL of 50 mM Tris-HCl pH 7.5, 1 mM ethylene glycol tetraacetic acid (EGTA), 10 mM dithiothreitol (DTT), 10 μg/mL

tert-amyl methyl ether (TAME), 10 μg/mL N-tosyl-l-phenylalanine chloromethyl ketone (TPCK), 10 μg/mL trypsin inhibitor, 10 μg/mL leupeptin, 10 μg/mL pepstatin A and 10 μg/mL N-benzoyl-l-arginine ethyl ester (BAEE). All chemicals were bought from Sigma-Aldrich Inc, UK. Afterwards, the re-suspended pellet was freeze/thawed three times and then centrifuged 64000 g for 30 minutes at 4ºC, followed by adding into the supernatant 5 mM $CaCl_2$.

The purification of CaM from the supernatant was carried out using phenyl sepharose CL-4B resin. (Sigma-Aldrich Inc, UK). 100 mL of the resin was washed using 10 L of 20 mM Tris/HCl pH 7.5 followed by a 2 L wash with Tris/HCl pH 7.5 containing 5 mM $CaCl_2$ and 500 mM NaCl and then the resin was heated and stirred at 35ºC for 20 minutes. After the washing process the resin was equilibrated with 2 L 20 mM Tris/HCl pH 7.5 containing 1 mM $CaCl_2$. It was at this stage that the supernatant containing CaM protein was mixed with the equilibrated resin and the mixture was heated and stirred at 35ºC for 20 minutes in order to increase the efficiency of the CaM-resin binding. The supernatant-resin mixture was cooled to 4ºC and then packed into a fast protein liquid chromatography (FPLC) column (Pharmcia Biotech, XK26). The FPLC machine that was used was the GE ÄKTA explorer (Amersham Pharmacia) system. The column was run using two buffers, both containing 20 mM Tris-HCl pH 7.5, 2 mM EGTA, 1 mM DTT, 0.2 mM phenylmethylsulfonyl fluoride (PMSF), 1 μg/mL of leupeptin and 1 μg/mL of pepstatin A. However, the first buffer contained 1 mM $CaCl_2$ and the second buffer contained 2 mM EGTA. The column was run in a gradient from a 100 % 1 mM $CaCl_2$ and 0 % 2 mM EGTA containing buffer to 0 % 1 mM $CaCl_2$ and 100 % 2 mM EGTA containing buffer in a total volume of 500 mL and collecting in 5 mL fractions/minute.

A second purification was carried out using a Q-sepharose column (Amersham Pharmacia) equilibrated with 10 column volumes of buffer containing 20 mM Tris-HCl pH 7.5, 2 mM EGTA, 1 mM DTT, 0.2 mM phenylmethylsulfonyl fluoride (PMSF), 1 μg/mL of leupeptin, 1 μg/mL of pepstatin A, and 2 mM EGTA. The protein solution was allowed to flow into the column and was eluted with two buffers both containing 20 mM Tris-HCl pH 7.5, 2 mM EGTA, 1 mM DTT, 0.2 mM

phenylmethylsulfonyl fluoride (PMSF), 1 μg/mL of leupeptin and 1 μg/mL of pepstatin A. However, only one of the buffers contained 2 mM EGTA. The elution run was carried out with a gradient from a 100 % buffer and 0 % buffer + 2 mM EGTA to 100 % buffer + 2 mM EGTA and 0% buffer. This was carried out in a total volume of 50 mL and collecting in 1 mL fractions/minute. The fractions containing CaM were determined at 278 nm (A_{278} 0.18 = 1 mg/mL CaM). In order to desalt the protein solution a PD10 column (Pharmacia Biotech, UK) was used. The equilibration of the column was carried out with 25 mL H_2O, followed by running the purified CaM solution through the column. The elution was carried out using 3.5 mL H_2O. The desalted CaM sample was then freeze-dried and stored in -20ºC.

2.10. Determination of protein concentration

To determine protein concentrations of cell lysates, the Bradford Assay (Bio-Rad Laboratories, Hertfordshire, UK) was used. To do this, BSA standards were prepared in a total of 200 uL of Bradford dye and appropriate PBS volumes with the following concentrations 0 mg/mL, 0.1 mg/mL, 0.2 mg/mL, 0.3 mg/mL, 0.5 mg/mL, 0.75 mg/mL, 1 mg/mL, 1.5 mg/mL and 2.0 mg/mL. The standards were vortexed and left for 5 minutes. The absorbance was measured at 595 nm wavelength using a spectrophotometer. Using the standard curve the 'unkown' samples were calculated from the equation of the line.

2.11. Site-directed fluorescence labelling of calmodulin

The Wt CaM cDNA cloned in the pAED4 vector, between *NdeI* and *PstI* sites, was mutated to generate CaM T34C mutant with the use of site-directed mutagenesis (see section 2.7) This vector construct was overexpressed in Escherichia coli (BL21 strain). The fluorophore – 6-bromoacetyl-2-dimethylaminonaphthalene (badan) was used to label CaMT34C. This was carried out by reacting 100 μg CaMT34C and 2 mM badan in a total volume of 1 mL solution of 150 mM KCl, 2 mM *tris* (2-carboxyethyl) phosphine (TCEP), and 20 mM MOPS (pH 7.2). This reaction was allowed to incubate for 2 hours at 22 ºC in the dark. Afterwards the reaction was stopped by 30 mM β-mercaptoehanol. In order to purify the CaM^{C34}-badan, the reaction mixture was run through a Sephadex G-15 column. This was

followed by two rounds of purification using high-performance liquid chromatography (HPLC) purification steps. The fraction containing CaM^{C34}-badan was used for the spectroscopic experiments. The concentration of the purified CaM^{C34}-badan was determined using the extinction coefficient (molar absorbance of badan) of 20,100 $cm^{-1}M^{-1}$ at 386 nm.

2.12. Reverse phase HPLC

Further purification of wild-type CaM and fluorescence-labelled CaM were carried out by using reverse phase high pressure liquid chromatography (HPLC). Proteins were separated with a linear gradient of the organic solvents. The gradient was 70% H_2O (containing 0.1 % trifluoroacetic acid, TFA) and 30% acetonitrile (0.082 % TFA) to 70% acetonitrile (0.082 % TFA) and 30% H_2O (0.1 % TFA).

2.13. Calmodulin-binding experiments

The fluorescently labelled CaMs (TA-CaM and DA-CaM) were kindly provided by Dr K. Török, St. George's, University of London, UK. CaM ^{C34}-badan was created in Dr K. Török's lab (see section 2.11). The TA-CaM is fluorescently labelled at lysine 75 to form 2-chloro-(epsilon-amino-Lys75)-[6-[4-(N,N-diethylamino)phenyl]- 1,3,5-triazin-4-yl]CaM. TA-CaM was excited at 366 nm wavelength and the emission was determined at 415 nm wavelength.

The DA-CaM had two native threonines replaced with cysteine (T34C/T110C) and randomly labelled with the donor 5-((((2-iodoacetyl)amino)ethyl)amino)naphthalene-1-sulfonic acid (1,5-IAEDANS) and the acceptor dimethylamino-3,5-dinitrophenyl (DDP). The fluorescent intensity depends on the distance between the donor and the acceptor. The quenching of fluorescence corresponded to a decrease in distance between the two Ca^{2+} -binding domains of CaM (which the 1, 5-IAEDANS and DDP are located). The DA-CaM used for this project has been fully characterized and exhibits undistinguishable kinetic characteristics to wild-type CaM (Török *et al*., 2001). DA-CaM excitation is 340 nm and the emission is 500 nm. The Absorbance was monitored at 250 nm.

All the labelled CaMs were double purified using high performance liquid chromatography (HPLC) and were experimented with using an assay buffer containing 1 mM $MgCl_2$, 100 mM NaCl, 50 mM K^+-PIPES (pH 7) in order to mimic physiological ionic strengths and pH. All the fluorometric experiments were carried using SLM spectrofluorimeter (8100 model) and the data was analysed using GraFit 7 (Erithacus Software Ltd, West Sussex, UK) and GraphPad Prism 5.0 (GraphPad Software, San Diego, USA).

2.14. Free Ca^{2+} calculation

The determination of the Ca^{2+} binding of CaM^{C34}-badan requires the precise control of free Ca^{2+} concentrations. This is achieved with an *in vitro* assay that has a high buffering capacity, utilising the chelating agent ethylene glycol tetraacetic acid (EGTA). Additionally, the calculation of free Ca^{2+} concentrations is dependent on the buffer's ionic strength, pH, and temperature. The dissociation constants (K_d) of EGTA for Ca^{2+} is 376 nM and for Mg^{2+} is 33.9 nM in a solution of pH 7 and at 20ºC (Tsien and Pozzan, 1989). This fundamental understanding allows for the determination of free Ca^{2+} concentration using the following equations:

$$Ca^{2+} + EGTA \rightleftharpoons Ca^{2+}.EGTA$$

The dissociation constant K_d is defined as:

$$K_d = [Ca^{2+}]_{free}\ [EGTA]_{free}/[Ca^{2+}.EGTA]$$

However

$$[Ca^{2+}.EGTA] = [Ca^{2+}]_{Total} - [Ca^{2+}]_{free}$$

Also

$$[EGTA]_{free} = [EGTA]_{Total} - [Ca^{2+}.EGTA]$$

Replacing $[EGTA]_{free}$ and $[Ca^{2+}.EGTA]$, changes the initial equation into

$$[Ca^{2+}]^2_{free} - ([Ca^{2+}]_{Total} - [EGTA]_{Total} - K_d) \times [Ca^{2+}]_{free} - K_d \times [Ca^{2+}]_{Total} = 0$$

This is a quadratic equation of the general form $\alpha x^2 + \beta x + \gamma = 0$. Upon solving this equation for $[Ca^{2+}]_{free}$ transforms into:

$$[Ca^{2+}]_{free} = -\ [([Ca^{2+}]_{Total} - [EGTA]_{Total} - K_d) \pm \Delta^{1/2}]/2 \times 1 \text{ (equation)}$$

where $\Delta = \beta^2 - 4\alpha\gamma = ([Ca^{2+}]_{Total} - [EGTA]_{Total} - K_d)^2 - 4 \times 1 \times (-K_d \times [Ca^{2+}]_{Total})$

Therefore the equation above is used for the calculation of the free Ca^{2+} concentration when the total Ca^{2+} and EGTA concentrations are given.

In order to determine the free Ca^{2+} concentrations in the CaM^{C34}-badan equilibrium Ca^{2+} binding experiments, an automated syringe pump (ALADDIN 1000, WPI) was used. The pump contained 325 mM $CaCl_2$ that was diluted at a 10 µL/min flow rate into a 3 mL cuvette containing 100 nM CaM^{C34}-badan, 50 mM K^+-HEPES (pH 7.5), 100 mM KCl, 2 mM $MgCl_2$, 5 mM EGTA. The flow rate values were converted into free Ca^{2+} concentrations using a two-chelator Maxchelator program. Validation checks of free Ca^{2+} concentrations were performed with the use of Fluo3 at K_d 325 nM. This was similar to the previously reported Ca^{2+} affinity for Fluo3 at K_d 390 nM in 100 mM KCl, 10 mM MOPS (pH 7.2) and at 22 ºC.(Haugland et al., 2005).

2.15. Steady state kinase activity assay

A derived quantitative description of enzyme catalysis is known as specific activity. This is calculated by a continuous spectrofluorimetric assay which is based on an ADP calibration (Török *et al.,* 1998). The amount of substrate (syntide-2) phosphorylation is equal to the amount of ADP production from the enzymatic reaction (*in vitro)*. This in turn is coupled to an NADH fluorescence assay, which decreases in fluorescence upon oxidation of NADH to NAD^+. The change in fluorescence is a direct correlation to syntide-2 phosphorylation. Consider the initial biochemical reaction (reaction **1**);

Reaction 1

$$\textbf{αCaMKII} + \textbf{Ca}^{2+} + \textbf{CaM} + \textbf{Syntide-2} + \textbf{ATP} \longrightarrow \textbf{Ca}^{2+}\textbf{.CaM.αCaMKII} + \textbf{Syntide-2}^{\textbf{-Phos.}} + \textbf{ADP}$$

The αCaMKII in the presence of CaM, Ca^{2+} and ATP will result in a complex of. Ca^{2+}.CaM.αCaMKII, which phosphorylates syntide-2 (syntide-2^{-Phos}), this reaction results in ADP production. However, the amount of substrate phosphorylation and ADP production is unquantifiable in real-time. To overcome this, a naturally fluorescent NADH assay is coupled to the above reaction **1**. Now consider the NADH assay below;

Reaction 2 **PEP + PK + ADP → Pyruvate + PK + ATP**

Reaction 3 **Pyruvate + LDH + NADH → Lactate + LDH + NAD^+**

Pyruvate kinase (PK) catalyses the transfer of a phosphate group from phosphoenolpyruvate (PEP) to ADP, yielding one molecule of pyruvate and one molecule of ATP (reaction **2**). Lactate dehydrogenase (LDH), which is a NADH dependent enzyme, converts pyruvate to lactate resulting in NADH oxidation to NAD^+ (reaction **3**). The combined reactions of **1, 2,** and **3** constitute the continuous spectrofluorimetric steady state coupled enzyme reaction (Figure 2.1). This provided continuous monitoring of NADH oxidation and thus a sensitive measurement of syntide-2 phosphorylation, ADP production and thus αCaMKII specific activity (Torok et al., 1998).

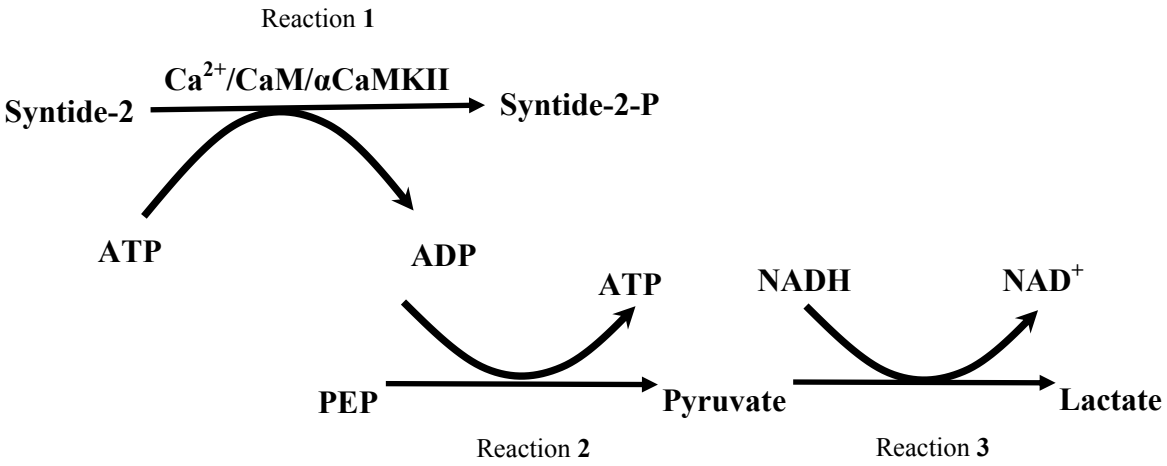

Figure 2.1 Steady state coupled enzyme reaction. The amount of substrate phosphorylation is equal to the amount of ADP produced by the enzyme reaction. The constant production of ADP corresponds to the constant fluorescence decrease of NADH upon oxidation to NAD^+. The individual reactions are labelled **1-3**.

The NADH fluorescence was measured using two spectrofluorimeter, the first was SLM spectrofluorimeter 8100 model consisting of a Xenon arc lamp (450 W) or mercury arc lamp (100 W). The excitation measured used in this instrument was 340 nm and the emission was 460 nm. Slit widths were 2, 2 nm for excitation and 16, 16 nm for emission. The other spectrofluorimeter used (and stated in the relevant results sections) was the FluroLog-3, manufactured by HORIBA scientific. Slit width was 2, 2 for excitation and 2, 2 for emissions.

All assays of steady state enzyme activities were carried with an assay buffer ($MgCl_2$ 1 mM, NaCl 100 mM, K^+-PIPES pH7 50 mM) containing 5 mM DTT, 50 μM syntide-2, 4 U/mL PK, 9 U/mL LDH, 2 mM PEP and 22 μM NADH. CaM, αCaMKII and Ca^{2+} concentrations were varied as indicated. The data analysis was carried out using GraFit 7 (Erithacus Software Ltd, West Sussex, UK).

T286 autophosphorylation was carried out using 1 μM αCaMKII, 6 μM CaM, (exception; CaM34, which was 60 μM in 220 μM $CaCl_2$), and 1 mM ATP in the presence of 50 mM K^+-PIPES, pH 7.0, 100 mM KCl, 2 mM $MgCl_2$, 5 mM DTT, and 0.05 mM $CaCl_2$ at 21 °C. At the indicated times, the reaction was stopped with 4 x SDS sample buffer. The samples were then run on a SDS-PAGE 4-12 % precast gels (Invitrogen). T286 phosphorylation was determined with western blotting and phospho-T286-αCaMKII-specific monoclonal antibody and fluorescent secondary antibody (IRDye 800CW goat antimouse IgG). Odyssey infrared imaging system (LI-COR Biotechnologies) was used to acquire the digital images. The densitometry values of the images obtained using ImageJ software (National Institutes of Health). The analysis was as follows: Densitometry values were taken from each band and time 0. The time 0 reaction was stopped before the addition of ATP. The following formula was used on an inverted scale: $(D_{\max} - Dt)/(D_{\max} - DB)$, where D_{max} represents the average density of the most fluorescent band, Dt – the average density of a time point, and DB – time 0 average density. By subtracting individual values with the highest densitometry value the scaling was inverted. The relative density is

represented with respect to the highest density. The data was fitted to an exponential function using GraFit software program, version 4.0.

2.16. ADP calibration

The ADP calibration is critical to the effectiveness of the steady state coupled enzyme reaction. It is derived by measuring the NADH fluorescence with reaction **2** and **3** (materials and methods – section 2.15) without ADP as a control and correlating the 2 μM ADP additions to fluorescence change. A typical ADP calibration would be:- 1 μM ADP corresponds to 1131 fluorescence counts. An ADP calibration was done every day preceding a steady state coupled enzyme activity experiment.

2.17. Calculation of CaMKII specific activity

After the ADP calibration an enzyme activity experiment was carried out. An assay mixture containing reactions of **1, 2,** and **3** (reactions in section 2.15), excluding αCaMKII from reaction **1** was measured in the spectrofluorimeter. An average gradient of fluorescence change is derived by using a PC with OS\2 operating system and SLM Aminco software attached to the SLM spectrofluorimeter. A typical value of an active enzyme is 300 fluorescence counts per second (fc/s). This value is then divided by a typical ADP calibration value of 1131 fluorescence counts per 1 μM ADP to give 26.5 x 10^{-3} μM ADP per second. At this stage of quantifying enzyme activity, the enzyme is producing 26.5 x 10^{-3} μM ADP and substrate phosphorylation per second. Finally, the formula below was used to calculate the specific enzyme activity.

$$Moles\ of\ product\ \times (amount\ of\ enzyme\ used)^{-1}\ \times (min)^{-1}$$
$$= \chi\ nmoles\ min^{-1}\ mg^{-1}$$

The 'moles of product' was calculated in nmoles/L of ADP. The 'amount of enzyme used' was expressed as milligrams, and the 'min' was 1 minute.

2.18. Cryopreservation and resurrection of cell-lines

Cell-lines were stored in liquid nitrogen (-196°C) containing a cryoprotectant of 10 % (v/v) dimethylsulphoxide (DMSO) and 90 % (v/v) foetal calf serum. The recovery procedure involved thawing the vials containing cell-lines in a 37°C water bath prior to being re-suspended in growth medium and seeded into culture flasks. In order to cryopreserve cell-lines, confluent cultures were passaged and harvested by centrifugation at 500 x g for 3 minutes. The culture medium was removed and the pellet was re-suspended in the cryoprotectant and slowly frozen using 'Mr Frosty' (Nalgene, Hereford, UK) container prefilled 100 % isopropanol and stored at -80 ^{o}C. After 24 hours, the vials were transferred to the liquid nitrogen tank.

2.19. Cell culture

The four different cell-lines used for this project were HEK-293, COS-7, GT1-7, and GnV3 cells. All the cell-lines were available in the laboratory of Dr Zhi-Liang Lu, Human Reproductive Science Unit, University of Edinburgh. The HEK-293, COS-7, and GT1-7 cells were maintained in Dulbecco's modified Eagles medium (DMEM; Sigma, UK) supplemented with 10% foetal calf serum, 2% glutamine and 1% penicillin (10,000units/mL)/streptomycin (10,000mg/mL). The GnV3 cells were maintained with Neurobasal A medium (Sigma, UK) containing 0.04 % B27 supplement (Gibco, UK), 500 µM glutamine, 25 µM glutamate, and 1% penicillin/streptomycin (Sigma, UK). All the cells were maintained at 37ºC in a humidified 5 % CO_2 atmosphere.

The cell-lines were passaged regularly with the use of trypsin/EGTA. To do this, the medium was removed from cell-line cultures approaching 80-100 % confluency and washed once in phosphate-buffered saline (PBS). To detach cells from the monolayer, 2 mL trypsin was added to 162 cm^2 cell culture flasks (Fisher Scientific, Leicestershire, UK) and allowed to incubate in the 37°C incubator for 5 minutes. Once the cells had fully detached, 8 mL of growth medium was added into the culture flask to terminate the trypsin action. The cell-lines were regularly passaged to 1:3 dilutions. In order to determine the cell number, a Neubauer haemocytometer was used. Briefly, the detached cells were diluted 1:10 in PBS and injected into the indicated inlets of the haemocytometer. The four counting areas

were utilised and an average was taken. The cell number was represented in x 10^5/mL. The dilution factor was also taken into consideration.

2.20. Confocal laser scanning microscopy

Confocal microscopy was used to characterise CaM-CFP interactions with KISS1R-YFP. The cDNA constructs were electroporated into HEK-293 cells (see materials and methods 2.21). The cDNA concentration used was 15 µg in the case of CFP-CaM only expressing cells and 15 µg for KISS1R-YFP only expressing cells. The combined co-transfection of CFP-CaM and KISS1R-YFP was carried out at 7 µg each. After electroporation the cells were placed into 3.5 cm plastic plates with glass cover bottoms (World Precision Instrument Inc, USA) and were left for 48 hours to reach 70 % confluency. Cell density when seeded was 1 x 10^6 cells/plate. Prior to imaging the cells were washed with Ca^{2+} free PBS and new medium was placed on the cells. The YFP was excited at 517 nm and the emission was measured at 528 nm wavelength. The CFP was excited at 436 nm and the emission was measured at 488 nm wavelength. The GnV3 cells were electroporated with 15 µg of cDNA GPR54-GFP (see materials and methods 2.21).

2.21. Transient transfection by electroporation

The transient expression of KISS1R in COS-7, HEK-293, GT1-7, and GnV3 cells was achieved using the electroporation method. All the cell-lines were electroporated using a Bio-rad Gene Pulser with cold (4 ^oC) Opti-MEM medium (Sigma-Aldrich Inc, UK). The HEK-293 cells were electroporated using 300 voltage (V) and of capacitance 950 µF. COS-7 cells were electroporated with 230 V and with 950 µF. GT1-7 cells were electroporated with 350 V and 960 µF and, while GnV3 cells were electroporated with 240 V and 700 µF. All the cells were electroporated with 4 mm cuvettes (Bio-Rad, UK) with infinite resistance.

2.22. KP-10 iodination and whole cell competitive radioligand binding assay

The iodination of kisspeptin-10 (KP-10) was carried out by Dr Kevin Morgan and Mr Robin Sellar. The KP-10 (Tyr-Asn-Trp-Asn-Ser-Phe-Gly-Leu-Arg-Phe-NH_2) was radiolabeled using the Chloramine-T method as described for GnRH (Flanagan et al., 1998). KP-10 (10 µL from 1 mM stock) was suspended into 50 µl PBS (pH7.2) and mixed with 10 µL (100 µCi/µL) of carrier-free $Na^{125}I$. Thereafter, 10 µl chloramine T (2 mg/ml) was added and the reaction was allowed to proceed for 10-15 seconds. Sodium metabisulfate (2 mg/ml) was added to terminate the reaction. The reaction was diluted into 1 ml running buffer (50 mM sodium acetate pH4.0, 50 mM N-acetylmethionine, 5 % sucrose, 2.5 % BSA, 0.1 % sodium azide) and then loaded onto a QAE Sephadex G25 size exclusion column. Fractions were collected in 1 ml vials and 10 µL was collected from each fraction and counted for 1 minute using a gamma counter to obtain the elution profile and identify fractions containing the radiolabelled peptide. The fractions to be kept were above 4,000 gamma counts. All the gamma counts in the peak (P) was added up and the 'specific activity' was calculated$= P \times 1{,}000 \div (TC \times 0.05)\mu Ci/\mu Mol$. Because we did not use a HPLC to gain > 99 % pure radiolabelled fraction, the 'specific activity' calculated is therefore an estimate for the purpose of standardisation between iodination batches.

With the use of the labelled KP-10, whole cell competition radioligand binding assay was performed using the method as previously described for GnRH (Flanagan et al., 1998). COS-7 cells were electroporated (see section 2.21) with KISS1R cDNA (see section 2.7) and seeding into 12-well plates. The peak KISS1R expression in COS-7 cells was optimised using confocal microscopy and western blotting. 48 hours post-transfection the media was aspirated and the cells were incubated for 4 hours at 4^{o}C in 0.5 mL binding media (DMEM supplemented with 10 mM HEPES and 0.1 % BSA) containing 100,000 cpm/well and increasing concentrations of unlabelled KP-10 ranging from 0 to 1µM. The estimated concentration [I^{125}]-KP10 tracer that was used in each well was about 25 pM. Hence, the tracer amount used in the experiments had little effect on the Cheng-Prusoff shift as determined for the GPCR – GnRH receptor (Flanagan et al., 1998) Non-specific

binding was determined in the presence of 1 μM unlabelled KP-10. After the incubation period unbound ligand was removed with two washes of cold PBS, followed by lysing the cells with 0.5 mL 0.1 NaOH. The radioactivity was measured using a γ counter. The raw data was represented as counts/minutes

2.23. Radioimmunoassay

The radioimmunoassay (RIA) was employed for the measurement of GnRH secretion in the characterisation of GV-3 and GT1-7 cell-lines, a cell model for GnRH neurons. To do this, 150 μL buffer (100 mM phosphate buffered saline gelatine pH 7.4), 100 μL primary anti-GnRHII antibody (1:10,000 dilution) and 50 μL of sample or standards was pre-mixed into 10 x 75 mm polypropylene test-tubes (Sarstedt Ltd., Leicester, UK) and incubated overnight at 4°C. On the second day, 100 μL of tracer was added and incubated for an additional 24 hours at 4°C. The tracer used was radioactively labelled GnRHII ligand with iodine-125 (I^{125}) at 20,000 cpm. The third day, 100 μL of normal rabbit serum (1:100 dilutions) was added and allowed to incubate for another 24 hours at 4°C. Finally, the fourth day, 1 mL of wash buffer was added into the tubes (polyethylene glycol 4%, saline 0.9%, triton 0.2%), and were centrifuged at 3000 rpm at 4ºC for 30 min. The supernatant was carefully decanted and the tubes were measured using a Wizard 1470 Automatic Gamma Counter (Perkin-Elmer Inc., MA, USA) which gave a reading in γ counts per minute. The raw data was analysed using the software AssayZAP (Biosoft, Cambridge, UK). The software generates a standard curve and calculates the unknown sample GnRH concentration.

2.24. Measurement of inositol phosphate turnover

HEK-293 and COS-7 cells were electroporated with DNA constructs (see section 2.21) and cultured 12 well culture dishes in complete DMEM. After 24 hours, the cells were washed twice with phosphate-buffered saline (PBS) prior to incubating the cells with special inositol free DMEM (Invitrogen, Paisley, UK) supplemented with 50 IU/mL penicillin-streptomycin, 1 % (v/v) dialysed foetal calf serum and 1 μCi/mL *myo*-D-[^{3}H] inositol (GE healthcare, Buckinghamshire, UK) in

a total volume of 500 µL for 16 hours. Thereafter, the cells were washed three times and then incubated with 500 µL of HEPES-DMEM containing 0.1 % BSA and 10 mM LiCl for 30 minutes at 37ºC to block inositol phosphate breakdown. After incubation, the medium was replaced with 500 µL of HEPES-DMEM/10 mM LiCl/0.1 % BSA containing varying concentrations of Kisspeptin-10 (10 pM – 1 mM) to stimulate the cells for 1 hr at 37 ºC. The cells were then lysed with 10 mM formic acid at 4ºC for 1 hr in order to extract the radioactive inositol phosphate. The lysates were transferred to plastic tubes containing 500 µL Dowex AGI-X8 ion exchange resin (Bio-Rad Laboratories, Hertfordshire, UK) in order to bind the radioactive inositol phosphate. The bound [^{3}H]inositol phosphate was washed with 1 mL deionised H_2O, then further washed with 60 mM ammonium formate / 5 mM sodium tetraborate. The resin bound [^{3}H]inositol phosphates was eluted with 1M NH_4 formate / 100 mM Formic acid. Finally, 800 µL of the eluted solution was transferred to vials containing 2.5 mL scintillation fluid and the radioactivity was measured on a Beta counter for 5 minutes.

2.25. Preparation of cell extracts

In order to carry out co-immunoprecipitation experiments, transfected or untransfected HEK-293 cell-lines were seeded onto a 150 mm cell culture dish (3 x 10^5 cells/1 mL) with 10 mLs of complete medium (DMEM supplemented with 10 % FCS, 2 mM glutamine, 50 IU/mL penicillin, 50 IU/mL streptomycin and 10 mM HEPES) and kept in the 37°C incubator. After 48 hours the medium was removed and replaced with 10 mL of fresh medium with or without the presence of kisspeptin ligand and inhibitors for durations that were indicated in the results figure legends. After the stimulation (indicated in the results figure legends) the medium was removed and the culture dishes were placed on ice and washed three times with cold PBS (10 mLs). Followed by adding the lysis buffer; nonidet P-40 solubilisation buffer (50 mM K^+-HEPES (pH8), 250 mM NaCl, 0.5 % (v/v) Nonidet P-40, 2 mM EDTA, 10 % (v/v) glycerol) that was supplemented with 1 mM phenylmethylsulfonyl floride (PMSF), 10 ug/mL leupeptin and 1 mM sodium orthovanodate fluoride. The lysate slurry was clarified by centrifugation at 4 °C,

20,000 x g for 15 minutes and the nuclear contents were sheared by sonication. The protein concentration was measured as described above.

2.26. Western blotting

Solubilised protein samples were mixed with sample buffer, Laemmli 2 x concentrated (LSB- 4% (v/v) SDS, 20% (v/v) glycerol, 10% (v/v) 2-mercaptoethanol, 0.004% (v/v) bromophenol blue and 0.125 M Tris-HCl, pH 6.8. The samples were then heated to 100^{o}C for 5 minutes. The protein samples were resolved using sodium dodecyl sulphate-polyacrylamide gel electrophoresis (SDS-PAGE) obtained from Invitrogen Life Technologies, Paisley, UK (20% Tris-Gly gels). Protein separation was carried out using SDS-PAGE running buffer (25 mM Tris, 192 mM glycine, 1 % (w/v) SDS) at 45 mA for 1 hour.

After the 1 hour of SDS-PAGE electrophoresis the gels were placed onto polyvinylidene difluoride (PVDF) membranes (NEN Life Science, Buckinghamshire, UK). The PVDF membranes were previously washed with 100 % methanol followed by several washes of distilled H_2O and equilibrated in semi-dry transfer buffer (20 mM Tris, 192 mM glycine, 20 % (v/v) methanol, 0.1 % (w/v) SDS) for 30 minutes. Also, six blotting papers (Bio-Rad Laboratories, Hertfordshire, UK) were pre-soaked in the transfer buffer for 30 minutes. A sandwich was created by placing three blotting papers onto the anode plate and the PVDF membrane placed on top of it. This was followed by placing the Tris-Gly gel onto the stack and another three blotting papers on top. Any trapped air bubbles were removed by rolling the sandwich with a glass test tube. The cathode plate was placed on top. The proteins were transferred from the gel to the PVDF membrane at 25 V for 1 hour.

The PVDF membranes were then washed with 3 x 10 minutes TBS-T (100 mM Tris (pH 7.0), 150 mM NaCl, 0.05% (v/v) Tween 20, 0.05% (v/v) Nonidet P-40) and blocked 3 x 10 minutes in 10 mL of blocking buffer (4 % (w/v) BSA, TBS-T) on the rocker. After the indicated times the blocking buffer was removed and the primary antibody (1:1000 dilutions in 10 mL blocking buffer) was incubated onto the PVDF membranes over night at 4 °C. The next day, the PVDF membranes were washed three times in TBS-T for 10 minutes after which the primary antibodies were detected with Goat IRDye800 conjugated anti-mouse antibodies (Rockland) and

Goat Alexa Fluor 680/700 conjugated anti-rabbit antibodies (Invitrogen Molecular Probes) at a 1:5000 dilution. The western blots were imaged using the Odyssey Li-Cor infrared imaging system (software version 2.1.12). The band intensities were quantified using Image J 1.46.

2.27 Software and data analysis

All the experiments shown in this thesis were repeated at least three independent times. The inositol phosphate and radio-ligand binding assays were carried out in triplicates of individual repeats. The data of these assays were represented as mean values and the standard error of the mean (SE). The statistically significant results were indicated by asterisks in the figures. The data analysis was performed using Students t-test or One-Way Anova with Dunnett's test using GraphPad Prism 5.0 (GraphPad Software, San Diego, USA). Sigmoidal dose response curves were fitted to the relevant data sets and the EC_{50} and E_{max} values were determined. The expression levels of the mutant KISS1R were expressed relative to wild-type KISS1R control included in the individual experiments. The αCaMKII activity data was fitted to a Michaelis-Menten equation using GraFit 7 (Erithacus Software Ltd, West Sussex, UK).

3. The physical association of calmodulin with kisspeptin receptor

The regulatory mechanisms that enable KISS1R to sense increased intracellular Ca^{2+} concentration and avoid Ca^{2+} excitotoxicity are unclear. In this chapter, the hypothesis is investigated whether an interaction between the KISS1R and the Ca^{2+} binding protein, calmodulin (CaM) may exist. The binding of CaM to KISS1R was tested by three different approaches. Firstly, spectrofluorimetric experiments were performed to see if CaM binds to intracellular loops IL1, IL2, IL3 or the C-terminal tail of KISS1R. Secondly, co-immunoprecipitation experiments were conducted using FLAG-KISS1R expressed in HEK-293 cells and immunoblotting for endogenous CaM. Thirdly, it was tested if in HEK-293 cells, CFP-CaM co-localises with YFP- KISS1R. The results of this chapter will be discussed in the context of how KISS1R is likely to function in high Ca^{2+} intracellular concentrations, desensitising itself to external stimuli by means of CaM binding.

3.1. Introduction

The kisspeptin receptor (KISS1R) is a 7-transmembrane G-protein coupled receptor (GPCR) that is critical for mammalian fertility and some endocrine cancers [as reviewed (Oakley et al., 2009)]. Upon KISS1R activation, its coupling partner, G-protein q/11 promotes cytosolic Ca^{2+} increase (Constantin et al., 2009, Kotani et al., 2001, Liu et al., 2008, Muir et al., 2001, Stafford et al., 2002). However, this linear set of events will lead to Ca^{2+} excitotoxicity if left un-regulated, thus we must determine the proteins that bind and regulate KISS1R function.

Like other GPCRs, the KISS1R contains three intracellular loops (IL1 to 3) and an intracellular C-terminal tail that function, in part, as contact sites for protein-protein interactions. GPCRs signal by forming macromolecular protein complexes consisting of G-proteins and other proteins (Davare et al., 2001, Venema et al., 1998, Kim et al., 2005, Guhan and Lu, 2004, Sjogren et al., 2013, Mahon and Segre, 2004). Proteins other than G-proteins that interact with GPCRs are known as GPCR-interacting proteins (GIPS). GIPs have been shown to directly interact with IL2 and IL3 of GPCRs, regulating their trafficking, function, and desensitisation [as reviewed in (Ritter and Hall, 2009, Bockaert et al., 2004). A detailed study of GIPs will increase our understanding of GPCR regulation mechanisms and potentially enable us to develop therapeutic drugs to modulate disease states.

In this regard, an increasing interest is being paid to – calmodulin (CaM), a Ca^{2+} regulated GIP that is known to modulate the functional properties of a variety of GPCRs [as reviewed in (Ritter and Hall, 2009). Binding of Ca^{2+} to CaM induces conformational changes that expose hydrophobic regions and enable CaM to bind to various target proteins. CaM binding motifs are highly variable, with secondary structure properties being critical for CaM binding. The Ca^{2+}/CaM binding motif is characterised by the existence of hydrophobic amino acids (F, W, I, L, or V) separated by basic residues (H, K, and R) in a 1-10, 1-12, 1-14 or 1-16 motif and governed by amphipathic α-helical feature. This criterion is derived from numerous structural studies of CaM binding to target proteins (Yap et al., 2000, Hultschig et al., 2004).

CaM is known to interact and regulate some GPCRs. These include the metabotropic glutamate receptor, μ-opioid receptor, angiotensin II AT_{1A} receptor, D2 dopamine receptor, V2-vasopressin receptor, 5-hydroxytryptamine receptor, 5-HT_{2A}, and 5-HT_{2C} receptors (O'Connor et al., 1999, Dev et al., 2001, El Far et al., 2001, Minakami et al., 1997, Ishikawa et al., 1999, Choi et al., 2011, Wang et al., 1999, Thomas et al., 1999, Nickols et al., 2004, Turner and Raymond, 2005, Labasque et al., 2008). The CaM binding regions of the above mentioned GPCRs vary. In the case of the μ-opioid and 5-HT_{1A} receptors, CaM binding is reported to occur via IL3 (Wang et al., 1999, Turner et al., 2004). Binding of CaM to IL2 and the C-terminal tail is observed in the 5-HT_{2C} receptor (Turner and Raymond, 2005). The general observation is that when CaM binding occurs via the intracellular loops of GPCRs then there is an attenuation of G-protein coupling [reviewed in (Ritter and Hall, 2009)].

The purpose of this chapter was to determine whether the repertoire of CaM-binding GPCRs extends to KISS1R. The work described in this chapter supports the role of CaM binding to KISS1R. However, the reader is directed to chapter 4 in order to appreciate the functional relevance of CaM binding to KISS1R.

3.2. Aim and hypothesis

The aim of this chapter is:

- Determine whether CaM binds to KISS1R, and if so, characterise the site(s) of interaction.

The hypothesis of this chapter is:

- Ca^{2+}/CaM binds to the KISS1R.

3.3. Results

3.3.1. Ca^{2+}/CaM binding to KISS1R intracellular loops

Several research groups have demonstrated that CaM can modulate the activity of a hand full of GPCRs [as reviewed in (Ritter and Hall, 2009)]. However, our knowledge is severely constrained as to the type and number of likely CaM binding GPCRs. Therefore, I have selected two GPCRs that are critical for reproductive health – the human kisspeptin receptor (KISS1R) and gonadotropin releasing hormone receptor (GnRHR). In order to determine whether CaM binds KISS1R and/or GnRHR, peptides that correspond to the intracellular loops of GnRHR and KISS1R, and the C-terminal tail (in the case of KISS1R) were titrated against fluorescently labelled CaM using a spectrofluorimetric CaM binding assays (see section 2.13).

Peptides that correspond to the intracellular loops (IL 1-3) of KISS1R and GnRHR, and the C-terminal tail (C-tail) of KISS1R were synthesized by EZBiolab, USA at > 95% purity (the peptide sequences are shown in Figures 3.1, 3.2, 3.4, and 3.6). These peptides were then reacted with two different CaM probes containing chemical fluorophores. The first of these probes was TA-CaM (see section 2.13), which allowed for the measurement of the hydrophobic conformational change of K^{75}. The probe is positioned in the flexible linker region of CaM. Another fluorescent probe termed DA-CaM was used. Briefly, double mutants (T34C/T110C) of CaM was generated and chemically labelled with IAEDANS and DDP fluorophores. The two probes form a Förster resonance energy transfer (FRET) pair. Upon DA-CaM binding to target peptide the donor IAEDANS fluorescence is quenched by the acceptor DDP, indicating close proximity of the probes, i.e. the closure of the N- and C- lobes of CaM (see section 2.13). Both the DA-CaM and TA-CaM had high basal fluorescence intensities, which decreased upon binding to target peptide.

The KISS1R intracellular loop 1 ($IL1^{67-80}$) peptide is 14 amino acids long and contains 4 basic residues positioned mainly in the N-terminus and 4 bulky hydrophobic residues mostly positioned at the C-terminus. The peptide sequence

contains a proline amino acid towards the half-way point (6th amino acid) of KISS1R-IL1$^{67-80}$ (Figure 3.2A). The titration of KISS1R-IL1$^{67-80}$ peptide (titration range: 0 to 100 μM) against TA-CaM gave little fluorescence reduction (Figure 3.2B). However, the titration of KISS1R-IL1$^{67-80}$ peptide against DA-CaM (titration range: 0 to 50 μM) gave an initial fluorescence reduction of approximately 10 % with the addition of 10 μM KISS1R-IL1$^{67-80}$ peptide, and gave no further fluorescence reduction with increased peptide concentration (Figure 3.2C). These observations were contrasted with the use of a high affinity CaM binding peptide called Trp peptide (RRKWQKTGHAVRAIGRL; single-letter amino acid code), the sequence is derived from the CaM binding domain of (residue 797-813) of smooth muscle myosin light chain kinase (MLCK) (Torok et al., 1998). The Trp peptide at 5 μM reduced DA-CaM fluorescence by approximately 85 % (Figure 3.2C).

The GnRHR-IL1$^{59-78}$ peptide is 20 amino acids long with 3 bulky hydrophobic residues spread along the full length of the peptide and 9 basic residues dispersed between them. This peptide sequence contains a glycine residue at the 12th amino acid position (Figure 3.2D). The GnRHR-IL1$^{59-78}$ peptide titrated against DA-CaM (titration range: 0 to 50 μM) gave undetectable fluorescence reduction, this was in stark contrast to the observation that 5 μM Trp peptide gave approximately 80 % fluorescence reduction of DA-CaM (Figure 3.2E)

The left shift of the spectral peaks of DA-CaM observed in panel C compared to panel E of figures 3.2, 3.3, and 3.5 were attributed to an instrumental artefact. Two different instruments were used, panel E was generated using FluroLog-3, manufactured by HORIBA scientific, and the remaining figures were generated using SLM aminco series spectrofluorimeter (8100 model).

The KISS1R intracellular loop 2 peptide (IL2$^{139-258}$) contains 20 amino acids with 8 bulky hydrophobic residues mostly positioned at the N-terminus and 6 basic residues mostly positioned at the C-terminus. This peptide sequence (KISS1R-IL2$^{139-258}$) contains two proline residues at the 9th and 19th amino acid positions (Figure 3.3A). The titration of KISS1R- IL2$^{139-258}$ peptide against TA- and DA-CaM (titration range: 0 to 500 nM) resulted in consistent reduction of fluorescence intensities (Figure 3.3B and 3.3C). The fluorescence intensity reduction observed for

DA-CaM was 32 ±13 % and TA-CaM was 27 ± 10 % upon saturating KISS1R-IL2$^{139-258}$ peptide (Figure 3.3). These levels were significantly lower than that of the 5 μM Trp peptide and DA-CaM mixture, which gave fluorescence reduction of approximately 80 %. The changes of the fluorescence intensities of TA-/DA-CaM were further analysed by plotting the emission fluorescence intensity values at 415 nm for TA-CaM and 480 nm for DA-CaM against peptide concentration (Figure 3.4 and Table 3.1). The obtained results show that KISS1R- IL2$^{139-258}$ peptide bound to DA-CaM with binding affinity of 23 ± 4 nM K_d and to TA-CaM at 82 ± 15 nM K_d (Table 3.1).

The GnRHR intracellular loop 2 (IL2$^{138-145}$) peptide contains 18 amino acids with 5 bulky hydrophobic and 4 basic residues dispersed among the sequence. The GnRHR-IL2$^{138-145}$ peptide contains a proline in the 9th amino acid position (Figure 3.3D). The DA-CaM mixed with GnRHR-IL2$^{138-145}$ peptide (titration range 0 to 50 μM) gave markedly less fluorescence intensity reduction (approx. 5 %) than that of 5 μM Trp peptide, which gave approximately 70 % reduction in fluorescence intensity (Figure 3.3E).

The KISS1R intracellular loop 3 (IL3$^{227-263}$) peptide contains 37 amino acids with 8 basic residues and 9 bulky hydrophobic residues spread throughout the length of the peptide. This sequence contains two proline amino acids at positions 12 and 14, and 3 glycine residues at positions 6, 21, and 29 (Figure 3.5A).The titration of KISS1R-IL3$^{227-263}$ peptide against TA-CaM and DA-CaM led to the largest reduction in fluorescence intensity (Figure 3.5C & D) compared with the other peptides tested (Figures 3.2, 3.3, and 3.7). Furthermore, 17 μM of KISS1R IL3$^{227-263}$ peptide was sufficient in quenching DA-CaM fluorescence similar to the extent with the addition of 5 μM Trp peptide (Figure 3.5D). The analysis of the changes of the fluorescence intensities of the spectral peaks (emission fluorescence values taken at 415 nm for TA-CaM and 480 nm for DA-CaM) showed a biphasic binding of the CaM probes to the KISS1R-IL3$^{227-263}$ peptide (Figure 3.6). Both TA-CaM and DA-CaM bound KISS1R-IL3$^{227-263}$ at two independent sites, with the first site having an affinity of 142 ± 65 nM for TA-CaM and 133 ± 98 nM for DA-CaM (Table 4.1). The second site of interaction was significantly lower in affinity for TA-CaM (12 ± 5 μM) and

DA-CaM (9 ± 3 μM). The level of the fluorescence reduction of TA-CaM binding to the first site of KISS1R-IL3$^{227-263}$ was 32 ± 2 % and the second site was 47 ± 4 %. The fluorescence reduction of DA-CaM to KISS1R-IL3$^{227-263}$ was 23 ± 5 % for the first site and 54 ± 4 % for the second site of KISS1R-IL3$^{227-263}$. Upon normalising the fluorescence reduction to saturating KISS1R-IL3$^{227-263}$ peptide concentrations, the B_{max} for TA-CaM binding to the first site was 41 ± 6 % and the second site was 60 ± 5 %. The B_{max} for DA-CaM binding to the first site of KISS1R-IL3$^{227-263}$ peptide was 30 ± 8 % and the second was 73 ± 6 % (Table 4.1).

The GnRHR intracellular loop 3 (IL3$^{230-270}$) peptide is composed of 40 amino acids with 12 bulky hydrophobic amino acids and 9 basic residues spread throughout the length of the peptide. The GnRHR-IL3$^{230-270}$ peptide contains 2 proline residues at amino acid positions 16 and 32 (Figure 3.5B). The addition of GnRHR-IL3$^{230-270}$ peptide against DA-CaM (titration range: 0 to 50 μM) gave approximately 15 % in fluorescence reduction and resulted in a left shift of the spectral peaks (Figure 3.5E)

The KISS1R C-terminal tail (C-tail$^{340-360}$) peptide is composed of 21 amino acids with 7 basic residues that mostly form 3 repeating motifs of PRR. This peptide sequence contains 7 proline residues in the amino acid position of 3, 6, 9, 12, 14, 17, and 20. Also contained in the KISS1R- C-tail$^{340-360}$ is a glycine residue in the 13th amino acid position. The titration of this peptide against TA- and DA-CaM gave undetectable change in fluorescence intensity (Figure 3.7)

To test whether CaM binding to KISS1R-IL3 peptide was Ca^{2+} dependent, DA-CaM binding to KISS1R-IL3$^{227-263}$ in the presence or absence of $CaCl_2$ was measured. In 100 μM $CaCl_2$, DA-CaM mixed with 100 μM KISS1R-IL3$^{227-263}$ reduced the fluorescence intensity by approximately 80 % and regained fluorescence intensity with the addition of 5 mM EGTA (Figure 3.8). This revealed that DA-CaM binding to KISS1R-IL3 peptide was Ca^{2+} dependent.

Next, I wanted to know whether peptides derived from the C-terminal region of the Gα-subunit of the heterotrimeric G proteins can displace the DA-CaM bound KISS1R-IL3$^{227-263}$ complex. To do this, C-terminal peptides from four different Gα-subunit of the heterotrimeric G proteins (Figure 3.9) were synthesized (EZBiolab) at

> 95 % purity. None of the heterotrimeric G protein peptides at 50 μM or less were found to displace DA-CaM bound to KISS1R-IL3$^{227-263}$ peptide (Figure 3.9).

In summary, the probes of TA- and DA-CaM gave significant fluorescence changes predominantly when titrated against KISS1R-IL3 and to a lesser extent -IL2, but not to -IL1 or -C-terminal tail (tested region). Nor did TA- and DA-CaM give significant fluorescence intensity change when titrated with intracellular loops of GnRHR. Furthermore, the binding of DA-CaM to KISS1R-IL3 was observed to be Ca^{2+} dependent. It was interesting to note that the Gα peptides did not displace the CaM.KISS1R-IL3 complex; this will later be evaluated in the discussion section of this chapter.

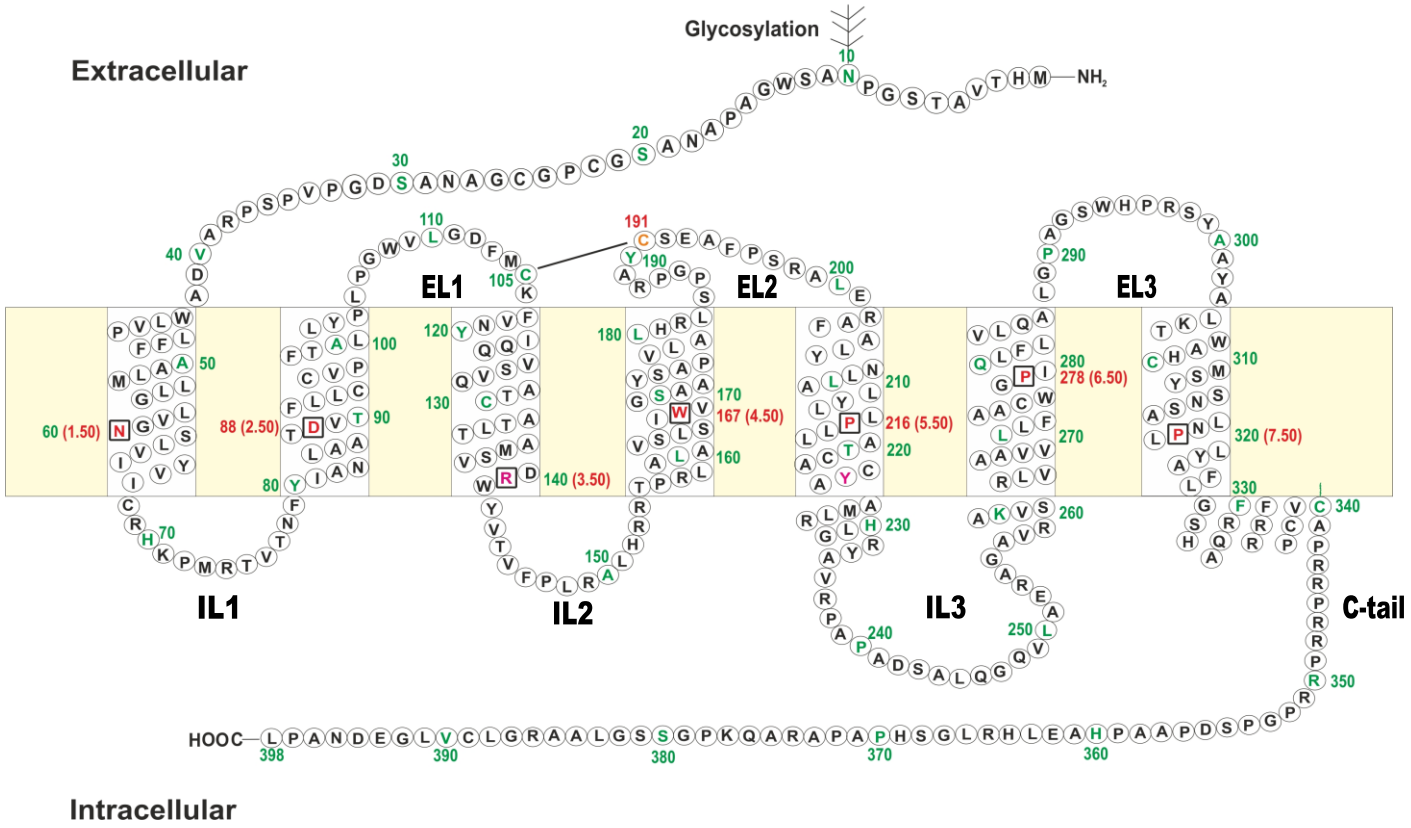

Figure 3.1 Schematic depiction of the human KISS1R primary amino acid sequence. This diagram shows the transmembrane domains embedded into the plasma membrane in yellow and connected by extracellular loops (EL1-3) and intracellular loops (IL1-3). The amino acid sequence is identifiable in green and the most highly conserved residues are indicated in red.

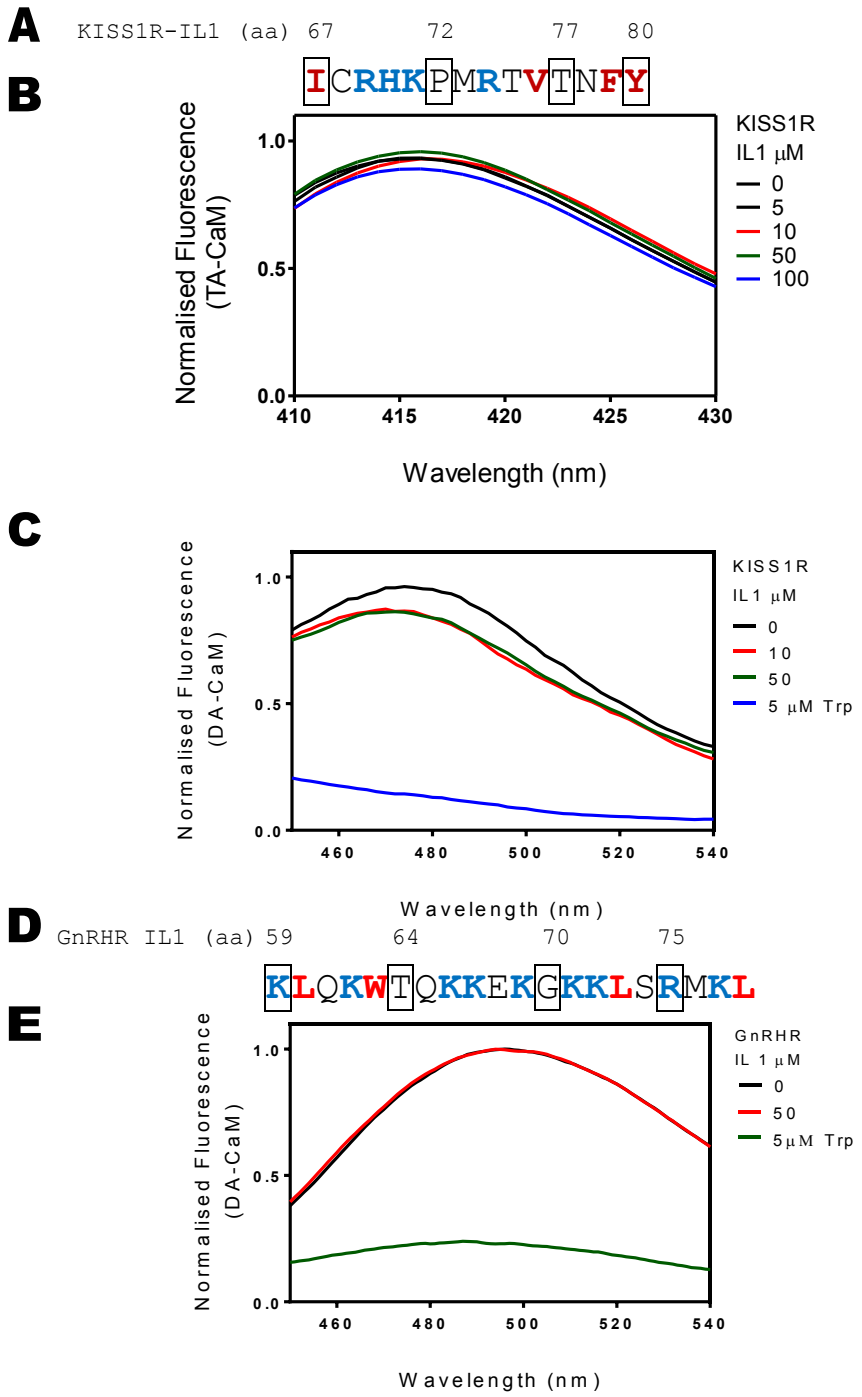

Figure 3.2 Emission fluorescence spectra of TA- and DA-CaM titrated against intracellular loop 1 peptides from KISS1R & GnRHR. The amino acid sequence of intracellular loop 1 (IL1) peptides derived from human KISS1R (**A**) and GnRHR (**D**) was synthesised; red indicates bulky hydrophobic amino acids, while blue depicts basic residues and the amino acid (aa) number is identifiable with numbering above the boxed letters. IL1 peptides were titrated against 100 nM TA-CaM (**B**) or 1 μM DA-CaM (**C & E**) in the presence of assay buffer (see section 2.13) containing 100 μM $CaCl_2$. TA-CaM (**B**) fluorescence was determined at excitation wavelength 366 nm and emission wavelength 410-430 nm. (**C & E**) DA-CaM fluorescence was measured at excitation wavelength 365 nm and emission wavelength 450-540 nm.

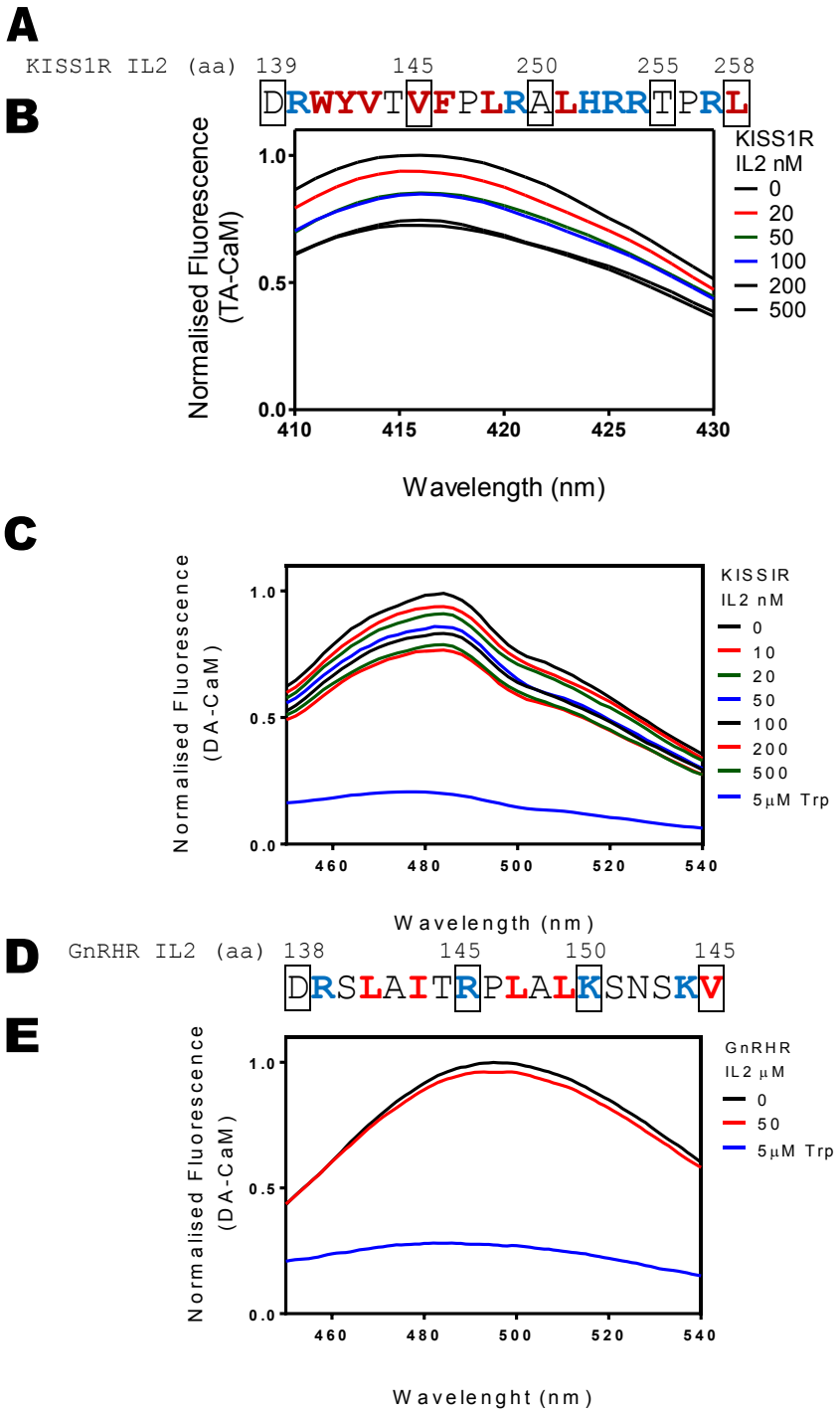

Figure 3.3 Emission fluorescence spectra of TA- and DA-CaM titrated against intracellular loop 2 peptides from KISS1R & GnRHR. The amino acid sequence of intracellular loop 2 (IL2) peptides derived from human KISS1R (**A**) and GnRHR (**D**) was synthesised; red indicates bulky hydrophobic amino acids, while blue depicts basic residues and the sequence is identifiable with numbering above the boxed letters. IL2 peptides were titrated against 100 nM TA-CaM (**B**) or 1 μM DA-CaM (**C & E**) in the presence of assay buffer (see section 2.13) containing 100 μM $CaCl_2$. TA-CaM (**B**) fluorescence was determined at excitation wavelength 366 nm and emission wavelength 410-430 nm. DA-CaM (**C & E**) fluorescence was measured at excitation wavelength 365 nm and emission wavelength 450-540 nm.

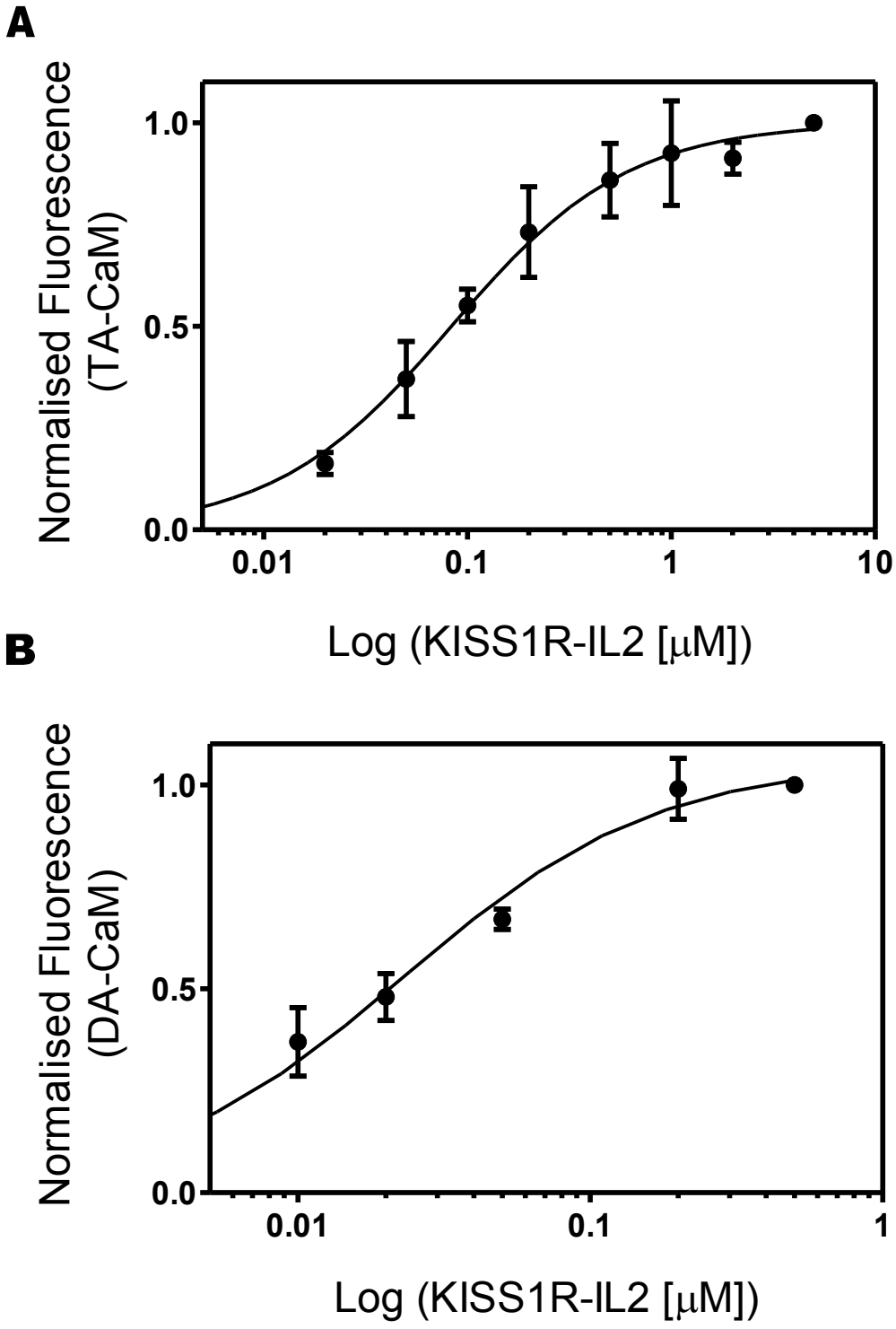

Figure 3.4 TA/DA-Calmodulin binding to KISS1R- IL2. (A) 100 nM TA-CaM or (B) 1 μM DA-CaM and 100 μM $CaCl_2$ were reacted with increasing concentrations of IL2 peptide. Fluorescence was determined at excitation wavelength at (A) 366 nm, (B) 365 nm and emission wavelength (A) 415 nm, (B) 480. The average values of three repeats were plotted and the error bars show the S.E.M. The data was fitted to a one-site model. The values are displayed in Table 4.1.

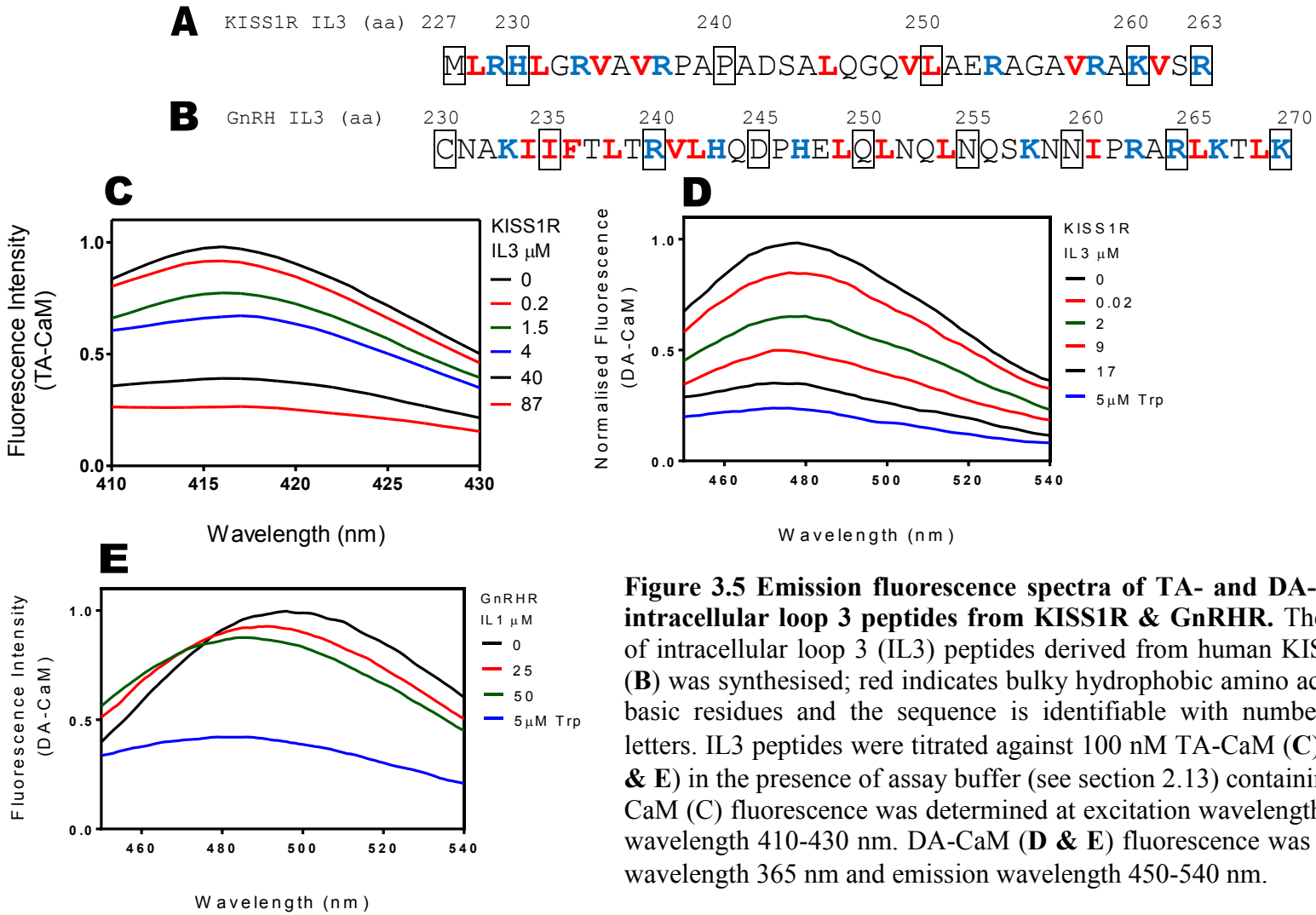

Figure 3.5 Emission fluorescence spectra of TA- and DA-CaM titrated against intracellular loop 3 peptides from KISS1R & GnRHR. The amino acid sequence of intracellular loop 3 (IL3) peptides derived from human KISS1R (**A**) and GnRHR (**B**) was synthesised; red indicates bulky hydrophobic amino acids, while blue depicts basic residues and the sequence is identifiable with numbering above the boxed letters. IL3 peptides were titrated against 100 nM TA-CaM (**C**) or 1 µM DA-CaM (**D & E**) in the presence of assay buffer (see section 2.13) containing 100 µM $CaCl_2$. TA-CaM (C) fluorescence was determined at excitation wavelength 366 nm and emission wavelength 410-430 nm. DA-CaM (**D & E**) fluorescence was measured at excitation wavelength 365 nm and emission wavelength 450-540 nm.

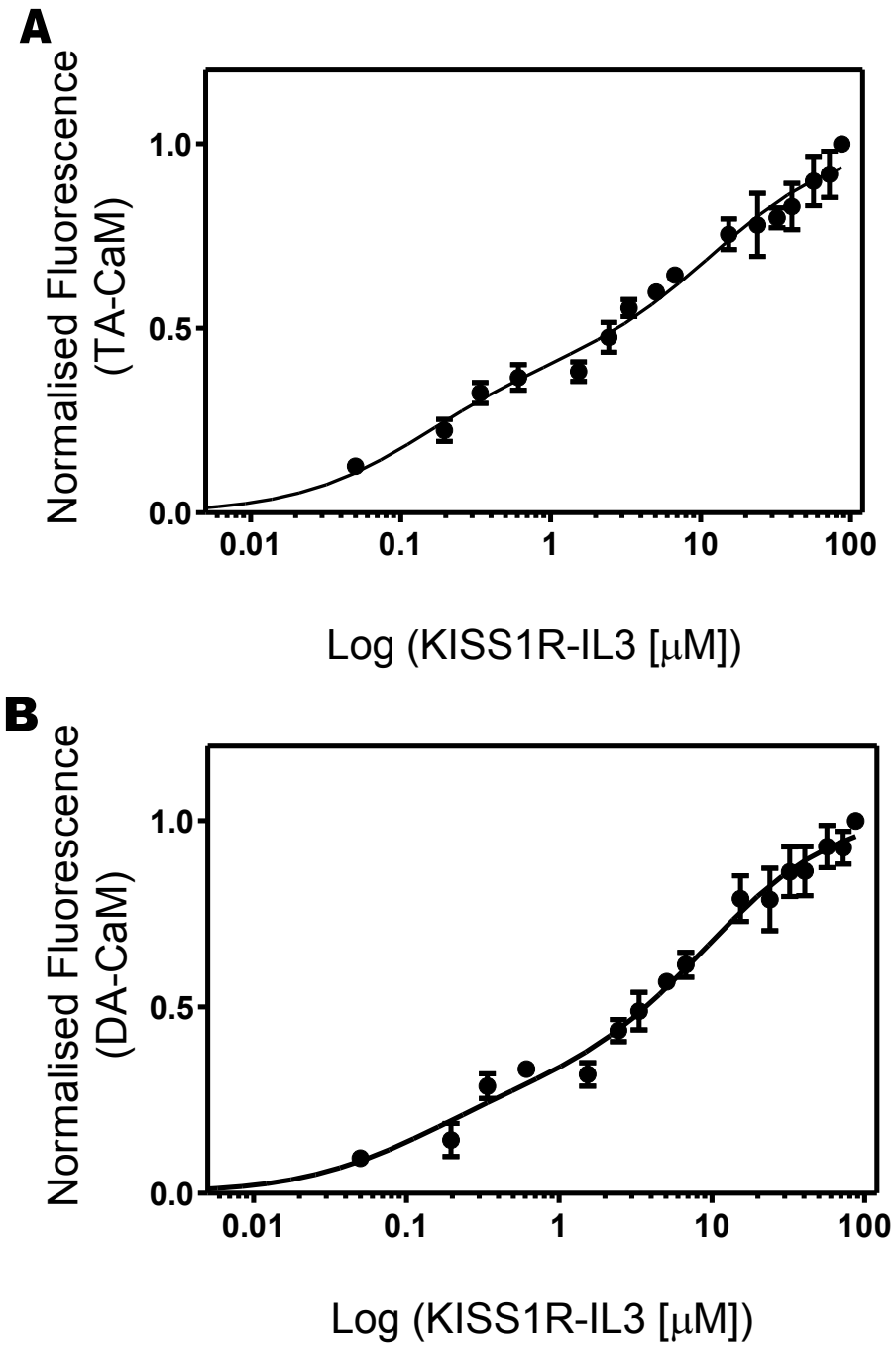

Figure 3.6 TA/DA-Calmodulin binding to KISS1R-IL3. (A) 100 nM TA-Calmodulin or (B) 1 μM DA-Calmodulin and 100 μM $CaCl_2$ was reacted with increasing concentrations of IL3 peptide. The experiments were carried out at 21°C, pH 7.0 in an assay buffer containing 100 mM KCl, 50 mM K^+- PIPES, and 2 mM $MgCl_2$. Fluorescence was determined at excitation wavelength at (A) 366 nm, (B) 365 and emission wavelength (A) 415 nm, (B) 480. The average values of three repeats were plotted and the error bars show the S.E.M. The data was fitted to a two-site model. The values are displayed in Table 4.1.

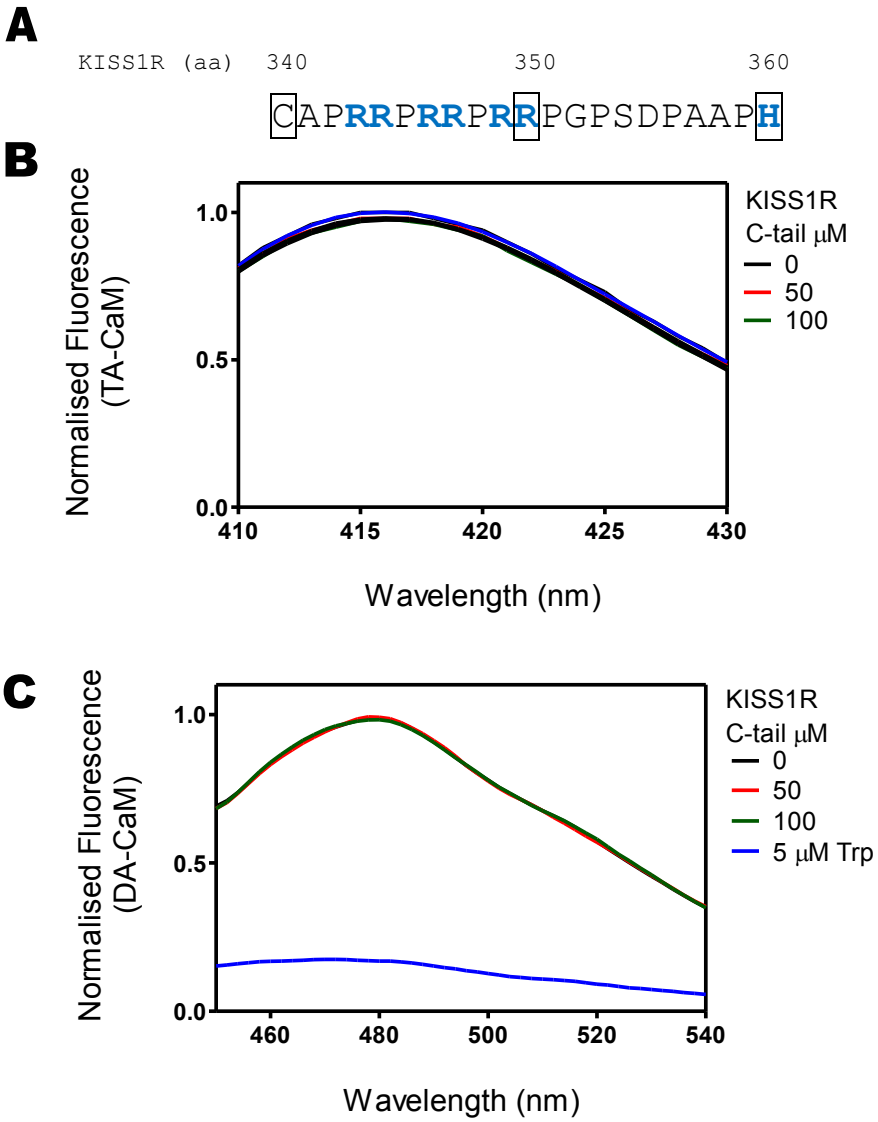

Figure 3.7 Emission fluorescence spectra of TA- and DA-CaM titrated against C-terminal tail fragment peptide of KISS1R. The amino acid sequence of the C-terminal fragment peptide (C-tail) derived from human KISS1R (**A**) was synthesised; red indicates bulky hydrophobic amino acids, while blue depicts basic residues and the sequence is identifiable with numbering above the boxed letters. The C-tail fragment peptide was titrated against 100 nM TA-CaM (**B**) or 1 μM DA-CaM (**C**) in the presence of assay buffer (see section 2.13) containing 100 μM $CaCl_2$. TA-CaM (**B**) fluorescence was determined at excitation wavelength 366 nm and emission wavelength 410-430 nm. DA-CaM (**C**) fluorescence was measured at excitation wavelength 365 nm and emission wavelength 450-540 nm.

Table 3.1 Summary of TA/DA-CaM binding to KISS1R-IL2 and IL3. This table shows the values of the plotted graphs shown in Figures 3.4 and 3.6. The standard error shows the error of the fit. Note, only IL3 had two site binding properties.

Intracellular region	K_d				B_{max}			
	Site -1 (nM)		Site-2 (μM)		Site -1 (%)		Site-2 (%)	
	TA-CaM	DA-CaM	TA-CaM	DA-CaM	TA-CaM	DA-CaM	TA-CaM	DA-CaM
IL 2	82 ± 15	23 ± 4	-	-	100	100	-	-
IL 3	142 ± 65	133 ± 98	12 ± 5	9 ± 3	41 ± 6	30 ± 8	60 ± 5	73 ± 6

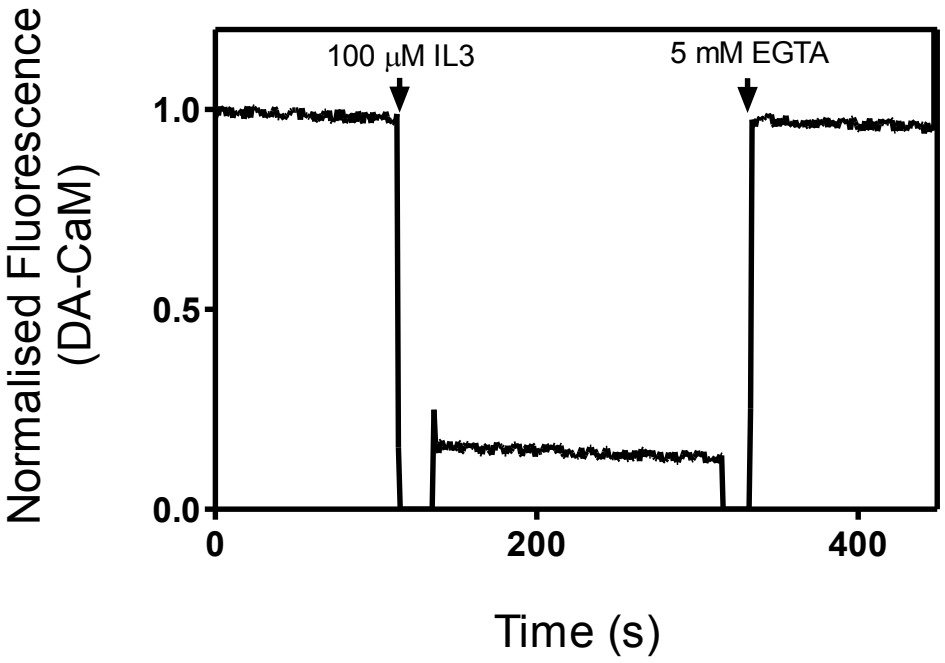

Figure 3.8 Ca^{2+} dependent DA-CaM binding to KISS1R-IL3. DA-CaM 1μM, in the presence of assay buffer (see section 2.13) containing 100 μM $CaCl_2$ was preincubated at 21 °C; DA-CaM fluorescence intensity was normalised to 1. At the point indicated by an *arrow*, 100 μM KISS1R-IL3 was added, resulting in substantial quenching of DA-CaM fluorescence, indicating a conformation in where the two globular domains of DA-CaM are compacted around KISS1R-IL3. As indicated by the second arrow, at 335 s, 5 mM EGTA was added, resulting in unquenching of DA-CaM fluorescence. This indicated the stretching of DA-CaM to an extended conformation and presumably releasing KISS1R-IL3. The excitation wavelength was set at 365 nm and emissions at 500 nm.

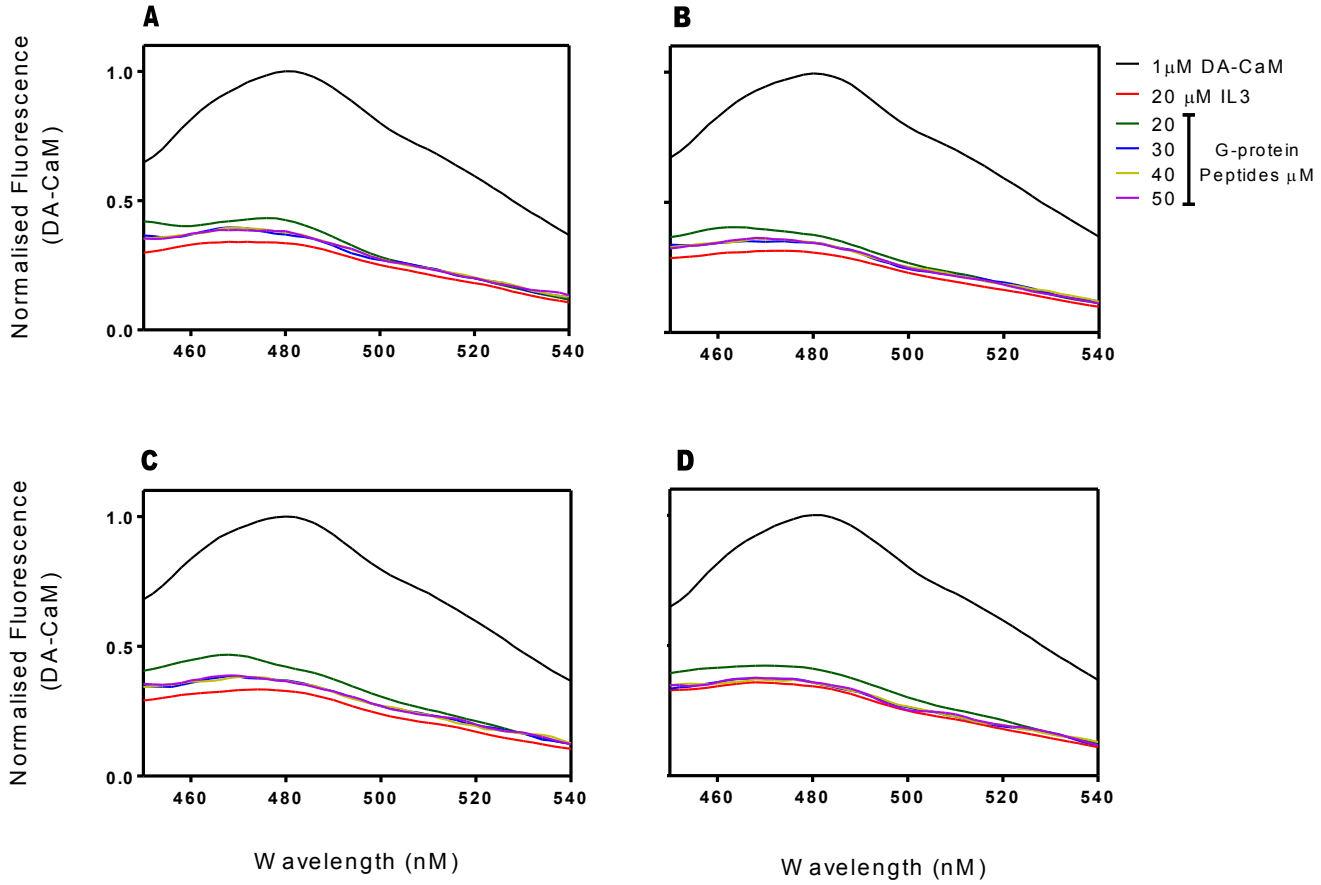

Figure 3.9 Peptides derived from the Gα-subunit of the heterotrimeric G proteins do not antagonise the CaM.KISS1R-IL3 complex. The G protein derived C-terminal peptides with variable amino acid sequences (table 3.2) were synthesised and titrated against 1 μM DA-CaM in the presence of assay buffer (see section 2.13) containing 100 μM $CaCl_2$. DA-CaM fluorescence was measured at excitation wavelength 365 nm and emission wavelength 480 nm. (A) Gqα peptide (B) G13α peptide (C) Gi3α peptide (D) Gsα peptide

Table 3.2 Human G protein α-subunits derived C-terminal peptides
The amino acid sequence of the peptides used in Figure 3.9. All the peptides were synthesised from EZ Biolabs at > 95 % purity.

Gα protein peptide	Amino Acid Sequence	NCBI Reference Sequence
(A) Gqα-C-Terminus (349-359)	LQLNLKEYNLV	P29992.2
(B) G13α-C-Terminus (272-282)	LHDNLKQLMLQ	NP_001269354.1
(C) Gi3α-C-Terminus (344-354)	IKNNLKECGLY	AAM12621.1
(D) Gsα-C-Terminus (384-394)	QRMHLRQYELL	P63092.1

3.3.2. Ca^{2+} and KP-10 dependent CaM binding to KISS1R

The selective binding of CaM to IL2 and IL3 peptides derived from the KISS1R, raised the important question of whether CaM can bind to the intact KISS1R expressed in cells, and whether the interaction is ligand and/or Ca^{2+} dependent. To answer this question, HEK-293 cells were used in co-immunoprecipitation experiments, transiently expressing FLAG-KISS1R and immunoblotting for endogenous CaM. Also, colocalisation experiments were carried using YFP-Chimeric-KISS1R and CFP-CaM co-expressed in HEK-293 cells.

To test the putative interaction between CaM and KISS1R in cells co-immunoprecipitation (Co-IP) experiments were carried out (see section 2.25). The cDNA vector of the N-terminal FLAG-tagged KISS1R was transiently transfected into HEK-293 cells. The FLAG-tag did not affect kisspeptin-10 (KP-10) binding or the signalling properties as compared to wild-type KISS1R (Figure 3.10, Table 3.3, Figure 3.11 and Table 3.4). The expression of FLAG-KISS1R was confirmed by the observation that the transfected-non-stimulated (TNS) band intensities were significantly ($P < 0.05$) increased relative to the non-transfected (NT) cells (Figure 3.12). Furthermore, the FLAG-KISS1R band intensities showed no significant ($P > 0.05$) change between KP-10 stimulated and TNS samples (Figure 3.12). These experiments revealed that FLAG-KISS1R could be detected when expressed and showed little variation in band intensity upon KP-10 stimulation. All the kisspeptin ligands bind to the KISS1R with nanomolar affinities and have indistinguishable signalling efficacies (Kotani et al., 2001). Therefore, the KP-10 ligand was used in further experiments because it was the shortest and the most stable peptide (Kotani et al., 2001). As expected, endogenous CaM was found to interact with the FLAG-KISS1R in Co-IP complex ($P < 0.05$) only upon KP-10 stimulation (Figure 3.12). This was determined by immunoblots with specific monoclonal anti-calmodulin antibody and the molecular weight was verified with purified calmodulin (Figure 3.12) as an indicator (Ind).

To test whether Ca^{2+} can promote CaM binding to FLAG-KISS1R expressed HEK-293 cell lysates, exogenous $CaCl_2$ was added into the lysate slurry (Figure 3.13). When the cells were not stimulated by KP-10 agonist, FLAG-KISS1R did not Co-IP with endogenous CaM, but did with exogenous addition of $CaCl_2$ concentrations (Figure 3.13). This interaction was disrupted by addition of the CaM inhibitor, calmidazolium (Figure 3.13).

To further validate the interaction between CaM and the KISS1R, co-localisation experiments were carried out using CFP-CaM and YFP-Chimeric-KISS1R transiently expressed in HEK-293 cells (Figure 3.14 and Figure 3.16). The YFP-Chimeric-KISS1R has the N-terminal region replaced with that of the Galanin receptor N-terminal region. The YFP-Chimeric-KISS1R was chosen for its properties of right-shift dose response curve (Figure 3.11), this enabled for the study of a receptor form that existed more in the inactive state than wild-type KISS1R, which had been shown to have constitutive activity (Pampillo and Babwah, 2010). The obtained confocal images showed that in CFP-CaM expressing cells the fluorophore appeared to be ubiquitously expressed throughout the cell (Figure 3.14). The YFP-Chimeric-KISS1R expressing cells appeared to be localised to the cell membrane and around what was presumed to be the nucleus (Figure 3.15). However, when both constructs were co-expressed in the same cell, a high degree of co-localisation in the membrane was observed. This basal colocalisation of CaM and KISS1R was observed in some populations of cells (Figure 3.16). However, the majority of cells did not express co-localisation.

Taken together, these results provided the first evidence that CaM selectively binds to IL2 and IL3 peptides derived from the KISS1R, and that CaM bind to the intact KISS1R expressed in HEK-293 cells in a KP-10/Ca^{2+} dependent manner. Additionally, the three independent methods of spectrofluorimetry, confocal microscopy, and co-immunoprecipitation, all validate each other. However, it remains to be further confirmed by testing the underlying sites of interaction(s) and the functional relevance of the interaction. In the following chapter these questions were experimentally addressed.

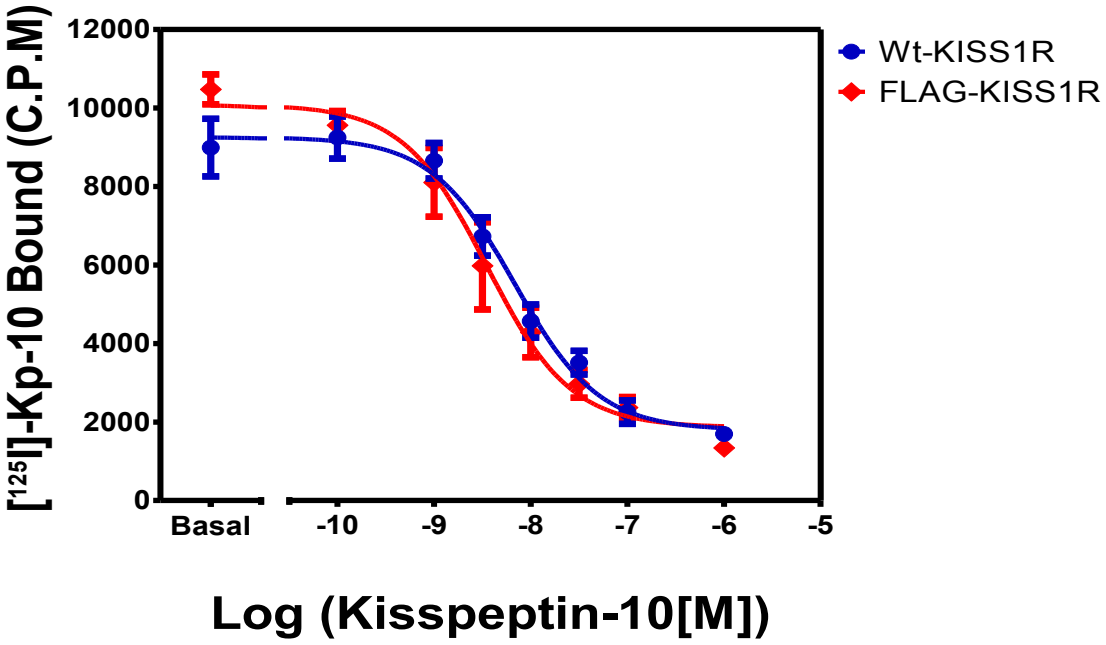

Figure 3.10 KP-10 binding to Wt-KISS1R and FLAG-KISS1R. COS-7 cells were transiently transfected with Wt-KISS1R (●) or N-terminal tagged FLAG-KISS1R (◆) 48 hours prior to the binding assay (see section 2.22). A representative trace of three independent repeats is shown.

Table 3.3 KP-10 binding to Wt-KISS1R and FLAG-KISS1R. The analysed data of Figure 3.10 shows the IC_{50} values of KP-10 binding to wild-type KISS1R FLAG-KISS1R transiently expressed in COS-7 cells.

Construct	IC_{50} [M]	S.E.M [M]
● Wt-KISS1R	7.44×10^{-9}	0.91×10^{-9}
◆ FLAG-KISS1R	5.21×10^{-9}	0.62×10^{-9}

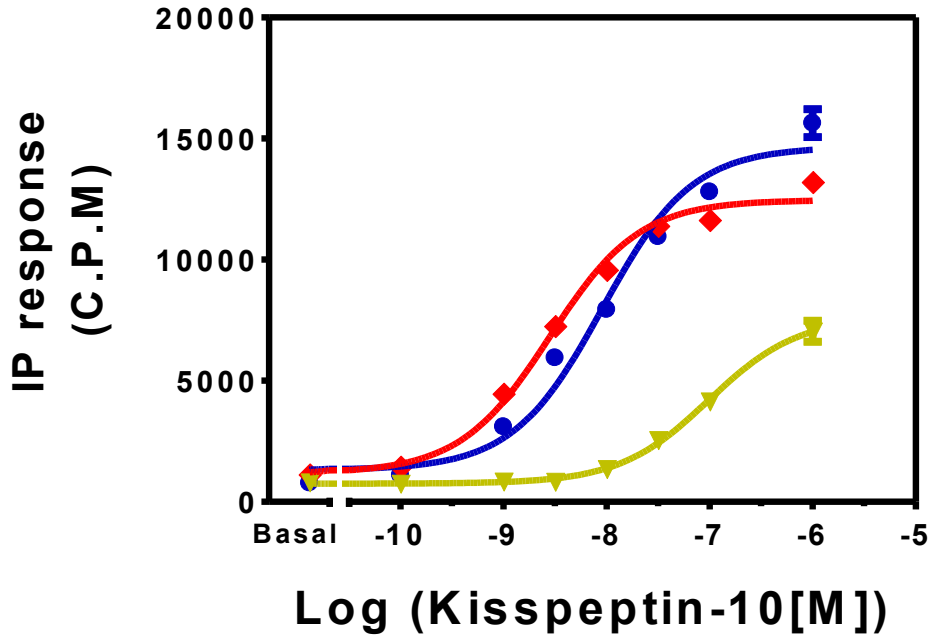

Figure 3.11 KP-10 induced IP_3 accumulation in COS-7 cells expressing KISS1R with or without tags. COS-7 cells were transiently transfected with different KISS1R constructs 48 hours prior to the IP_3 accumulation assay (see section 2.24). Wt-KISS1R (●), N-terminal fused FLAG-KISS1R (◆), and N-terminal YFP-Chimeric-KISS1R (▼) in where the N-terminal is replaced for the Galanin receptor. The results of the three independent experiments are shown with mean ± S.E.M.

Table 3.4 Comparison of KP-10 potency of the different tagged KISS1R constructs. Analysed data of Figure 3.11 show the EC_{50} values of KP-10 in stimulating IP_3 turnover transfected with different tagged KISS1R constructs. Asterisks (*) denote statistical significance (* P<0.05) as calculated with student 't' test.

Construct	EC_{50} [M]	S.E.M [M]
● Wt-KISS1R	3.4×10^{-9}	1.7×10^{-9}
◆ FLAG-KISS1R	5.27×10^{-9}	0.85×10^{-9}
▼ YFP-Chimeric-KISS1R	9×10^{-8}*	5.5×10^{-8}

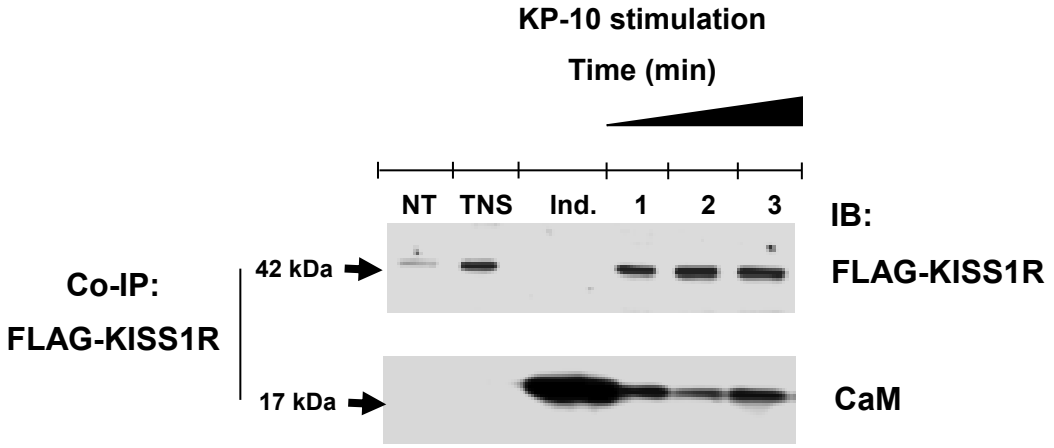

Figure 3.12 KP-10 dependent binding of FLAG-KISS1R to endogenous CaM. FLAG-KISS1R was transiently transfected into HEK-293 cells. At 48 hours post transfection the cells were stimulated with 100 nM KP-10 at 1 minute intervals and processed using the Co-IP method (see section 2.25). The samples were later immunoblotted (IB) with anti-FLAG M2 and anti-CaM antibodies. Lane NT denotes non-transfected cells and TNS is transfected non-stimulated stimulated cells. Purified CaM from bovine testes was used as the positive control (indicator, Ind.). A representative blot of three independent repeats is shown.

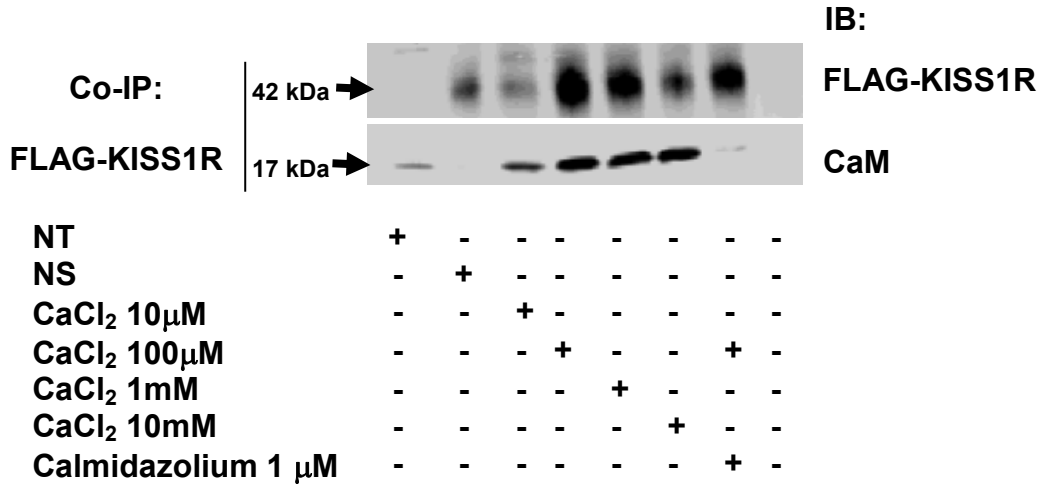

Figure 3.13 Ca^{2+} dependent binding of FLAG-KISS1R to endogenous CaM. HEK-293 cells were transiently transfected with FLAG-KISS1R 48 hours before incubation in lyses buffer containing indicated Ca^{2+} concentrations and Calmidazolium inhibitor. CaM and FLAG were detected via immunoblotting (IB). A representative blot of three independent repeats is shown.

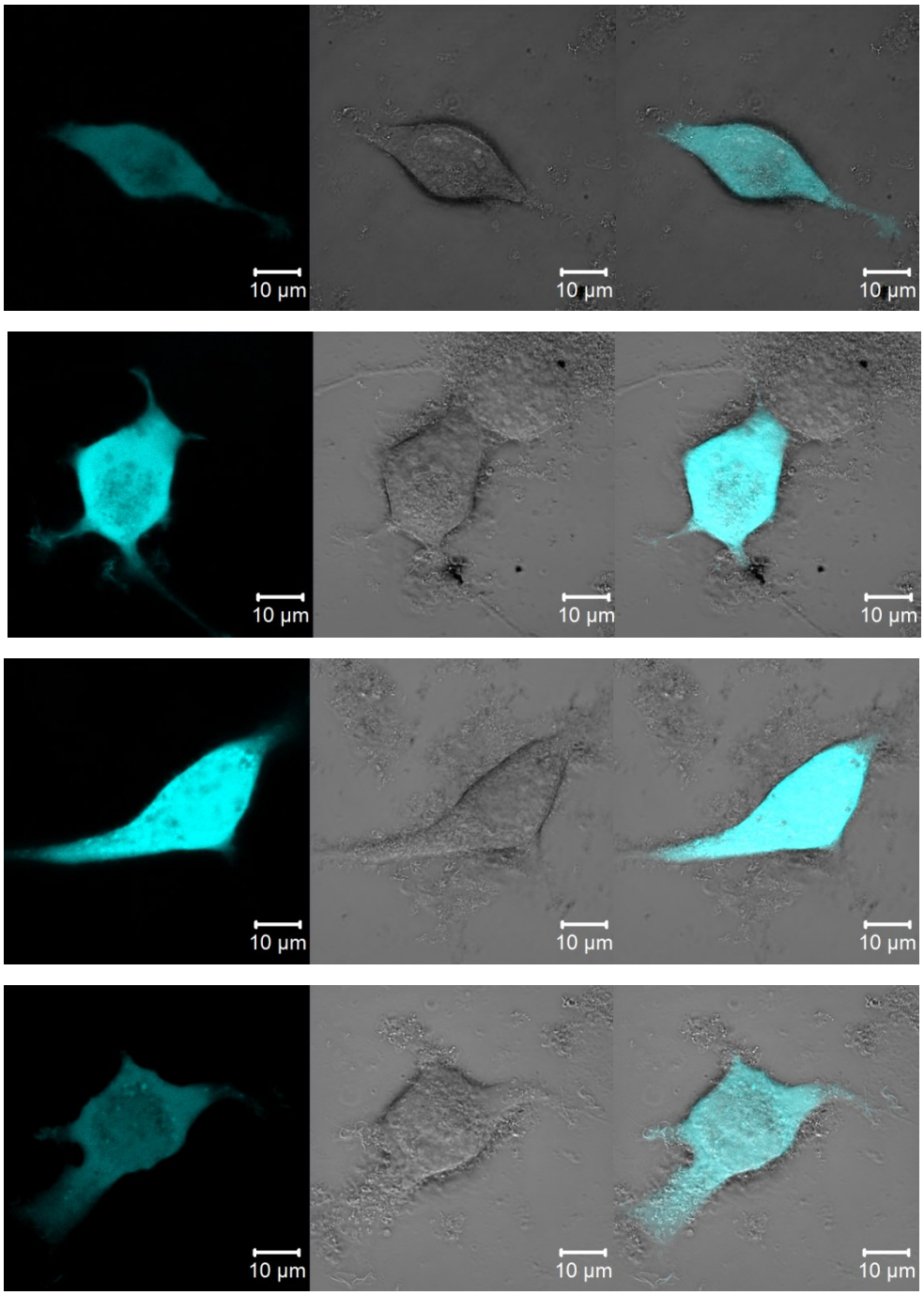

Figure 3.14 Ubiquitous expression of CFP-CaM in HEK-293 cells. Live cell imaging was made by using HEK-293 cells that were transiently transfected with CFP-CaM (Cyan colour) 48 h before confocal imaging. The right column is the fluorescence channel, the middle column is bright field and the left column is merged images.

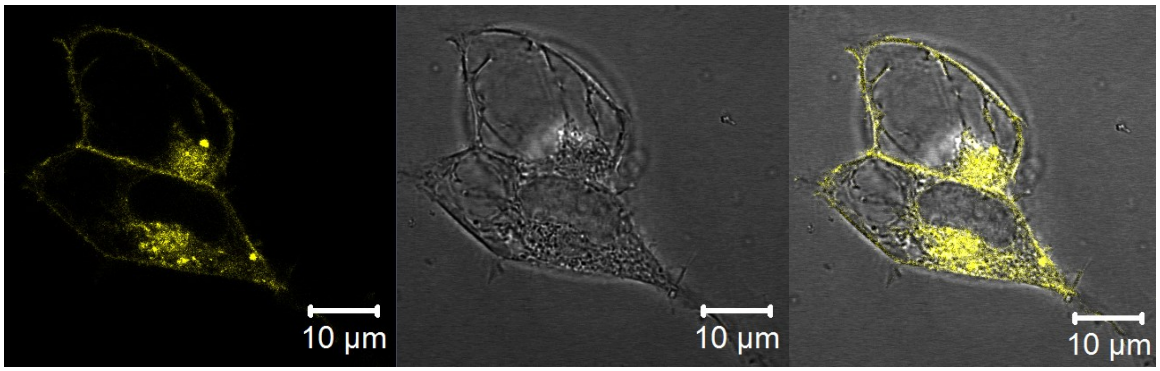

Figure 3.15 YFP-Chimeric-KISS1R expression in HEK-293 cells. Live cell imaging was obtained using HEK-293 cells that were transiently transfected with YFP-Chimeric-KISS1R (Yellow colour) 48 h before confocal imaging. The right column is the fluorescence channel, the middle column is bright field and the left column is the merged images.

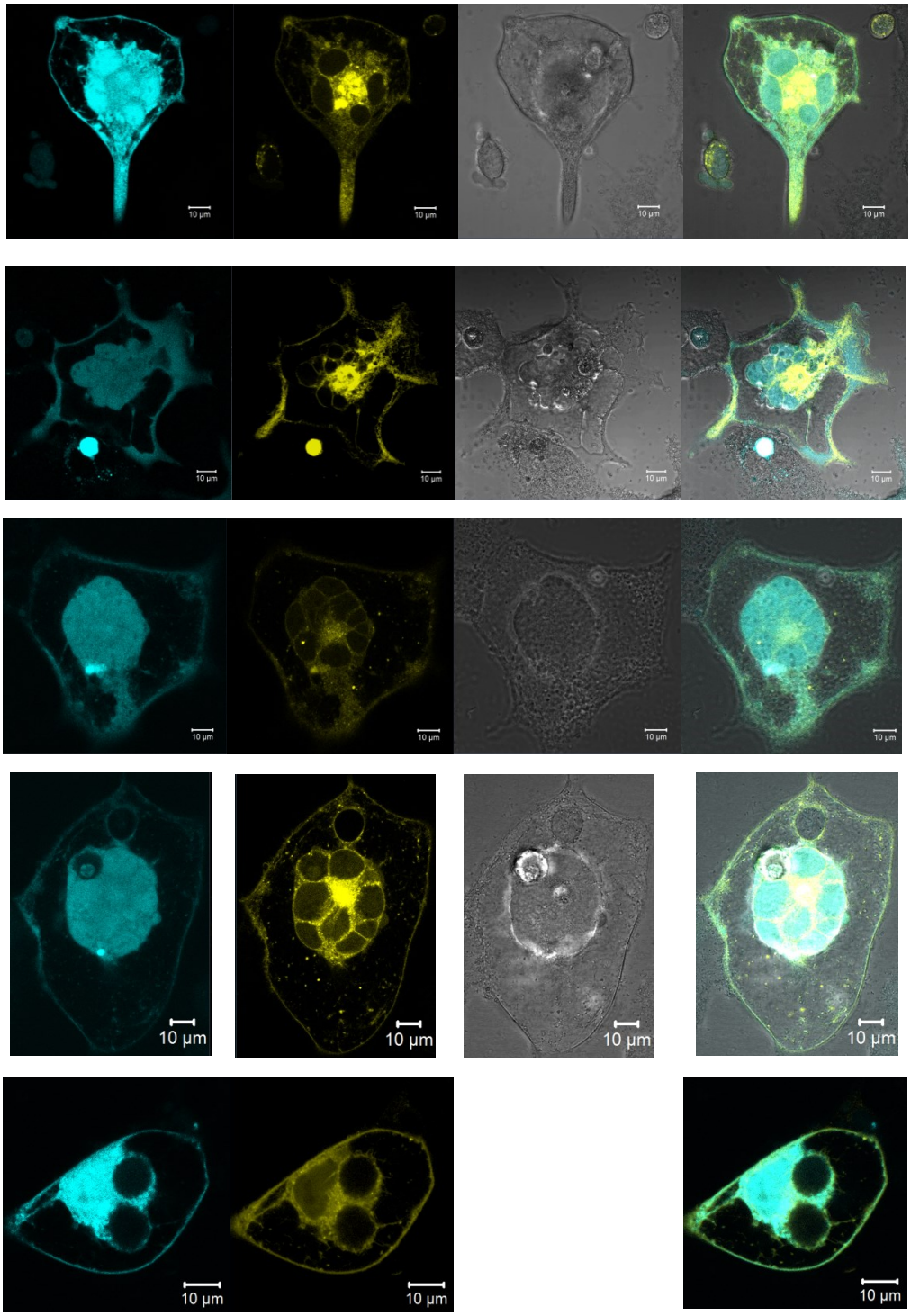

Figure 3.16 Colocalisation of CFP-CaM and YFP-Chimeric-KISS1R in HEK-293 cells. Live cell imaging of HEK-293 cells were carried out by transiently transfection of YFP-Chimeric-KISS1R (Yellow colour) and CFP-CaM (Cyan colour) 48 h before confocal imaging. From the left, CFP-CaM fluorescence channel, then the YFP-Chimeric-KISS1R fluorescence channel, followed by the bright field channel (with exception of the bottom image), and finally the merged images.

3.4 Discussion

Calmodulin (CaM) is a multifunctional signalling adaptor protein that transduces Ca^{2+} signals by binding Ca^{2+} ions and then interacts with target proteins to modify their structure and function. These include several GPCRs, which have been shown to interact with CaM [Reviewed in (Ritter and Hall, 2009)]. However, whether the CaM binding GPCRs extends to the kisspeptin receptor (KISS1R) was not known. Therefore, following the reductionist approach, this study set out to determine the affinity of CaM binding to the intracellular regions of KISS1R. Indeed, there was CaM binding to IL2 and IL3 and not to IL1, or C-terminal tail (tested region) of the KISS1R, or to IL1-IL3 of GnRHR. Further validation was carried out with confocal imaging, which appeared to show that CaM and KISS1R colocalise in the periphery of the cell in some cells. Also, KISS1R was found to interact with endogenous CaM in a ligand and Ca^{2+} dependent manner by assays.

The binding of CaM to the intact KISS1R in cells was confirmed by co-immunoprecipitation (Co-IP) experiments. In HEK-293 cells, endogenous CaM and transiently transfected FLAG-KISS1R were found to Co-IP in an agonist- and Ca^{2+}-dependent manner at a time of $\leq$ 1 minute post stimulation (Figure 3.10 and 3.11). The rapid binding of CaM to the KISS1R upon agonist stimulation was deemed to be faster than the initiation of KISS1R internalization, which was shown to be ~ 5 minutes by Pampillo and Babwah (Pampillo and Babwah, 2010). Therefore, CaM binding to the KISS1R occurs before the initiation of the agonist-induced KISS1R internalization. Furthermore, the KISS1R has been shown to exhibit basal constitutive activity and internalization (Pampillo and Babwah, 2010). It was thus unclear whether CaM binds the inactive state of the KISS1R.

In an attempt to address this, a chimeric KISS1R was utilised, where the N-terminal of KISS1R was replaced with that of the Galanin receptor and the C-terminal was fused with YFP. The YFP-chimeric-KISS1R construct exhibited a (10-fold) right-shifted dose-response curve (Figure 3.11), implying that the chimeric receptor has decreased ligand potency and signalling efficacy, but remains functional in terms of activating G-proteins. The expressed protein was observed to colocalise with CFP-CaM in the cell periphery of HEK-293 cells (Figure 3.14). The basal

colocalisation was observed in some cells and not all. The cells that showed colocalisaiton were abnormal in shape and large in size implying that these cells are perhaps undergoing cell division or apoptosis. Apoptosis is known require increased cytosolic Ca^{2+} (Mattson and Chan, 2003). Therefore, if the cells are apoptotic the increased Ca^{2+} may drive the colocalisation. Another explanation may be due to the inherent Ca^{2+} dynamics in the cell throughout the mammalian cell-cycle, and especially during early G_1 and G_1/S and G_2/M transitions (Roderick and Cook, 2008). The first major Ca^{2+} transient occurs before cells enter mitosis, and the second is during the metaphase-anaphase transition (Roderick and Cook, 2008, Groigno and Whitaker, 1998). Additionally, the downstream protein targets for Ca^{2+} are also implicated in the cell cycle (Patel et al., 1999, Rasmussen and Means, 1989). Therefore, the basal colocalisation that is observed in some population of cells may be the result of those cells undergoing cell division or apoptosis and thus increased cytosolic Ca^{2+} that promotes CaM binding to KISS1R.

Although supported by Figure 3.13**,** showing the Ca^{2+} dependent binding of CaM to KISS1R in Co-IP, the confocal imaging results have significant limitations, these include; that the minority of cells that showed colocalisation were also of poor viability. The study examined the basal interaction and not the KP10 stimulated interaction. KP10 stimulation was attempted but exhibited technical difficulties in terms of simultaneous stimulation and imaging and the high KP10 concentration that was required to activate the YFP-chimeric-KISS1R. YFP-chimeric-KISS1R may have altered trafficking properties because of the replaced N-terminal. The Wild-type KISS1R-YFP was created to address some of these issues but the expression was poor, possibly due to the pEYFP vector. Immunohistochemistry (IHC) was considered but ruled out because the real-time dynamic interaction will not be appreciated and direct protein-protein interactions cannot be determined even with IHC-FRET, as the spatial distance of the probes via primary and secondary antibodies will increase the measured distance of the interaction significantly to ~140 Å, and are substantially flexible to influence their absolute positions (Snapp and Hegde, 2006). Future experiments should entail the optimisation of Wild-type KISS1R-YFP expression, the use of CFP-CaM in a FRET study with and without KP10 stimulation, and a perfusion culture chamber to properly administer the KP10

while simultaneously imaging the live-cells. This approach will determine the spatial distance of CaM and KISS1R to < 100 Å and image the real-time dynamic interaction (Selvin, 2000). This approached although desirable will have limitation in the photobleaching of CFP and YFP and therefore increased the signal-to-noise ratio. Furthermore, the probes may interfere with the structural interaction between KISS1R and CaM.

These results are in concurrence with other research showing CaM Co-IP with some GPCRs. For example, CaM has been shown to interact with 5-Hydroxytryptamine 2A and 2C (5-HT_{2A} and 5-HT_{2C}) receptors in a Ca^{2+} and agonist dependent manner (Labasque et al., 2008, Turner and Raymond, 2005). Also, CaM Co-IP with the Vasopressin (V2) receptor has been shown to be Ca^{2+} dependent (Nickols et al., 2004). These results are in contrast with the finding that CaM Co-IPs with the 5-HT_{1A} and Dopamine D_2 receptor in a constitutive, agonist-independent manner (Turner et al., 2004). However, intracellular Ca^{2+} signalling is complex and this constitutive interaction may partially be the result of 'cross-talk' from other signalling pathways, which may in turn promote CaM binding to D_2 and 5-HT_{1A}.

The inherent limitations of Co-IP experiments involving CaM and GPCRs cannot exclude the potential of indirect protein-protein interactions. For instance, one argument that may challenge CaM.KISS1R Co-IP is the following logic; CaM has been shown to bind G protein-coupled receptor kinases (GRKs) and β-arrestin (Pronin et al., 1997, Levay et al., 1998, Wu et al., 2006). Both β-arrestin and GRK-2 in turn have been shown to bind KISS1R (Pampillo et al., 2009). Thus, β-arrestin and GRK-2 may function to mediate CaM interaction with KISS1R.

However, upon careful consideration these arguments are refuted with the following explanations; CaM binds to the concave surface of the C-domain and a finger loop in the middle of the ß-arrestin molecule. These CaM-binding sites on the β-arrestin also overlap with receptor and microtubule binding sites. In fact, CaM binds ß-arrestin with a K_d of ~ 7 μM, and ß-arrestin binds its cognate receptors in the nanomolar affinity range. This means that ß-arrestin cannot bind to CaM and receptor simultaneously because these two interactions are mutually exclusive, making CaM an ineffective competitor for ß-arrestin binding in the presence of

highly expressed receptors (Wu et al., 2006). Therefore, ß-arrestin is unlikely to function as an intermediary interacting protein linking CaM and KISS1R.

Ca^{2+} bound CaM has been shown to inhibit the catalytic activity of all the GRKs (GRK2, -3, -4, -5, and -6) except GRK1 (Chuang et al., 1996). With GRK5 being the most sensitive to CaM (IC_{50} 40-50 nM) and GRK2 being the least sensitive (IC_{50} ~2 μM) (Chuang et al., 1996, Pronin et al., 1997). Pampillo (Pampillo et al., 2009) showed GRK2 interacted with KISS1R in the absence and presence of KP-10 agonist, implying that GRK2 and KISS1R form basal interaction. In addition, myc-GRK2 was found to interact predominantly with GST-IL2 of KISS1R, but in this thesis CaM was found to bind to IL3 of KISS1R (Figure 3.5 and 3.6). In addition, Pampillo overexpressed myc-GRK2 and FLAG-KISS1R in HEK-293 cells which may artificially increase KISS1R-GRK2 interactions. Thus, further studies involving Co-IP of FLAG-KISS1R and endogenous GRK2 are required to determine whether there is an actual basal interaction. However, other unknown intermediary proteins linking CaM and KISS1R Co-IP complex were not ruled out.

In order to circumvent the inherent limitations of the Co-IP method, cell-free spectrofluorimetric CaM binding assays were utilized to study the physical interactions between CaM and KISS1R intracellular regions. In those studies, fluorophore labelled CaM was found to bind exclusively to IL2 and IL3 derived peptides of the KISS1R, but not to the peptides of IL1, the C-terminal tail (tested region) or any of the three intracellular loops of GnRHR (Figure 3.2-3.7). As far as one can tell from the literature, the biphasic nature of CaM binding to IL3 is the first reported case of CaM biphasic binding to target peptide. The two distinct DA-CaM binding sites of IL3 are both within physiological concentrations, as HEK-293 cells have been shown to contain intracellularly available CaM at a concentration of 8.8 ± 2.2 μM (Black et al., 2004). The binding of TA/DA-CaM to IL2 and IL3 (Table 3.1) were in agreement with published data of CaM binding to other GPCRs. Fluorescence labelled dansyl-CaM has been shown to bind to IL3 of 5-HT_{1A} in two separate peptide regions (K_d - 87 nM ± 23 nM and 1.7 μM ± 0.16 μM), D2 Dopamine receptor (K_d ~100 nM), and Opioid receptor (IC_{50} 42 nM ± 3 nM). The binding of dansyl-CaM has also been shown to bind to IL2 of the 5-HT_{2A} (K_d 65 ± 30

nM). Also, all these interactions are Ca^{2+} dependent (Turner et al., 2004, Bofill-Cardona et al., 2000, Wang et al., 1999, Turner and Raymond, 2005). Furthermore, numerous studies have indicated IL3 of GPCRs as being critical for G-protein activation (Cai et al., 2001, Kang et al., 2005, Geiser et al., 2006, Nanoff et al., 2006, Johnston and Siderovski, 2007). Additionally, Gq coupling was found occur at IL2 of the KISS1R (Wacker et al., 2008). Taken together, KISS1R IL2 and IL3 constitute significant sites for Gq activation and therefore CaM binding to those sites is proposed to compete with Gq.

This chapter set out to determine whether CaM binds the KISS1R, and if so where were the sites of interaction(s). The three independent experiments of spectrofluorimetry, confocal imaging and co-immunoprecipitation all validate each other to provide the first evidence of the physical interaction between CaM and KISS1R via IL2 and IL3. The intracellular loop regions are also critical sites of heterotrimeric Gq binding, implying that CaM binding may function to attenuate Gq coupling. In the next chapter, the amino acid sequence of IL2 and IL3 of KISS1R will be analysed for CaM binding motifs and then the critical amino acids will be replaced by alanine to determine whether KISS1R/Gq coupling can be enhanced. This approach will allow for closer examination of the sites of interaction and at the same time determine the function of these sites in KISS1R function.

4. The functional relevance of calmodulin binding to kisspeptin receptor

Having established that CaM binds to IL2 and IL3 of KISS1R, the functional importance of this interaction was studied with alanine substitution by site-directed mutagenesis of the putative critical binding residues. This method revealed the importance of bulky hydrophobic amino acids at the juxtamembrane regions of IL3. These results were used to model CaM binding to KISS1R-IL3 peptide. The site-directed mutagenesis and modelling data was validated with site-directed fluorescence labelling of CaM to determine the importance of the juxtamembrane regions of KISS1R-IL3 in CaM binding.

4.1. Introduction

There is increasing evidence to suggest that the kisspeptin (KP) pathway is a therapeutic target for the potential treatment for hypogonadotropic hypogonadism (HH), delayed puberty, and many endocrine cancers (Nash et al., 2007, Clarkson et al., 2008, Makri et al., 2008, Roa et al., 2009). However, two main hurdles must be overcome to realise this potential. Firstly, KISS1R will internalise through the process of endocytosis to desensitise against the stimulation of KP ligands (Pampillo and Babwah, 2010). Secondly, the endogenous expression levels of KISS1R vary in space and time and may limit the potential KP ligand-based hormone therapy (Ohtaki et al., 2001). A solution might be to determine the structural features of KP ligands in order to engineer more potent analogues, but this approach poses considerable challenges. As noticed by Shin et al., 2009, the KP-54 in sodium dodecyl sulphate (S.D.S) micelles "exhibits greater than 90 % random coil content, with no significant β sheet or α-helical content" as studied by nuclear magnetic resonance (NMR) techniques (Shin et al., 2009). The authors conclude that the lack of distinguishable structural elements in KP-54 make it difficult to engineer more potent analogues (Shin et al., 2009). Nevertheless, promising work carried out by Orsini et al., 2007, revealed that the shorter KP-13 in detergent (S.D.S micelles) adopted a stable helical structure in the last seven residues using NMR spectroscopy (Orsini et al., 2007). With this information the authors generated full agonists, but with reduced potency compared to KP-13 (Orsini et al., 2007). However, Tomita and colleagues of 2006 were more successful in generating agonists with increased potency (compound 34), albeit with reduced maximum agonistic activity relative to KP-10 (Tomita et al., 2006).

Engineering ligands that target the extracellular regions of KISS1R may one day prove useful in disease modulation, but currently considerable challenges exist, therefore other approaches need to be considered. Thus, the intracellular regions of KISS1R were explored in our search for novel drug targets against protein-protein interactions. A number of studies utilising site-directed or alanine scanning mutagenesis approaches have suggested that the intracellular loops 2 and 3 (IL2 and IL3) of GPCRs are paramount for G–protein coupling and activation (Moro et al.,

1993, Blin et al., 1995, Arora et al., 1995, Burstein et al., 1998, Zhou et al., 1999, Gaborik et al., 2003, Cai et al., 2001, Kang et al., 2005, Geiser et al., 2006, Nanoff et al., 2006, Johnston and Siderovski, 2007, Audet and Bouvier, 2012). Furthermore, it was previously shown that in the class A GPCRs, a sequence element that was termed DRY (E/DRY) motif played a role in receptor activation. Numerous structural studies have revealed the presence of a polar interaction between the arginine of the above mentioned motif positioned at the bottom of transmembrane 3 (TM3) and a glutamate located in TM6. The ionic lock that is formed between TM3 and TM6 involves IL2 and IL3 and is proposed to stabilise the inactive state of GPCRs [as reviewed in (Audet and Bouvier, 2012)]. This would therefore imply that IL2 and IL3 function as conduits for transducing the activation of GPCRs into the modulation of the multi-domain GPCR-G protein interface, and thus regulating G-protein activity.

One particular GPCR interacting protein that has drawn increasing interest lately is calmodulin (CaM), because of its direct involvement in attenuating G-protein activation via interactions with IL2 and IL3 of GPCRs [as reviewed in (Ritter and Hall, 2009)]. Consistent with this, I have shown that CaM binds to KISS1R via IL2 and IL3 (see chapter 3). Herein, I aim to determine the functional relevance of CaM binding to IL2 and IL3 of KISS1R. The method used was alanine substitution by site-directed mutagenesis of the putative CaM binding motifs of KISS1R, as well as modelling the KISS1R.CaM interaction. This approach aims to advance our understanding of the KISS1R.CaM complex with the strategic vision to develop novel therapeutic co-agonists.

4.2. Aims and hypotheses

The aims of this chapter are:

To test the hypothesis that calmodulin binding motifs regulate G-protein coupling/activation.

- Propose a testable structural model of CaM.KISS1R complex
- Test the CaM.KISS1R model.

The hypotheses of this chapter are:

- The putative CaM binding motifs in KISS1R-IL3 regulateKISS1R-CaM interactions
- The interaction of KISS1R with CaM via the putative CaM binding motifs in KISS1R-IL3 regulates KISS1R signalling efficacy but not ligand affinity.

4.3. Results

4.3.1. The critical sites of KISS1R-CaM binding motifs

KISS1R IL2 and IL3 contain CaM-binding motifs and thus may constitute the foundation of the CaM.KISS1R interactions. In order to test this, alanine substitution by site-directed mutagenesis was used to replace the putative crucial amino acids that make up the CaM binding motifs of the KISS1R (Figure 4.1), and followed by studying the effects of mutation on ligand binding and receptor functional activity (see section 2.22 and 2.24, respectively). This approach might be useful in the identification of specific CaM binding sites of KISS1R. The experimentally proposed CaM binding sites were then used to validate an *in silico* model of the CaM-IL3 complex.

The IL3 region of KISS1R contains 6 complete CaM binding motifs and 4 more binding motifs extended into the transmembrane domains (TM) 5 or 6. The IL2 in contrast contains only 1 CaM binding motif (Figure 4.1). The bulky hydrophobic amino acids and the basic residues that are characteristic of the CaM binding motifs were mutated into alanine (Ala) using site-directed mutagenesis (Figure 4.1). The Ala mutants were transiently transfected into COS-7 cells and the receptor expression level was measured using radio-ligand binding assay (see section 2.22). The expression profile of the Ala mutants showed reduced expression level (relative to wild-type KISS1R) in KISS1R-IL2 mutants W141A (12.59 % ±10.54 %), Y142A (11.19 % ± 2.15 %). Also the KISS1R-IL3 N-terminus mutants were also reduced, these were R229A (10.97 % ± 1.81 %), V236A (5.10 % ± 5.31 %), as well as the KISS1R-IL3 C-terminus mutants of R253A (34.30 % ± 2.27 %), R258A (31.00 % ± 6.20 %), K260A (25.02 % ± 3.04 %), and K263A (23.52 % ± 2.84 %). All these low expressing mutants were statistically significant (ranging from $P<0.001$ to $P<0.05$) from wild-type KISS1R expression levels (Figure 4.2, Table 4.1).

The KP-10 ligand bound to wild-type KISS1R with an IC_{50} value of 5.21 ± 0.62 nM, and this was similar to most of the KISS1R Ala mutants that ranged between an IC_{50} value of 2.37 ± 0.24 nM (R237A) and 8.44 ± 2.18 nM (V234A). Unfortunately, the IC_{50} values of W141A, Y142A, and V236A were undetectable

(Figure 4.3 and Table 4.1), due to their low expression levels (Figure 4.2 and Figure 4.3, respectively).

Next, the effect of KP-10 ligand induced IP_3 turnover in cells expressing KISS1R alanine mutants was studied. The Ala mutants were transiently expressed in COS-7 cells and then functionally analysed by IP_3 accumulation assays (see section 2.24). The relative maximum responsiveness was calculated by the ratio of E_{max}/R_{exp} relative to KISS1R wild-type KISS1R, where the receptors were saturated and the ligand binding affinity became unimportant. Interestingly, only one mutant (L245A) displayed a 6-fold reduction in the relative maximum responsiveness (Figure 4.1) with also a 4-fold increase in EC_{50} value (Table 4.1). In contrast, two mutants (W141A and Y142A) of IL2 gave a 4 to 5-fold increase in relative maximum responsiveness. Mutations to KISS1R-IL3 revealed that the N-terminal region residues of R229A and V236A gave a 4 and 16-fold increase in relative maximum responsiveness, respectively (Figure 4.5 and Table 4.1). However, all the mutants tested did not show significant increases in basal activity (Figure 4.6).

The Ala mutagenesis studies were complemented with computational modelling of the CaM-IL3 interaction. To do this, the amino acid sequence of IL3 and the flanking regions (P216– P278) of KISS1R was aligned to their comparative regions of bovine rhodopsin, using the highly conserved proline residues positioned in transmembrane 5.50 (TM) and TM 6.50 (Figure 4.7) using www.tcoffee.org. This was then homology-modelled against the determined structure of bovine rhodopsin (PDB 2X72) using easy modeller GUI. In addition to this, the CaM structure (1CM1) was obtained from the determined structure of CaM binding to the auto inhibitory domain of CaMKII. Both these structures were then uploaded onto the www.cluspro.bu.edu protein-protein docking web server for predicting the CaM-IL3 interaction. The third highest scoring model was chosen as it fitted the Ala mutagenesis results (Figure 4.7). The CaM-IL3 model showed CaM binding to the juxtamembrane regions KISS1R-IL3, with the N-terminal of IL3 binding to the C-terminal of CaM (Figure 4.7).

Taken together, these results supported the hypothesis that the CaM binding motifs of KISS1R participates in regulating receptor activity, and in particular the juxtamembrane regions of KISS1R-IL3 and the N-terminal region of KISS1R-IL2 Alanine mutations of IL2 and IL3 of KISS1R had little effect on the binding affinity of KP-10, suggesting little global structural disturbance by the alanine mutations, which simply delete the side-chain beyond the β-carbon. The marked increase in the signalling efficacy of the mutants, especially R229A and V236A, may be caused by the abolishment of the mutant receptor interaction with CaM. Unfortunately this could not be further validated by Co-IP due to very low expression of the mutant receptors.

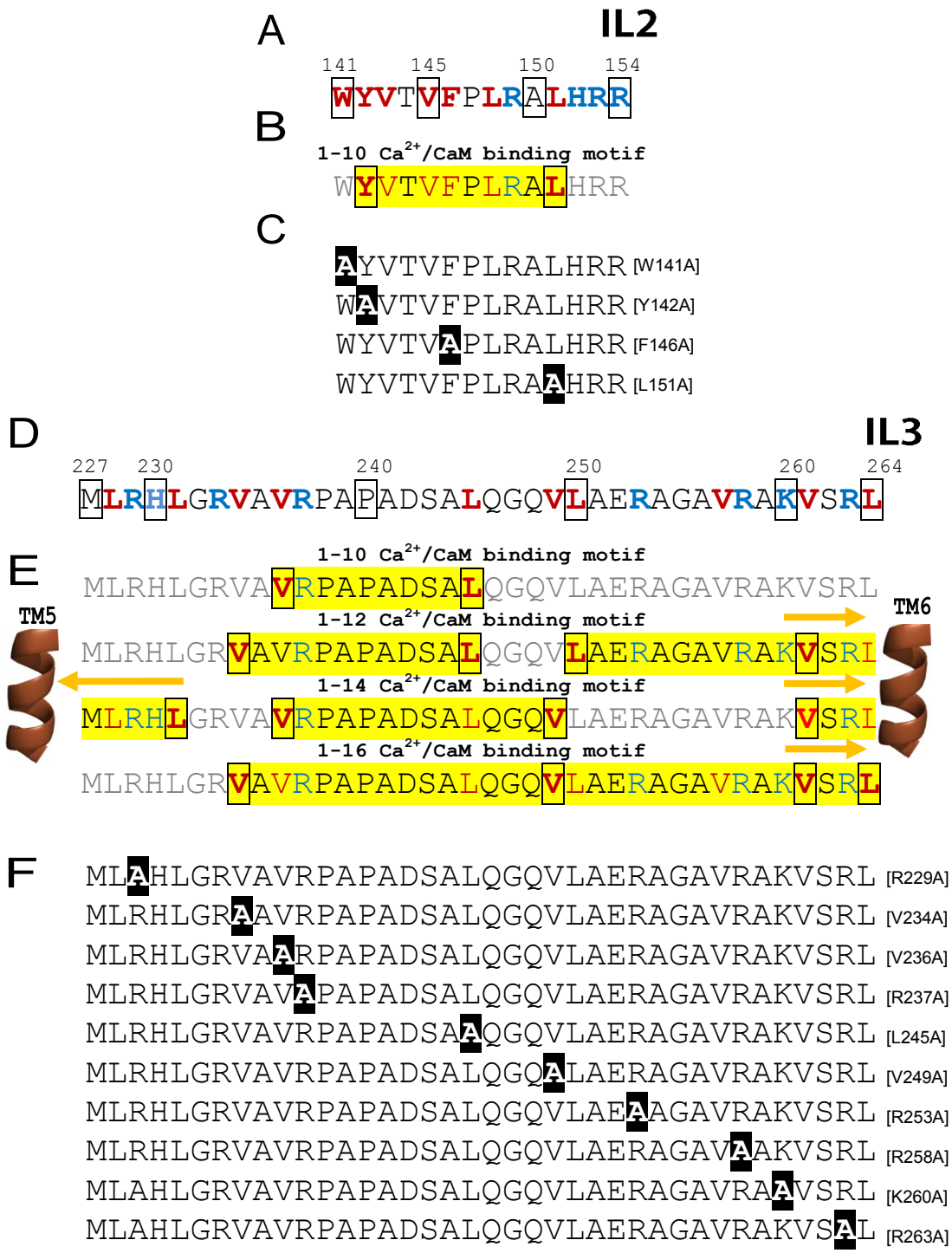

Figure 4.1 Putative Calmodulin-binding motifs of KISS1R-IL2 and IL3. The amino acid sequences of KISS1R-IL2 (**A-C**) and -IL3 (**D-F**) have many basic amino acids (blue) dispersed between flanking bulky hydrophobic residues (red) that are characteristic of CaM binding motifs. IL2 has only one putative CaM binding motif (highlighted in yellow, **B**). However, IL3 contains 6 full-length putative CaM binding motifs with 4 more motifs extending into transmembranes 5 and 6 (**E**). Alanine substitution by site-directed mutagenesis to the suggested crucial CaM binding residues was carried out in order to investigate the role of these CaM binding motifs (**C** and **F**, highlighted in black).

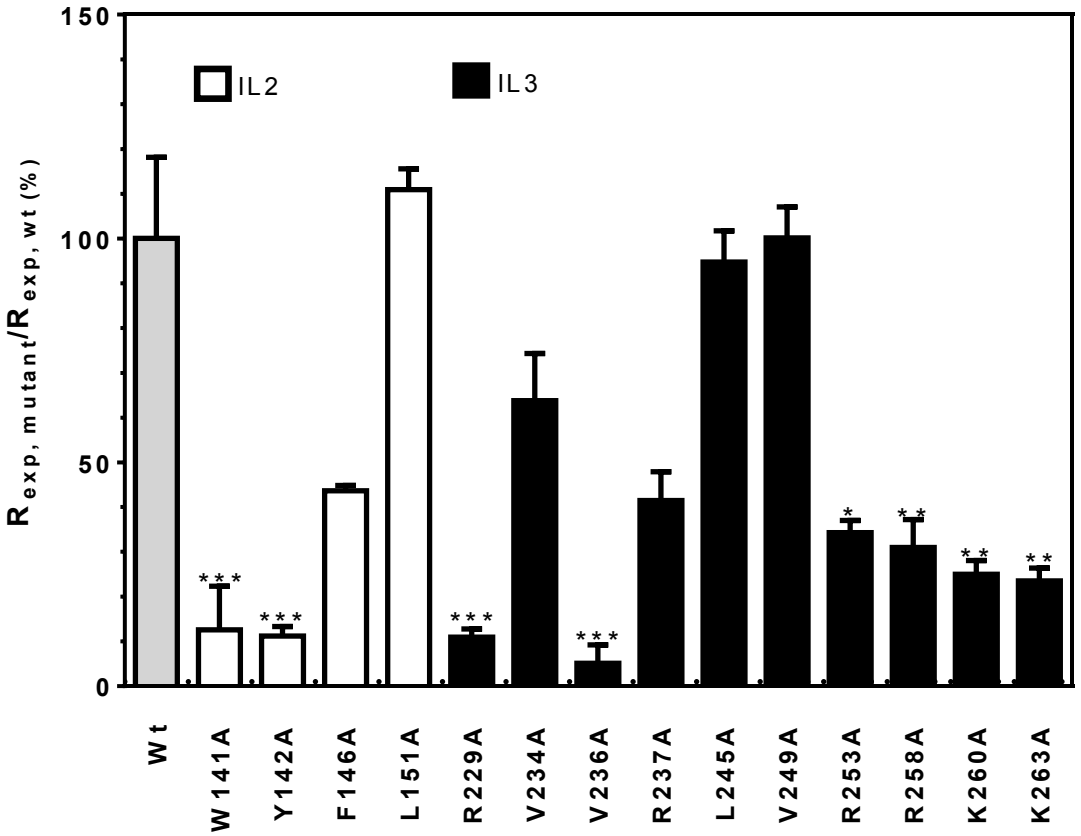

Figure 4.2 Cell surface expression levels of KISS1R mutants. COS-7 cells were transiently transfected with KISS1R 48 hours prior to the radio-ligand binding assay (see section 2.22). The average values of three experimental repeats are shown with the error bars (S.E.M.) Asterisks (*) denote statistical significance (* $P<0.05$, ** $P<0.01$, *** $P< 0.001$) as calculated by One-Way Anova with Dunnett's test.

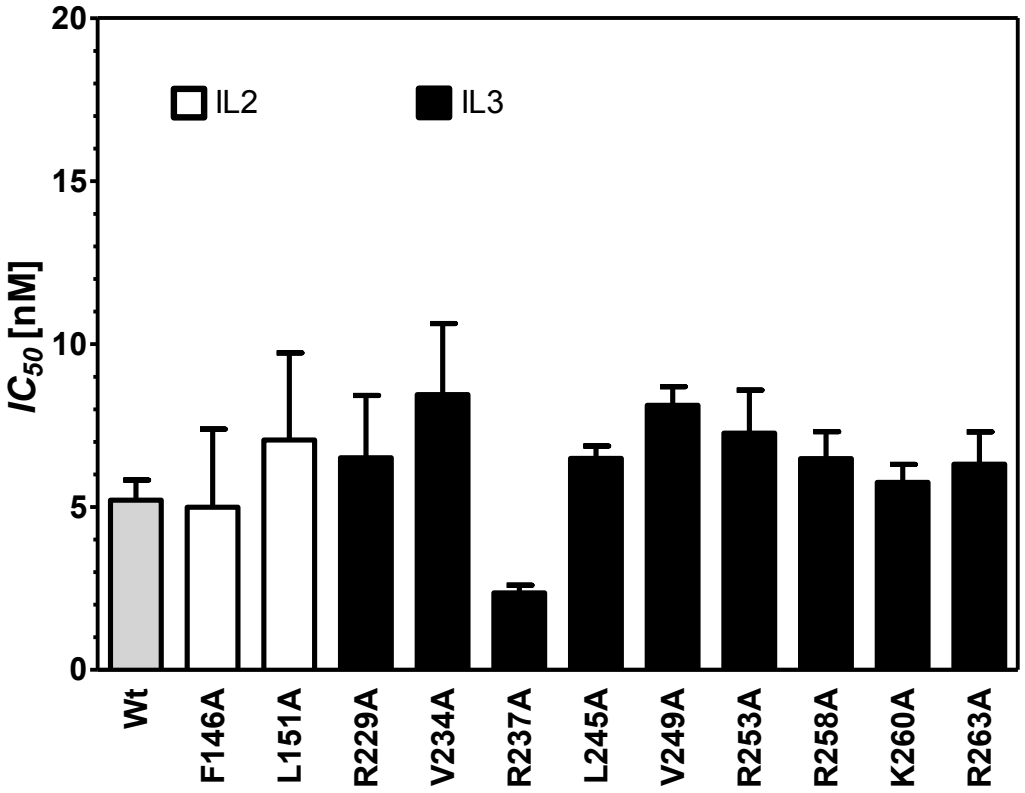

Figure 4.3 KP-10 binding properties of KISS1R-mutants. COS-7 cells were transiently transfected with KISS1R 48 hours prior to the radio-ligand binding assay (see section 2.22). The average values of three repeats are shown with the error bars denoting standard error of the mean (S.E.M.). The mutations showed little effect on KP-10 binding ($P>0.05$ calculated by One-Way Anova with Dunnett's test).

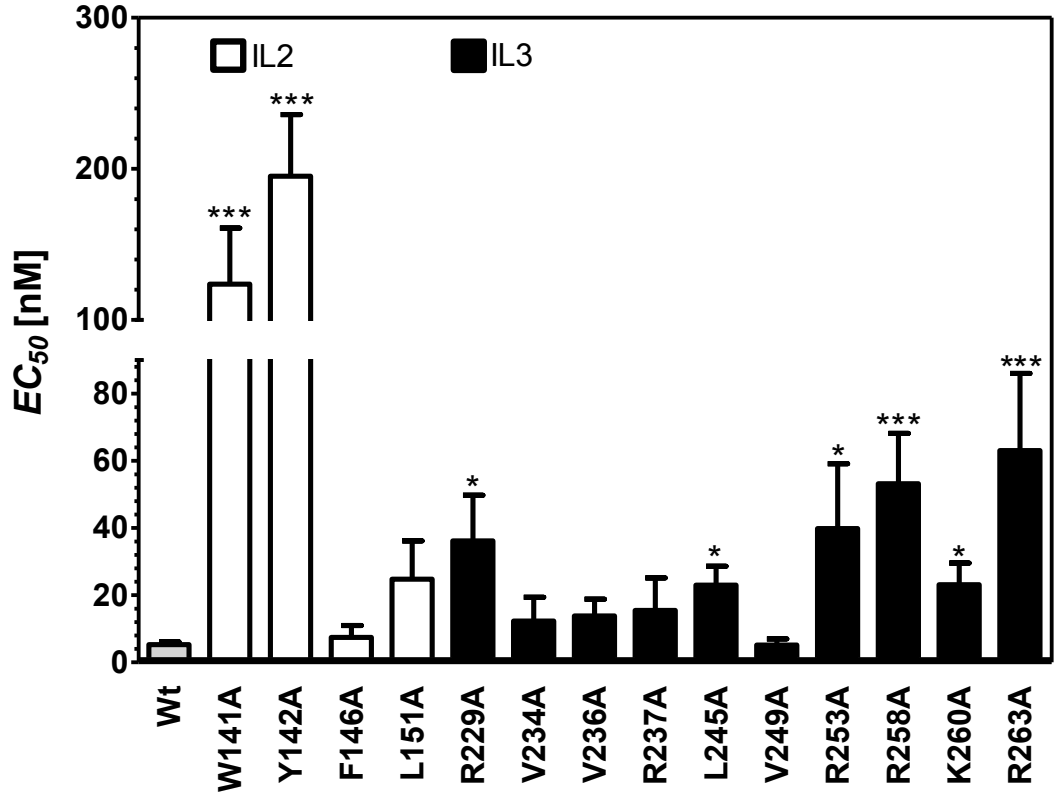

Figure 4.4 The signalling potency of KP-10/KISS1R-mutants. COS-7 cells were transiently transfected with wild-type and mutant KISS1Rs 48 hours before stimulation with KP-10 for 60 minutes, and the IP_3 accumulation was measured (see section 2.24). The average EC_{50} values of the three repeats are shown with the error bars constituting S.E.M. Asterisks (*) denote statistical significance (* $P<0.05$, ** $P<0.01$, *** $P< 0.001$) as calculated by One-Way Anova with Dunnett's test.

.

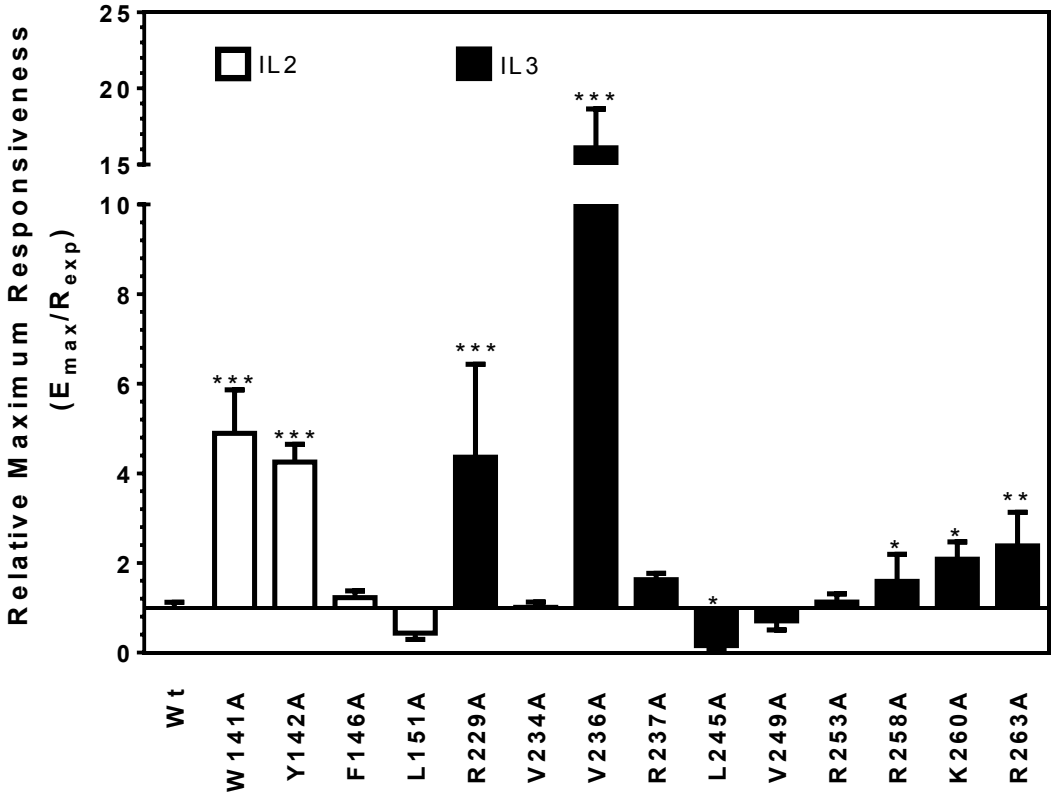

Figure 4.5 The relative maximum responsiveness of KP-10/KISS1R-mutations. COS-7 cells were transiently transfected with KISS1R wild-type and mutant receptors 48 hours before stimulation with KP-10 for 60 minutes, and the IP_3 accumulation was measured (see section 2.24). The average of three repeats is shown with the error bars constituting S.E.M. Asterisks (*) denote statistical significance (* $P<0.05$, ** $P<0.01$, *** $P< 0.001$) as calculated by One-Way Anova with Dunnett's test.

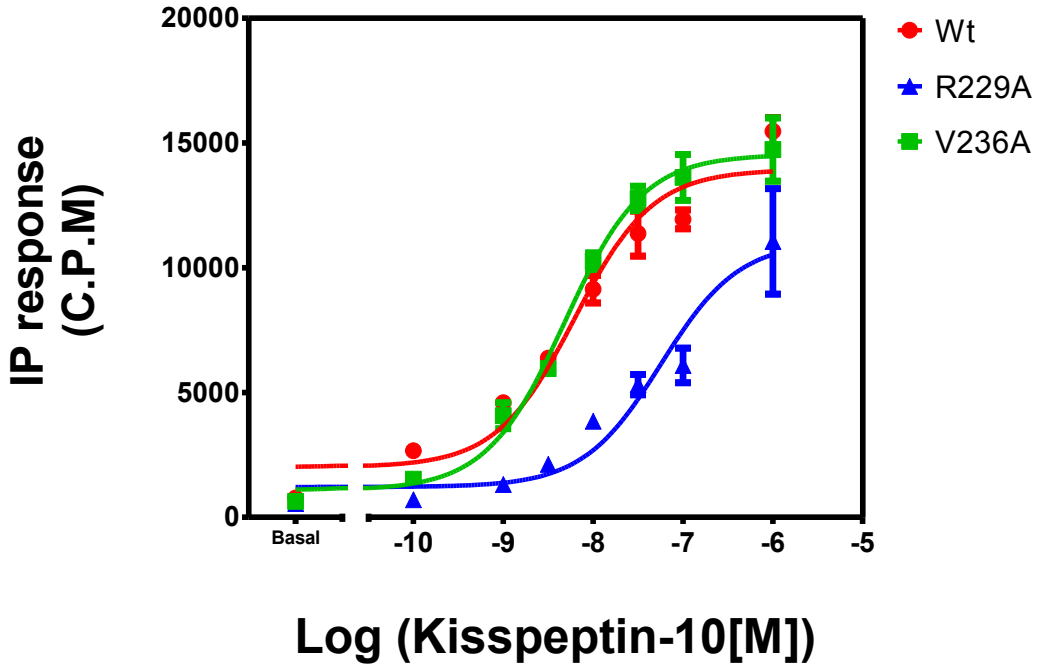

Figure 4.6 Effects of mutations of R229 and V236- KISS1R to Ala on IP_3 production. COS-7 cells were transiently transfected with KISS1R wild-type and mutant receptors 48 hours before stimulation with KP-10 for 60 minutes, and the IP_3 accumulation was measured (see section 2.24). A representative trace of three independent repeats is shown.

Table 4.1 Alanine substitution of putative sites of the CaM-binding motifs of KISS1R. COS-7 cells were transiently transfected with wild-type and mutant receptors 48 hours prior to the binding assay and IP_3 assay (see section 2.22 and 2.24 respectively). The shaded section depicts IL2 mutations. [a] Normalised to itself [b] Normalised to the average of the experimental repeats Asterisks (*) denote statistical significance (* P<0.05, ** P<0.01, *** P< 0.001) as calculated by One-Way Anova with Dunnett's test. –‡ denotes - could not be measured accurately.

Mutant	Binding		IP_3 Responses		Relative Maximum Responsiveness
	R_{exp}	IC_{50}	E_{max}	EC_{50}	E_{max}/R_{exp}
	% WT	*(nM)*	*% WT*	*(nM)*	*Fold Change*
WT	100[a]	5.21 ± 0.62	100[a]	5.27 ± 0.85	1.00 ± 0.13[b]
W141A	12.59 ± 10.54***	–‡	61.62 ± 12.24	123.64 ± 37.23***	4.89 ± 0.97***
Y142A	11.19 ± 2.15***	–‡	47.60 ± 3.62	195.15 ± 33.27***	4.25 ± 0.40***
F146A	43.63 ± 1.21	4.99 ± 2.40	53.58 ± 6.64	7.42 ± 3.58	1.23 ± 0.15
L151A	110.89 ± 4.64	7.06 ± 2.67	48.57 ± 15.98	24.76 ± 11.40	0.44 ± 0.14
R229A	10.97 ± 1.81***	6.51 ± 1.91	47.82 ± 22.73	36.17 ± 13.62**	4.36 ± 2.07***
V234A	63.79 ± 10.52	8.44 ± 2.18	64.52 ± 7.59	12.32 ± 7.10	1.01 ± 0.12
V236A	5.10 ± 5.31***	–‡	81.02 ± 16.72	13.84 ± 4.98	16.10 ± 2.55***
R237A	41.46 ± 6.41	2.37 ± 0.24	67.45 ± 4.87	15.46 ± 7.90	1.63 ± 0.14
L245A	94.75 ± 6.97	6.49 ± 0.38	15.83 ± 4.08**	22.98 ± 5.64*	0.16 ± 0.07
V249A	100.11 ± 6.93	8.12 ± 0.58	88.51 ± 13.58	5.15 ± 1.84	0.71 ± 0.2
R253A	34.30 ± 2.72	7.26 ± 1.32	38.76 ± 6.31	39.82 ± 19.30*	1.13 ± 0.18
R258A	31.00 ± 6.20*	6.48 ± 0.83	49.35 ± 18.66	53.19 ± 15.03***	1.59 ± 0.60*
K260A	25.02 ± 3.04*	5.75 ± 0.55	54.83 ± 7.18	23.10 ± 6.50*	2.08 ± 0.39*
R263A	23.52 ± 2.84**	6.31 ± 0.99	56.01 ± 17.71	63.10 ± 22.91***	2.38 ± 0.75**

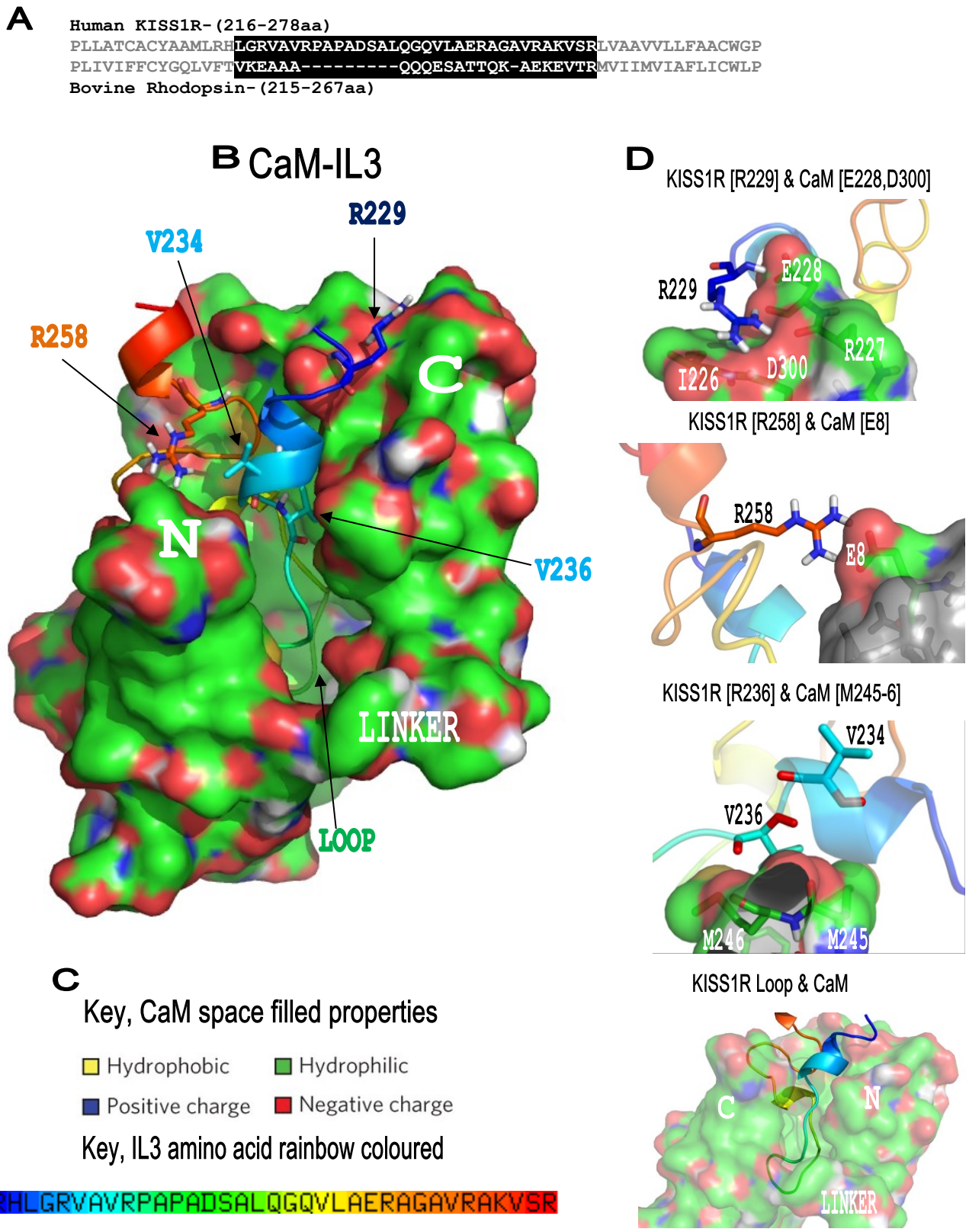

Figure 4.7 A proposed model for CaM-IL3 complex. The amino acid alignment of bovine rhodopsin and human KISS1R (A) is shown with the full alignment in grey and the selected IL3 sequence in black & white. Space filled CaM (B) has unique amino acid characteristics (C) and is identifiable with C- and N- terminal domains connected by the linker region. The IL3 peptide amino acid sequence (C) is represented in rainbow colour to better identify the cartoon structure docked in the centre of CaM (B). The amino acids of IL3 that were identified of having a role in modulating KISS1R activity are pointed out. A zoomed image of specific sites of interest is shown in D

4.3.2. The functional relevance of KISS1R-IL3 juxtamembrane regions

The site-directed mutagenesis study suggested that the CaM binding motifs of KISS1R particularly that of the juxtamembrane regions of IL3 may play an important role in CaM binding. Furthermore, modelling (Figure 4.7) the CaM.IL3 interaction revealed the interaction of CaM with the juxtamembrane regions of IL3. However, these experiments do not constitute a direct evidence of CaM.IL3 interactions, thus further experiments were conducted to validate these observations. In order to measure the importance of CaM binding to the juxtamembrane regions of KISS1R-IL3 (227-263 aa) a shortened version termed KISS1R-IL3^{short} (234-254 aa) was synthesized by EZbiolabs with > 95 % purity (Figure 4.8). Da-CaM was used to test whether the two CaM globular domains come in close proximity to one another in the presence of KISS1R-IL3^{short}. Da-CaM has its endogenous T34 and T110 replaced for the amino acid Cys. This double mutant (T34C/T110C) CaM was chemically labelled with IAEDANS and DDP fluorophores. The two probes form a Förster resonance energy transfer (FRET) pair. Upon DA-CaM binding to target peptide the donor IAEDANS fluorescence is quenched by the acceptor DDP, indicating close proximity of the probes, i.e. the closure of the N- and C- lobes of CaM (see section 2.13). I also tested the Ca^{2+} dependency of CaM binding with KISS1R-IL3 and KISS1R-IL3^{short} peptides using CaM^{C34}-badan, in which the amino acid T34 was replaced for Cys and then labelled with badan, an environmentally sensitive fluorescent probe.

The KISS1R-IL3 (227-263) peptide contains 37 amino acids with 8 basic residues dispersed between 9 bulky hydrophobic residues that form 6 complete CaM binding motifs. The KISS1R-IL3^{short} (234-254 aa) peptide contains 2 basic residues and 5 bulky hydrophobic residues that form 4 complete CaM binding motifs. The KISS1R-IL3 peptide contains 2 proline residues at the 12th, 14th amino acid positions, as well as 3 glycine residues at positions 6, 21, and 29. The KISS1R-IL3^{short} peptide lacks the two glycine residues of KISS1R-IL3 at positions 6 and 29 (Figure 4.8).

The reaction mixture of KISS1R-IL3 peptide with DA-CaM in an assay buffer (see section 2.13) containing 100 μM $CaCl_2$ led to a large reduction in fluorescence intensity as compared to the addition of KISS1R-IL3^{short} (Figure 4.9). The level of fluorescence reduction of DA-CaM upon adding 20 μM KISS1R-IL3^{short} was 7% and upon adding an equal amount of 20 μM KISS1R-IL3 peptide the fluorescence reduction was. 61 %. With the use of the high affinity Trp peptide the fluorescence reduction was reduced further to 82 % (Figure 4.9).

The proposed *in silico* model revealed the possible role of the C-terminal domain of CaM in its interaction with the juxtamembrane regions of IL3 (Figure 4.7). In order to test this experimentally, a site-directed fluorophore called badan was attached to the N-terminal domain of CaM (CaM^{C34}-badan) (see section 2.11). This construct was previously shown to be a powerful tool to monitor CaM conformational changes and the interaction interface between CaM and target proteins (Gangopadhyay et al., 2004). The CaM^{C34}-badan construct was sensitive to Ca^{2+} with *Kd* of 792 ± 39.53 nM and Hill coefficient (*n*) of 4.58 ± 0.22. The Ca^{2+} affinity for CaM^{C34}-badan was increased by the pre-incubation of KISS1R-IL3 (*Kd* 398 ± 25.21 nM and *n*- 5.60 ± 0.63). However, the Ca^{2+} affinity of CaM^{C34}-badan premixed with KISS1R-IL3^{short} with gave a similar affinity to CaM^{C34}-badan without peptides with an affinity of *Kd* 802 ± 15.07 nM and *n* of 4.74 ± 0.22 (Figure 4.10 and Table 4.2).

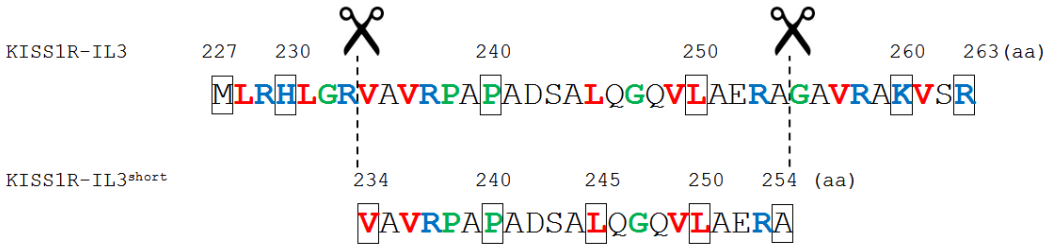

Figure 4.8 Peptide sequence KISS1R-IL 3 fragments. Two related peptides were synthesised; the first was KISS1R- intracellular loop 3 (IL3) (227-263 aa), and the second was KISS1R-IL3^{short} (234-254 aa). Red indicates bulky hydrophobic amino acids, while blue depicts basic residues, and the green represents flexible residues. The amino acid (aa) number is identifiable with numbering above the boxed letters. The scissor symbol represents the juxtamembrane regions that were removed from KISS1R-IL3 to generate KISS1R IL3^{short}.

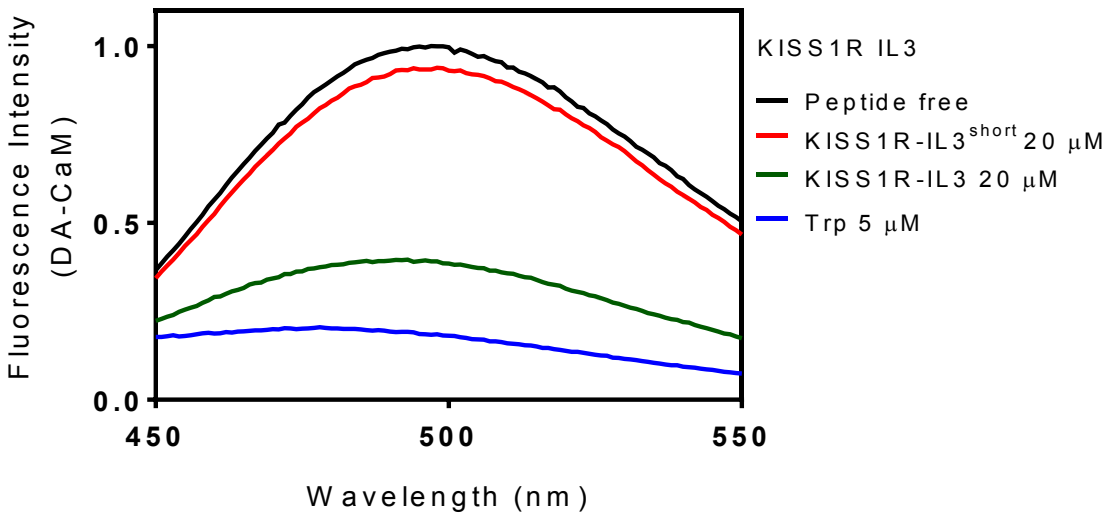

Figure 4.9 Emission fluorescence spectra of DA-CaM titrated against KISS1R-IL 3 peptides fragments. KISS1R derived intracellular loop 3 (IL3) peptide fragments were titrated against 1 μM DA-CaM in the assay buffer (see section 2.13) containing 100 μM $CaCl_2$. DA-CaM fluorescence was measured at excitation wavelength 365 nm and emission wavelength 450-550 nm.

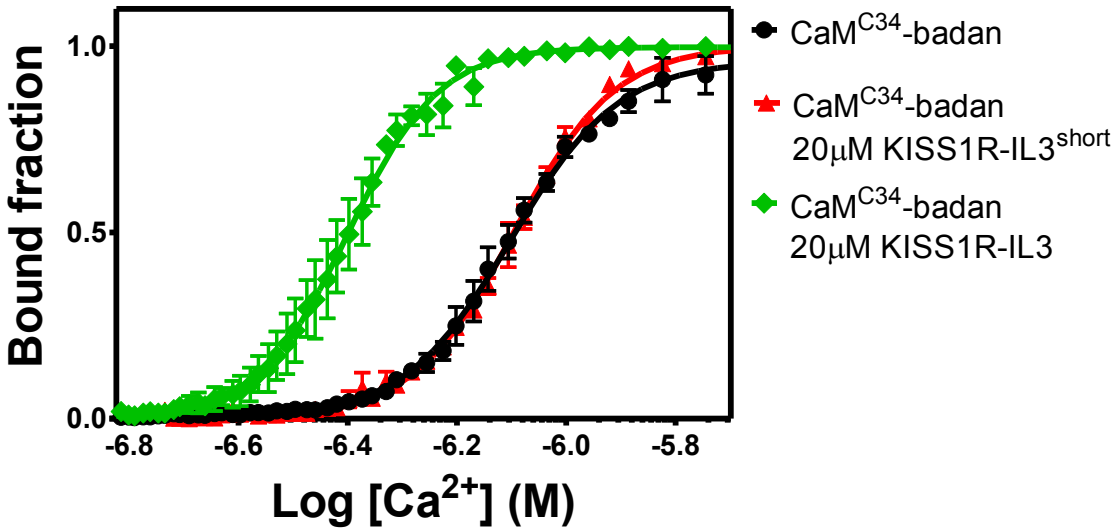

Figure 4.10 Ca^{2+} dependence of CaM^{C34}-badan in the presence of KISS1R-IL3 fragments. Equilibrium Ca^{2+} binding assay was carried out with 100 nM CaM^{C34}-badan (black line) in assay buffer (see section 2.14). The addition of KISS1R-IL3 (green line-227-263 aa) and $KISS1R\text{-}IL3^{short}$ (red line-234-254 aa) peptides were premixed with CaM^{C34}-badan prior to experimentations. CaM^{C34}-badan fluorescence was measured at excitation wavelength 368 nm and emission wavelength 455 nm. All experiments were carried out at 20 ºC.

Table 4.2 CaM^{C34}-badan Ca^{2+} dependencies in the presence of KISS1R-IL3. This table shows the values of the plotted graphs shown in Figures 4.10. The standard error shows S.E.M of three independent repeats.

CaM^{C34}-badan mix	$K_{d\ (nM)}$	Hill coefficient
CaM^{C34}-badan only	792 ± 40	4.58 ± 0.22
KISS1R-IL3	398 ± 25	5.60 ± 0.63
$KISS1R\text{-}IL3_{short}$	802 ± 15	4.74 ± 0.22

4.4. Discussion

This chapter aimed to characterise the interactions between CaM and the KISS1R. The approaches used were alanine mutagenesis of the putative CaM-binding motifs of KISS1R, molecular modelling of the CaM.KISS1R complex, and spectrofluorimetric CaM binding assays using KISS1R derived peptides. Herein, evidence is provided for the binding of CaM to KISS1R via the juxtamembrane regions of IL3, resulting in the attenuation heteromeric G protein activation.

Calmodulin (CaM) regulates a wide array of cellular processes via its interaction with specific binding motifs of proteins. These include several GPCRs that have been shown to interact with CaM [Reviewed in (Ritter and Hall, 2009)]. Therefore, following the tradition of identifying CaM binding regions, this study set out to examine the primary amino acid sequence of KISS1R and to determine whether there exist CaM-binding motif(s). Indeed, there were CaM-binding motifs in IL2 and IL3 of KISS1R (Figure 4.1). The putative CaM-binding motif of IL3 (245-263aa) was confirmed with the use of the Calmodulin Target Database search engine (http://calcium.uhnres.utoronto.ca/ctdb/ctdb/sequence.html). However, the search engine did not identify IL2, even though there is a "1-10" CaM-binding motif (142-151aa). This is thought to be due to the lack of alpha-helical propensity of the CaM-binding motif of IL2, a critical criterion for the identification of putative CaM-binding motifs. Another explanation might be due to the selective criterion of the search engine, which was derived from numerous structural analyses of CaM binding to none-GPCR proteins (Yap et al., 2000).

The solved structures of CaM bound proteins gave potential to the idea of determining the structure of CaM bound to KISS1R-IL3. In light of this, crystallisation trials were carried out; however, no crystals were observed. The reason for this may be due to the non-homogenous nature of the biphasic binding of CaM to KISS1R-IL3 (Figure 3.5), and the significant unstructured region of KISS1R-IL3. Future crystallisation trails should detail the use of optimised KISS1R-IL3 peptides. Nevertheless, a new approach was sought in determining the CaM binding sites of KISS1R.

KISS1R IL2 and IL3 are the only intracellular regions that contain CaM-binding motifs, and they have been shown to bind CaM exclusively (see chapter 3). With this in mind, an in-depth understanding of the CaM.KISS1R interaction via IL2 and IL3 was sought by alanine mutagenesis of the CaM binding motifs (Figure 4.1), homogenous competition ligand binding and inositol phosphate accumulation studies.

4.4.1 Ligand binding assay with radiolabeled KP-10

Although saturation ligand binding assay is the most appropriate approach to measure receptor expression and ligand binding affinity, it is often infeasible for labelled peptide ligands (Mamputha et al., 2007, Kuohung et al., 2010). The KISS1R saturation ligand binding assays presented a technical problem because of its high non-specific binding of ^{125}I-leballed kisspeptin peptides and KP-10 forming aggregates (Kuohung et al., 2010, Nielsen et al., 2010). Furthermore, my colleague Kevin Morgan has previously found that increasing the concentrations of radiolabeled KP-10 in binding assays leads to increased non-specific binding, which makes it difficult to distinguish between specific and non-specific binding. Consequently, it is not technically feasible to use increased tracer concentrations or saturation binding assays to determine ligand binding affinities of the wild-type and mutant KISS1R receptors. As a result, a competition ligand binding assay was carried out as that previously described for GnRH (Flanagan et al., 1998). The concentration of used radioligand is about 25 pM. Hence, it is likely to have little effect on the Cheng-Prusoff shift. Furthermore, homogenous competition binding experiments of ^{125}I-KP-10 on intact cells transiently transfected with wild-type and mutant receptors demonstrated little or only marginal shift in affinity for any of the mutants compared to the wild type receptor. Therefore, in most cases, the B_o values of the specific binding measured in the absence of competitive ligands reflect the relative expression levels (R_{exp}) of receptors on the cell surface.

4.4.1.1 Receptor Reserve and Responsiveness.

It is important to take into account the spare receptors when calculating efficacy. Our lab has previously used irreversible antagonists to estimate receptor reserve (Lu et al., 1997). However, due to the lack of irreversible antagonists for KISS1R, it is difficult to estimate the receptor reserve for KISS1R. However, the little change between the IC_{50}/K_d and EC_{50} values of KP-10 for wild-type KISS1R suggests little presence of a receptor reserve. Hence, the relative maximum signalling efficacy of KP-10 was estimated by normalization of the maximum IP responses to the cell surface receptor binding sites as the receptor population is saturated, and the affinity is not an issue (Takino et al., 2003, Kenakin, 2002a). The decreases in KP-10 potency for mutant receptors are potentially the product of combined decreased coupling efficiency/activation with decreased affinity of the mutant receptor. The low expressing mutants often show a decreased potency (larger EC_{50} values, (Lu et al., 1997). However, mutation of certain constrained amino acids may increase signalling potency/efficacy, as the mutants become super-active (Lu et al., 2005, Lu et al., 2007). The increased relative maximum responsiveness (relative to wild-type KISS1R) of KISS1R mutations of the N-termini of IL2 (W141A and Y142A) and IL3 (R229A, V236A), as well as the C-terminus of IL3 (R258A, K260A and K263A) may indicate super-coupling and/or the inhibition of intramolecular constraints. In contrast the decreased efficacy of the mutants may indicate that they may be involved in receptor G protein coupling such as L151A, L245A and V249A. However, KP-10 IC_{50} of KISS1R W141A, Y142A and V236A could not be accurately measured and require future investigation. As with all such mutagenesis studies, there remains the possibility that hypothetical changes in the receptor's cell surface expression, G protein interactions or desensitization could have some influence on observations.

Due to the inherent complexity involved in the folding and trafficking of seven-transmembrane proteins, GPCRs must fulfil stringent quality control mechanisms that will enable them to express normally at the cell surface (Conn et al., 2006). It was therefore not surprising that most of the KISS1R mutants showed decreased receptor expression on the cell surface (Figure 4.2). One explanation to

this might be due to an increase in intracellular retention, due to KISS1R misfolding and subsequently becoming misrouted within the cell. Intracellular retention is the most prevalent mechanism by which clinical mutations of GPCRs cause disease (Meyer et al., 1992, Tan et al., 2004). For example, of the 21 clinical mutations recorded in the gonadotropin-releasing hormone receptor, ~17 are shown to be the result of intracellular retention (Conn et al., 2007). Another explanation to why some KISS1R mutants showed decreased receptor expression on the cell surface might be due to increased constitutive activity and thus increased constitutive internalisation. This explanation is supported with the evidence that the KISS1R mutants with decreased expression levels on the cell surface positively correlated with an observed increase in the relative maximum responsiveness (Figure 4.5). Future experiments should entail dissecting these two explanations by immunocytochemistry and internalisation assays.

The KISS1R mutants with increased EC_{50} values (decreased potency) (Figure 4.2, Figure 4.3, and Table 4.1) is likely the result of the markedly decreased receptor expression level on the cell surface. This conclusion is reached because those KISS1R mutants also had increased relative maximum responsiveness, and a similar phenomenon was observed by Lu and colleagues 1997 when performing mutation studies on the m1 muscarinic receptor.

GPCR intracellular loops undergo large conformational changes as part of ligand binding and receptor activation, implying high conformational flexibility (Rasmussen et al., 2011a, Lebon et al., 2011, Xu et al., 2011, Standfuss et al., 2011, Choe et al., 2011, Park et al., 2008, Scheerer et al., 2008). Mutations in the intracellular regions of KISS1R showed little effect on ligand binding affinity (IC_{50} values) of all the KISS1R mutants tested (Figure 4.3, Table 4.1). Additionally, the disease causing mutant L148S of KISS1R also showed a markedly reduced ligand potency, but unchanged ligand binding affinity (Wacker et al., 2008).

The intracellular-transmembrane regions (IC-TM) harbour many functionally important features that are conserved in class A GPCRs [as reviewed in (Katritch et al., 2012, Audet and Bouvier, 2012)]. Among these is the conserved (D/E) $R^{3.50}$ (Y/W) motif [$R^{3.50}$, as according to the Ballesteros/Weinstein numbering (Ballesteros et al., 1998)] located at the bottom of TM3 in which $R^{3.50}$ may interact with a $E^{6.30}$

residue in TM6 in certain receptors (Rovati et al., 2007). The interaction between $R^{3.50}$ and $E^{6.30}$ is thought to stabilise the inactive state of GPCRs through a mechanism known as 'ionic lock', which brings together TM3 and TM6 in close proximity (Rovati et al., 2007). The KISS1R contains the highly conserved $R^{3.50}$ (in the aa position 140, Figure 3.1), as indeed do 96 % of class A GPCRs (Mirzadegan et al., 2003). However, in the KISS1R, the equivalent position 6.30 is occupied by a positive charged residue (R258) (Figure 3.1), which is unlike 32 % of class A GPCRs (Springael et al., 2007). Therefore, the KISS1R is unlikely to form an ionic lock. Indeed, most peptide GPCRs (> 90%) cannot form an ionic lock due to the lack of an acidic residue in position 6.30 (Mirzadegan et al., 2003). Therefore, the increased EC_{50} values of W141A and Y142A (C-terminus to TM3) and R253A, R258A, K260A, and R263A (N-terminal to TM6) is not related to the ionic lock concept.

GPCRs are known to act as guanine nucleotide exchange factors (GEF) and drive G-protein activation, however the structural basis for GPCR-catalysed nucleotide exchange is presently unclear (Oldham and Hamm, 2008). Nevertheless, important crystallographic studies have suggested that G-protein activation requires conformational changes of the Gα switch I, II, III to relieve a GDP clamp formed between the GTPase and α-helical domains (Oldham and Hamm, 2006). In the inactive Gαβγ heterotrimer, the Gα switch II region is sequestered by Gβγ and in theory GPCRs utilise Gβγ as a lever against the Gα switch II region to relieve the GDP clamp (Iiri et al., 1998). More recently, the structure of active β_2 adrenergic receptor (β_2AR) in complex with Gαs protein was solved (Rasmussen et al., 2011b, Chung et al., 2011). The β_2AR-Gαs interface is formed by IL2 and the juxtamembrane regions IL3 (Rasmussen et al., 2011b). Therefore, the KISS1R mutants of IL2 and the juxtamembrane regions of IL3 with increased relative maximum responsiveness are likely the result of Gq/11 super-coupling.

In that regard, the increased relative maximum responsiveness observed in the juxtamembrane regions of KISS1R-IL3; R229A, V236A, R258A, K260A, and R263A are likely to be the result of impaired CaM binding and increased G-protein activation. These observations were similar to Lu and colleagues, 2005, where they show super coupling after rescuing GnRH mutant receptors (Lu et al., 2005). These

results complements previous reports that GPCRs interact with Gα via the basic residues of the juxtamembrane regions of IL3 [as reviewed in (Denis et al., 2012)]. This would suggest that removing the biochemical basis for CaM binding increases KISS1R maximum efficacy. Furthermore, this finding agrees with the report that CaM competes with ^{35}S-labeled guanosine 5'-3-*O*-(tio)triphosphate binding to G-proteins, in membranes containing OP_3 and D_2 receptors (Bofill-Cardona et al., 2000, Wang et al., 1999).

In order to further validate these observations I carried out spectrofluorimetric CaM binding experiments with KISS1R-IL3 peptide lacking the juxtamembrane regions. The KISS1R-IL3 contains landmarks in the form of specific amino acids strategically positioned to convey flexibility, i.e., G 232 and G 255 flanking the central region of IL3 (Figure 4.8). The central region of IL3 contains 2 Pro and 1 Gly residues that provide more flexibility. The removal of the juxtamembrane regions around the landmarks, created KISS1R-IL3^{short} peptide. The KISS1R-IL3^{short} peptide did not lead to FRET produced by the proximity of the globular domains due to CaM binding to peptides (Figure 4.9). This was in stark contrast to the KISS1R-IL3 peptide that gave a significant reduction in DA-CaM fluorescence, which means that the N- and C-terminal lobs of CaM come in close proximity, wrapping around KISS1R-IL3 (Figure 4.9). I therefore conclude that the juxtamembrane regions of KISS1R-IL3 constitute distinct binding sites critical for CaM binding, which support the proposal derived from the site-directed mutagenesis study. A similar observation exists in the binding of CaM to the IL3 of 5-$HT_{1A,}$ which also involves two distinct bindings sites positioned in the N- and C-terminal region of 5-HT_{1A}-IL3 (Turner et al., 2004).

The Ca^{2+} affinity for CaM^{C34}-badan was determined to be 792 ± 39.53 nM, which is similar to the previous report of ~700 nM (Gangopadhyay et al., 2004). The increased Ca^{2+} affinity of CaM^{C34}-badan pre-mixed with KISS1R-IL3 peptide revealed an interesting possibility that the KISS1R-IL3 induces conformational changes of CaM^{C34}-badan that favours the EF-hand regions to bind Ca^{2+}more efficiently. Therefore, it may be possible that Ca^{2+}CaM binding to KISS1R-IL3 juxtamembrane regions may create a $Ca^{2+/}$CaM.KISS1R complex that is more responsive to Ca^{2+}.

Although CaM binding to GPCRs has been known since the 1990s, the literature lacks a testable model. Herein is proposed the first such model of CaM binding to the juxtamembrane regions of IL3 (Figure 4.7). The model aims to initiate the realistic and testable conceptualisation of an important interaction. The model consolidates the site-directed mutagenesis data and the spectrofluorimetric CaM binding experiments. Notably, IL2 is absent from model, the reason is as follows: Firstly, IL2 titration against TA/DA-CaM gave a relatively small amplitude change (see Figure 3.3), implying a non-conventional binding. Secondly, the site-directed mutagenesis data revealed that only the N-terminus of the CaM-binding motif of IL2 increased KISS1R activity. This would imply that a very small portion of the CaM binding motif of IL2 is involved. Furthermore, these residues are very close to the membrane, while TM5 and TM6 have extended alpha-helical structures (Standfuss et al., 2011). Therefore, I propose that CaM binding occurs mainly to IL3 and with a peripheral contact to IL2.

In conclusion the site-directed mutagenesis study and molecular modelling revealed the functional importance of CaM binding motifs present in the juxtamembrane regions of KISS1R-IL3 and the N-terminal region of KISS1R-IL2. In addition, the relative maximum responsiveness of KISS1R mutants varied, but the ligand binding (IC_{50}) remained similar. This would therefore suggest that the receptor-G protein coupling may be fine-tuned by Ca^{2+}/CaM.

The knowledge gained from chapters 3 and 4 is integrated into a CaM.IL3 model. This model and subsequent validations revealed how CaM is likely to interact with the juxtamembrane regions of IL3. It is therefore proposed that CaM binding to KISS1R IL3 attenuates G-protein activation via steric hindrance.

5. αCaMKII targets kisspeptin receptor to down-regulate the HPG axis

This thesis has so far provided evidence for the role of Ca^{2+}/CaM in the regulation of KISS1R function. However, can a closely related kinase also regulate KISS1R function? A-Ca^{2+}/calmodulin-dependent protein kinase II (αCaMKII) phosphorylates substrates possessing specific consensus sequences. Therefore, the KISS1R amino acid sequence was examined for αCaMKII consensus sequence. Indeed, there was such a motif and subsequent kinase assays were performed with IL1, IL2, IL3, and C-terminal tail peptides. Phosphomimetic mutations of KISS1R revealed the potential importance of the phosphorylation event in the regulation of KISS1R function. These in vitro data were validated with in vivo experiments from my collaborator, which involved perturbation studies of rat HPG axis using a αCaMKII inhibitor.

5.1. Introduction

Mammalian Kisspeptins (KPs) are important regulators of the hypothalamic-pituitary-gonadal axis (HPG) (Oakley et al., 2009). KPs activate KISS1R expressed on the surface of hypothalamic GnRH neurons, leading to the consequent increase in intracellular Ca^{2+} which drives GnRH pulsatile secretion (Constantin et al., 2009, Liu et al., 2008). However, researchers do not know to the full extent by which the multifarious effects of Ca^{2+} cause GnRH pulsatile secretion (Liu et al., 2008). Nevertheless, GnRH stimulates gonadotropic cells of the pituitary to secrete luteinising hormone (LH) and follicle stimulating hormone (FSH) into the blood stream, which in turn orchestrates the reproductive processes of mammals (Sisk and Foster, 2004).

Ca^{2+}/calmodulin-dependent protein kinase II (αCaMKII) is a multifunctional Ser/Thr protein kinase that is abundant in brain cells, particularly at neuronal dendritic spines (Hudmon and Schulman, 2002b, Schulman and Greengard, 1978a, Schulman and Greengard, 1978b). Binding of Ca^{2+}/CaM to αCaMKII exposes the substrate binding regions of the catalytic domain and facilitates T286 autophosphorylation (Lisman, 1994, Meyer et al., 1992, Torok et al., 2001). The function of T286 autophosphorylation is to stabilise the active state of αCaMKII (Ishida et al., 1996, Tzortzopoulos and Torok, 2004). Thereafter, the enzyme auto-inactivates in ~1 minute due to T305/306 autophosphorylation (Jama et al., 2009, Lee et al., 2009). As such, αCaMKII functions as a Ca^{2+} frequency decoder, integrating the diverse forms of Ca^{2+} transients and decoding it into various forms of phosphorylation states that leads to neuronal synaptic plasticity (Eshete and Fields, 2001, Dupont and Goldbeter, 1998, Lisman et al., 2012, Jama et al., 2011). For instance, αCaMKII has been shown to phosphorylate α-amino-3-hydroxy-5-methyl-4-isoxazolepropionic acid receptor (AMPA) to increase channel conductance and thus neuronal synaptic strength (Benke et al., 1998). Another example is the important role of αCaMKII in GPCR functional regulation. Both the inhibitory phosphorylation of dopamine D_3 receptor (D_3R) and the stimulatory phosphorylation of M_4 muscarinic acetylcholine receptor (M_4 mAChR) by αCaMKII contributes to dopamine homeostasis (Liu et al., 2009, Guo et al., 2010).

The highly expressed neuronal αCaMKII is believed to target multifarious substrates containing the basic consensus sequence of **K**/**R**-*X*-*X*-**S**/**T** (Pearson et al., 1985, White et al., 1998). Currently, a limited number of substrates have been identified (Colbran, 2004). This limits our understanding of how cytoplasmic Ca^{2+} synchronises the panoply of signalling events through αCaMKII. In search for new αCaMKII substrates, the KISS1R amino acid sequence was examined for the consensus sequences, followed by kinase assays to determine the catalytic relationship between αCaMKII and KISS1R derived peptides. The *in vivo* role of αCaMKII inhibition was studied with perturbation studies of rat HPG axis. Taken together, this chapter reveals the mechanism by which αCaMKII targets KISS1R to down-regulate the HPG axis.

5.2. Aims and hypothesis

The aims of this chapter are:

- To determine whether αCaMKII phosphorylates the consensus sequences of the KISS1R derived peptides.
- To identify the function of the phosphorylation of KISS1R by the αCaMKII

The hypothesis of this chapter is:

- αCaMKII phosphorylates T77 of KISS1R, modulating receptor activity.

5.3. Results

5.3.1. αCaMKII phosphorylates T77 of KISS1R

α-Ca^{2+}/calmodulin-dependent protein kinase II (αCaMKII) is a serine/threonine protein kinase that is known to recognise and phosphorylate the consensus sequence – **K/R**-*X*-*X*-**S/T** (White et al., 1998, Pearson et al., 1985). A similar sequence exists in the intracellular loop 1 (IL1) and the C-terminal tail (C-tail) of the human KISS1R (Table 5.1). To explore whether these sites are substrates for αCaMKII, the intracellular loops (IL1, IL2 and IL3) and the putative phosphorylation sequence of the C-terminal tail (C-Tail) of KISS1R (Table 5.1) were synthesised at > 95% purity from EzBiolabs. A steady state kinase assay was used to determine the specific activity of αCaMKII in the presence of synthetic peptides (see section 2.15). Furthermore, the activation mechanisms αCaMKII by Ca^{2+}/CaM dynamics were investigated by mutation of Ca^{2+} binding sites in different lobes, in order to put into the context of the possible role of αCaMKII phosphorylation of the putative sites of KISS1R.

As expected (Jama et al., 2011, Jama et al., 2009), the specific activity of αCaMKII in the presence of saturating Syntide-2 (a well-known positive control) gave a value of 5506 ± 297 nmol x min^{-1} x mg^{-1}. The velocity of αCaMKII phosphorylation for IL1 peptide was lower than that of Syntide-2, giving a specific activity of 922 ± 37.4 nmol·min^{-1}·mg^{-1}. The speed of αCaMKII phosphorylation was at undetectable level (i.e. extremely reduced) with the pre-mixing of 80 μM IL2, IL3 or C-Tail peptides (Figure 5.1 and Table 5.1). The phosphorylation affinity (K_m) of αCaMKII for IL1 was 19 ± 1 μM, which was similar to Syntide-2 at 12 ± 2 μM (Table 5.1). The six-fold difference in specific activities of IL1 and Syntide-2 and their comparable K_m values imply that αCaMKII may favour a longer interaction with IL1 as opposed to Syntide-2. It was observed that IL1 contains two T residues separated by a V. To determine the site of phosphorylation, two different peptides were synthesised (IL1-T75A and IL1-T77A). αCaMKII was found to phosphorylate only IL1-T75A peptide with a specific activity of 80.7 ± 1.4 nmol x min^{-1} x mg^{-1}, implying that T77 of IL1 is the site of phosphorylation (Figure 5.2 and Table 5.1).

However, the catalytic activity of αCaMKII was ~11-fold lower for IL1-T75A relative to the parent IL1 (Table 5.1). Thus, the side chain of T75 in IL1 may be configurationally important in supporting T77 phosphorylation. Interestingly, IL1 and IL1-T75A phosphorylation exhibited positively cooperative kinetics with a Hill coefficient (*n*) of 4.4 ± 0.83 and 3.3 ± 0.15, respectively. This was in stark contrast to Syntide-2 phosphorylation, which was observed to have non-cooperative kinetics.

GPCRs are known to form receptosomes, consisting of macromolecular protein complexes with divergent roles (Bockaert et al., 2004). Moreover, the activation of the KISS1R is thought to activate the canonical transient receptor potential (TRPC) channel (Zhang et al., 2013). Thus, the KISS1R may function in a unique microenvironment with local Ca^{2+} dynamics. In order to understand the role of Ca^{2+} in the activation of αCaMKII, T286 autophosphorylation experiments were carried with wild type and CaM mutants with submaximal Ca^{2+} binding.

The C-terminal domain of CaM is thought to have an inherently higher affinity for Ca^{2+} than the N-terminal domain (Martin et al., 1985). This would imply that CaM C-terminal domain is populated by low amplitude/frequency Ca^{2+} whereas CaM N-terminal domain is populated with high amplitude/frequency Ca^{2+} (Jama et al., 2011). With this in mind, CaM mutants deficient in the Ca^{2+} binding sites of the N-terminal domain (CaM1 and CaM2) and the C-terminal domain (CaM 3 and CaM 4) were generated by single site mutation of the first coordinating Asp of the Ca^{2+} binding EF-hand motifs to Ala (CaM1-D21A, CaM2-D56A, CaM3-D93A and CaM4-D131A). Because calcium ions are coordinated in a pentagonal configuration around the EF-hand motif, the first Asp and the last Glu of the motif provides two oxygen atoms, each for binding calcium. Additionally, the negatively charged Asp and Glu will make a charge-interaction with the positively charged calcium ion. Thus replacing the first Asp and/or last the Glu to Ala will remove the functionality of the respective EF-hand motif (Martin et al., 1992, Babu et al., 1985).

The rate of αCaMKII Thr^{286} autophosphorylation by wild-type CaM was previously determined to be very fast at ~ 5 s^{-1} by quenched flow (Bradshaw et al., 2002). In another study, manual mixing experiments showed that wild-type CaM induced complete Thr^{286} autophosphorylation in less than 15 s (Tzortzopoulos et al.,

2004). However, when following the reaction for 1 hour, a second slower phase became apparent (Figure 5.3, Table 5.2).

Wild-type and mutant CaMs were reacted with αCaMKII in the presence of assay buffer (see section 2.15) and the time course of the reaction was determined by western blotting (see section 2.26). The fastest possible sampling time was 15 s, at this time point the reaction was ~ 50 % complete. Therefore, we decided to plot the data with two phases, the first being constrained to 5 s^{-1}, in line with the previously determined fast rate (Bradshaw et al., 2002). This enabled the deconvolution of the second phase of the Thr^{286} autophosphorylation rates. Wild-type CaM induced the second rate Thr286 autophosphorylation by 0.006 s^{-1} (Table 5.2). With regards to CaM2 and CaM3, the T286 autophosphorylation rates were similar to the time courses of wild type CaM. This was in stark contrast to the T286 autophosphorylation time courses of CaM1, CaM4, CaM12, and CaM34, which showed a much diminished fast phase, and a significantly slower second phase at 0.0014, 0.002, 0.0024, and 0.0008 s^{-1} ($p < 0.05$), respectively (Figure 5.3 and Table 5.2).

In summary, the steady state kinase assay revealed that αCaMKII selectively phosphorylates IL1 of the KISS1R and that the phosphate group is likely attached to T77. Additionally, the phosphorylation of IL1 by αCaMKII exhibited cooperative kinetics unlike Syntide-2. Furthermore, the role of Ca^{2+} dynamics in αCaMKII T286 autophosphorylation was determined to involve both CaM domains and thus suggests that αCaMKII activation and the subsequent KISS1R-IL1 phosphorylation requires local and global Ca^{2+} dynamics.

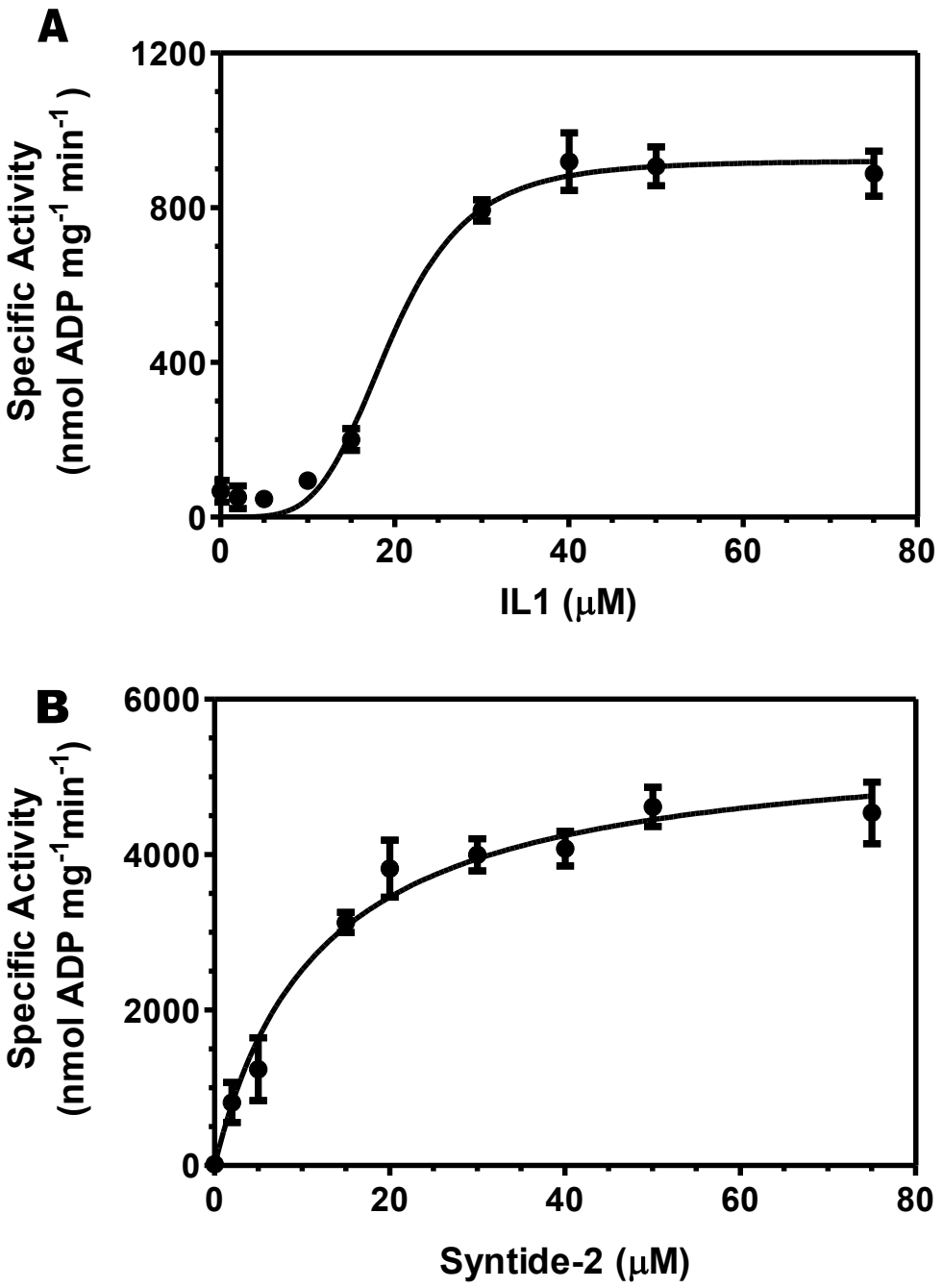

Figure 5.1 KISS1R-IL1 and syntide-2 phosphorylation by αCaMKII. 6 μM Calmodulin and 50 μM $CaCl_2$ were reacted with varying concentrations of IL1 peptide in the presence of **(A)** 50 nM αCaMKII or **(B)** 35 nM αCaMKII. The experiments were carried out at 21°C, pH 7.0 in the spectrofluorimetry-coupled enzyme reaction assay containing 100 mM KCl, 50 mM K^+- PIPES, and 2 mM $MgCl_2$, 2 mM PEP, 1 mM ATP, 22 μM NADH, 5 mM DTT. NADH fluorescence was determined at excitation wavelength 346 nm and emission wavelength 460 nm. The average of three repeats was plotted and the error bars show the S.E.M. The data was fitted to a Michaelis-Menten model. The standard error displayed in Table 5.1 shows the error of the fit.

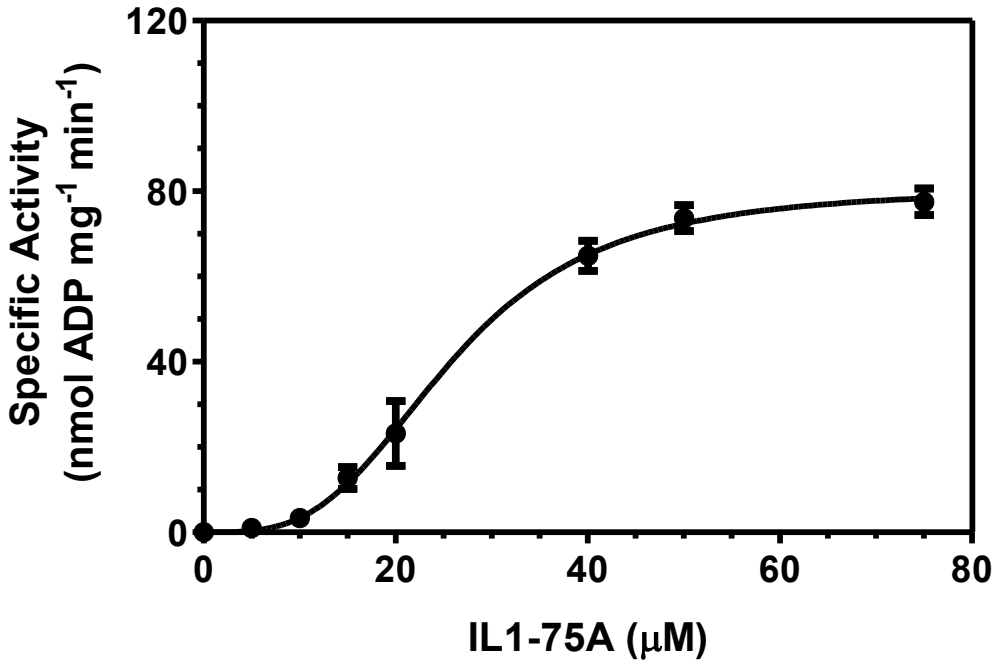

Figure 5.2 KISS1R-IL1 T75A phosphorylation by αCaMKII. 50 nM αCaMKII, 6 μM Calmodulin and 50 μM $CaCl_2$ were reacted with varying concentrations of IL1-T^{75A} peptide. The experiment was carried out at 21°C, pH 7.0 in the spectrofluorimetry-coupled enzyme reaction assay containing 100 mM KCl, 50 mM K^+- PIPES, and 2 mM $MgCl_2$, 2 mM PEP, 1 mM ATP, 22 μM NADH, 5 mM DTT. NADH fluorescence was determined at excitation wavelength 346 nm and emission wavelength 460 nm. The average of three repeats was plotted and the error bars show the S.E.M. The data was fitted to a Michaelis-Menten model. The standard error displayed in Table 5.1 shows the error of the fit.

Table 5.1 Summary of αCaMKII catalyzed phosphorylation kinetics of the synthesized peptides derived from the intracellular regions of KISS1R. Bold **A** letters represent the introduced mutations. Blue represents the initiation of the αCaMKII consensus sequence. Red denotes the potential phosphorylation residue. IL is the abbreviation for intracellular loops and C-Tail means C-terminal tail region of KISS1R.

Peptide	Sequence	K_m	Hill coefficient	Specific Activity V_{max} (*nmol of ADP*)
		μM	*n*	min^{-1} mg^{-1}
Syntide-2	PLA**R**TL**S**VAGLPGKK	12 ± 2	-	5506 ± 297
IL1(I67-Y80)	ICRHKPM**R**TV**T**NFY	19.6 ± 1.4	4.4 ± 0.83	922 ± 37.4
IL1-T75A (I67-Y80)	ICRHKPM**R****A**V**T**NFY	25.9 ± 0.6	3.3 ± 0.15	80.7 ± 1.4
IL1-T77A (I67-Y80)	ICRHKPMRTV**A**NFY	-	-	Undetectable
IL2 (W141-R154)	WYVTVFPLRALHRR	-	-	Undetectable
IL3 (M227-R263)	MLRHLGRVAVRPAPADSA-LQGQVLAERAGAVRAKVSR	-	-	Undetectable
C-Tail (C340-H360)	CAPRRPRRPRRPGPSDPAAPH	-	-	Undetectable
C-Tail (A361-A371)	AELH**R**LG**S**HPA	-	-	Undetectable

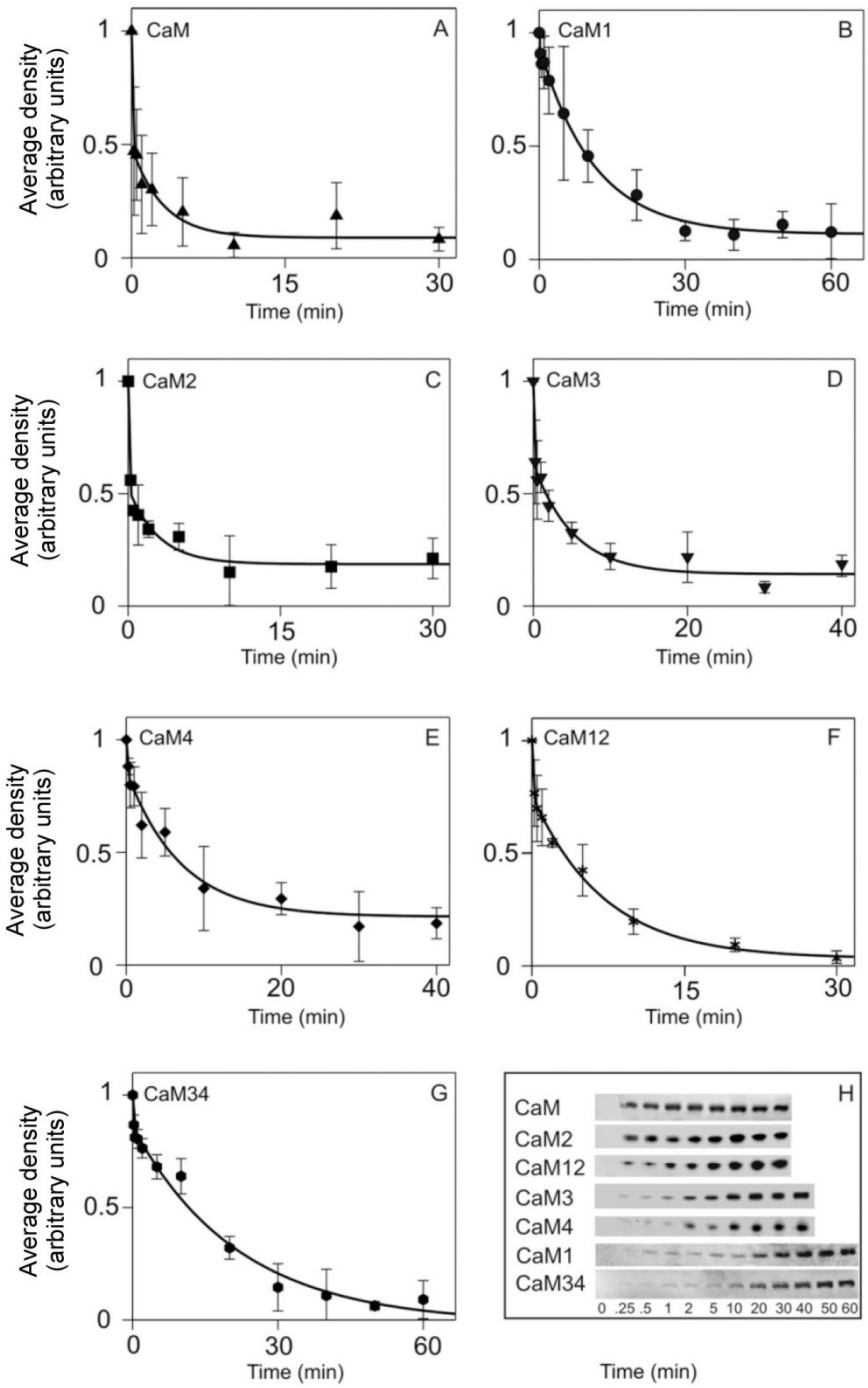

Figure 5.3 Time courses of αCaMKII T286 autophosphorylation induced by wild type and mutant CaMs. A–G, Densitometric analysis of the western blots (immunoblots shown in **H** and described in section 2.15) for wild type CaM (**A**), CaM1 (**B**), CaM2 (**C**), CaM3 (**D**), CaM4 (**E**), CaM12 (**F**), and CaM34 (**G**) were performed as previously described (see section 2.15) and fitted an exponential function. The rate constant amplitudes are shown in Table 5.2. The error bars represent the S.D. from three repeats.

Table 5.2 Summary of the rates of αCaMKII T286 autophosphorylation by CaM mutants. The time courses were fitted to a double exponential. The amplitudes (***A***) and rates (***k***) for each phase is given. The values are the mean of three measurements. The standard errors are the S.E.M. ‡ Denotes statistically significant (P > 0.05) values compared to the second phase (s^{-1}) of wild-type CaM Thr^{286} autophosphorylation. See section 2.15 for more details.

	k_1	A_1	k_2	A_2
	s^{-1}		s^{-1}	
CaM	5 ± 0	0.6 ± 0.1	0.006 ± 0.002	0.4 ± 0.1
CaM1	5 ± 0	0.1 ± 0.03	0.0014 ± 0.0001‡	0.9 ± 0.02
CaM2	5 ± 0	0.6 ± 0.1	0.006 ± 0.003	0.4 ± 0.1
CaM3	5 ± 0	0.4 ± 0.1	0.003 ± 0.001	0.6 ± 0.1
CaM4	3 ± 0	0.2 ± 0.11	0.002 ± 0.001‡	0.8 ± 0.1
CaM12	5 ± 0	0.2 ± 0.1	0.0024 ± 0.0003‡	0.8 ± 0.1
CaM34	5 ± 0	0.14 ± 0.06	0.0008 ± 0.0002‡	0.86 ± 0.07

5.3.2. Phosphomimetic mutations of KISS1R-T77.

The functional significance of phosphorylated KISS1R-T77 was investigated. To do this, phosphorylation-deficient KISS1R-T77A and the phosphomimetic KISS1R-T77D and KISS1R-T77E mutants were generated (see section 2.7). The effect of the mutations was studied with radio-ligand binding and inositol phosphate (IP_3) turnover assays (see sections 2.22 and 2.27, respectively). The results showed that the phosphomimetic mutations abolished IP_3 turnover, but had unchanged ligand binding affinity (IC_{50}) (Figure 5.4, Figure 5.5, and Table 5.3). In addition, co-transfection of GFP-αCaMKII and KISS1R in COS-7 cells led to a reduced KP-10 *Emax* as compared to KISS1R only transfected COS-7 cells (Figure 5.6).

αCaMKII selectively phosphorylates T77 KISS1R (see section 5.3.1). Therefore, the role of this residue in receptor function was investigated by replacing it with phosphomimetic aspartic acid (D) and glutamic acid (E). Furthermore, phosphorylation deficient KISS1R-T77 was studied with alanine (A) substitution, which deletes the side-chain beyond the β-carbon. The KISS1R constructs were transiently transfected into COS-7 cells and their function was studied with radio-ligand binding and IP_3 turnover assays (see section 2.22 and 2.24, respectively). The expression levels of the KISS1R mutants were moderately reduced relative to wild-type KISS1R. The expression level of T77A (48 % ± 4 %), T77D (56 % ± 2 %) and T77E (65 % ± 11 %) were however sufficiently expressed to measure KP-10 binding affinity, which showed IC_{50} values ranging from 3.2 ± 0.4 to 5.3 ± 0.2 nM and were similar to wild-type KISS1R with an IC_{50} value of 5.2 ± 0.6 nM (Figure 5.4 and Table 5.3). The IP_3 turnover study of these mutant KISS1Rs showed that T77A had unchanged relative maximum responsiveness relative to wild-type (Figure 5.5 and Table 5.3). In contrast, KISS1R-T77D/E gave very little IP_3 responses, (Figure 5.5 and Table 5.3). This suggested that the phosphomimetic mutations may cause deleterious effects on the receptor-G protein coupling. Furthermore, of the three KISS1R mutants tested, only the T77A gave a moderate IP_3 response to KP-10 stimulation, showing a 2.2-fold increase in EC_{50} value and 50 % reduction in *Emax*. This was thought to be caused by the reduced receptor expression level on the cell

surface. The mutant T77A gave a relative maximum responsiveness that was similar to wild-type by taking into account receptor expression levels.

The role of αCaMKII in KISS1R mediated IP_3 response was investigated further. Wild-type KISS1R and GFP-αCaMKII were transiently co-transfected into COS-7 cells. The increased expression of αCaMKII levels reduced the maximum IP_3 responses relative to the wild-type KISS1R co-transfected with vector DNA at the same amount of GFP-αCaMKII. The pre-incubation (30 minutes) of KN-93 inhibitor with cells co-expressing KISS1R and GFP-αCaMKII reversed the reduced KP-10 *Emax* (Figure 5.6). This indicated that inhibition of αCaMKII increased KP-10 induced IP_3 response, suggesting an inhibitory role of αCaMKII in KISS1R-elicited IP_3 turnover.

In conclusion, phosphomimetic mutations at T77 of KISS1R-IL1 nearly abolished IP_3 responses without altering KP-10 binding affinity. In addition, increasing the expression of αCaMKII decreases KISS1R elicited maximum IP_3 response. This suggested that the phosphorylation of KISS1R-T77 by αCaMKII would inhibit KISS1R-Gq/11 coupling, and that αCaMKII functions to desensitise KISS1R activity.

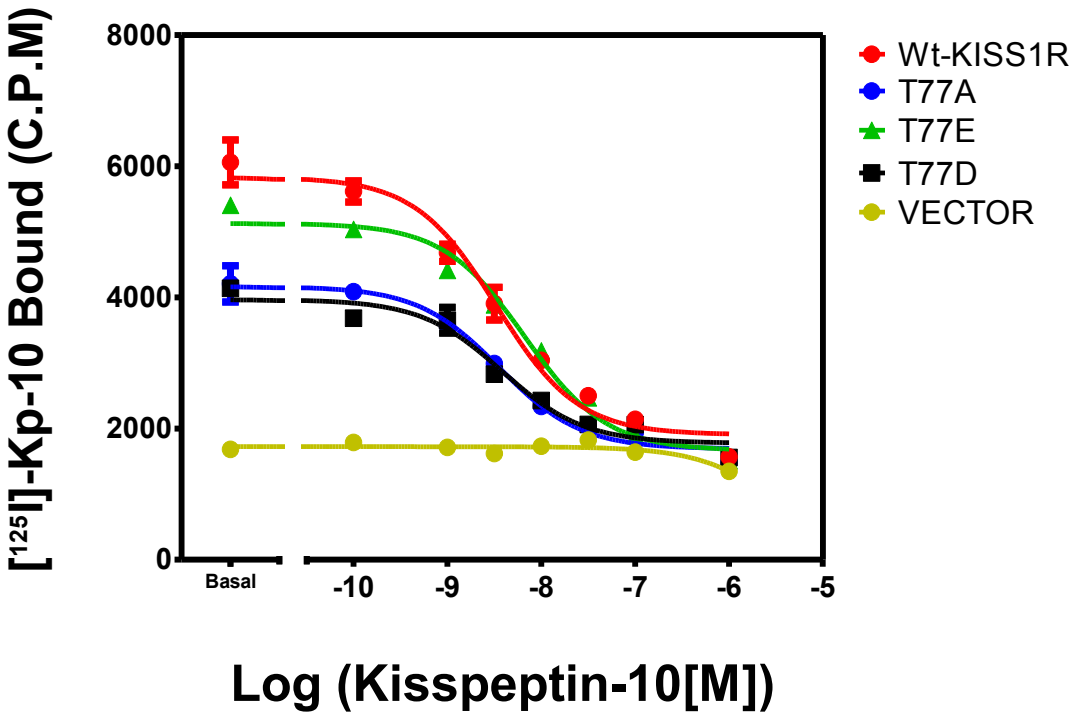

Figure 5.4 Effects of KISS1R-T77 mutation on KP-10 ligand binding. COS-7 cells were transiently transfected with KISS1R constructs and incubated for 48 hour prior to processing with radio-ligand binding assay (see section 2.22). A representative of three independent experiments is presented.

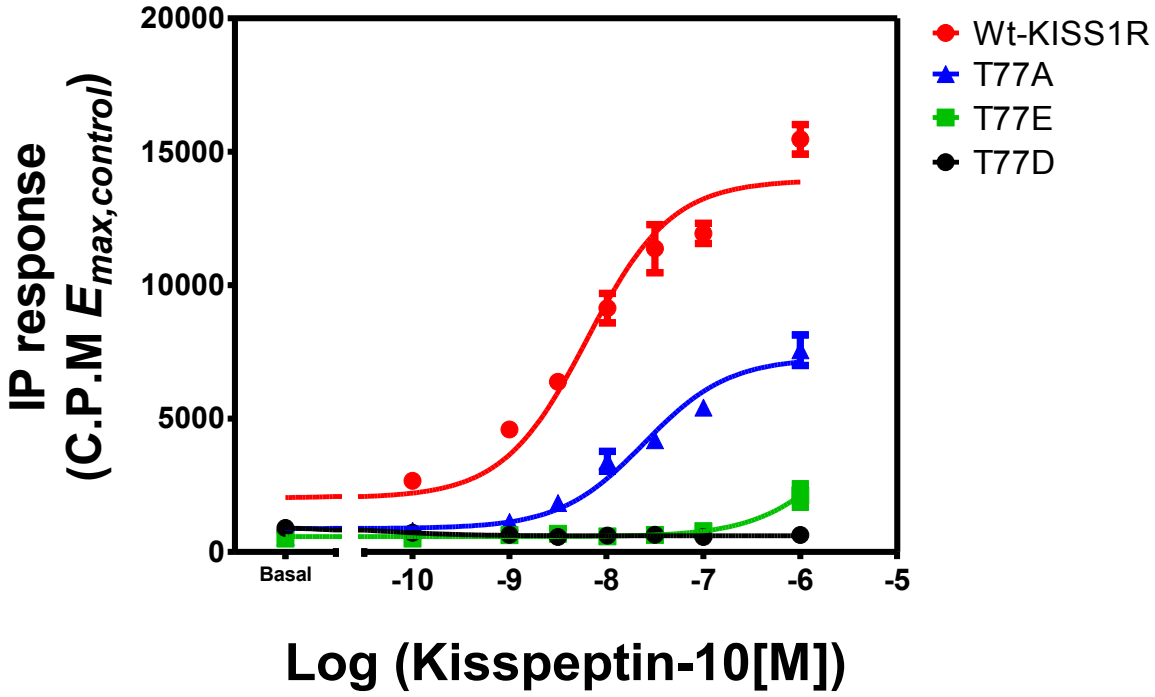

Figure 5.5 KP-10 induced IP_3 response of KISS1R-T77 mutants. COS-7 cells were transiently transfected with KISS1R constructs 48 hours before stimulation with KP-10 for 60 minutes, and then by followed be measuring IP_3 turnover (see section 2.24). A representative of three independent repeats is presented.

Table 5.3 Effects of mutations of KISS1R-T77 on receptor binding functional response. COS-7 cells were transiently transfected with KISS1R constructs 48 hours prior to processing with radio-ligand binding IP_3 assays (see section 2.22 and 2.24, respectively). [a] Normalised to itself [b] Normalised to the average of the experimental repeats Asterisks (*) denote statistical significance (* P<0.05, ** P<0.01, *** P< 0.001) as calculated by One-Way Anova with Dunnett's test.

Mutant	Binding		IP_3 Responses		Relative Maximum Responsiveness
	R_{exp}	IC_{50}	E_{max}	EC_{50}	E_{max}/R_{exp}
	% WT	*(nM)*	*% WT*	*(nM)*	*Fold Change*
WT	100[a]	5.2 ± 0.6	100[a]	5.3 ± 0.62	1.00 ± 0.13[b]
T77A	48 ± 4**	4.1 ± 0.5	50 ± 2	11.7 ± 6.4	1.04 ± 0.03
T77D	56 ± 2**	3.2 ± 0.4	4 ± 2	(undetectable)	0.16 ± 0.01 (uncoupled)***
T77E	65 ± 11*	5.3 ± 0.2	19 ± 13	(undetectable)	0.07 ± 0.03 (uncoupled)**

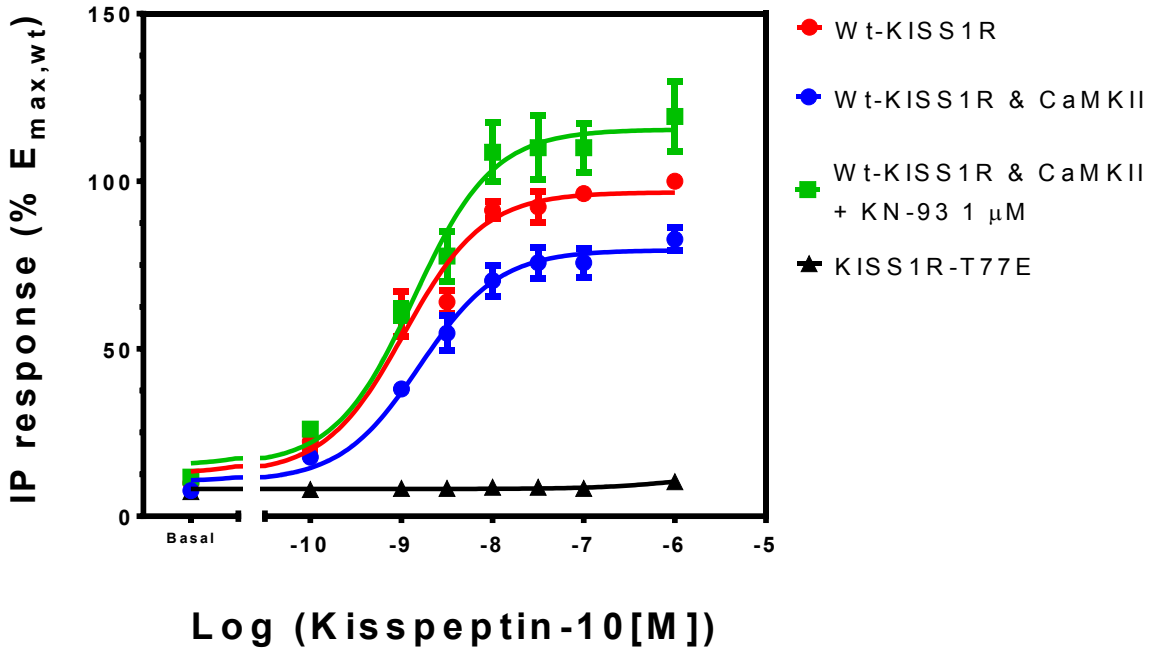

Figure 5.6 Effect of αCaMKII on KISS1R-elicited IP_3 response. COS-7 cells were transiently co-transfected with KISS1R and GFP-αCaMKII or vector DNA 48 hours prior to IP_3 assay (see section 2.17). An average of three experiments is shown.

5.3.3. Perturbation of αCaMKII function in rat HPG axis

The physiological significance of αCaMKII in the regulation of hypothalamic-pituitary-gonadal axis (HPG) by KPs was investigated. In order to do this, I collaborated with Professor Kevin O'Byrne of Kings College London, United Kingdom. The model organism we chose was ovariectomised (OVX). The OVX rats were intracerebroventricularly (ICV) treated with N-terminal myristoylated autocamtide-2 related inhibitory peptide (Myr-AIP) for 10 minutes prior to KP-10 ICV administration. The obtained results revealed that Myr-AIP and KP-10 administered rats exhibited augmented luteinizing hormone (LH) responses relative to KP-10 only treated rats, as measured by plasma LH concentrations.

The full-length human KISS1R shares 80 % amino acid sequence homology with the rat KISS1R (Kotani et al., 2001). Furthermore, the intracellular loop 1 (IL1) of KISS1R, and particularly the phosphorylatable T77 of the human KISS1R is fully conserved among fish, amphibians and mammals (Figure 5.7). However, the R74 residue at IL1 of the human KISS1R that is part of the αCaMKII consensus motif is changed to Q in the rat KISS1R at the equivalent position. The consequence of this alteration is unknown. An attempt to study the effect of this change on αCaMKII specific activity was made, but the synthesised rat IL1 peptide could not be dissolved in the assay buffer, presumably because it was too hydrophobic. This made the kinetic studies unfeasible. The significance of the amino acid change is discussed further in the discussion section of this chapter.

In order to inhibit αCaMKII *in vivo,* the AIP inhibitor was selected because of its characteristics of high specificity, potency, and high-affinity. AIP inhibits αCaMKII with an IC_{50} value of 100 nM, but does not affect the catalytic activity of protein kinases A and C (PKA and PKC), and CaMKIV (Ishida et al., 1995). Myr-AIP was used to increase cell permeability. The OVX rats showed unchanged LH pulses after ICV administration with 4 nmol Myr-AIP, indicating that Myr-AIP and the subsequent inhibition of αCaMKII did not affect the basal LH responses (Figure 5.8 C). The ICV administration of 1 nmol of KP-10 increased the plasma LH concentration (basal ~ 2 ng/ml: KP-10 5.6 ng/ml LH) (Figure 5.8 A). The ICV

administration of 4 nmol Myr-AIP 10 minutes prior to 1 nmol KP-10 treatment revealed an augmented LH spike (basal ~2 ng/ml: Myr-AIP+KP-10 8 ng/ml LH) and prolonged duration of the response (Figure 5.8 B). This was observed in 4 repeats (a representative results is shown). Thus, the amplitude of LH spike in the KP-10 only treated rats had to be kept low in order to circumvent the 'ceiling effect' of Myr-AIP + KP-10 synergistic effects.

Interestingly, increasing the concentration of Myr-AIP treatment (40 nmol) prior to KP-10 (1 nmol) administration had an unexpected effect. The expected augmentation observed in 4 nmol Myr-AIP was not observed in the rats pre-treated with 40 nmol Myr-AIP (Figure 5.9). It is presently unclear why the increased concentration of Myr-AIP had this effect, but one explanation may be a side-effect.

Taken together these results indicate that the human αCaMKII consensus sequence in IL1 is on the whole conserved amongst vertebrates with changes to R74 to Q in rodents. Also, inhibiting αCaMKII prior to KP-10 administration augments LH secretion. However, increasing the concentration of Myr-AIP appears to exhibit side-effects that are yet unknown.

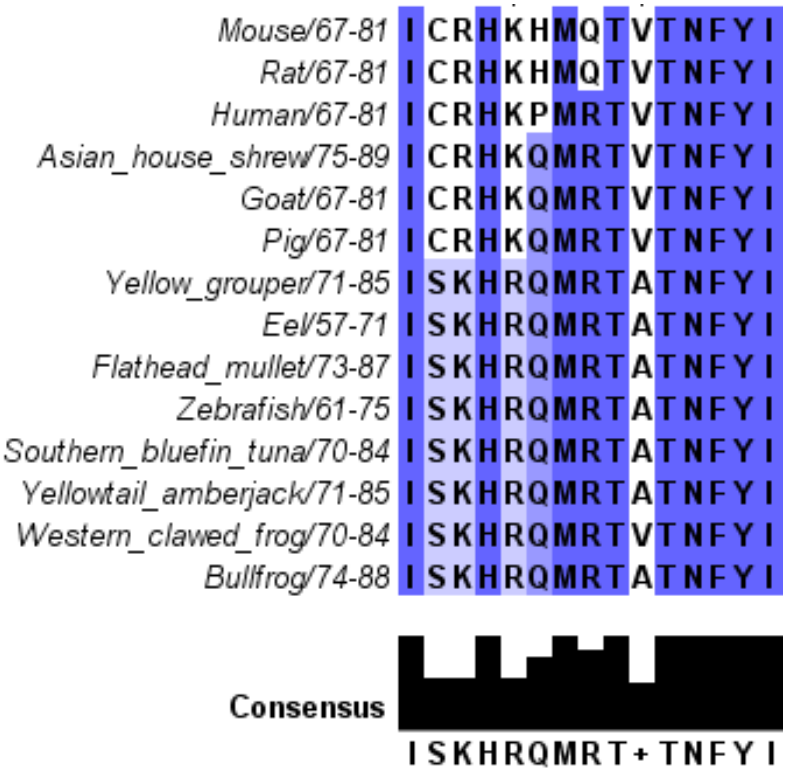

Figure 5.7 The amino acid sequence of KISS1R-IL1 is evolutionarily conserved among fish, amphibians and mammals. The amino acid sequences were obtained from Pubmed. The sequence alignments were performed with the full length sequences of KISS1R and only the IL1 region is shown. The blue represents identical amino acids. The 'Quality' is calculated used the Blosum 62 score. The image was analysed in Jalview2.7.

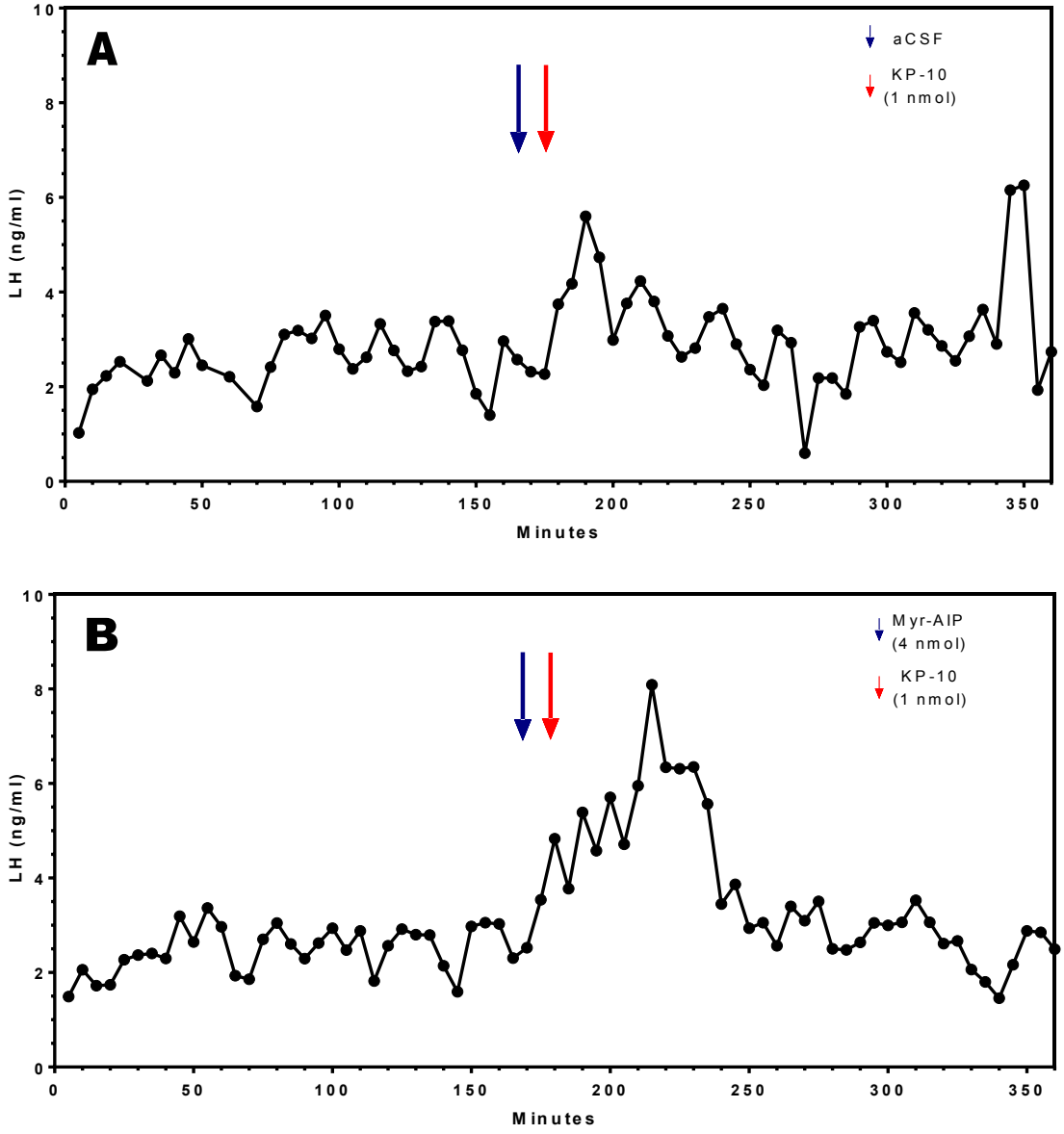
A
aCSF
KP-10
(1 nmol)
LH (ng/ml)
Minutes
0
2
4
6
8
10
0
50
100
150
200
250
300
350
B
Myr-AIP
(4 nmol)
KP-10
(1 nmol)
LH (ng/ml)
Minutes

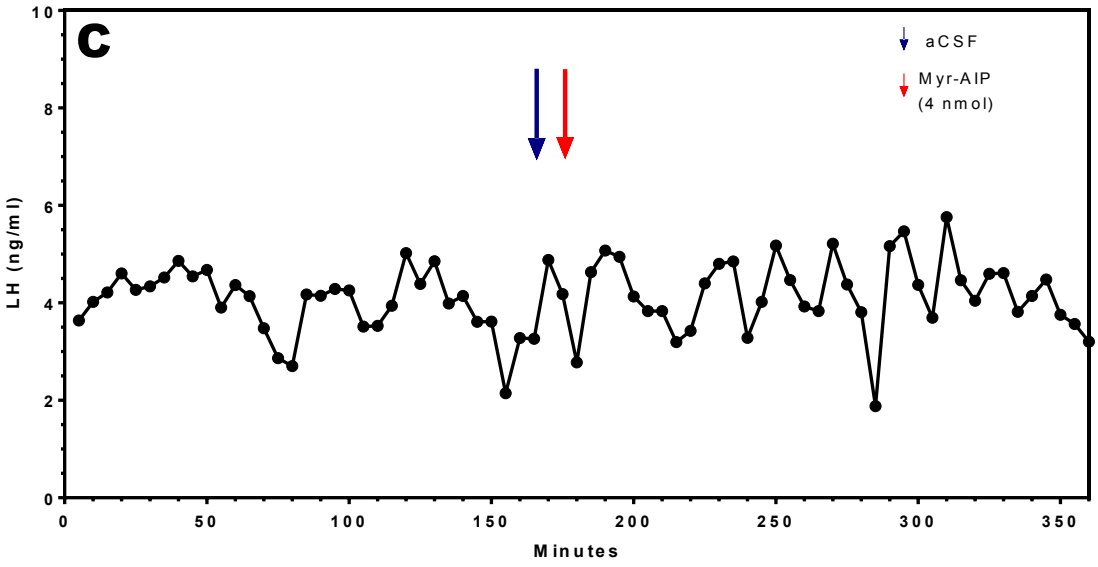

Figure 5.8 ICV administration of Myr-AIP at 4 nmol augments KP-10 stimulated LH spike in OVX rats. Ovariectomized (OVX) rats were intracerebroventricularly (ICV) treated with **(A)** 4 µL artificial cerebrospinal fluid (aCSF, blue arrow, 165 minutes) followed by 1 nmol/4 µL of the KP-10 (red arrow, 175 minutes). **(B)** ICV treatment with 4 nmol/4 µL of myristoylated autocamtide-2 related inhibitory peptide (Myr-AIP, blue arrow, 165 minutes) followed by 1 nmol/4 µL of the KP-10 (red arrow, 175 minutes). **(C)** ICV treatment with 4 µL aCSF (blue arrow, 165 minutes) followed by 4 nmol/4 µL of Myr-AIP (blue arrow, 175 minutes). All figure are representatives of at least three repeats with the exception of **A**, which was repeated twice. The second repeat of **A** did not show any spike.

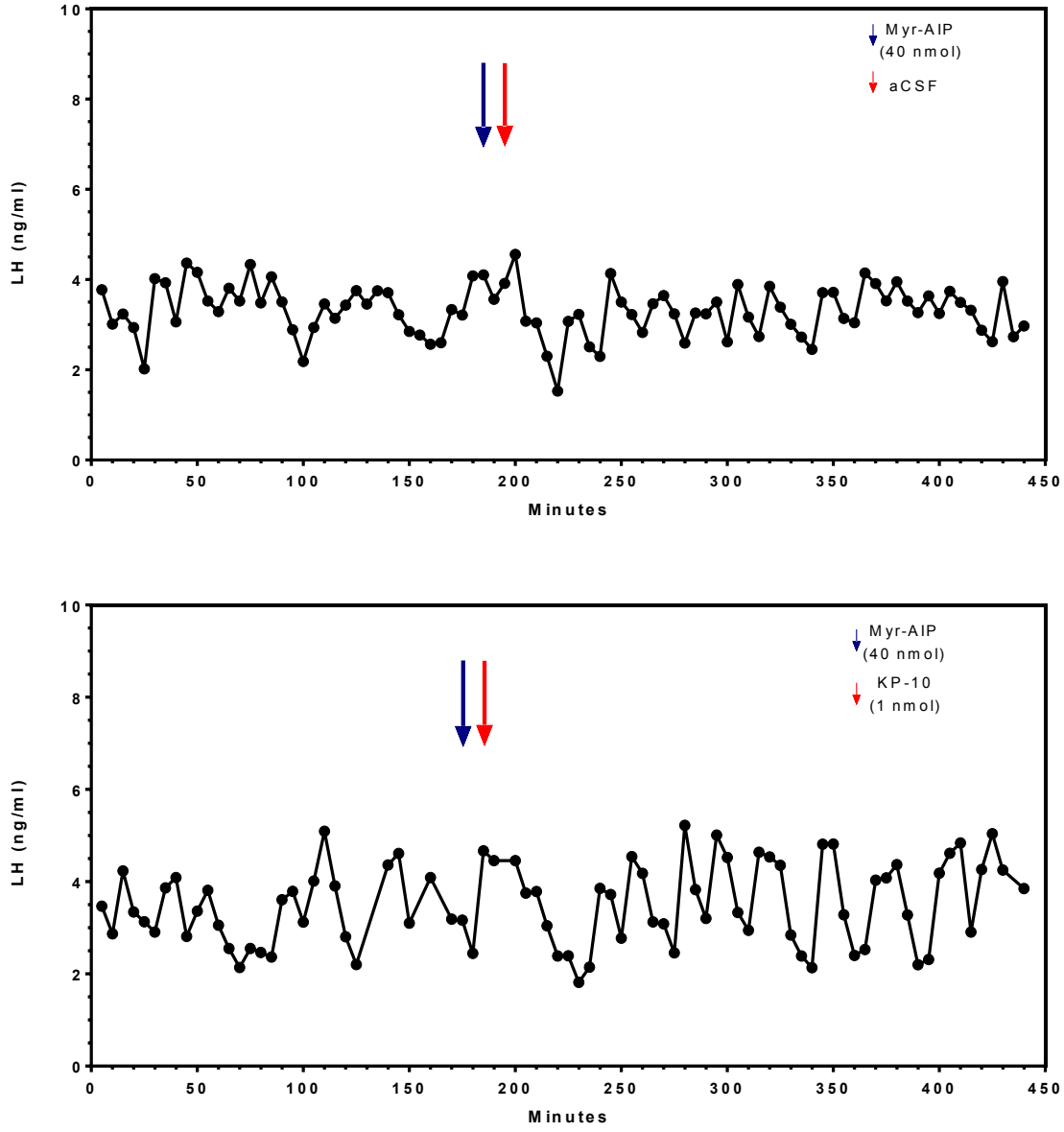

Figure 5.9 Effect of ICV Myr-AIP at 40 nmol on KP-10 stimulated LH spike in OVX rats. Ovariectomized (OVX) rats were intracerebroventricularly (ICV) treated with 40 nmol/4 µL Myr-AIP (blue arrow, 165 minutes) followed by 1 nmol/4 µL of KP-10 (red arrow, 175 minutes). Myr-AIP denotes myristoylated autocamtide-2 related inhibitory peptide and aCSF denotes artificial cerebrospinal fluid. Both figures are representatives of at least three repeats.

5.4 Discussion

In this chapter I uncovered an inhibitory phosphorylation of KISS1R by αCaMKII. Although the human KISS1R contains two αCaMKII consensus motifs positioned in IL1 and the C-terminal tail, it was determined that αCaMKII cooperatively phosphorylates only IL1 at T77. The functional significance of a phosphate group attached to T77 was investigated with phosphomimetic mutations. The results revealed that KISS1R-T77D and KISS1R-T77E were functionally deficient in eliciting inositol phosphate turnover (IP_3). Furthermore, the role of Ca^{2+} in the activation of αCaMKII was determined to require a diverse range of Ca^{2+} dynamics. In addition, the *in vivo* functional significance of αCaMKII interactions with KISS1R was studied with OXV rats ICV treated with Myr-AIP prior to KP-10 administration. The results showed that αCaMKII inhibition augments the effects of KP-10 stimulated blood LH levels. The data of this chapter identifies a new link between KP-10/KISS1R and the reproductive axis via αCaMKII.

Notably, human KISS1R contains two R*XX*S/T motifs in the first intracellular loop and the C-terminal tail (Table 5.1). This sequence is consistent with the consensus substrate recognition motif (R*XX*S/T) for αCaMKII (White et al., 1998). However, only IL1 was observed to be phosphorylated by αCaMKII. It is plausible that αCaMKII is unable to phosphorylate the C-terminal tail fragment (A361-A371) due to the bulky hydrophobic L363 and L365 flanking the crucial R365, and thus masking the initiation of the recognition motif. Furthermore, the S368 of the motif might be very flexible due to the presence of G367, making the recognition motif unable to be phosphorylated by αCaMKII. Future studies should be carried out to determine whether these amino acids are factors in the inability of αCaMKII to phosphorylate the C-terminal tail fragment (A361-A371). In addition, the recognition motif (R*XX*S/T) is known to be a target for other kinases, such as protein kinase A, C (PKA and PKC) and Akt/PKB (Montminy, 1997, Pearson and Kemp, 1991). Thus, future studies to investigate whether these kinases can phosphorylate IL1 are required and may increase our understanding of the proteomic networks that are involved in down-regulating KISS1R activity.

The rat and human KISS1R share 80 % sequence homology, as well as similar KP ligand binding affinity and potency (Kotani et al., 2001). Nevertheless, the R74 of the human KISS1R, that is part of the αCaMKII recognition motif, is changed to Q in the rat KISS1R. However, a valid αCaMKII recognition motif still exists in IL1 of rat KISS1R in the form of H*XX*T motif. It is possible that histidine can replace arginine in the consensus sequence as long as it carries a positive charge. This corresponds to H72 and upon protonation at pH 6.5 it is possible that T75 becomes the phosphorylatable residue. A similar observation is reported in the inhibitory phosphorylation of the human HMG-CoA reductase by αCaMKII via the sequence H869-D-R-S872 (Clarke and Hardie, 1990). The authors show that αCaMKII phosphorylation of HMG-CoA increases at pH 6.5 compared to pH 7.2 (Clarke and Hardie, 1990). In this study, an attempt was made to verify this, however, the synthesised IL1 peptide was unable to be dissolved in assay buffer, because the peptide was too hydrophobic (see section 2.20). Future experiments should entail synthesising a peptide that can be dissolved in order to verify whether the rat KISS1R-IL1 can be phosphorylated by αCaMKII and whether pH plays any role.

The cooperative phosphorylation of the human KISS1R IL1 by αCaMKII means that the initial catalytic domain involved in IL1 phosphorylation positively affects adjacent catalytic domains preferentially over those located more distantly within the dodecameric structure. Furthermore, the IL1-T75A peptide exhibited cooperative phosphorylation and thus the two threonine residues of IL1 (T75 and T77) were unlikely to be the cause of the cooperative phosphorylation. In contrast, Syntide-2 phosphorylation was non-cooperative, implying that one αCaMKII catalytic domain does not sequentially affect another catalytic domain. It is presently unclear the exact cause of this kinetic phenomenon, but is likely due to the difference in the amino acid sequence of Syntide-2 and IL1 peptides. Also, the speed (velocity) at which αCaMKII phosphorylated IL1 was observed to be ~6 times slower than syntide-2 phosphorylation. Although αCaMKII's Hill coefficient of (n) 4.4 ± 0.83 in the phosphorylation of IL1 may account partially for the reduced speed, it is possible that other contributing factor(s) exist. A similar observation was reported in the

phosphorylation of the limbic dopamine receptor (D2R) by αCaMKII. The authors report αCaMKII recognises a binding motif at the N-terminus of D2R IL3 and phosphorylates S229 at a speed of 4.0 ± 0.2 pmol/μg/min and affinity of *Km* 65.9 ± 1.2 nM (Liu et al., 2009). The specific activity of αCaMKII in the phosphorylation D2R IL3 was 4-fold faster than the phosphorylation of KISS1R IL1. This may be explained by the observation that the D2R IL3 is non-cooperatively phosphorylated by αCaMKII (Liu et al., 2009). Thus αCaMKII's Hill coefficient of (*n*) 4.4 ± 0.83 in the phosphorylation of IL1 may account for the reduced speed.

The autophosphorylation of αCaMKII (T286) by Ca^{2+}/CaM is critical for its *in vivo* function (Giese et al., 1998). The Ca^{2+} binding sites 1, 3, and 4 are sufficient in promoting αCaMKII T286 autophosphorylation. This is supported with the observation that CaM mutants with submaximal Ca^{2+} binding sites 1, 3, and 4 significantly inhibited the rate of αCaMKII T286 autophosphorylation (Figure 3). Furthermore, CaM C-terminal domain is populated by low amplitude/frequency Ca^{2+} whereas CaM N-terminal domain is populated with high amplitude/frequency Ca^{2+} (Jama et al., 2011). With this in mind, Ca^{2+}/CaM decode global and local Ca^{2+} dynamics and transduce αCaMKII T286 autophosphorylation. Therefore, αCaMKII is likely to integrate a diverse Ca^{2+} dynamic into the phosphorylation of KISS1R IL1

To date, very little is known about the significance of IL1 in the activation mechanisms of KISS1R. Herein, evidence is presented that IL1-T77 phosphorylation confers onto KISS1R the uncoupling of heterotrimeric G protein – Gq/11 and the inhibition of IP_3 turnover. Whether a phosphate group at IL1-T77 is permanent or not is presently unknown. However, the KISS1R is known to physically interact with phosphatase 2A (PP2A-C). This interaction may enable the dephosphorylation IL1-T77 (Evans et al., 2008).

The inhibition of αCaMKII function by Myr-AIP in the hypothalamus of OVX rats revealed an expected augmentation of KP-10 induced role of the HPG axis. Unexpectedly however, the increased dose of 40 nmol Myr-AIP abolished the observed augmentation. This may be explained by the side-effect of the high dose of Myr-AIP. One such side-effect may be the unintended inhibition αCaMKII phosphorylation of the α-amino-3-hydroxy-5-methyl-4-isoxazolepropionic acid

(AMPA) receptor, and thus impairing synaptic functioning, which is critical for neuronal communication [as reviewed in (Derkach, 2011)].

In conclusion, the human KISS1R was identified to contain two consensus motifs for αCaMKII phosphorylation. They are located in the intracellular loop 1 (IL1) and the C-terminal tail of KISS1R. Upon further examination αCaMKII was found to selectively phosphorylate IL1 at residue T77. The phosphorylation of IL1 was observed to be cooperative, which implied that the dodecameric αCaMKII must utilise several catalytic domains in that effort. Furthermore, decrypting the Ca^{2+} dynamics that regulate αCaMKII function revealed that global and local Ca^{2+} ooscillations have important roles. Phosphomimetic mutations (E/D) of KISS1R-T77 revealed a significant reduction in inositol phosphate turnover following KP-10 stimulation, but exhibited unchanged IC_{50} ligand binding. Micro-injections of the αCaMKII inhibitor – autocamtide-2 related inhibitory peptide (AIP) into the hypothalamus of ovariectomized rats exhibited augmented KP induced blood plasma LH surge, relative to KP-10 only administered rats. Taken together, these results reveal that αCaMKII down-regulates the activity of KISS1R through phosphorylation of the IL1, and thus participates in KP-LH homeostasis.

6. Conclusion

The kisspeptin receptor (KISS1R), functioning as the metastasis suppressor and gate-keeper of GnRH neurons, is a potent activator of intracellular Ca^{2+}. Upon KISS1R activation, phospholipase Cβ (PLC_β) drives the production of inositol phosphate (IP_3), which in turn promotes Ca^{2+} release from the endoplasmic reticulum. However, the regulatory mechanisms that enables KISS1R to sense the increased intracellular Ca^{2+} concentration and avoid Ca^{2+} excitotoxicity via a signalling off-switch remains unclear. In this thesis, evidence is provided for a novel protein-protein interaction between KISS1R and the Ca^{2+} regulated proteins of Ca^{2+}/calmodulin (Ca^{2+}/CaM) and αCa^{2+}/CaM dependent protein kinase II (αCaMKII).

The interaction between CaM and KISS1R was determined with three independent methods of colocalisation with confocal microscopy, co-immunoprecipitation (Co-IP), and cell-free spectrofluorimetric CaM binding experiments. The KISS1R in HEK-293 cells was found to colocalise with CaM, as well as Co-IP with endogenous CaM in a ligand/Ca^{2+} dependent manner. Moreover, the KISS1R derived intracellular loop 2 & 3 (IL2 and IL3) peptides were found to exclusively bind CaM (see chapter 3). Further examination of the sites of interaction revealed extensive CaM binding motifs mainly positioned in IL3 of KISS1R. The alanine substitution of critical residues of the juxtamembrane regions of IL3 created a KISS1R variant with increased relative maximum responsiveness, but unchanged ligand binding affinity. These experiments were further validated with the observation that the IL3 peptide lacking the juxtamembrane regions did not bind CaM in the cell-free spectrofluorimetric CaM binding experiments (see chapter 4).

The knowledge gained from chapters 3 and 4 developed the hypothesis that αCaMKII, a closely associated kinase to Ca^{2+}/CaM, may also interact with KISS1R. This theory was validated with the observation that αCaMKII selectively phosphorylated T77 KISS1R-IL1. Interestingly, the kinetics of the phosphorylation was cooperative. The phosphomimetic mutations of KISS1R-T77D/E created a receptor that was unable to elicit IP_3 production in COS-7 cells. Finally, *in vivo*

perturbation studies with ovariectomised rats revealed that the intracerebroventricularly administrated cell-permeable αCaMKII inhibitor, autocamtide-2 related inhibitory peptide (AIP), augments the 1 nmol KP-10 stimulation of plasma luteinizing hormone (LH) levels (see chapter 5).

Taken together, these results suggest that KISS1R contains two distinct off-switch mechanisms. The first of which is the dynamic binding of Ca^{2+}/CaM to KISS1R-IL3. This is postulated to attenuate G-protein activity via steric hindrance. The second mechanism is theorised to involve the permanent inhibitory phosphorylation of KISS1R by αCaMKII. The interplay between dynamic regulation vs permanent termination of KISS1R activity, is likely determined by intracellular Ca^{2+} levels.

7. References

ANG, L. P., LEE, H. M., AU EONG, K. G., YAP, E. Y. & LIM, A. T. 2000. Endogenous Klebsiella endophthalmitis. *Eye,* 14**,** 855-60.

ARORA, K. K., SAKAI, A. & CATT, K. J. 1995. Effects of second intracellular loop mutations on signal transduction and internalization of the gonadotropin-releasing hormone receptor. *J Biol Chem,* 270**,** 22820-6.

AUDET, M. & BOUVIER, M. 2012. Restructuring G-protein- coupled receptor activation. *Cell,* 151**,** 14-23.

AYDIN, M., OKTAR, S., YONDEN, Z., OZTURK, O. H. & YILMAZ, B. 2010. Direct and indirect effects of kisspeptin on liver oxidant and antioxidant systems in young male rats. *Cell biochemistry and function,* 28**,** 293-9.

BABU, Y. S., BUGG, C. E. & COOK, W. J. 1988. Structure of calmodulin refined at 2.2 A resolution. *Journal of molecular biology,* 204**,** 191-204.

BABU, Y. S., SACK, J. S., GREENHOUGH, T. J., BUGG, C. E., MEANS, A. R. & COOK, W. J. 1985. Three-dimensional structure of calmodulin. *Nature,* 315**,** 37-40.

BALLESTEROS, J., KITANOVIC, S., GUARNIERI, F., DAVIES, P., FROMME, B. J., KONVICKA, K., CHI, L., MILLAR, R. P., DAVIDSON, J. S., WEINSTEIN, H. & SEALFON, S. C. 1998. Functional microdomains in G-protein-coupled receptors. The conserved arginine-cage motif in the gonadotropin-releasing hormone receptor. *J Biol Chem,* 273**,** 10445-53.

BARROW, A. D. & TROWSDALE, J. 2006. You say ITAM and I say ITIM, let's call the whole thing off: the ambiguity of immunoreceptor signalling. *European journal of immunology,* 36**,** 1646-53.

BASS, C., KATANSKI, C., MAYNARD, B., ZURRO, I., MARIANE, E., MATTA, M., LOI, M., MELIS, V., CAPPONI, V., MURONI, P., SETZU, M. & NICHOLS, R. 2013. Conserved residues in RF-NH receptor models identify predicted contact sites in ligand-receptor binding. *Peptides,* 26**,** 009.

BECAMEL, C., ALONSO, G., GALEOTTI, N., DEMEY, E., JOUIN, P., ULLMER, C., DUMUIS, A., BOCKAERT, J. & MARIN, P. 2002. Synaptic multiprotein complexes associated with 5-HT(2C) receptors: a proteomic approach. *The EMBO journal,* 21**,** 2332-42.

BECHTOLD, D. A. & LUCKMAN, S. M. 2007. The role of RFamide peptides in feeding. *Journal of Endocrinology,* 192**,** 3-15.

BECKER, J. A. J., MIRJOLET, J.-F., BERNARD, J., BURGEON, E., SIMONS, M.-J., VASSART, G., PARMENTIER, M. & LIBERT, F. 2005. Activation of GPR54 promotes cell cycle arrest and apoptosis of human tumor cells through a specific transcriptional program not shared by other Gq-coupled receptors. *Biochemical and Biophysical Research Communications,* 326**,** 677-686.

BELCHETZ, P. E., PLANT, T. M., NAKAI, Y., KEOGH, E. J. & KNOBIL, E. 1978. Hypophysial responses to continuous and intermittent delivery of hypopthalamic gonadotropin-releasing hormone. *Science,* 202**,** 631-3.

BENKE, T. A., LUTHI, A., ISAAC, J. T. & COLLINGRIDGE, G. L. 1998. Modulation of AMPA receptor unitary conductance by synaptic activity. *Nature,* 393**,** 793-7.

BENOVIC, J. L., PIKE, L. J., CERIONE, R. A., STANISZEWSKI, C., YOSHIMASA, T., CODINA, J., CARON, M. G. & LEFKOWITZ, R. J. 1985. Phosphorylation of the mammalian beta-adrenergic receptor by cyclic AMP-dependent protein kinase. Regulation of the rate of receptor phosphorylation and dephosphorylation by agonist occupancy and effects on coupling of the receptor to the stimulatory guanine nucleotide regulatory protein. *The Journal of biological chemistry,* 260**,** 7094-101.

BENOVIC, J. L., STRASSER, R. H., CARON, M. G. & LEFKOWITZ, R. J. 1986. Beta-adrenergic receptor kinase: identification of a novel protein kinase that phosphorylates the agonist-occupied form of the receptor. *Proceedings of the National Academy of Sciences of the United States of America,* 83**,** 2797-801.

BLACK, D. J., TRAN, Q. K. & PERSECHINI, A. 2004. Monitoring the total available calmodulin concentration in intact cells over the physiological range in free Ca2+. *Cell Calcium,* 35**,** 415-25.

BLIN, N., YUN, J. & WESS, J. 1995. Mapping of single amino acid residues required for selective activation of Gq/11 by the m3 muscarinic acetylcholine receptor. *J Biol Chem,* 270**,** 17741-8.

BOCKAERT, J., ROUSSIGNOL, G., BECAMEL, C., GAVARINI, S., JOUBERT, L., DUMUIS, A., FAGNI, L. & MARIN, P. 2004. GPCR-interacting proteins (GIPs): nature and functions. *Biochemical Society transactions,* 32**,** 851-5.

BOFILL-CARDONA, E., KUDLACEK, O., YANG, Q., AHORN, H., FREISSMUTH, M. & NANOFF, C. 2000. Binding of calmodulin to the D2-dopamine receptor reduces receptor signaling by arresting the G protein activation switch. *J Biol Chem,* 275**,** 32672-80.

BONINI, J. A., JONES, K. A., ADHAM, N., FORRAY, C., ARTYMYSHYN, R., DURKIN, M. M., SMITH, K. E., TAMM, J. A., BOTEJU, L. W., LAKHLANI, P. P., RADDATZ, R., YAO, W.-J., OGOZALEK, K. L., BOYLE, N., KOURANOVA, E. V., QUAN, Y., VAYSSE, P. J., WETZEL, J. M., BRANCHEK, T. A., GERALD, C. & BOROWSKY, B. 2000. Identification and Characterization of Two G Protein-coupled Receptors for Neuropeptide FF. *Journal of Biological Chemistry,* 275**,** 39324-39331.

BRADSHAW, J. M., HUDMON, A. & SCHULMAN, H. 2002. Chemical quenched flow kinetic studies indicate an intraholoenzyme autophosphorylation mechanism for Ca2+/calmodulin-dependent protein kinase II. *The Journal of biological chemistry,* 277**,** 20991-8.

BRAKEMAN, P. R., LANAHAN, A. A., O'BRIEN, R., ROCHE, K., BARNES, C. A., HUGANIR, R. L. & WORLEY, P. F. 1997. Homer: a protein that selectively binds metabotropic glutamate receptors. *Nature,* 386**,** 284-8.

BROTHERS, S. P., JANOVICK, J. A. & CONN, P. M. 2006. Calnexin regulated gonadotropin-releasing hormone receptor plasma membrane expression. *Journal of molecular endocrinology,* 37**,** 479-88.

BRUZZONE, F., LECTEZ, B., TOLLEMER, H., LEPRINCE, J., DUJARDIN, C., RACHIDI, W., CHATENET, D., BARONCINI, M., BEAUVILLAIN, J. C., VALLARINO, M., VAUDRY, H. & CHARTREL, N. 2006. Anatomical distribution and biochemical characterization of the novel RFamide peptide 26RFa in the human hypothalamus and spinal cord. *J Neurochem,* 99**,** 616-27.

BURSTEIN, E. S., SPALDING, T. A. & BRANN, M. R. 1998. The second intracellular loop of the m5 muscarinic receptor is the switch which enables G-protein coupling. *J Biol Chem,* 273**,** 24322-7.

CAHILL, M., CAHILL, S. & CAHILL, K. 2002. Proteins wriggle. *Biophysical journal,* 82**,** 2665-70.

CAI, K., ITOH, Y. & KHORANA, H. G. 2001. Mapping of contact sites in complex formation between transducin and light-activated rhodopsin by covalent crosslinking: use of a photoactivatable reagent. *Proc Natl Acad Sci U S A,* 98**,** 4877-82.

CAVALLARO, U. & CHRISTOFORI, G. 2004. Cell adhesion and signalling by cadherins and Ig-CAMs in cancer. *Nature reviews. Cancer,* 4**,** 118-32.

CERRATO, F., SHAGOURY, J., KRALICKOVA, M., DWYER, A., FALARDEAU, J., OZATA, M., VAN VLIET, G., BOULOUX, P., HALL, J. E., HAYES, F. J., PITTELOUD, N., MARTIN, K. A., WELT, C. & SEMINARA, S. B. 2006. Coding sequence analysis of GNRHR and GPR54 in patients with congenital and adult-onset forms of hypogonadotropic hypogonadism. *European Journal of Endocrinology,* 155**,** S3-S10.

CHARTREL, N., DUJARDIN, C., ANOUAR, Y., LEPRINCE, J., DECKER, A., CLERENS, S., DO-REGO, J. C., VANDESANDE, F., LLORENS-CORTES, C., COSTENTIN, J., BEAUVILLAIN, J. C. & VAUDRY, H. 2003. Identification of 26RFa, a hypothalamic neuropeptide of the RFamide peptide family with orexigenic activity. *Proc Natl Acad Sci U S A,* 100**,** 15247-52.

CHEN, J. C., LEE, W. H., CHEN, P. C., TSENG, C. P. & HUANG, E. Y. 2006. Rat NPFF(1) receptor-mediated signaling: functional comparison of neuropeptide FF (NPFF), FMRFamide and PFR(Tic)amide. *Peptides,* 27**,** 1005-14.

CHOE, H. W., KIM, Y. J., PARK, J. H., MORIZUMI, T., PAI, E. F., KRAUSS, N., HOFMANN, K. P., SCHEERER, P. & ERNST, O. P. 2011. Crystal structure of metarhodopsin II. *Nature,* 471**,** 651-5.

CHOI, K. Y., CHUNG, S. & ROCHE, K. W. 2011. Differential binding of calmodulin to group I metabotropic glutamate receptors regulates receptor trafficking and signaling. *J Neurosci,* 31**,** 5921-30.

CHRISTOPOULOS, A., CHRISTOPOULOS, G., MORFIS, M., UDAWELA, M., LABURTHE, M., COUVINEAU, A., KUWASAKO, K., TILAKARATNE, N. & SEXTON, P. M. 2003. Novel receptor partners and function of receptor activity-modifying proteins. *The Journal of biological chemistry,* 278**,** 3293-7.

CHUANG, T. T., PAOLUCCI, L. & DE BLASI, A. 1996. Inhibition of G protein-coupled receptor kinase subtypes by Ca2+/calmodulin. *J Biol Chem,* 271**,** 28691-6.

CHUNG, K. Y., RASMUSSEN, S. G., LIU, T., LI, S., DEVREE, B. T., CHAE, P. S., CALINSKI, D., KOBILKA, B. K., WOODS, V. L., JR. & SUNAHARA, R. K. 2011. Conformational changes in the G protein Gs induced by the beta2 adrenergic receptor. *Nature,* 477**,** 611-5.

CLAPHAM, D. E. 2007. Calcium signaling. *Cell,* 131**,** 1047-58.

CLARKE, I. J., QI, Y., PUSPITA SARI, I. & SMITH, J. T. 2009. Evidence that RF-amide related peptides are inhibitors of reproduction in mammals. *Frontiers in Neuroendocrinology,* 30**,** 371-378.

CLARKE, I. J., SARI, I. P., QI, Y., SMITH, J. T., PARKINGTON, H. C., UBUKA, T., IQBAL, J., LI, Q., TILBROOK, A., MORGAN, K., PAWSON, A. J., TSUTSUI, K., MILLAR, R. P. & BENTLEY, G. E. 2008. Potent action of RFamide-related peptide-3 on pituitary gonadotropes indicative of a hypophysiotropic role in the negative regulation of gonadotropin secretion. *Endocrinology,* 149**,** 5811-21.

CLARKE, P. R. & HARDIE, D. G. 1990. Calmodulin-dependent multiprotein kinase and protein kinase C phosphorylate the same site on HMG-CoA reductase as the AMP-activated protein kinase. *FEBS Lett,* 269**,** 213-7.

CLARKSON, J., D'ANGLEMONT DE TASSIGNY, X., MORENO, A. S., COLLEDGE, W. H. & HERBISON, A. E. 2008. Kisspeptin-GPR54 signaling is essential for preovulatory gonadotropin-releasing hormone neuron activation and the luteinizing hormone surge. *J Neurosci,* 28**,** 8691-7.

CLARKSON, J. & HERBISON, A. E. 2006. Development of GABA and glutamate signaling at the GnRH neuron in relation to puberty. *Molecular and Cellular Endocrinology,* 254-255**,** 32-8.

COHEN, P. & KLEE, C. B. 1988. *Calmodulin,* Amsterdam ; New York, Elsevier.

COLBRAN, R. J. 1993. Inactivation of Ca2+/calmodulin-dependent protein kinase II by basal autophosphorylation. *The Journal of biological chemistry,* 268**,** 7163-70.

COLBRAN, R. J. 2004. Targeting of calcium/calmodulin-dependent protein kinase II. *Biochem J,* 378**,** 1-16.

COLBRAN, R. J. & SODERLING, T. R. 1990. Calcium/calmodulin-independent autophosphorylation sites of calcium/calmodulin-dependent protein kinase II. Studies on the effect of phosphorylation of threonine 305/306 and serine 314

on calmodulin binding using synthetic peptides. *The Journal of biological chemistry,* 265**,** 11213-9.

COLLEDGE, W. H. 2004. GPR54 and puberty. *Trends in Endocrinology & Metabolism,* 15**,** 448-453.

COLLEDGE, W. H. 2009. Transgenic mouse models to study Gpr54/kisspeptin physiology. *Peptides,* 30**,** 34-41.

CONN, P. M., JANOVICK, J. A., BROTHERS, S. P. & KNOLLMAN, P. E. 2006. 'Effective inefficiency': cellular control of protein trafficking as a mechanism of post-translational regulation. *J Endocrinol,* 190**,** 13-6.

CONN, P. M., ULLOA-AGUIRRE, A., ITO, J. & JANOVICK, J. A. 2007. G protein-coupled receptor trafficking in health and disease: lessons learned to prepare for therapeutic mutant rescue in vivo. *Pharmacological reviews,* 59**,** 225-50.

CONSTANTIN, S., CALIGIONI, C. S., STOJILKOVIC, S. & WRAY, S. 2009. Kisspeptin-10 facilitates a plasma membrane-driven calcium oscillator in gonadotropin-releasing hormone-1 neurons. *Endocrinology,* 150**,** 1400-12.

COTSIKI, M., LOCK, R. L., CHENG, Y., WILLIAMS, G. L., ZHAO, J., PERERA, D., FREIRE, R., ENTWISTLE, A., GOLEMIS, E. A., ROBERTS, T. M., JAT, P. S. & GJOERUP, O. V. 2004. Simian virus 40 large T antigen targets the spindle assembly checkpoint protein Bub1. *Proc Natl Acad Sci U S A,* 101**,** 947-52.

COULTRAP, S. J. & BAYER, K. U. 2012. CaMKII regulation in information processing and storage. *Trends in neurosciences,* 35**,** 607-18.

COULTRAP, S. J., BUARD, I., KULBE, J. R., DELL'ACQUA, M. L. & BAYER, K. U. 2010. CaMKII autonomy is substrate-dependent and further stimulated by Ca2+/calmodulin. *The Journal of biological chemistry,* 285**,** 17930-7.

CURTIS, A. E., COOKE, J. H., BAXTER, J. E., PARKINSON, J. R., BATAVELJIC, A., GHATEI, M. A., BLOOM, S. R. & MURPHY, K. G. 2010. A kisspeptin-10 analog with greater in vivo bioactivity than kisspeptin-10. *Am J Physiol Endocrinol Metab,* 298**,** 24.

D'ANGLEMONT DE TASSIGNY, X. & COLLEDGE, W. H. 2010. The Role of Kisspeptin Signaling in Reproduction. *Physiology,* 25**,** 207-217.

D'ANGLEMONT DE TASSIGNY, X., FAGG, L. A., DIXON, J. P. C., DAY, K., LEITCH, H. G., HENDRICK, A. G., ZAHN, D., FRANCESCHINI, I., CARATY, A., CARLTON, M. B. L., APARICIO, S. A. J. R. & COLLEDGE, W. H. 2007. Hypogonadotropic hypogonadism in mice lacking a functional Kiss1 gene. *Proceedings of the National Academy of Sciences,* 104**,** 10714-10719.

DA SILVA, A. C. & REINACH, F. C. 1991. Calcium binding induces conformational changes in muscle regulatory proteins. *Trends in biochemical sciences,* 16**,** 53-7.

DALKYZ, M., OZCAN, A., YAPAR, M., GOKAY, N. & YUNCU, M. 2000. Evaluation of the effects of different biomaterials on bone defects. *Implant dentistry,* 9**,** 226-35.

DAVARE, M. A., AVDONIN, V., HALL, D. D., PEDEN, E. M., BURETTE, A., WEINBERG, R. J., HORNE, M. C., HOSHI, T. & HELL, J. W. 2001. A beta2 adrenergic receptor signaling complex assembled with the Ca2+ channel Cav1.2. *Science,* 293**,** 98-101.

DE ROUX, N., GENIN, E., CAREL, J.-C., MATSUDA, F., CHAUSSAIN, J.-L. & MILGROM, E. 2003. Hypogonadotropic hypogonadism due to loss of function of the KiSS1-derived peptide receptor GPR54. *Proceedings of the National Academy of Sciences,* 100**,** 10972-10976.

DENIS, C., SAULIERE, A., GALANDRIN, S., SENARD, J. M. & GALES, C. 2012. Probing heterotrimeric G protein activation: applications to biased ligands. *Current pharmaceutical design,* 18**,** 128-44.

DERKACH, V. 2011. Zooming in on AMPA receptor regulation by CaMKII. *Nat Neurosci,* 14**,** 674-5.

DEV, K. K., NAKANISHI, S. & HENLEY, J. M. 2001. Regulation of mglu(7) receptors by proteins that interact with the intracellular C-terminus. *Trends in pharmacological sciences,* 22**,** 355-61.

DHAMI, G. K. & FERGUSON, S. S. 2006. Regulation of metabotropic glutamate receptor signaling, desensitization and endocytosis. *Pharmacology & therapeutics,* 111**,** 260-71.

DHAR, D. K., NAORA, H., KUBOTA, H., MARUYAMA, R., YOSHIMURA, H., TONOMOTO, Y., TACHIBANA, M., ONO, T., OTANI, H. & NAGASUE, N. 2004. Downregulation of KiSS-1 expression is responsible for tumor invasion and worse prognosis in gastric carcinoma. *Int J Cancer,* 111**,** 868-72.

DONG, C., FILIPEANU, C. M., DUVERNAY, M. T. & WU, G. 2007. Regulation of G protein-coupled receptor export trafficking. *Biochimica et Biophysica Acta,* 1768**,** 853-70.

DUPONT, G. & GOLDBETER, A. 1998. CaM kinase II as frequency decoder of Ca2+ oscillations. *Bioessays,* 20**,** 607-10.

DUVERNAY, M. T., FILIPEANU, C. M. & WU, G. 2005. The regulatory mechanisms of export trafficking of G protein-coupled receptors. *Cellular signalling,* 17**,** 1457-65.

EL FAR, O., BOFILL-CARDONA, E., AIRAS, J. M., O'CONNOR, V., BOEHM, S., FREISSMUTH, M., NANOFF, C. & BETZ, H. 2001. Mapping of calmodulin and Gbetagamma binding domains within the C-terminal region of the metabotropic glutamate receptor 7A. *J Biol Chem,* 276**,** 30662-9.

ELLGAARD, L. & HELENIUS, A. 2001. ER quality control: towards an understanding at the molecular level. *Current opinion in cell biology,* 13**,** 431-7.

ENGSTRÖM, M., BRANDT, A., WURSTER, S., SAVOLA, J.-M. & PANULA, P. 2003. Prolactin Releasing Peptide Has High Affinity and Efficacy at Neuropeptide FF2 Receptors. *Journal of Pharmacology and Experimental Therapeutics,* 305**,** 825-832.

ERICKSON, J. R., JOINER, M. L., GUAN, X., KUTSCHKE, W., YANG, J., ODDIS, C. V., BARTLETT, R. K., LOWE, J. S., O'DONNELL, S. E., AYKIN-BURNS, N., ZIMMERMAN, M. C., ZIMMERMAN, K., HAM, A. J., WEISS, R. M., SPITZ, D. R., SHEA, M. A., COLBRAN, R. J., MOHLER, P. J. & ANDERSON, M. E. 2008. A dynamic pathway for calcium-independent activation of CaMKII by methionine oxidation. *Cell,* 133**,** 462-74.

ESHETE, F. & FIELDS, R. D. 2001. Spike frequency decoding and autonomous activation of Ca2+-calmodulin-dependent protein kinase II in dorsal root ganglion neurons. *J Neurosci,* 21**,** 6694-705.

EVANS, B. J., WANG, Z., MOBLEY, L., KHOSRAVI, D., FUJII, N., NAVENOT, J. M. & PEIPER, S. C. 2008. Physical association of GPR54 C-terminal with protein phosphatase 2A. *Biochem Biophys Res Commun,* 377**,** 1067-71.

FALLON, J. L. & QUIOCHO, F. A. 2003. A closed compact structure of native Ca(2+)-calmodulin. *Structure,* 11**,** 1303-7.

FERGUSON, S. S. 2001. Evolving concepts in G protein-coupled receptor endocytosis: the role in receptor desensitization and signaling. *Pharmacological reviews,* 53**,** 1-24.

FERGUSON, S. S., BARAK, L. S., ZHANG, J. & CARON, M. G. 1996. G-protein-coupled receptor regulation: role of G-protein-coupled receptor kinases and arrestins. *Canadian journal of physiology and pharmacology,* 74**,** 1095-110.

FERNANDEZ-FERNANDEZ, R., MARTINI, A. C., NAVARRO, V. M., CASTELLANO, J. M., DIEGUEZ, C., AGUILAR, E., PINILLA, L. & TENA-SEMPERE, M. 2006. Novel signals for the integration of energy balance and reproduction. *Molecular and Cellular Endocrinology,* 254–255**,** 127-132.

FINDEISEN, M., RATHMANN, D. & BECK-SICKINGER, A. G. 2011. RFamide Peptides: Structure, Function, Mechanisms and Pharmaceutical Potential. *Pharmaceuticals,* 4**,** 1248-1280.

FINK, G. 2000. Neuroendocrine Regulation of Pituitary Function. *In:* CONN, P. M. & FREEMAN, M. (eds.) *Neuroendocrinology in physiology and medicine.* Humana Press.

FLANAGAN, C. A., FROMME, B. J., DAVIDSON, J. S. & MILLAR, R. P. 1998. A high affinity gonadotropin-releasing hormone (GnRH) tracer, radioiodinated at position 6, facilitates analysis of mutant GnRH receptors. *Endocrinology,* 139**,** 4115-9.

FORMAN, M. S., LEE, V. M. & TROJANOWSKI, J. Q. 2003. 'Unfolding' pathways in neurodegenerative disease. *Trends in neurosciences,* 26**,** 407-10.

FRASER, I. D., CONG, M., KIM, J., ROLLINS, E. N., DAAKA, Y., LEFKOWITZ, R. J. & SCOTT, J. D. 2000. Assembly of an A kinase-anchoring protein-beta(2)-adrenergic receptor complex facilitates receptor phosphorylation and signaling. *Curr Biol,* 10**,** 409-12.

FUNES, S., HEDRICK, J. A., VASSILEVA, G., MARKOWITZ, L., ABBONDANZO, S., GOLOVKO, A., YANG, S., MONSMA, F. J. & GUSTAFSON, E. L. 2003. The KiSS-1 receptor GPR54 is essential for the development of the murine reproductive system. *Biochemical and Biophysical Research Communications,* 312**,** 1357-1363.

GABORIK, Z., JAGADEESH, G., ZHANG, M., SPAT, A., CATT, K. J. & HUNYADY, L. 2003. The role of a conserved region of the second intracellular loop in AT1 angiotensin receptor activation and signaling. *Endocrinology,* 144**,** 2220-8.

GANGOPADHYAY, J. P., GRABAREK, Z. & IKEMOTO, N. 2004. Fluorescence probe study of Ca2+-dependent interactions of calmodulin with calmodulin-binding peptides of the ryanodine receptor. *Biochem Biophys Res Commun,* 323**,** 760-8.

GARCÍA-GALIANO, D., NAVARRO, V. M., ROA, J., RUIZ-PINO, F., SÁNCHEZ-GARRIDO, M. A., PINEDA, R., CASTELLANO, J. M., ROMERO, M., AGUILAR, E., GAYTÁN, F., DIÉGUEZ, C., PINILLA, L. & TENA-SEMPERE, M. 2010. The Anorexigenic Neuropeptide, Nesfatin-1, Is Indispensable for Normal Puberty Onset in the Female Rat. *The Journal of Neuroscience,* 30**,** 7783-7792.

GARDNER, L. A., TAVALIN, S. J., GOEHRING, A. S., SCOTT, J. D. & BAHOUTH, S. W. 2006. AKAP79-mediated targeting of the cyclic AMP-dependent protein kinase to the beta(1)-arenergic receptor promotes recycling and functional resensitization of the receptor. *Journal of Biological Chemistry,* 281**,** 33537-33553.

GEISER, A. H., SIEVERT, M. K., GUO, L. W., GRANT, J. E., KREBS, M. P., FOTIADIS, D., ENGEL, A. & RUOHO, A. E. 2006. Bacteriorhodopsin chimeras containing the third cytoplasmic loop of bovine rhodopsin activate transducin for GTP/GDP exchange. *Protein Sci,* 15**,** 1679-90.

GIESE, K. P., FEDOROV, N. B., FILIPKOWSKI, R. K. & SILVA, A. J. 1998. Autophosphorylation at Thr286 of the alpha calcium-calmodulin kinase II in LTP and learning. *Science,* 279**,** 870-3.

GNEGY, M. E. 1993. Calmodulin in neurotransmitter and hormone action. *Annual review of pharmacology and toxicology,* 33**,** 45-70.

GROIGNO, L. & WHITAKER, M. 1998. An anaphase calcium signal controls chromosome disjunction in early sea urchin embryos. *Cell,* 92**,** 193-204.

GUHAN, N. & LU, B. 2004. Homer-PIKE complex: a novel link between mGluRI and PI 3-kinase. *Trends Neurosci,* 27**,** 645-8.

GUO, M. L., FIBUCH, E. E., LIU, X. Y., CHOE, E. S., BUCH, S., MAO, L. M. & WANG, J. Q. 2010. CaMKIIalpha interacts with M4 muscarinic receptors to control receptor and psychomotor function. *EMBO J,* 29**,** 2070-81.

GUTIÉRREZ-PASCUAL, E., LEPRINCE, J., MARTÍNEZ-FUENTES, A. J., SÉGALAS-MILAZZO, I., PINEDA, R., ROA, J., DURAN-PRADO, M., GUILHAUDIS, L., DESPERROIS, E., LEBRETON, A., PINILLA, L., TONON, M.-C., MALAGÓN, M. M., VAUDRY, H., TENA-SEMPERE, M. & CASTAÑO, J. P. 2009. In Vivo and in Vitro Structure-Activity Relationships and Structural Conformation of Kisspeptin-10-Related Peptides. *Molecular Pharmacology,* 76**,** 58-67.

HAN, S.-K., GOTTSCH, M. L., LEE, K. J., POPA, S. M., SMITH, J. T., JAKAWICH, S. K., CLIFTON, D. K., STEINER, R. A. & HERBISON, A. E. 2005. Activation of Gonadotropin-Releasing Hormone Neurons by Kisspeptin as a Neuroendocrine Switch for the Onset of Puberty. *The Journal of Neuroscience,* 25**,** 11349-11356.

HANSON, P. I. & SCHULMAN, H. 1992a. Inhibitory autophosphorylation of multifunctional Ca2+/calmodulin-dependent protein kinase analyzed by site-directed mutagenesis. *The Journal of biological chemistry,* 267**,** 17216-24.

HANSON, P. I. & SCHULMAN, H. 1992b. Neuronal Ca2+/calmodulin-dependent protein kinases. *Annual review of biochemistry,* 61**,** 559-601.

HARTL, F. U. & HAYER-HARTL, M. 2002. Molecular chaperones in the cytosol: from nascent chain to folded protein. *Science,* 295**,** 1852-8.

HASHIMOTO, Y., SCHWORER, C. M., COLBRAN, R. J. & SODERLING, T. R. 1987. Autophosphorylation of Ca2+/calmodulin-dependent protein kinase II. Effects on total and Ca2+-independent activities and kinetic parameters. *The Journal of biological chemistry,* 262**,** 8051-5.

HATA, K., DHAR, D. K., WATANABE, Y., NAKAI, H. & HOSHIAI, H. 2007. Expression of metastin and a G-protein-coupled receptor (AXOR12) in epithelial ovarian cancer. *Eur J Cancer,* 43**,** 1452-9.

HAUGLAND, R. P., SPENCE, M. T. Z. & JOHNSON, I. D. 2005. *The Handbook: A Guide to Fluorescent Probes and Labeling Technologies*, Molecular Probes.

HE, B. J., JOINER, M. L., SINGH, M. V., LUCZAK, E. D., SWAMINATHAN, P. D., KOVAL, O. M., KUTSCHKE, W., ALLAMARGOT, C., YANG, J., GUAN, X., ZIMMERMAN, K., GRUMBACH, I. M., WEISS, R. M., SPITZ, D. R., SIGMUND, C. D., BLANKESTEIJN, W. M., HEYMANS, S., MOHLER, P. J. & ANDERSON, M. E. 2011. Oxidation of CaMKII determines the cardiotoxic effects of aldosterone. *Nature medicine,* 17**,** 1610-8.

HELENIUS, I. J., TIKKANEN, H. O. & HAAHTELA, T. 1997. Association between type of training and risk of asthma in elite athletes. *Thorax,* 52**,** 157-60.

HERBISON, A. E. 2006. Chapter 28 - Physiology of the Gonadotropin-Releasing Hormone Neuronal Network. *In:* JIMMY, D. N., TONY, M. P., DONALD, W. P., JOHN, R. G. C., DAVID, M. D. K., JOANNE, S. R. & WASSARMAN, P. M. (eds.) *Knobil and Neill's Physiology of Reproduction (Third Edition).* St Louis: Academic Press.

HERBISON, A. E. & MOENTER, S. M. 2011. Depolarising and Hyperpolarising Actions of GABAA Receptor Activation on Gonadotrophin-Releasing Hormone Neurones: Towards an Emerging Consensus. *Journal of Neuroendocrinology,* 23**,** 557-569.

HESLING, C., D'INCAN, M., MANSARD, S., FRANCK, F., CORBIN-DUVAL, A., CHEVENET, C., DECHELOTTE, P., MADELMONT, J. C., VEYRE, A., SOUTEYRAND, P. & BIGNON, Y. J. 2004. In vivo and in situ modulation of the expression of genes involved in metastasis and angiogenesis in a patient treated with topical imiquimod for melanoma skin metastases. *Br J Dermatol,* 150**,** 761-7.

HINO, T., ARAKAWA, T., IWANARI, H., YURUGI-KOBAYASHI, T., IKEDA-SUNO, C., NAKADA-NAKURA, Y., KUSANO-ARAI, O., WEYAND, S., SHIMAMURA, T., NOMURA, N., CAMERON, A. D., KOBAYASHI, T., HAMAKUBO, T., IWATA, S. & MURATA, T. 2012. G-protein-coupled receptor inactivation by an allosteric inverse-agonist antibody. *Nature,* 482**,** 237-40.

HINUMA, S., SHINTANI, Y., FUKUSUMI, S., IIJIMA, N., MATSUMOTO, Y., HOSOYA, M., FUJII, R., WATANABE, T., KIKUCHI, K., TERAO, Y., TAKAHIKO, Y., TAKANORI, Y., YUJI, K., YUGO, H., MARI, A., CHIEKO, K., TSUTOMU, K., HARUO, O., OSAMU, N., MASAKI, T., YASUHIKO, I. & MASAHIKO, F. 2000. New neuropeptides containing carboxy-terminal RFamide and their receptor in mammals. *Nature Cell Biology,* 2**,** 703-708.

HOELZ, A., NAIRN, A. C. & KURIYAN, J. 2003. Crystal structure of a tetradecameric assembly of the association domain of Ca2+/calmodulin-dependent kinase II. *Molecular cell,* 11**,** 1241-51.

HORI, A., HONDA, S., ASADA, M., OHTAKI, T., ODA, K., WATANABE, T., SHINTANI, Y., YAMADA, T., SUENAGA, M., KITADA, C., ONDA, H., KUROKAWA, T., NISHIMURA, O. & FUJINO, M. 2001. Metastin suppresses the motility and growth of CHO cells transfected with its receptor. *Biochem Biophys Res Commun,* 286**,** 958-63.

HUDMON, A. & SCHULMAN, H. 2002a. Neuronal CA2+/calmodulin-dependent protein kinase II: the role of structure and autoregulation in cellular function. *Annual review of biochemistry,* 71**,** 473-510.

HUDMON, A. & SCHULMAN, H. 2002b. Structure-function of the multifunctional Ca2+/calmodulin-dependent protein kinase II. *Biochem J,* 364**,** 593-611.

HULTSCHIG, C., HECHT, H. J. & FRANK, R. 2004. Systematic delineation of a calmodulin peptide interaction. *J Mol Biol,* 343**,** 559-68.

IIRI, T., FARFEL, Z. & BOURNE, H. R. 1998. G-protein diseases furnish a model for the turn-on switch. *Nature,* 394**,** 35-8.

IKEGUCHI, M., YAMAGUCHI, K. & KAIBARA, N. 2004. Clinical significance of the loss of KiSS-1 and orphan G-protein-coupled receptor (hOT7T175) gene expression in esophageal squamous cell carcinoma. *Clin Cancer Res,* 10**,** 1379-83.

IRWIG, M. S., FRALEY, G. S., SMITH, J. T., ACOHIDO, B. V., POPA, S. M., CUNNINGHAM, M. J., GOTTSCH, M. L., CLIFTON, D. K. & STEINER, R. A. 2004. Kisspeptin activation of gonadotropin releasing hormone neurons and regulation of KiSS-1 mRNA in the male rat. *Neuroendocrinology,* 80**,** 264-72.

ISHIDA, A., KAMESHITA, I., OKUNO, S., KITANI, T. & FUJISAWA, H. 1995. A novel highly specific and potent inhibitor of calmodulin-dependent protein kinase II. *Biochem Biophys Res Commun,* 212**,** 806-12.

ISHIDA, A., KITANI, T. & FUJISAWA, H. 1996. Evidence that autophosphorylation at Thr-286/Thr-287 is required for full activation of calmodulin-dependent protein kinase II. *Biochim Biophys Acta,* 1311**,** 211-7.

ISHIKAWA, K., NASH, S. R., NISHIMUNE, A., NEKI, A., KANEKO, S. & NAKANISHI, S. 1999. Competitive interaction of seven in absentia homolog-1A and Ca2+/calmodulin with the cytoplasmic tail of group 1 metabotropic glutamate receptors. *Genes to cells : devoted to molecular & cellular mechanisms,* 4**,** 381-90.

JACOBI, J. S., MARTIN, C., NAVA, G., JEZIORSKI, M. C., CLAPP, C. & MARTINEZ DE LA ESCALERA, G. 2007. 17-Beta-estradiol directly regulates the expression of adrenergic receptors and kisspeptin/GPR54 system in GT1-7 GnRH neurons. *Neuroendocrinology,* 86**,** 260-9.

JACOBY, E., BOUHELAL, R., GERSPACHER, M. & SEUWEN, K. 2006. The 7 TM G-protein-coupled receptor target family. *ChemMedChem,* 1**,** 761-82.

JAMA, A. M., FENTON, J., ROBERTSON, S. D. & TOROK, K. 2009. Time-dependent autoinactivation of phospho-Thr286-alphaCa2+/calmodulin-dependent protein kinase II. *J Biol Chem,* 284**,** 28146-55.

JAMA, A. M., GABRIEL, J., AL-NAGAR, A. J., MARTIN, S., BAIG, S. Z., SOLEYMANI, H., CHOWDHURY, Z., BEESLEY, P. & TOROK, K. 2011. Lobe-specific functions of Ca2+.calmodulin in alphaCa2+.calmodulin-dependent protein kinase II activation. *J Biol Chem,* 286**,** 12308-16.

JHAMANDAS, J. H. & GONCHARUK, V. 2013. Role of Neuropeptide FF (NPFF) in central cardiovascular and neuroendocrine regulation. *Frontiers in Endocrinology,* 4.

JOHNSON, M. A., TSUTSUI, K. & FRALEY, G. S. 2007. Rat RFamide-related peptide-3 stimulates GH secretion, inhibits LH secretion, and has variable effects on sex behavior in the adult male rat. *Hormones and behavior,* 51**,** 171-80.

JOHNSTON, C. A. & SIDEROVSKI, D. P. 2007. Structural basis for nucleotide exchange on G alpha i subunits and receptor coupling specificity. *Proc Natl Acad Sci U S A,* 104**,** 2001-6.

JURADO, L. A., CHOCKALINGAM, P. S. & JARRETT, H. W. 1999. Apocalmodulin. *Physiological Reviews,* 79**,** 661-82.

KANG, H., LEE, W. K., CHOI, Y. H., VUKOTI, K. M., BANG, W. G. & YU, Y. G. 2005. Molecular analysis of the interaction between the intracellular loops of the human serotonin receptor type 6 (5-HT6) and the alpha subunit of GS protein. *Biochem Biophys Res Commun,* 329**,** 684-92.

KAPLOWITZ, P. B. 2008. Link between body fat and the timing of puberty. *Pediatrics,* 121 Suppl 3**,** S208-17.

KATRITCH, V., CHEREZOV, V. & STEVENS, R. C. 2012. Diversity and modularity of G protein-coupled receptor structures. *Trends in pharmacological sciences,* 33**,** 17-27.

KELLY, E., BAILEY, C. P. & HENDERSON, G. 2008. Agonist-selective mechanisms of GPCR desensitization. *British journal of pharmacology,* 153 Suppl 1**,** S379-88.

KELLY, M. J., ZHANG, C., QIU, J. & RONNEKLEIV, O. K. 2013. Pacemaking Kisspeptin Neurons. *Exp Physiol,* 30**,** 30.

KENAKIN, T. 2002a. Drug efficacy at G protein-coupled receptors. *Annual review of pharmacology and toxicology,* 42**,** 349-79.

KENAKIN, T. 2002b. Efficacy at G-protein-coupled receptors. *Nature reviews. Drug discovery,* 1**,** 103-10.

KIM, K. M., GAINETDINOV, R. R., LAPORTE, S. A., CARON, M. G. & BARAK, L. S. 2005. G protein-coupled receptor kinase regulates dopamine D3 receptor signaling by modulating the stability of a receptor-filamin-beta-arrestin complex. A case of autoreceptor regulation. *J Biol Chem,* 280**,** 12774-80.

KING, J. C., TOBET, S. A., SNAVELY, F. L. & ARIMURA, A. A. 1982. LHRH immunopositive cells and their projections to the median eminence and organum vasculosum of the lamina terminalis. *The Journal of comparative neurology,* 209**,** 287-300.

KINSEY-JONES, J. S., LI, X. F., KNOX, A. M. I., WILKINSON, E. S., ZHU, X. L., CHAUDHARY, A. A., MILLIGAN, S. R., LIGHTMAN, S. L. & O'BYRNE, K. T. 2009. Down-Regulation of Hypothalamic Kisspeptin and its Receptor, Kiss1r, mRNA Expression is Associated with Stress-Induced Suppression of Luteinising Hormone Secretion in the Female Rat. *Journal of Neuroendocrinology,* 21**,** 20-29.

KIRBY, H. R., MAGUIRE, J. J., COLLEDGE, W. H. & DAVENPORT, A. P. 2010. International Union of Basic and Clinical Pharmacology. LXXVII. Kisspeptin receptor nomenclature, distribution, and function. *Pharmacological reviews,* 62**,** 565-78.

KOTANI, M., DETHEUX, M., VANDENBOGAERDE, A., COMMUNI, D., VANDERWINDEN, J.-M., LE POUL, E., BRÉZILLON, S., TYLDESLEY, R., SUAREZ-HUERTA, N., VANDEPUT, F., BLANPAIN, C., SCHIFFMANN, S. N., VASSART, G. & PARMENTIER, M. 2001. The Metastasis Suppressor Gene KiSS-1 Encodes Kisspeptins, the Natural Ligands of the Orphan G Protein-coupled Receptor GPR54. *Journal of Biological Chemistry,* 276**,** 34631-34636.

KUBONIWA, H., TJANDRA, N., GRZESIEK, S., REN, H., KLEE, C. B. & BAX, A. 1995. Solution structure of calcium-free calmodulin. *Nature structural biology,* 2**,** 768-76.

KUOHUNG, W., BURNETT, M., MUKHTYAR, D., SCHUMAN, E., NI, J., CROWLEY, W. F., GLICKSMAN, M. A. & KAISER, U. B. 2010. A high-throughput small-molecule ligand screen targeted to agonists and antagonists of the G-protein-coupled receptor GPR54. *Journal of biomolecular screening,* 15**,** 508-17.

LABASQUE, M., REITER, E., BECAMEL, C., BOCKAERT, J. & MARIN, P. 2008. Physical interaction of calmodulin with the 5-hydroxytryptamine2C receptor C-terminus is essential for G protein-independent, arrestin-dependent receptor signaling. *Mol Biol Cell,* 19**,** 4640-50.

LAGERSTROM, M. C. & SCHIOTH, H. B. 2008. Structural diversity of G protein-coupled receptors and significance for drug discovery. *Nature reviews. Drug discovery,* 7**,** 339-57.

LANFRANCO, F., GROMOLL, J., VON ECKARDSTEIN, S., HERDING, E. M., NIESCHLAG, E. & SIMONI, M. 2005. Role of sequence variations of the GnRH receptor and G protein-coupled receptor 54 gene in male idiopathic hypogonadotropic hypogonadism. *European Journal of Endocrinology,* 153**,** 845-852.

LANGMEAD, C. J., SZEKERES, P. G., CHAMBERS, J. K., RATCLIFFE, S. J., JONES, D. N., HIRST, W. D., PRICE, G. W. & HERDON, H. J. 2000. Characterization of the binding of [(125)I]-human prolactin releasing peptide (PrRP) to GPR10, a novel G protein coupled receptor. *Br J Pharmacol,* 131**,** 683-8.

LAPATTO, R., PALLAIS, J. C., ZHANG, D., CHAN, Y.-M., MAHAN, A., CERRATO, F., LE, W. W., HOFFMAN, G. E. & SEMINARA, S. B. 2007. Kiss1−/− Mice Exhibit More Variable Hypogonadism than Gpr54−/− Mice. *Endocrinology,* 148**,** 4927-4936.

LEBON, G., WARNE, T., EDWARDS, P. C., BENNETT, K., LANGMEAD, C. J., LESLIE, A. G. & TATE, C. G. 2011. Agonist-bound adenosine A2A receptor structures reveal common features of GPCR activation. *Nature,* 474**,** 521-5.

LEBON, G., WARNE, T. & TATE, C. G. 2012. Agonist-bound structures of G protein-coupled receptors. *Current opinion in structural biology,* 22**,** 482-90.

LEE, D. K., NGUYEN, T., O'NEILL, G. P., CHENG, R., LIU, Y., HOWARD, A. D., COULOMBE, N., TAN, C. P., TANG-NGUYEN, A. T., GEORGE, S. R.

& O'DOWD, B. F. 1999. Discovery of a receptor related to the galanin receptors. *FEBS Lett,* 446**,** 103-7.

LEE, J.-H., MIELE, M. E., HICKS, D. J., PHILLIPS, K. K., TRENT, J. M., WEISSMAN, B. E. & WELCH, D. R. 1996a. KiSS-1, a Novel Human Malignant Melanoma Metastasis-Suppressor Gene. *Journal of the National Cancer Institute,* 88**,** 1731-1737.

LEE, J. H., LEE, J., CHOI, K. Y., HEPP, R., LEE, J. Y., LIM, M. K., CHATANI-HINZE, M., ROCHE, P. A., KIM, D. G., AHN, Y. S., KIM, C. H. & ROCHE, K. W. 2008. Calmodulin dynamically regulates the trafficking of the metabotropic glutamate receptor mGluR5. *Proceedings of the National Academy of Sciences of the United States of America,* 105**,** 12575-80.

LEE, J. H., MIELE, M. E., HICKS, D. J., PHILLIPS, K. K., TRENT, J. M., WEISSMAN, B. E. & WELCH, D. R. 1996b. KiSS-1, a novel human malignant melanoma metastasis-suppressor gene. *J Natl Cancer Inst,* 88**,** 1731-7.

LEE, J. H. & WELCH, D. R. 1997. Suppression of metastasis in human breast carcinoma MDA-MB-435 cells after transfection with the metastasis suppressor gene, KiSS-1. *Cancer Res,* 57**,** 2384-7.

LEE, S. J., ESCOBEDO-LOZOYA, Y., SZATMARI, E. M. & YASUDA, R. 2009. Activation of CaMKII in single dendritic spines during long-term potentiation. *Nature,* 458**,** 299-304.

LEE, S. J. & YASUDA, R. 2009. Spatiotemporal Regulation of Signaling in and out of Dendritic Spines: CaMKII and Ras. *The open neuroscience journal,* 3**,** 117-127.

LEHMAN, M. N., COOLEN, L. M. & GOODMAN, R. L. 2010. Minireview: Kisspeptin/Neurokinin B/Dynorphin (KNDy) Cells of the Arcuate Nucleus: A Central Node in the Control of Gonadotropin-Releasing Hormone Secretion. *Endocrinology,* 151**,** 3479-3489.

LEVAY, K., SATPAEV, D. K., PRONIN, A. N., BENOVIC, J. L. & SLEPAK, V. Z. 1998. Localization of the sites for Ca2+-binding proteins on G protein-coupled receptor kinases. *Biochemistry,* 37**,** 13650-9.

LI, X. F., KNOX, A. M. I. & O'BYRNE, K. T. 2010. Corticotrophin-releasing factor and stress-induced inhibition of the gonadotrophin-releasing hormone pulse generator in the female. *Brain Research,* 1364**,** 153-163.

LINSE, S., HELMERSSON, A. & FORSEN, S. 1991. Calcium binding to calmodulin and its globular domains. *The Journal of biological chemistry,* 266**,** 8050-4.

LISMAN, J. 1994. The CaM kinase II hypothesis for the storage of synaptic memory. *Trends Neurosci,* 17**,** 406-12.

LISMAN, J., SCHULMAN, H. & CLINE, H. 2002. The molecular basis of CaMKII function in synaptic and behavioural memory. *Nat Rev Neurosci,* 3**,** 175-90.

LISMAN, J., YASUDA, R. & RAGHAVACHARI, S. 2012. Mechanisms of CaMKII action in long-term potentiation. *Nat Rev Neurosci,* 13**,** 169-82.

LIU, Q., GUAN, X.-M., MARTIN, W. J., MCDONALD, T. P., CLEMENTS, M. K., JIANG, Q., ZENG, Z., JACOBSON, M., WILLIAMS, D. L., YU, H., BOMFORD, D., FIGUEROA, D., MALLEE, J., WANG, R., EVANS, J., GOULD, R. & AUSTIN, C. P. 2001. Identification and Characterization of Novel Mammalian Neuropeptide FF-like Peptides That Attenuate Morphine-induced Antinociception. *Journal of Biological Chemistry,* 276**,** 36961-36969.

LIU, X., LEE, K. & HERBISON, A. E. 2008. Kisspeptin excites gonadotropin-releasing hormone neurons through a phospholipase C/calcium-dependent pathway regulating multiple ion channels. *Endocrinology,* 149**,** 4605-14.

LIU, X. Y., MAO, L. M., ZHANG, G. C., PAPASIAN, C. J., FIBUCH, E. E., LAN, H. X., ZHOU, H. F., XU, M. & WANG, J. Q. 2009. Activity-dependent modulation of limbic dopamine D3 receptors by CaMKII. *Neuron,* 61**,** 425-38.

LIU, Y., BUCK, D. C., MACEY, T. A., LAN, H. & NEVE, K. A. 2007. Evidence that calmodulin binding to the dopamine D2 receptor enhances receptor signaling. *Journal of receptor and signal transduction research,* 27**,** 47-65.

LOHSE, M. J., ANDEXINGER, S., PITCHER, J., TRUKAWINSKI, S., CODINA, J., FAURE, J. P., CARON, M. G. & LEFKOWITZ, R. J. 1992. Receptor-specific desensitization with purified proteins. Kinase dependence and receptor specificity of beta-arrestin and arrestin in the beta 2-adrenergic receptor and rhodopsin systems. *The Journal of biological chemistry,* 267**,** 8558-64.

LOU, L. L. & SCHULMAN, H. 1989. Distinct autophosphorylation sites sequentially produce autonomy and inhibition of the multifunctional Ca2+/calmodulin-dependent protein kinase. *The Journal of neuroscience : the official journal of the Society for Neuroscience,* 9**,** 2020-32.

LU, Z. L., COETSEE, M., WHITE, C. D. & MILLAR, R. P. 2007. Structural determinants for ligand-receptor conformational selection in a peptide G protein-coupled receptor. *The Journal of biological chemistry,* 282**,** 17921-9.

LU, Z. L., CURTIS, C. A., JONES, P. G., PAVIA, J. & HULME, E. C. 1997. The role of the aspartate-arginine-tyrosine triad in the m1 muscarinic receptor: mutations of aspartate 122 and tyrosine 124 decrease receptor expression but do not abolish signaling. *Mol Pharmacol,* 51**,** 234-41.

LU, Z. L., GALLAGHER, R., SELLAR, R., COETSEE, M. & MILLAR, R. P. 2005. Mutations remote from the human gonadotropin-releasing hormone (GnRH) receptor-binding sites specifically increase binding affinity for GnRH II but not GnRH I: evidence for ligand-selective, receptor-active conformations. *The Journal of biological chemistry,* 280**,** 29796-803.

LUO, M., GUAN, X., LUCZAK, E. D., LANG, D., KUTSCHKE, W., GAO, Z., YANG, J., GLYNN, P., SOSSALLA, S., SWAMINATHAN, P. D., WEISS,

R. M., YANG, B., ROKITA, A. G., MAIER, L. S., EFIMOV, I. R., HUND, T. J. & ANDERSON, M. E. 2013. Diabetes increases mortality after myocardial infarction by oxidizing CaMKII. *The Journal of clinical investigation,* 123**,** 1262-74.

MADABUSHI, S., GROSS, A. K., PHILIPPI, A., MENG, E. C., WENSEL, T. G. & LICHTARGE, O. 2004. Evolutionary trace of G protein-coupled receptors reveals clusters of residues that determine global and class-specific functions. *The Journal of biological chemistry,* 279**,** 8126-32.

MAEDA, A., OKANO, K., PARK, P. S., LEM, J., CROUCH, R. K., MAEDA, T. & PALCZEWSKI, K. 2010a. Palmitoylation stabilizes unliganded rod opsin. *Proceedings of the National Academy of Sciences of the United States of America,* 107**,** 8428-33.

MAEDA, K.-I., OHKURA, S., UENOYAMA, Y., WAKABAYASHI, Y., OKA, Y., TSUKAMURA, H. & OKAMURA, H. 2010b. Neurobiological mechanisms underlying GnRH pulse generation by the hypothalamus. *Brain Research,* 1364**,** 103-115.

MAHON, M. J. & SEGRE, G. V. 2004. Stimulation by parathyroid hormone of a NHERF-1-assembled complex consisting of the parathyroid hormone I receptor, phospholipase Cbeta, and actin increases intracellular calcium in opossum kidney cells. *J Biol Chem,* 279**,** 23550-8.

MAHON, M. J. & SHIMADA, M. 2005. Calmodulin interacts with the cytoplasmic tails of the parathyroid hormone 1 receptor and a sub-set of class b G-protein coupled receptors. *FEBS Lett,* 579**,** 803-7.

MAKRI, A., PISSIMISSIS, N., LEMBESSIS, P., POLYCHRONAKOS, C. & KOUTSILIERIS, M. 2008. The kisspeptin (KiSS-1)/GPR54 system in cancer biology. *Cancer Treat Rev,* 34**,** 682-92.

MAMPUTHA, S., LU, Z. L., ROESKE, R. W., MILLAR, R. P., KATZ, A. A. & FLANAGAN, C. A. 2007. Conserved amino acid residues that are important for ligand binding in the type I gonadotropin-releasing hormone (GnRH) receptor are required for high potency of GnRH II at the type II GnRH receptor. *Molecular endocrinology,* 21**,** 281-92.

MANSUY, V., GELLER, S., REY, J. P., CAMPAGNE, C., BOCCARD, J., POULAIN, P., PREVOT, V. & PRALONG, F. P. 2011. Phenotypic and molecular characterization of proliferating and differentiated GnRH-expressing GnV-3 cells. *Molecular and cellular endocrinology,* 332**,** 97-105.

MARTIN, S. R., ANDERSSON TELEMAN, A., BAYLEY, P. M., DRAKENBERG, T. & FORSEN, S. 1985. Kinetics of calcium dissociation from calmodulin and its tryptic fragments. A stopped-flow fluorescence study using Quin 2 reveals a two-domain structure. *European journal of biochemistry / FEBS,* 151**,** 543-50.

MARTIN, S. R., MAUNE, J. F., BECKINGHAM, K. & BAYLEY, P. M. 1992. Stopped-flow studies of calcium dissociation from calcium-binding-site

mutants of Drosophila melanogaster calmodulin. *European journal of biochemistry / FEBS,* 205**,** 1107-14.

MARTINS, C. M., FERNANDES, B. F., ANTECKA, E., DI CESARE, S., MANSURE, J. J., MARSHALL, J. C. & BURNIER, M. N., JR. 2008. Expression of the metastasis suppressor gene KISS1 in uveal melanoma. *Eye (Lond),* 22**,** 707-11.

MASUI, T., DOI, R., MORI, T., TOYODA, E., KOIZUMI, M., KAMI, K., ITO, D., PEIPER, S. C., BROACH, J. R., OISHI, S., NIIDA, A., FUJII, N. & IMAMURA, M. 2004. Metastin and its variant forms suppress migration of pancreatic cancer cells. *Biochem Biophys Res Commun,* 315**,** 85-92.

MATTSON, M. P. & CHAN, S. L. 2003. Calcium orchestrates apoptosis. *Nature Cell Biology,* 5**,** 1041-3.

MAY, T., HAUSER, H. & WIRTH, D. 2004. Transcriptional control of SV40 T-antigen expression allows a complete reversion of immortalization. *Nucleic Acids Res,* 32**,** 5529-38.

MAYER, C., ACOSTA-MARTINEZ, M., DUBOIS, S. L., WOLFE, A., RADOVICK, S., BOEHM, U. & LEVINE, J. E. 2010. Timing and completion of puberty in female mice depend on estrogen receptor α-signaling in kisspeptin neurons. *Proceedings of the National Academy of Sciences,* 107**,** 22693-22698.

MEADOR, W. E., MEANS, A. R. & QUIOCHO, F. A. 1993. Modulation of calmodulin plasticity in molecular recognition on the basis of x-ray structures. *Science,* 262**,** 1718-21.

MELLON, P. L., WINDLE, J. J., GOLDSMITH, P. C., PADULA, C. A., ROBERTS, J. L. & WEINER, R. I. 1990. Immortalization of hypothalamic GnRH neurons by genetically targeted tumorigenesis. *Neuron,* 5**,** 1-10.

MEYER, T., HANSON, P. I., STRYER, L. & SCHULMAN, H. 1992. Calmodulin trapping by calcium-calmodulin-dependent protein kinase. *Science,* 256**,** 1199-202.

MIGUES, P. V., LEHMANN, I. T., FLUECHTER, L., CAMMAROTA, M., GURD, J. W., SIM, A. T., DICKSON, P. W. & ROSTAS, J. A. 2006. Phosphorylation of CaMKII at Thr253 occurs in vivo and enhances binding to isolated postsynaptic densities. *Journal of neurochemistry,* 98**,** 289-99.

MILLER, S. G. & KENNEDY, M. B. 1986. Regulation of brain type II Ca2+/calmodulin-dependent protein kinase by autophosphorylation: a Ca2+-triggered molecular switch. *Cell,* 44**,** 861-70.

MINAKAMI, R., JINNAI, N. & SUGIYAMA, H. 1997. Phosphorylation and calmodulin binding of the metabotropic glutamate receptor subtype 5 (mGluR5) are antagonistic in vitro. *J Biol Chem,* 272**,** 20291-8.

MIRZADEGAN, T., BENKO, G., FILIPEK, S. & PALCZEWSKI, K. 2003. Sequence analyses of G-protein-coupled receptors: similarities to rhodopsin. *Biochemistry,* 42**,** 2759-67.

MITCHELL, D. C., ABDELRAHIM, M., WENG, J., STAFFORD, L. J., SAFE, S., BAR-ELI, M. & LIU, M. 2006. Regulation of KiSS-1 metastasis suppressor gene expression in breast cancer cells by direct interaction of transcription factors activator protein-2alpha and specificity protein-1. *J Biol Chem,* 281**,** 51-8.

MONTMINY, M. 1997. Transcriptional regulation by cyclic AMP. *Annual review of biochemistry,* 66**,** 807-22.

MORELLO, J. P., SALAHPOUR, A., PETAJA-REPO, U. E., LAPERRIERE, A., LONERGAN, M., ARTHUS, M. F., NABI, I. R., BICHET, D. G. & BOUVIER, M. 2001. Association of calnexin with wild type and mutant AVPR2 that causes nephrogenic diabetes insipidus. *Biochemistry,* 40**,** 6766-75.

MORO, O., LAMEH, J., HOGGER, P. & SADEE, W. 1993. Hydrophobic amino acid in the i2 loop plays a key role in receptor-G protein coupling. *J Biol Chem,* 268**,** 22273-6.

MORRIS, E. P. & TOROK, K. 2001. Oligomeric structure of alpha-calmodulin-dependent protein kinase II. *Journal of molecular biology,* 308**,** 1-8.

MOULEDOUS, L., MOLLEREAU, C. & ZAJAC, J. M. 2010. Opioid-modulating properties of the neuropeptide FF system. *Biofactors,* 36**,** 423-9.

MUIR, A. I., CHAMBERLAIN, L., ELSHOURBAGY, N. A., MICHALOVICH, D., MOORE, D. J., CALAMARI, A., SZEKERES, P. G., SARAU, H. M., CHAMBERS, J. K., MURDOCK, P., STEPLEWSKI, K., SHABON, U., MILLER, J. E., MIDDLETON, S. E., DARKER, J. G., LARMINIE, C. G., WILSON, S., BERGSMA, D. J., EMSON, P., FAULL, R., PHILPOTT, K. L. & HARRISON, D. C. 2001. AXOR12, a novel human G protein-coupled receptor, activated by the peptide KiSS-1. *J Biol Chem,* 276**,** 28969-75.

MUKHERJI, S. & SODERLING, T. R. 1994. Regulation of Ca2+/calmodulin-dependent protein kinase II by inter- and intrasubunit-catalyzed autophosphorylations. *The Journal of biological chemistry,* 269**,** 13744-7.

MURAKAMI, M., MATSUZAKI, T., IWASA, T., YASUI, T., IRAHARA, M., OSUGI, T. & TSUTSUI, K. 2008. Hypophysiotropic role of RFamide-related peptide-3 in the inhibition of LH secretion in female rats. *The Journal of endocrinology,* 199**,** 105-12.

NAGAI, K., DOI, R., KATAGIRI, F., ITO, T., KIDA, A., KOIZUMI, M., MASUI, T., KAWAGUCHI, Y., TOMITA, K., OISHI, S., FUJII, N. & UEMOTO, S. 2009. Prognostic value of metastin expression in human pancreatic cancer. *J Exp Clin Cancer Res,* 28**,** 9.

NAKAJIMA, Y., YAMAMOTO, T., NAKAYAMA, T. & NAKANISHI, S. 1999. A relationship between protein kinase C phosphorylation and calmodulin binding to the metabotropic glutamate receptor subtype 7. *The Journal of biological chemistry,* 274**,** 27573-7.

NAKAYAMA, S. & KRETSINGER, R. H. 1994. Evolution of the EF-hand family of proteins. *Annual review of biophysics and biomolecular structure,* 23**,** 473-507.

NANOFF, C., KOPPENSTEINER, R., YANG, Q., FUERST, E., AHORN, H. & FREISSMUTH, M. 2006. The carboxyl terminus of the Galpha-subunit is the latch for triggered activation of heterotrimeric G proteins. *Mol Pharmacol,* 69**,** 397-405.

NASH, K. T., PHADKE, P. A., NAVENOT, J. M., HURST, D. R., ACCAVITTI-LOPER, M. A., SZTUL, E., VAIDYA, K. S., FROST, A. R., KAPPES, J. C., PEIPER, S. C. & WELCH, D. R. 2007. Requirement of KISS1 secretion for multiple organ metastasis suppression and maintenance of tumor dormancy. *J Natl Cancer Inst,* 99**,** 309-21.

NATHANSON, N. M. 2000. A multiplicity of muscarinic mechanisms: enough signaling pathways to take your breath away. *Proceedings of the National Academy of Sciences of the United States of America,* 97**,** 6245-7.

NAVARRO, V. M., FERNANDEZ-FERNANDEZ, R., CASTELLANO, J. M., ROA, J., MAYEN, A., BARREIRO, M. L., GAYTAN, F., AGUILAR, E., PINILLA, L., DIEGUEZ, C. & TENA-SEMPERE, M. 2004. Advanced vaginal opening and precocious activation of the reproductive axis by KiSS-1 peptide, the endogenous ligand of GPR54. *The Journal of Physiology,* 561**,** 379-86.

NAVARRO, V. M., FERNÁNDEZ-FERNÁNDEZ, R., NOGUEIRAS, R., VIGO, E., TOVAR, S., CHARTREL, N., LE MAREC, O., LEPRINCE, J., AGUILAR, E., PINILLA, L., DIEGUEZ, C., VAUDRY, H. & TENA-SEMPERE, M. 2006. Novel role of 26RFa, a hypothalamic RFamide orexigenic peptide, as putative regulator of the gonadotropic axis. *The Journal of Physiology,* 573**,** 237-249.

NAVARRO, V. M., GOTTSCH, M. L., CHAVKIN, C., OKAMURA, H., CLIFTON, D. K. & STEINER, R. A. 2009. Regulation of Gonadotropin-Releasing Hormone Secretion by Kisspeptin/Dynorphin/Neurokinin B Neurons in the Arcuate Nucleus of the Mouse. *The Journal of Neuroscience,* 29**,** 11859-11866.

NICKOLS, H. H., SHAH, V. N., CHAZIN, W. J. & LIMBIRD, L. E. 2004. Calmodulin interacts with the V2 vasopressin receptor: elimination of binding to the C terminus also eliminates arginine vasopressin-stimulated elevation of intracellular calcium. *J Biol Chem,* 279**,** 46969-80.

NIELSEN, S. B., FRANZMANN, M., BASAIAWMOIT, R. V., WIMMER, R., MIKKELSEN, J. D. & OTZEN, D. E. 2010. beta-Sheet aggregation of kisspeptin-10 is stimulated by heparin but inhibited by amphiphiles. *Biopolymers,* 93**,** 678-89.

NIIDA, A., WANG, Z., TOMITA, K., OISHI, S., TAMAMURA, H., OTAKA, A., NAVENOT, J.-M., BROACH, J. R., PEIPER, S. C. & FUJII, N. 2006. Design and synthesis of downsized metastin (45–54) analogs with

maintenance of high GPR54 agonistic activity. *Bioorganic & Medicinal Chemistry Letters,* 16**,** 134-137.

NIMRI, R., LEBENTHAL, Y., LAZAR, L., CHEVRIER, L., PHILLIP, M., BAR, M., HERNANDEZ-MORA, E., DE ROUX, N. & GAT-YABLONSKI, G. 2011. A novel loss-of-function mutation in GPR54/KISS1R leads to hypogonadotropic hypogonadism in a highly consanguineous family. *J Clin Endocrinol Metab,* 96**,** 2010-1676.

NYGAARD, R., FRIMURER, T. M., HOLST, B., ROSENKILDE, M. M. & SCHWARTZ, T. W. 2009. Ligand binding and micro-switches in 7TM receptor structures. *Trends in pharmacological sciences,* 30**,** 249-59.

O'CONNOR, V., EL FAR, O., BOFILL-CARDONA, E., NANOFF, C., FREISSMUTH, M., KARSCHIN, A., AIRAS, J. M., BETZ, H. & BOEHM, S. 1999. Calmodulin dependence of presynaptic metabotropic glutamate receptor signaling. *Science,* 286**,** 1180-4.

OAKLEY, A. E., CLIFTON, D. K. & STEINER, R. A. 2009. Kisspeptin signaling in the brain. *Endocr Rev,* 30**,** 713-43.

OHTAKI, T., SHINTANI, Y., HONDA, S., MATSUMOTO, H., HORI, A., KANEHASHI, K., TERAO, Y., KUMANO, S., TAKATSU, Y., MASUDA, Y., ISHIBASHI, Y., WATANABE, T., ASADA, M., YAMADA, T., SUENAGA, M., KITADA, C., USUKI, S., KUROKAWA, T., ONDA, H., NISHIMURA, O. & FUJINO, M. 2001. Metastasis suppressor gene KiSS-1 encodes peptide ligand of a G-protein-coupled receptor. *Nature,* 411**,** 613-7.

OJEDA, S., LOMNICZI, A., SANDAU, U. & MATAGNE, V. 2009. New concepts on the control of the onset of puberty.

OJEDA, S. R., LOMNICZI, A., MASTRONARDI, C., HEGER, S., ROTH, C., PARENT, A.-S., MATAGNE, V. & MUNGENAST, A. E. 2006. Minireview: The Neuroendocrine Regulation of Puberty: Is the Time Ripe for a Systems Biology Approach? *Endocrinology,* 147**,** 1166-1174.

OJEDA, S. R., LOMNICZI, A. & SANDAU, U. S. 2008. Glial–Gonadotrophin Hormone (GnRH) Neurone Interactions in the Median Eminence and the Control of GnRH Secretion. *Journal of Neuroendocrinology,* 20**,** 732-742.

OLDHAM, W. M. & HAMM, H. E. 2006. Structural basis of function in heterotrimeric G proteins. *Quarterly reviews of biophysics,* 39**,** 117-66.

OLDHAM, W. M. & HAMM, H. E. 2008. Heterotrimeric G protein activation by G-protein-coupled receptors. *Nature reviews. Molecular cell biology,* 9**,** 60-71.

ORSINI, M. J., KLEIN, M. A., BEAVERS, M. P., CONNOLLY, P. J., MIDDLETON, S. A. & MAYO, K. H. 2007. Metastin (KiSS-1) Mimetics Identified from Peptide Structure−Activity Relationship-Derived Pharmacophores and Directed Small Molecule Database Screening. *Journal of Medicinal Chemistry,* 50**,** 462-471.

OSUGI, T., UKENA, K., SOWER, S. A., KAWAUCHI, H. & TSUTSUI, K. 2006. Evolutionary origin and divergence of PQRFamide peptides and

LPXRFamide peptides in the RFamide peptide family. *FEBS Journal,* 273**,** 1731-1743.

OVERINGTON, J. P., AL-LAZIKANI, B. & HOPKINS, A. L. 2006. How many drug targets are there? *Nature reviews. Drug discovery,* 5**,** 993-6.

PAGE, R. B. & DOVEY-HARTMAN, B. J. 1984. Neurohemal contact in the internal zone of the rabbit median eminence. *J Comp Neurol,* 226**,** 274-88.

PAMPILLO, M. & BABWAH, A. V. 2010. Assessment of constitutive activity and internalization of GPR54 (KISS1-R). *Methods Enzymol,* 484**,** 75-93.

PAMPILLO, M., CAMUSO, N., TAYLOR, J. E., SZERESZEWSKI, J. M., AHOW, M. R., ZAJAC, M., MILLAR, R. P., BHATTACHARYA, M. & BABWAH, A. V. 2009. Regulation of GPR54 signaling by GRK2 and {beta}-arrestin. *Mol Endocrinol,* 23**,** 2060-74.

PANULA, P. 2009. Neuropeptide FF and Receptors. *In:* EDITOR-IN-CHIEF: LARRY, R. S. (ed.) *Encyclopedia of Neuroscience.* Oxford: Academic Press.

PARK, J. H., SCHEERER, P., HOFMANN, K. P., CHOE, H. W. & ERNST, O. P. 2008. Crystal structure of the ligand-free G-protein-coupled receptor opsin. *Nature,* 454**,** 183-7.

PATEL, R., HOLT, M., PHILIPOVA, R., MOSS, S., SCHULMAN, H., HIDAKA, H. & WHITAKER, M. 1999. Calcium/calmodulin-dependent phosphorylation and activation of human Cdc25-C at the G2/M phase transition in HeLa cells. *J Biol Chem,* 274**,** 7958-68.

PATTON, B. L., MILLER, S. G. & KENNEDY, M. B. 1990. Activation of type II calcium/calmodulin-dependent protein kinase by Ca2+/calmodulin is inhibited by autophosphorylation of threonine within the calmodulin-binding domain. *The Journal of biological chemistry,* 265**,** 11204-12.

PEARSON, R. B. & KEMP, B. E. 1991. Protein kinase phosphorylation site sequences and consensus specificity motifs: tabulations. *Methods in enzymology,* 200**,** 62-81.

PEARSON, R. B., WOODGETT, J. R., COHEN, P. & KEMP, B. E. 1985. Substrate specificity of a multifunctional calmodulin-dependent protein kinase. *The Journal of biological chemistry,* 260**,** 14471-6.

PERSECHINI, A. & KRETSINGER, R. H. 1988. The central helix of calmodulin functions as a flexible tether. *The Journal of biological chemistry,* 263**,** 12175-8.

PIELECKA-FORTUNA, J., CHU, Z. & MOENTER, S. M. 2008. Kisspeptin acts directly and indirectly to increase gonadotropin-releasing hormone neuron activity and its effects are modulated by estradiol. *Endocrinology,* 149**,** 1979-86.

PINEDA, R., GARCIA-GALIANO, D., ROSEWEIR, A., ROMERO, M., SANCHEZ-GARRIDO, M. A., RUIZ-PINO, F., MORGAN, K., PINILLA,

L., MILLAR, R. P. & TENA-SEMPERE, M. 2010. Critical roles of kisspeptins in female puberty and preovulatory gonadotropin surges as revealed by a novel antagonist. *Endocrinology,* 151**,** 722-30.

PINILLA, L., AGUILAR, E., DIEGUEZ, C., MILLAR, R. P. & TENA-SEMPERE, M. 2012. Kisspeptins and Reproduction: Physiological Roles and Regulatory Mechanisms. *Physiological Reviews,* 92**,** 1235-1316.

PRALONG, F. P. 2010. Insulin and NPY pathways and the control of GnRH function and puberty onset. *Molecular and Cellular Endocrinology,* 324**,** 82-86.

PRONIN, A. N., SATPAEV, D. K., SLEPAK, V. Z. & BENOVIC, J. L. 1997. Regulation of G protein-coupled receptor kinases by calmodulin and localization of the calmodulin binding domain. *J Biol Chem,* 272**,** 18273-80.

QUAYNOR, S., HU, L., LEUNG, P. K., FENG, H., MORES, N., KRSMANOVIC, L. Z. & CATT, K. J. 2007. Expression of a functional g protein-coupled receptor 54-kisspeptin autoregulatory system in hypothalamic gonadotropin-releasing hormone neurons. *Molecular endocrinology,* 21**,** 3062-70.

RADFORD, S. E. & DOBSON, C. M. 1999. From computer simulations to human disease: emerging themes in protein folding. *Cell,* 97**,** 291-8.

RASMUSSEN, C. D. & MEANS, A. R. 1989. Calmodulin is required for cell-cycle progression during G1 and mitosis. *EMBO J,* 8**,** 73-82.

RASMUSSEN, S. G., CHOI, H. J., FUNG, J. J., PARDON, E., CASAROSA, P., CHAE, P. S., DEVREE, B. T., ROSENBAUM, D. M., THIAN, F. S., KOBILKA, T. S., SCHNAPP, A., KONETZKI, I., SUNAHARA, R. K., GELLMAN, S. H., PAUTSCH, A., STEYAERT, J., WEIS, W. I. & KOBILKA, B. K. 2011a. Structure of a nanobody-stabilized active state of the beta(2) adrenoceptor. *Nature,* 469**,** 175-80.

RASMUSSEN, S. G., DEVREE, B. T., ZOU, Y., KRUSE, A. C., CHUNG, K. Y., KOBILKA, T. S., THIAN, F. S., CHAE, P. S., PARDON, E., CALINSKI, D., MATHIESEN, J. M., SHAH, S. T., LYONS, J. A., CAFFREY, M., GELLMAN, S. H., STEYAERT, J., SKINIOTIS, G., WEIS, W. I., SUNAHARA, R. K. & KOBILKA, B. K. 2011b. Crystal structure of the beta2 adrenergic receptor-Gs protein complex. *Nature,* 477**,** 549-55.

REITER, E. & LEFKOWITZ, R. J. 2006. GRKs and beta-arrestins: roles in receptor silencing, trafficking and signaling. *Trends in endocrinology and metabolism: TEM,* 17**,** 159-65.

RELLOS, P., PIKE, A. C., NIESEN, F. H., SALAH, E., LEE, W. H., VON DELFT, F. & KNAPP, S. 2010. Structure of the CaMKIIdelta/calmodulin complex reveals the molecular mechanism of CaMKII kinase activation. *PLoS biology,* 8**,** e1000426.

RITTER, S. L. & HALL, R. A. 2009. Fine-tuning of GPCR activity by receptor-interacting proteins. *Nat Rev Mol Cell Biol,* 10**,** 819-30.

ROA, J., CASTELLANO, J. M., NAVARRO, V. M., HANDELSMAN, D. J., PINILLA, L. & TENA-SEMPERE, M. 2009. Kisspeptins and the control of gonadotropin secretion in male and female rodents. *Peptides,* 30**,** 57-66.

ROA, J., VIGO, E., CASTELLANO, J. M., NAVARRO, V. M., FERNÁNDEZ-FERNÁNDEZ, R., CASANUEVA, F. F., DIEGUEZ, C., AGUILAR, E., PINILLA, L. & TENA-SEMPERE, M. 2006. Hypothalamic Expression of KiSS-1 System and Gonadotropin-Releasing Effects of Kisspeptin in Different Reproductive States of the Female Rat. *Endocrinology,* 147**,** 2864-2878.

RODERICK, H. L. & COOK, S. J. 2008. Ca2+ signalling checkpoints in cancer: remodelling Ca2+ for cancer cell proliferation and survival. *Nature reviews. Cancer,* 8**,** 361-75.

ROSENBERG, O. S., DEINDL, S., COMOLLI, L. R., HOELZ, A., DOWNING, K. H., NAIRN, A. C. & KURIYAN, J. 2006. Oligomerization states of the association domain and the holoenyzme of Ca2+/CaM kinase II. *The FEBS journal,* 273**,** 682-94.

ROSENBERG, O. S., DEINDL, S., SUNG, R. J., NAIRN, A. C. & KURIYAN, J. 2005. Structure of the autoinhibited kinase domain of CaMKII and SAXS analysis of the holoenzyme. *Cell,* 123**,** 849-60.

ROVATI, G. E., CAPRA, V. & NEUBIG, R. R. 2007. The highly conserved DRY motif of class A G protein-coupled receptors: beyond the ground state. *Mol Pharmacol,* 71**,** 959-64.

ROZELL, T. G., DAVIS, D. P., CHAI, Y. & SEGALOFF, D. L. 1998. Association of gonadotropin receptor precursors with the protein folding chaperone calnexin. *Endocrinology,* 139**,** 1588-93.

SALVI, R., CASTILLO, E., VOIROL, M. J., GLAUSER, M., REY, J. P., GAILLARD, R. C., VOLLENWEIDER, P. & PRALONG, F. P. 2006. Gonadotropin-releasing hormone-expressing neurons immortalized conditionally are activated by insulin: implication of the mitogen-activated protein kinase pathway. *Endocrinology,* 147**,** 816-26.

SAMSON, W. K., KEOWN, C., SAMSON, C. K., SAMSON, H. W., LANE, B., BAKER, J. R. & TAYLOR, M. M. 2003. Prolactin-releasing peptide and its homolog RFRP-1 act in hypothalamus but not in anterior pituitary gland to stimulate stress hormone secretion. *Endocrine,* 20**,** 59-66.

SANCHEZ-CARBAYO, M., BELBIN, T. J., SCOTLANDI, K., PRYSTOWSKY, M., BALDINI, N., CHILDS, G. & CORDON-CARDO, C. 2003a. Expression profiling of osteosarcoma cells transfected with MDR1 and NEO genes: regulation of cell adhesion, apoptosis, and tumor suppression-related genes. *Lab Invest,* 83**,** 507-17.

SANCHEZ-CARBAYO, M., CAPODIECI, P. & CORDON-CARDO, C. 2003b. Tumor suppressor role of KiSS-1 in bladder cancer: loss of KiSS-1 expression is associated with bladder cancer progression and clinical outcome. *Am J Pathol,* 162**,** 609-17.

SANDERS, C. R. & NAGY, J. K. 2000. Misfolding of membrane proteins in health and disease: the lady or the tiger? *Current opinion in structural biology,* 10**,** 438-42.

SANTORO, N., FILICORI, M. & CROWLEY, W. F., JR. 1986. Hypogonadotropic disorders in men and women: diagnosis and therapy with pulsatile gonadotropin-releasing hormone. *Endocr Rev,* 7**,** 11-23.

SCHEERER, P., PARK, J. H., HILDEBRAND, P. W., KIM, Y. J., KRAUSS, N., CHOE, H. W., HOFMANN, K. P. & ERNST, O. P. 2008. Crystal structure of opsin in its G-protein-interacting conformation. *Nature,* 455**,** 497-502.

SCHLYER, S. & HORUK, R. 2006. I want a new drug: G-protein-coupled receptors in drug development. *Drug Discov Today,* 11**,** 481-93.

SCHRAG, J. D., PROCOPIO, D. O., CYGLER, M., THOMAS, D. Y. & BERGERON, J. J. 2003. Lectin control of protein folding and sorting in the secretory pathway. *Trends in biochemical sciences,* 28**,** 49-57.

SCHULMAN, H. & GREENGARD, P. 1978a. Ca2+-dependent protein phosphorylation system in membranes from various tissues, and its activation by "calcium-dependent regulator". *Proc Natl Acad Sci U S A,* 75**,** 5432-6.

SCHULMAN, H. & GREENGARD, P. 1978b. Stimulation of brain membrane protein phosphorylation by calcium and an endogenous heat-stable protein. *Nature,* 271**,** 478-9.

SCHWANZEL-FUKUDA, M. & PFAFF, D. W. 1989. Origin of luteinizing hormone-releasing hormone neurons. *Nature,* 338**,** 161-4.

SCHWARTZ, N. 2000a. Neuroendocrine Regulation of Reproductive Cyclicity. *In:* CONN, P. M. & FREEMAN, M. (eds.) *Neuroendocrinology in physiology and medicine.* Humana Press.

SCHWARTZ, N. B. 2000b. Neuroendocrine regulation of reproductive cyclicity. *Neuroendocrinology in physiology and medicine***,** 135-146.

SCOTT, J. A., XIE, L., LI, H., LI, W., HE, J. B., SANDERS, P. N., CARTER, A. B., BACKS, J., ANDERSON, M. E. & GRUMBACH, I. M. 2012. The multifunctional Ca2+/calmodulin-dependent kinase II regulates vascular smooth muscle migration through matrix metalloproteinase 9. *American journal of physiology. Heart and circulatory physiology,* 302**,** H1953-64.

SEINSOTH, S., UHLMANN-SCHIFFLER, H. & STAHL, H. 2003. Bidirectional DNA unwinding by a ternary complex of T antigen, nucleolin and topoisomerase I. *EMBO reports,* 4**,** 263-8.

SELVIN, P. R. 2000. The renaissance of fluorescence resonance energy transfer. *Nature structural biology,* 7**,** 730-4.

SEMINARA, S. B., MESSAGER, S., CHATZIDAKI, E. E., THRESHER, R. R., ACIERNO, J. S., SHAGOURY, J. K., BO-ABBAS, Y., KUOHUNG, W., SCHWINOF, K. M., HENDRICK, A. G., ZAHN, D., DIXON, J., KAISER, U. B., SLAUGENHAUPT, S. A., GUSELLA, J. F., O'RAHILLY, S.,

CARLTON, M. B. L., CROWLEY, W. F., APARICIO, S. A. J. R. & COLLEDGE, W. H. 2003. The GPR54 Gene as a Regulator of Puberty. *New England Journal of Medicine,* 349**,** 1614-1627.

SEMPLE, R. K., ACHERMANN, J. C., ELLERY, J., FAROOQI, I. S., KARET, F. E., STANHOPE, R. G., O'RAHILLY, S. & APARICIO, S. A. 2005. Two Novel Missense Mutations in G Protein-Coupled Receptor 54 in a Patient with Hypogonadotropic Hypogonadism. *Journal of Clinical Endocrinology & Metabolism,* 90**,** 1849-1855.

SHAHAB, M., MASTRONARDI, C., SEMINARA, S. B., CROWLEY, W. F., OJEDA, S. R. & PLANT, T. M. 2005. Increased hypothalamic GPR54 signaling: a potential mechanism for initiation of puberty in primates. *Proceedings of the National Academy of Sciences of the United States of America,* 102**,** 2129-34.

SHIH, M., LIN, F., SCOTT, J. D., WANG, H. Y. & MALBON, C. C. 1999. Dynamic complexes of beta2-adrenergic receptors with protein kinases and phosphatases and the role of gravin. *J Biol Chem,* 274**,** 1588-95.

SHIN, R., WELCH, D. R., MISHRA, V. K., NASH, K. T., HURST, D. R. & RAMA KRISHNA, N. 2009. Nuclear magnetic resonance and circular dichroism study of metastin (Kisspeptin-54) structure in solution. *Clin Exp Metastasis,* 26**,** 527-33.

SHIRASAKI, F., TAKATA, M., HATTA, N. & TAKEHARA, K. 2001. Loss of expression of the metastasis suppressor gene KiSS1 during melanoma progression and its association with LOH of chromosome 6q16.3-q23. *Cancer Res,* 61**,** 7422-5.

SHOJI, S., TANG, X. Y., UMEMURA, S., ITOH, J., TAKEKOSHI, S., SHIMA, M., USUI, Y., NAGATA, Y., UCHIDA, T., OSAMURA, R. Y. & TERACHI, T. 2009. Metastin inhibits migration and invasion of renal cell carcinoma with overexpression of metastin receptor. *European urology,* 55**,** 441-9.

SILVEIRA, L. G., NOEL, S. D., SILVEIRA-NETO, A. P., ABREU, A. P., BRITO, V. N., SANTOS, M. G., BIANCO, S. D. C., KUOHUNG, W., XU, S., GRYNGARTEN, M., ESCOBAR, M. E., ARNHOLD, I. J. P., MENDONCA, B. B., KAISER, U. B. & LATRONICO, A. C. 2010. Mutations of the KISS1 Gene in Disorders of Puberty. *Journal of Clinical Endocrinology & Metabolism,* 95**,** 2276-2280.

SIMONNEAUX, V., ANSEL, L., REVEL, F. G., KLOSEN, P., PÉVET, P. & MIKKELSEN, J. D. 2009. Kisspeptin and the seasonal control of reproduction in hamsters. *Peptides,* 30**,** 146-153.

SISK, C. L. & FOSTER, D. L. 2004. The neural basis of puberty and adolescence. *Nat Neurosci,* 7**,** 1040-7.

SITIA, R. & BRAAKMAN, I. 2003. Quality control in the endoplasmic reticulum protein factory. *Nature,* 426**,** 891-4.

SJOGREN, T., NORD, J., EK, M., JOHANSSON, P., LIU, G. & GESCHWINDNER, S. 2013. Crystal structure of microsomal prostaglandin E2 synthase provides insight into diversity in the MAPEG superfamily. *Proc Natl Acad Sci U S A,* 110**,** 3806-11.

SLACK, A., CERVONI, N., PINARD, M. & SZYF, M. 1999. DNA methyltransferase is a downstream effector of cellular transformation triggered by simian virus 40 large T antigen. *J Biol Chem,* 274**,** 10105-12.

SMITH, J. T., ACOHIDO, B. V., CLIFTON, D. K. & STEINER, R. A. 2006. KiSS-1 neurones are direct targets for leptin in the ob/ob mouse. *Journal of Neuroendocrinology,* 18**,** 298-303.

SMITH, J. T. & CLARKE, I. J. 2010. Gonadotropin inhibitory hormone function in mammals. *Trends in endocrinology and metabolism: TEM,* 21**,** 255-260.

SMITH, M. S. & GROVE, K. L. 2002. Integration of the regulation of reproductive function and energy balance: lactation as a model. *Frontiers in Neuroendocrinology,* 23**,** 225-256.

SNAPP, E. L. & HEGDE, R. S. 2006. Rational design and evaluation of FRET experiments to measure protein proximities in cells. *Current protocols in cell biology / editorial board, Juan S. Bonifacino ... [et al.],* Chapter 17**,** Unit 17 9.

SORENSEN, S. D., MACEK, T. A., CAI, Z., SAUGSTAD, J. A. & CONN, P. J. 2002. Dissociation of protein kinase-mediated regulation of metabotropic glutamate receptor 7 (mGluR7) interactions with calmodulin and regulation of mGluR7 function. *Molecular Pharmacology,* 61**,** 1303-12.

SPRINGAEL, J. Y., DE POORTER, C., DEUPI, X., VAN DURME, J., PARDO, L. & PARMENTIER, M. 2007. The activation mechanism of chemokine receptor CCR5 involves common structural changes but a different network of interhelical interactions relative to rhodopsin. *Cellular signalling,* 19**,** 1446-56.

STAFFORD, L. J., XIA, C., MA, W., CAI, Y. & LIU, M. 2002. Identification and characterization of mouse metastasis-suppressor KiSS1 and its G-protein-coupled receptor. *Cancer Res,* 62**,** 5399-404.

STANDFUSS, J., EDWARDS, P. C., D'ANTONA, A., FRANSEN, M., XIE, G., OPRIAN, D. D. & SCHERTLER, G. F. 2011. The structural basis of agonist-induced activation in constitutively active rhodopsin. *Nature,* 471**,** 656-60.

SWAMINATHAN, P. D., PUROHIT, A., SONI, S., VOIGT, N., SINGH, M. V., GLUKHOV, A. V., GAO, Z., HE, B. J., LUCZAK, E. D., JOINER, M. L., KUTSCHKE, W., YANG, J., DONAHUE, J. K., WEISS, R. M., GRUMBACH, I. M., OGAWA, M., CHEN, P. S., EFIMOV, I., DOBREV, D., MOHLER, P. J., HUND, T. J. & ANDERSON, M. E. 2011. Oxidized CaMKII causes cardiac sinus node dysfunction in mice. *The Journal of clinical investigation,* 121**,** 3277-88.

TAKINO, T., KOSHIKAWA, N., MIYAMORI, H., TANAKA, M., SASAKI, T., OKADA, Y., SEIKI, M. & SATO, H. 2003. Cleavage of metastasis suppressor gene product KiSS-1 protein//metastin by matrix metalloproteinases. *Oncogene,* 22**,** 4617-4626.

TAN, C. M., BRADY, A. E., NICKOLS, H. H., WANG, Q. & LIMBIRD, L. E. 2004. Membrane trafficking of G protein-coupled receptors. *Annual review of pharmacology and toxicology,* 44**,** 559-609.

TAO, J., WANG, H. Y. & MALBON, C. C. 2003. Protein kinase A regulates AKAP250 (gravin) scaffold binding to the beta2-adrenergic receptor. *EMBO J,* 22**,** 6419-29.

TELES, M. G., BIANCO, S. D. C., BRITO, V. N., TRARBACH, E. B., KUOHUNG, W., XU, S., SEMINARA, S. B., MENDONCA, B. B., KAISER, U. B. & LATRONICO, A. C. 2008. A GPR54-Activating Mutation in a Patient with Central Precocious Puberty. *New England Journal of Medicine,* 358**,** 709-715.

TENA-SEMPERE, M. 2007. Roles of ghrelin and leptin in the control of reproductive function. *Neuroendocrinology,* 86**,** 229-41.

TENENBAUM-RAKOVER, Y., COMMENGES-DUCOS, M., IOVANE, A., AUMAS, C., ADMONI, O. & DE ROUX, N. 2007. Neuroendocrine Phenotype Analysis in Five Patients with Isolated Hypogonadotropic Hypogonadism due to a L102P Inactivating Mutation of GPR54. *Journal of Clinical Endocrinology & Metabolism,* 92**,** 1137-1144.

THOMAS, W. G., PIPOLO, L. & QIAN, H. 1999. Identification of a Ca2+/calmodulin-binding domain within the carboxyl-terminus of the angiotensin II (AT1A) receptor. *FEBS Lett,* 455**,** 367-71.

TOBET, S. A. & SCHWARTING, G. A. 2006. Minireview: recent progress in gonadotropin-releasing hormone neuronal migration. *Endocrinology,* 147**,** 1159-65.

TOBIN, A. B., BUTCHER, A. J. & KONG, K. C. 2008. Location, location, location...site-specific GPCR phosphorylation offers a mechanism for cell-type-specific signalling. *Trends in pharmacological sciences,* 29**,** 413-20.

TODMAN, M. G., HAN, S. K. & HERBISON, A. E. 2005. Profiling neurotransmitter receptor expression in mouse gonadotropin-releasing hormone neurons using green fluorescent protein-promoter transgenics and microarrays. *Neuroscience,* 132**,** 703-712.

TOMASZEWSKA-ZAREMBA, D. & HERMAN, A. 2009. The role of immunological system in the regulation of gonadoliberin and gonadotropin secretion. *Reprod Biol,* 9**,** 11-23.

TOMITA, K., NIIDA, A., OISHI, S., OHNO, H., CLUZEAU, J., NAVENOT, J.-M., WANG, Z.-X., PEIPER, S. C. & FUJII, N. 2006. Structure–activity relationship study on small peptidic GPR54 agonists. *Bioorganic & Medicinal Chemistry,* 14**,** 7595-7603.

TOMITA, K., OISHI, S., OHNO, H., PEIPER, S. C. & FUJII, N. 2008. Development of Novel G-Protein-Coupled Receptor 54 Agonists with Resistance to Degradation by Matrix Metalloproteinase. *Journal of Medicinal Chemistry,* 51**,** 7645-7649.

TOROK, K., COWLEY, D. J., BRANDMEIER, B. D., HOWELL, S., AITKEN, A. & TRENTHAM, D. R. 1998. Inhibition of calmodulin-activated smooth-muscle myosin light-chain kinase by calmodulin-binding peptides and fluorescent (phosphodiesterase-activating) calmodulin derivatives. *Biochemistry,* 37**,** 6188-98.

TOROK, K., TZORTZOPOULOS, A., GRABAREK, Z., BEST, S. L. & THOROGATE, R. 2001. Dual effect of ATP in the activation mechanism of brain Ca(2+)/calmodulin-dependent protein kinase II by Ca(2+)/calmodulin. *Biochemistry,* 40**,** 14878-90.

TROMBETTA, E. S. & PARODI, A. J. 2003. Quality control and protein folding in the secretory pathway. *Annual review of cell and developmental biology,* 19**,** 649-76.

TSIEN, R. & POZZAN, T. 1989. Measurement of cytosolic free Ca2+ with quin2. *Methods Enzymol,* 172**,** 230-62.

TSUTSUI, K., SAIGOH, E., UKENA, K., TERANISHI, H., FUJISAWA, Y., KIKUCHI, M., ISHII, S. & SHARP, P. J. 2000. A novel avian hypothalamic peptide inhibiting gonadotropin release. *Biochem Biophys Res Commun,* 275**,** 661-7.

TU, J. C., XIAO, B., YUAN, J. P., LANAHAN, A. A., LEOFFERT, K., LI, M., LINDEN, D. J. & WORLEY, P. F. 1998. Homer binds a novel proline-rich motif and links group 1 metabotropic glutamate receptors with IP3 receptors. *Neuron,* 21**,** 717-26.

TUNG, H. H. & LEE, S. L. 2012. Neural transmembrane protease and endothelial Gs protein activation in cell contact-dependent signaling between neural stem/progenitor cells and brain endothelial cells. *J Biol Chem,* 287**,** 22497-508.

TURNER, J. H., GELASCO, A. K. & RAYMOND, J. R. 2004. Calmodulin interacts with the third intracellular loop of the serotonin 5-hydroxytryptamine1A receptor at two distinct sites: putative role in receptor phosphorylation by protein kinase C. *J Biol Chem,* 279**,** 17027-37.

TURNER, J. H. & RAYMOND, J. R. 2005. Interaction of calmodulin with the serotonin 5-hydroxytryptamine2A receptor. A putative regulator of G protein coupling and receptor phosphorylation by protein kinase C. *J Biol Chem,* 280**,** 30741-50.

TZORTZOPOULOS, A., BEST, S. L., KALAMIDA, D. & TOROK, K. 2004. Ca2+/calmodulin-dependent activation and inactivation mechanisms of alphaCaMKII and phospho-Thr286-alphaCaMKII. *Biochemistry,* 43**,** 6270-80.

TZORTZOPOULOS, A. & TOROK, K. 2004. Mechanism of the T286A-mutant alphaCaMKII interactions with Ca2+/calmodulin and ATP. *Biochemistry,* 43**,** 6404-14.

UBUKA, T., MORGAN, K., PAWSON, A., OSUGI, T., CHOWDHURY, V., MINAKATA, H., TSUTSUI, K., MILLAR, R. & BENTLEY, G. 2009. Identification of human GnIH homologs,RFRP-1 and RFRP-3, and the cognate receptor, GPR147 in the hypothalamic pituitary axis. *PLoS One,* 4 e8400.

VASSILAKOS, A., MICHALAK, M., LEHRMAN, M. A. & WILLIAMS, D. B. 1998. Oligosaccharide binding characteristics of the molecular chaperones calnexin and calreticulin. *Biochemistry,* 37**,** 3480-90.

VENEMA, R. C., JU, H., VENEMA, V. J., SCHIEFFER, B., HARP, J. B., LING, B. N., EATON, D. C. & MARRERO, M. B. 1998. Angiotensin II-induced association of phospholipase Cgamma1 with the G-protein-coupled AT1 receptor. *J Biol Chem,* 273**,** 7703-8.

VENKATAKRISHNAN, A. J., DEUPI, X., LEBON, G., TATE, C. G., SCHERTLER, G. F. & BABU, M. M. 2013. Molecular signatures of G-protein-coupled receptors. *Nature,* 494**,** 185-94.

WACKER, J. L., FELLER, D. B., TANG, X. B., DEFINO, M. C., NAMKUNG, Y., LYSSAND, J. S., MHYRE, A. J., TAN, X., JENSEN, J. B. & HAGUE, C. 2008. Disease-causing mutation in GPR54 reveals the importance of the second intracellular loop for class A G-protein-coupled receptor function. *J Biol Chem,* 283**,** 31068-78.

WALL, M. E., CLARAGE, J. B. & PHILLIPS, G. N. 1997. Motions of calmodulin characterized using both Bragg and diffuse X-ray scattering. *Structure,* 5**,** 1599-612.

WANG, D., QUILLAN, J. M., WINANS, K., LUCAS, J. L. & SADEE, W. 2001. Single nucleotide polymorphisms in the human mu opioid receptor gene alter basal G protein coupling and calmodulin binding. *The Journal of biological chemistry,* 276**,** 34624-30.

WANG, D., SADEE, W. & QUILLAN, J. M. 1999. Calmodulin binding to G protein-coupling domain of opioid receptors. *J Biol Chem,* 274**,** 22081-8.

WANG, D., SURRATT, C. K. & SADEE, W. 2000. Calmodulin regulation of basal and agonist-stimulated G protein coupling by the mu-opioid receptor (OP(3)) in morphine-pretreated cell. *Journal of neurochemistry,* 75**,** 763-71.

WAXHAM, M. N., TSAI, A. L. & PUTKEY, J. A. 1998. A mechanism for calmodulin (CaM) trapping by CaM-kinase II defined by a family of CaM-binding peptides. *The Journal of biological chemistry,* 273**,** 17579-84.

WESS, J. 1996. Molecular biology of muscarinic acetylcholine receptors. *Critical reviews in neurobiology,* 10**,** 69-99.

WHITE, R. R., KWON, Y. G., TAING, M., LAWRENCE, D. S. & EDELMAN, A. M. 1998. Definition of optimal substrate recognition motifs of Ca2+-calmodulin-dependent protein kinases IV and II reveals shared and distinctive features. *The Journal of biological chemistry,* 273**,** 3166-72.

WHORTON, M. R., BOKOCH, M. P., RASMUSSEN, S. G., HUANG, B., ZARE, R. N., KOBILKA, B. & SUNAHARA, R. K. 2007. A monomeric G protein-coupled receptor isolated in a high-density lipoprotein particle efficiently activates its G protein. *Proceedings of the National Academy of Sciences of the United States of America,* 104**,** 7682-7.

WRAY, S. 2002. Molecular Mechanisms for Migration of Placodally Derived GnRH Neurons. *Chemical Senses,* 27**,** 569-572.

WRAY, S., GRANT, P. & GAINER, H. 1989a. Evidence that cells expressing luteinizing hormone-releasing hormone mRNA in the mouse are derived from progenitor cells in the olfactory placode. *Proc Natl Acad Sci U S A,* 86**,** 8132-6.

WRAY, S., GRANT, P. & GAINER, H. 1989b. Evidence that cells expressing luteinizing hormone-releasing hormone mRNA in the mouse are derived from progenitor cells in the olfactory placode. *Proceedings of the National Academy of Sciences,* 86**,** 8132-8136.

WU, N., HANSON, S. M., FRANCIS, D. J., VISHNIVETSKIY, S. A., THIBONNIER, M., KLUG, C. S., SHOHAM, M. & GUREVICH, V. V. 2006. Arrestin binding to calmodulin: a direct interaction between two ubiquitous signaling proteins. *J Mol Biol,* 364**,** 955-63.

XIAO, B., TU, J. C., PETRALIA, R. S., YUAN, J. P., DOAN, A., BREDER, C. D., RUGGIERO, A., LANAHAN, A. A., WENTHOLD, R. J. & WORLEY, P. F. 1998. Homer regulates the association of group 1 metabotropic glutamate receptors with multivalent complexes of homer-related, synaptic proteins. *Neuron,* 21**,** 707-16.

XU, F., WU, H., KATRITCH, V., HAN, G. W., JACOBSON, K. A., GAO, Z. G., CHEREZOV, V. & STEVENS, R. C. 2011. Structure of an agonist-bound human A2A adenosine receptor. *Science,* 332**,** 322-7.

YAN, C., WANG, H. & BOYD, D. D. 2001. KiSS-1 represses 92-kDa type IV collagenase expression by down-regulating NF-kappa B binding to the promoter as a consequence of Ikappa Balpha -induced block of p65/p50 nuclear translocation. *J Biol Chem,* 276**,** 1164-72.

YANG, E. & SCHULMAN, H. 1999. Structural examination of autoregulation of multifunctional calcium/calmodulin-dependent protein kinase II. *The Journal of biological chemistry,* 274**,** 26199-208.

YANG, Y., TURNER, R. S. & GAUT, J. R. 1998. The chaperone BiP/GRP78 binds to amyloid precursor protein and decreases Abeta40 and Abeta42 secretion. *The Journal of biological chemistry,* 273**,** 25552-5.

YAP, K. L., KIM, J., TRUONG, K., SHERMAN, M., YUAN, T. & IKURA, M. 2000. Calmodulin target database. *J Struct Funct Genomics,* 1**,** 8-14.

YAPHE, J., RIGGE, M., HERXHEIMER, A., MCPHERSON, A., MILLER, R., SHEPPERD, S. & ZIEBLAND, S. 2000. The use of patients' stories by self-help groups: a survey of voluntary organizations in the UK on the register of the College of Health. *Health expectations : an international journal of public participation in health care and health policy,* 3**,** 176-181.

YI, X., LI, C. Y., ZHANG, S. H., WANG, X. H., LI, Z. Q. & YANG, F. 2008. [Relationship and clinical significance of KiSS-1, nuclear factor kappa B (NF-kappaB), p50, and matrix metalloproteinase 9 expression in breast cancer]. *Zhonghua Bing Li Xue Za Zhi,* 37**,** 238-42.

YOSHIOKA, K., OHNO, Y., HORIGUCHI, Y., OZU, C., NAMIKI, K. & TACHIBANA, M. 2008. Effects of a KiSS-1 peptide, a metastasis suppressor gene, on the invasive ability of renal cell carcinoma cells through a modulation of a matrix metalloproteinase 2 expression. *Life Sci,* 83**,** 332-8.

ZHANG, C., BOSCH, M. A., RONNEKLEIV, O. K. & KELLY, M. J. 2013. Kisspeptin activation of TRPC4 channels in female GnRH neurons requires PIP2 depletion and cSrc kinase activation. *Endocrinology,* 154**,** 2772-83.

ZHANG, J., FERGUSON, S. S., BARAK, L. S., MENARD, L. & CARON, M. G. 1996. Dynamin and beta-arrestin reveal distinct mechanisms for G protein-coupled receptor internalization. *The Journal of biological chemistry,* 271**,** 18302-5.

ZHANG, J., XUE, F. & CHANG, Y. 2009. Agonist- and antagonist-induced conformational changes of loop F and their contributions to the rho1 GABA receptor function. *The Journal of Physiology,* 587**,** 139-53.

ZHAO, S. & KRIEGSFELD, L. J. 2009. Daily changes in GT1-7 cell sensitivity to GnRH secretagogues that trigger ovulation. *Neuroendocrinology,* 89**,** 448-57.

ZHOU, H., YAN, F., YAMAMOTO, S. & TAI, H. H. 1999. Phenylalanine 138 in the second intracellular loop of human thromboxane receptor is critical for receptor-G-protein coupling. *Biochem Biophys Res Commun,* 264**,** 171-5.

8. Appendix

8.1. Characterising cell-line models for GnRH neurons

Physiologically relevant cell-line models that are similar to GnRH neurons and secrete GnRH would be good cell model candidates to study cellular physiology. To date, the best candidates are the GT1-7 and GnV3 cell-lines. Furthermore, GnRH neurons have been reported to express endogenous KISS1R and that when stimulated with KP-10 induce fast action potentials and secrete GnRH [as reviewed in (Oakley et al., 2009)]. Thus, in order to determine whether GT1-7 and GnV3 cells express endogenous KISS1R, ^{125}I-KP-10 binding (see section 2.22), and inositol phosphate (IP_3) turnover (see section 2.24) were examined. As a comparison, COS-7 cells were used, with and without transient expression (see section 2.21) of KISS1R.

The GnV3 cell-line contains a Tet-On system which drives the transcription of v-myc (the immortalisation agent) upon doxycycline (DOX) administration. The proliferation of GnV3 cells is stimulated with DOX, while in DOX free medium GnV3 cells differentiate back into 'GnRH neurons' (Salvi et al., 2006, Mansuy et al., 2011). GT1-7 constitutively expresses the immortalisation agent SV40 T-antigen (Mellon et al., 1990).

The GT1-7 and GnV3 cells were determined to have undetectable endogenous KISS1R expression (GnV3 cells were cultured in the absence of DOX), as both cell types gave undetectable ^{125}I-KP-10 binding and IP_3 turnover. (Figure 6.1 and Figure 6.2). In contrast, COS-7 cells, which are frequently used to express GPCRs, showed approximately 7-fold increase in the maximum ^{125}I-KP-10 binding of transiently expressing KISS1R ($P < 0.05$) (Figure 6.1) Furthermore, the COS-7 cells transiently expressing KISS1R gave a 20-fold increase in KP-10 induced IP_3 turnover relative to the vector control ($P < 0.05$) (Figure 6.2).

In order to determine whether GT1-7 and GnV3 cells secrete GnRH upon potassium stimulation a radioimmunoassay was carried. It was observed that GT1-7 and GnV3 cells were unable to secrete GnRH, or the levels below the methodological sensitivity of tens of pg/mL GnRH (Figure 6.3).

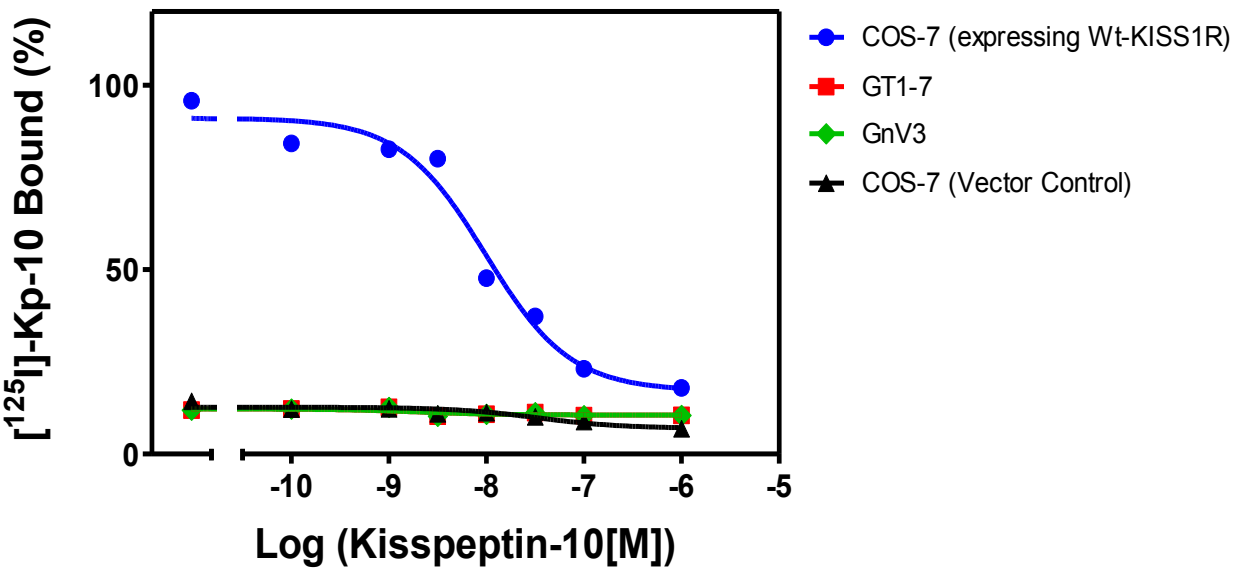

Figure 8.1 KP-10 binding to COS-7, GT1-7, and GnV3 cells. All cell-lines were prepared following the receptor binding assay protocol (see section 2.22) and the KISS1R cDNA transfection was carried out using the protocol in section 2.21. COS-7 cells transiently transfected with KISS1R (blue line) or vector (pcDNA3.1+) (black line) were compared to untransfected native GT1-7 (red line) and GnV3 (green line) cells. The GnV3 cells were cultured in the absence of doxycycline (-DOX) 48 hours prior to the assay. The error bars are the standard error of the mean (S.E.M).

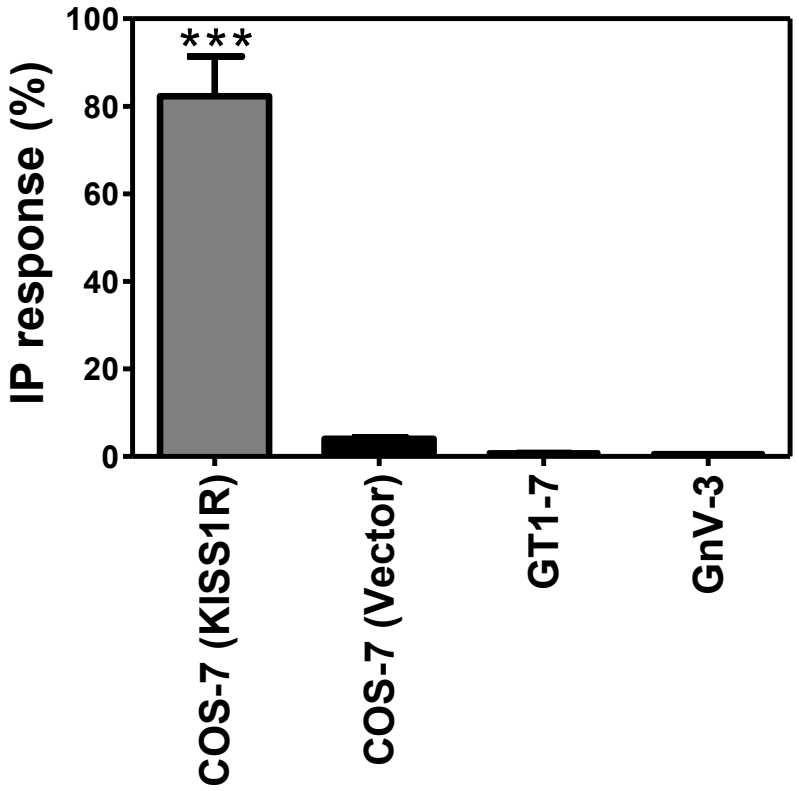

Figurer 8.2 KP-10 induced effects on IP_3 response in COS-7, GT1-7, and GnV3 cells. All cells were treated with KP-10 (1 μM) and processed using the IP_3 accumulation assay (see section 2.24). COS-7 cells were transiently transfected with control vector (pcDNA3.1+) or KISS1R cDNA and native GT1-7 and GnV-3 cells were used. GnV3 cells were incubated in the absence of doxycycline (-DOX) for 48 prior the assay. Asterisks (*) denote statistical significance (** $P<0.01$) as calculated by One-Way Anova with Dunnett's test.

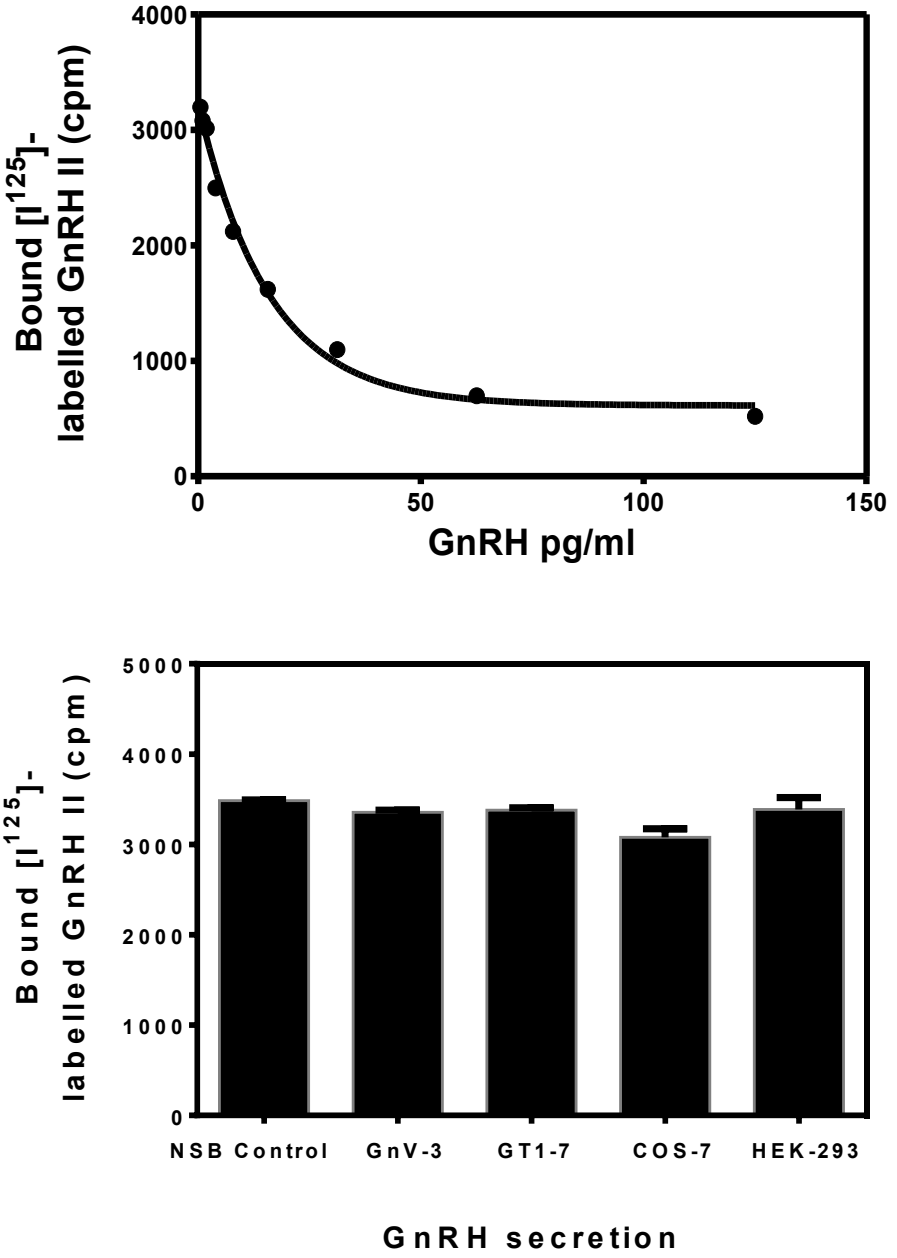

Figure 8.3 GnRH secretion studies of GnV3, GT1-7, COS-7, and HEK-293 cell-lines. *Top*; calibration curve using GnRH II concentration gradient to determine the sensitively of the radioimmunoassay. *Bottom;* indicated cell-lines were treated with 60 mM of K^+ for 30 minutes in their respective culture media. GnV3 cells were cultured in doxycycline 24 hours prior. 50 μL of medium (from 10mL) was removed as sample for the radioimmunoassay (see section 2.23).

8.1.1. Discussion

The aim of this section was to characterise GnV3 and GT1-7 cells for the purpose of studying KISS1R interacting proteins. To do this, a radio-ligand binding assay was used to determine the presence of endogenous KISS1R in GT1-7 and GnV3 cells. Also, in order to determine whether the KISS1R was functional, inositol IP_3 turnover was measured. These biochemical assays were complemented by determining whether these cell-lines secrete GnRH upon depolarisation with potassium chloride stimulation.

Some important phenotypic characteristics of GnRH neurons found *in vivo* must be present in the *in vitro* cell-line models in order to study cellular physiology. These characteristics should include the expression of endogenous KISS1R. Indeed, several research groups demonstrated the existence of KISS1R in GT1-7 and GnV3 cells (Zhao and Kriegsfeld, 2009, Quaynor et al., 2007, Jacobi et al., 2007). However, in this, the results revealed that GT1-7 and GnV3 cell-lines do not express, on their cell surface endogenous KISS1R and that they do not secrete GnRH. One reason for this might be the lack of KISS1R trafficking proteins. Another possibility is that these cells have differentiated away from their previously reported characteristics.

In conclusion, cell-line models for GnRH neurons pose considerable challenges, mainly the inability to maintain their phenotypes. Therefore, future experiments pertaining to the study of KISS1R interacting proteins should rely on the use of the common cell-lines like COS-7 and HEK-293, which can transiently express GPCRs well.